



8-2019

Materials Science and Engineering

Joshua P. Steimel

University of the Pacific, jsteimel@pacific.edu

Follow this and additional works at: <https://scholarlycommons.pacific.edu/open-textbooks>

 Part of the [Materials Science and Engineering Commons](#)



This work is licensed under a [Creative Commons Attribution-NonCommercial-No Derivative Works 4.0 International License](#).

Recommended Citation

Steimel, Joshua P., "Materials Science and Engineering" (2019). *Pacific Open Texts*. 8.
<https://scholarlycommons.pacific.edu/open-textbooks/8>

This Book is brought to you for free and open access by the Open Educational Resources at Pacific at Scholarly Commons. It has been accepted for inclusion in Pacific Open Texts by an authorized administrator of Scholarly Commons. For more information, please contact mgibney@pacific.edu.

MATERIALS SCIENCE AND ENGINEERING

By

JOSHUA PAUL STEIMEL

The University of the Pacific

Material Science and Engineering

by

Joshua Paul Steimel

Preface:

This text serves to provide a brief overview of some of the myriad of topics available for study in the field of Materials Science. This is by no means a comprehensive compilation of Materials Science and Engineering topics but is instead meant as an introduction to the topic for entry-level undergraduates who want to pursue a career studying materials.

Acknowledgments

The information presented in this OER would not have been possible without the outpouring support from many family members, faculty, colleagues, and friends. In particular I would like to point out Professor Sam Allen, Krystyn Van Vliet, Michael Cima, Alfredo Alexander-Katz, Reid Van Lehn, and Yoda Patta.

Table of Contents

Part I	Bonding, Structure, and Defects	15
1	Bonding, Bragg, Beginning of Structure	17
1.1	Topics Covered in this Class	17
1.2	The Materials Tetrahedron	17
1.3	Atomic Structure and Bonding:	18
1.4	Types of Bonding: Covalent, Ionic, Metallic, and Van Der Waals	23
2	Structure: Structure: Crystalline, Amorphous, Non-Crystalline, and Liquid	
	Crystal Materials	31
2.1	Crystal Structures:	31
2.2	Lattice, Primitive Unit Cell, Basis Vectors, Lattice Constants	31
2.3	Crystal Systems: Simple Cubic, BCC, FCC, HCP	32
2.4	Simple Cubic	37
2.5	Body Center Cubic (BCC)	38
2.6	Face Centered Cubic (FCC)	40
2.7	Hexagonal Close Packed (HCP)	42
2.8	Close-Packed Structures	42
2.9	Structure of Non-Crystalline Materials:	45
3	Defects in Crystalline Materials	51
3.1	Crystalline Point Defects (0D)	51
3.2	Point Defects, Kröger-Vink Notation, and Schottky and Frenkel Defects .	55
3.3	Impurities in Kröger-Vink	56
3.4	Dislocation Defects (1D)	57
3.5	Grain Boundaries, External Surfaces, Phase Boundaries, Twin Boundaries, and Stacking Faults (2D)	60
3.6	Bulk or Volume Defects (3D)	61
Part II	Kinetics	62
4	Kinetics	63

4.1	Diffusion and Fick's First Law	63
4.2	Kirkendall Effect	64
4.3	C-Frame:	65
4.4	V-Frame	66
4.5	Conjugate Forces to Drive Diffusion	68
4.6	Fick's Second Law	71
4.7	Engineering Approximation Diffusion Depth	74
4.8	Arrhenius Temperature Dependence of Diffusion and Anisotropy	75
4.9	Diffusion as Random Walk	76
4.10	Diffusion in Relation to Kroger-Vink	78
4.11	Diffusion Depends on Local Environment	79
 Part III Phase Diagrams and Microstructural Evolution		81
5	Phase Diagrams	83
5.1	Lowest Energy Wins!	83
5.2	Phase Diagrams of Single-Component Materials	84
5.3	Gibbs Phase Rule	84
5.4	Multi-Component Phase Diagrams	86
5.5	The Lever Rule:	88
5.6	Phase Transitions Congruent vs Incongruent	89
5.7	Eutectic Phase Diagram	89
5.8	Eutectic, Eutectoid, Peritectic, Peritectoid, and Monotectic	90
5.9	Stable vs. Metastable Phase Boundaries: Cahn-Hilliard Spinodal Decom- position	94
5.10	First Order vs Second Order Phase Transitions	95
6	Nucleation, Growth, and Oswald Ripening	99
6.1	Surface Tension/Energy and Chemical Potential	99
6.2	Flux Across a Grain	100
6.3	Grain Growth:	103
6.4	Oswald Ripening and Coarsening	105
6.5	Homogeneous Nucleation	108
6.6	Heterogeneous Nucleation	111
6.7	Time-Temperature-Transformation Diagrams	115
 Part IV Mechanical Behavior of Materials		116
7	Mechanical Behavior of Materials	117

7.1	Sign Conventions:	117
7.2	Stress-Strain Curve:	117
7.3	1. Elastic Regime:	119
7.4	2. Plastic Regime	141
7.5	3. Fracture Regime	149
Part V Electrochemistry		155
8	Electrochemistry	157
8.1	Types of Corrosion:	157
8.2	Electrochemical Nature of Corrosion: Redox Reactions	158
8.3	Electrochemical Cell	158
8.4	Standard emf Series:	160
8.5	Half Cell and Full Cell Reactions:	160
8.6	What Material Corrodes in Galvanic Corrosion?	162
8.7	Nernst Equation:	163
8.8	Methods to Protect Against Galvanic Corrosion:	164
8.9	Redox Reactions with Kroger Vink Notation:	165
Part VI Polymeric Electrical, Optical, and Magnetic Materials		170
9	Polymers, Soft Matter, and Composites	171
9.1	Soft Matter	171
9.2	Polymer Chain Conformations:	172
9.3	The Chemist's Polymer Chain Model	177
9.4	Effect of Solvent on Polymer Chain MSD	180
9.5	Physicist's Ideal Chain	182
9.6	Real Polymer Chains : Swelling and Excluded Volume	184
9.7	Flory Full Free Energy:	190
9.8	Scaling Behavior in Solvents:	191
9.9	Non-Crystalline/Amorphous Polymers:	193
9.10	XRD Analysis:	198
9.11	DSC Analysis:	200
10	Electrical, Optical, and Magnetic Properties of Materials	203
10.1	Electrical, Optical, and Magnetic Materials	203
10.2	Electronic Band Structure and Block Waves	203
10.3	Optical Properties	204
10.4	Magnetic Properties	204

List of Figures

Chapter 1	17
1-1 Materials Tetrahedron.	17
1-2 Double Slit Experiment.	19
1-3 Interference Pattern.	19
1-4 Constructive Interference.	20
1-5 Destructive Interference.	20
1-6 Bragg Diffraction.	21
1-7 Electron Orbitals.	22
1-8 LJ Potential.	24
1-9 Bonding Schematic.	25
1-10 Covalent Hybridization.	26
1-11 Isomeric States.	27
1-12 Dichloroethene.	28
1-13 Stereoisomers.	28
1-14 RIS States.	29
 Chapter 2	 31
2-1 Parallelogram Lattice.	32
2-2 Rectangular Lattice.	32
2-3 Crystal Systems.	33
2-4 Crystal Systems.	33
2-5 Directions.	34
2-6 What Direction is this?	35
2-7 What Plane is this?	36
2-8 What Plane is this?	36
2-9 What Plane is this?.	37
2-10 Simple Cubic.	38
2-11 Simple Cubic Atomic Packing Factor.	39
2-12 Body Centered Cubic.	39
2-13 Body Centered Cubic Atomic Packing Factor.	40
2-14 Face Centered Cubic.	41
2-15 Face Centered Cubic Atomic Packing Factor.	41

2-16	Hexagonal Close Packed.	42
2-17	ABC or ABAB Stacking.	43
2-18	Planar Density.	44
2-19	Planar Density.	44
2-20	Planar Density.	45
2-21	Radial Distribution Function.	46
2-22	Generic RDF.	47
2-23	Metal RDF.	47
2-24	Liquid Crystal.	48
Chapter 3		51
3-1	Point Defects.	52
3-2	Arrhenius Relationships.	53
3-3	Arrhenius Plots.	54
3-4	Edge Dislocation.	57
3-5	Edge Dislocation.	58
3-6	Screw Dislocation.	58
3-7	Burgers Circuit.	59
3-8	Right Hand Screw.	59
3-9	Left Hand Screw.	60
3-10	Grain Boundaries.	61
Chapter 4		63
4-1	Diffusion Schematic.	63
4-2	SS Diffusion.	64
4-3	Diffusion Mechanisms.	65
4-4	Diffusion Couple.	67
4-5	Kirkendall Effect.	68
4-6	Destruction and Creation of Half Planes.	68
4-7	Destruction and Creation of Half Planes.	69
4-8	Electric Field Driven Diffusion.	69
4-9	Temperature Driven Diffusion.	70
4-10	Curvature Driven Diffusion.	70
4-11	Stress Driven Diffusion.	71
4-12	Diffusion Couple.	72
4-13	Semi-Infinite Diffusion.	74
4-14	Diffusion of Impurities in Silicon.	75
4-15	Vacancy Diffusion.	77
4-16	Interstitial Diffusion.	78

4-17	Concentration and Diffusion of Vacancies.	80
4-18	Diffusion in Different Environments.	80
Chapter 5		83
5-1	Free Energy Curves Melting.	83
5-2	Free Energy Curves Melting and Vaporization.	84
5-3	Single Component Phase Diagram.	85
5-4	Binary Lens Phase Diagram.	87
5-5	Free Energy Curves Binary Phase Diagram.	88
5-6	Lever Rule.	88
5-7	Congruent Melting.	90
5-8	Eutectic Phase Diagram.	91
5-9	Microstructure Evolution.	91
5-10	Invariant Points.	92
5-11	Invariant Points.	93
5-12	Stability.	95
5-13	Nucleation and Growth vs. Spinodal Decomposition.	95
5-14	First and Second Order Phase Transitions.	96
6-1	Curvature.	101
6-2	Grain Boundary Motion.	102
6-3	Energy Landscape.	103
6-4	Grain Growth Schematic.	104
6-5	Oswald Ripening.	107
6-6	Measuring process.	109
6-7	Free Energy Change Upon Undercooling.	109
6-8	Interfacial vs. Volumetric Energy Contribution.	110
6-9	Nucleation Rate.	112
6-10	Nucleation Rate.	112
6-11	Nucleation on a Surface.	113
6-12	Heterogeneous Nucleation Lowers Energy Barrier.	114
6-13	Critical Undercooling Heterogeneous Nucleation.	114
6-14	TTT Diagrams.	115
Chapter 7		117
7-1	Stress Strain Curves.	117
7-2	Normal and Shear Stress.	119
7-3	3D Stress State.	120
7-4	Infinitesimal Strain Theory.	123

7-5	Biaxial Stress State.	124
7-6	Jewelry Die.	130
7-7	Pressure Vessels.	131
7-8	Resolving Stresses.	132
7-9	Maxwell and Kelvin-Voigt Models.	135
7-10	Storage and Loss Modulus.	139
7-11	Composites.	140
7-12	Composite Modulus vs. Fraction of Fibers.	141
7-13	Yield Criterion.	142
7-14	Work Hardening.	144
7-15	Solute Strengthening.	145
7-16	Grain Size Strengthening.	145
7-17	Bowing vs. Cutting.	146
7-18	Shear Banding vs. Crazing.	147
7-19	Deformation Mechanism Maps.	149
7-20	Stress Concentrator.	150
7-21	Cracking Modes.	152
7-22	Fatigue Regimes.	153
7-23	S-N Curve.	154
Chapter 8		157
8-1	Electrochemical Cell.	159
8-2	Cu-Fe.	159
8-3	Cu-Fe.	160
8-4	SEP Table.	161
8-5	Fe-Zn.	162
8-6	Fe-Zn.	163
8-7	Sacrificial Anode.	165
8-8	Imposed Current.	166
8-9	Brouwer Diagram.	169
Chapter 9		171
9-1	End-to-End Distance.	173
9-2	Rigid vs. Coiled Polymer.	174
9-3	Ideal Chain Model.	174
9-4	Mathematician's Ideal Chain.	175
9-5	Chemist's Chain Model.	178
9-6	RIS States.	179
9-7	Solvent Quality.	181

9-8	Physicist's Ideal Chain Model.	182
9-9	Radius of Gyration.	183
9-10	LJ Potential.	187
9-11	Excluded Volume.	188
9-12	Enthalpic Schematic.	190
9-13	XRD Curves.	198
9-14	Methacrylates.	199
9-15	PMMA Schematic.	199
9-16	Amorphous Vs. Crystalline.	200
9-17	Thermoplastic Vs. Thermoset.	201
Chapter 10		203
10-1	Electronic Band Structure.	203
10-2	Diamagnetic.	205
10-3	Paramagnetic.	206
10-4	Ferromagnetic.	206
10-5	Superparamagnetic.	207

List of Tables

Part I

Bonding, Structure, and Defects

THIS PAGE INTENTIONALLY LEFT BLANK

CHAPTER 1

BONDING, BRAGG, BEGINNING OF STRUCTURE

1.1 Topics Covered in this Class

1. **Part I:** Bonding, Structure, Defects, Diffusion, Phase Diagrams
2. **Part II:** Nucleation and Growth, Mechanics
3. **Part III:** Electrochemistry, Electrical, Optical, and Magnetic Properties

1.2 The Materials Tetrahedron

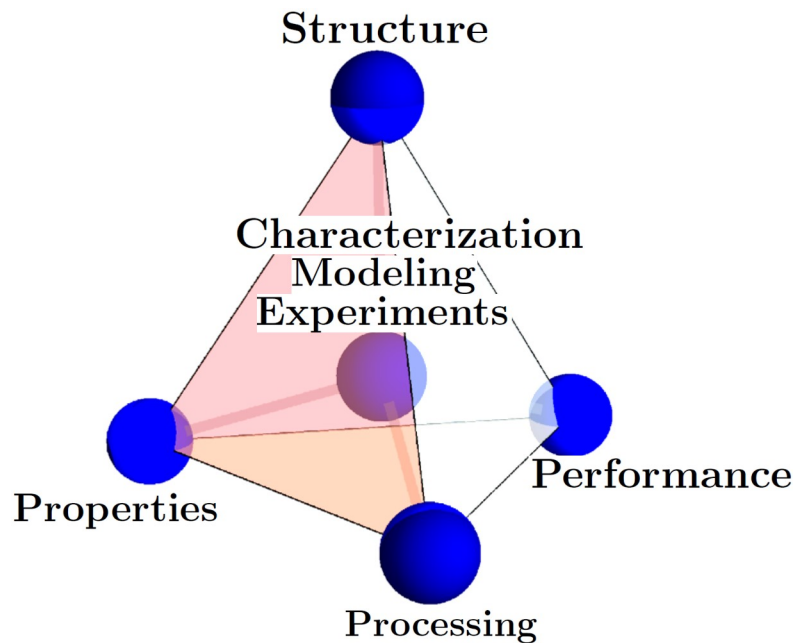


Figure 1-1: Materials Tetrahedron

The four corners of the Materials Science and Engineering Tetrahedron are: **Structure, Processing, Properties, Performance**. At the center is a combination of **Characterization/Modeling/Experiments**.

A couple of quick examples if you **process** sheet metal by cold rolling you change the **structure** and induce more dislocations in the material. This in turn will change the yield strength (**property**) and thus the **performance** of that sheet metal in the application of interest. As materials scientists at the core of what we do is try to characterize material with **experimentation and simulation** to better understand this materials tetrahedron and to eventually reach a point where we can begin to predict some material responses.

Any other examples where we can apply this materials tetrahedron?

- Lead Titanate
- Cold Rolling Titanium Sheet
- Cross-Linked Rubber or Kevlar

Different Types or Classifications of Materials:

- Metals
- Polymers
- Ceramics
- Composites
- Active Matter
- Piezoelectric
- Shape Memory Alloys
- Ferromagnetic Materials

Material Properties:

- Mechanical
- Thermal
- Magnetic
- Optical
- Electrical
- Structure

1.3 Atomic Structure and Bonding:

Before diving into materials structure, we need to start at the basics and build up from the sub-atomic to atomic, nano, micro, and then macrostructure. So hopefully we all remember from our chemistry classes...

An atom is composed of a **nucleus** of **protons** and **neutrons**. A cloud of **electrons** surrounds the nucleus. The **atomic number** of an element is denoted by the **number of protons in the nucleus**. **Atomic mass** is the sum of the masses of proton and neutrons. **Atomic weight** of an element is the weighted average of the atomic masses. The atomic mass unit (amu) is defined as $\frac{1}{12}$ the atomic mass of Carbon 12 [1].

When we discuss the different types of bonding we are typically interested in the **electronic structure** of an element or a material. In particular, we are interested in the **valence electrons or the outermost electrons**. Now electrons have **particle-wave duality**, i.e. electrons are governed by quantum mechanics. The classical example being the **double slit experiment**. It was conducted by Thomas Young in 1801 where he showed that light and later Davisson and Germer demonstrated that electrons display an interference pattern when shot at a double slit [1]. This is because electrons can behave like particles and waves and when a wave passes through a double slit there will be **constructive** and **destructive** interference of the waves.

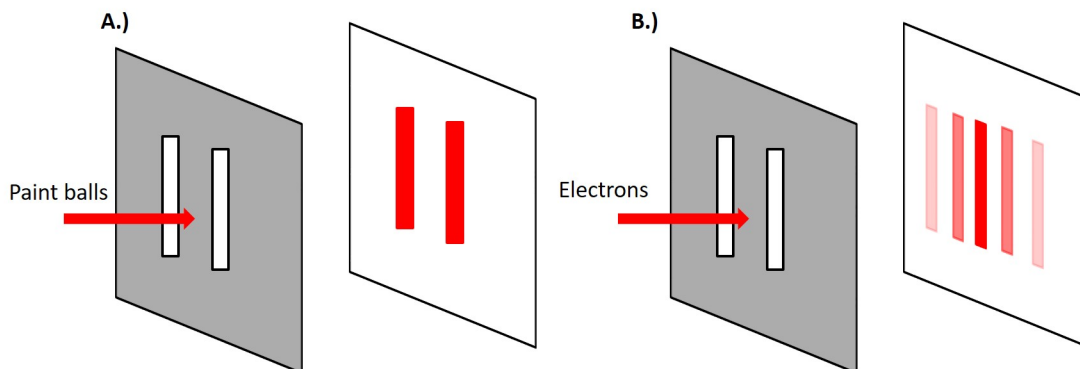


Figure 1-2: Double Slit Experiment. A) Particle pattern and B) Electron pattern.

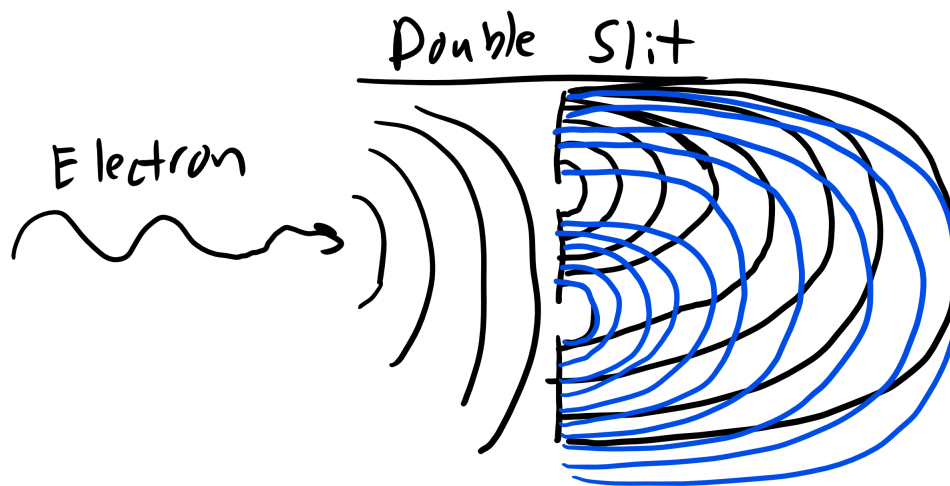


Figure 1-3: Double Slit Experiment: Electron pattern.

This phenomenon is particularly relevant to X-Ray Diffraction (XRD). This is a technique we will use in our first lab to investigate the atomic structures of several different materials. In general, **diffraction** will occur when a wave encounters a **series of regularly spaced obstacles** or slits that are capable of scattering the wave **and** have **spacings** that are **comparable** to the

magnitude of the wavelength of the incident wave [2].

Let's look at an example of **constructive** vs. **destructive** interference as seen below. Consider the first set of waves that are incident to the scattering event. After they pass through the scattering event you see that the waves are still in phase so the resultant waves constructively interfere with each other and produce the resultant diffracted wave that is now twice the amplitude [1]. We previously assumed that the two incident waves were both of the same magnitude and wavelength. Conversely for **destructive** interference after the waves encounter the scattering event they are out of phase which results in the waves canceling each other out or in other words **destruction** [1].

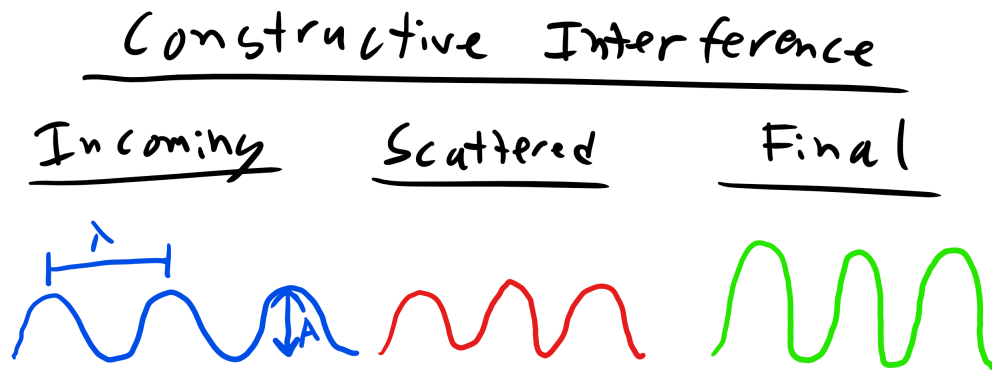


Figure 1-4: Constructive vs. Destructive Interference

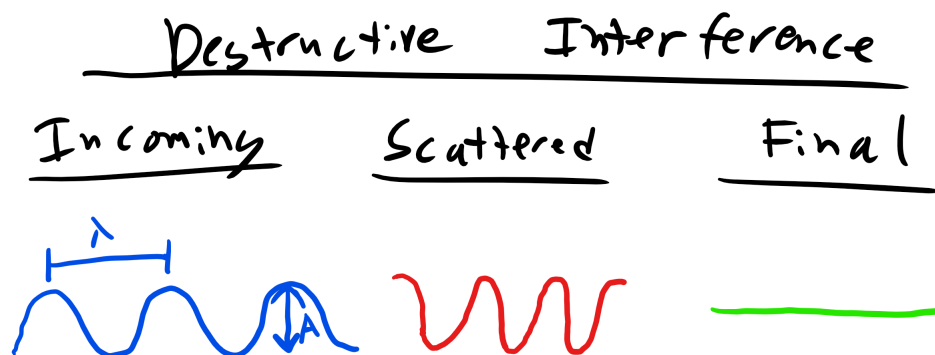


Figure 1-5: Constructive vs. Destructive Interference

1.3.1 Bragg Diffraction

Sir William Lawrence Bragg was a very brilliant scientist and he won the Nobel Prize for Bragg Diffraction when he was 25 and he won it with his father [1]. Bragg realized that if we want to deduce material structure we can actually investigate this with X-rays. Cu-K $_{\alpha}$ radiation has a wavelength of 1.542Å. This is on the order of the spacing of atomic structures which meets one of our criterion for diffraction and crystal structures are made of regularly spaced obstacles for which a beam of X-rays can scatter. Bragg saw that in doing so it would be possible deduce the inter-atomic or inter-planar spacing between atoms for a given incident wavelength [1]. Look at 2D schematic below

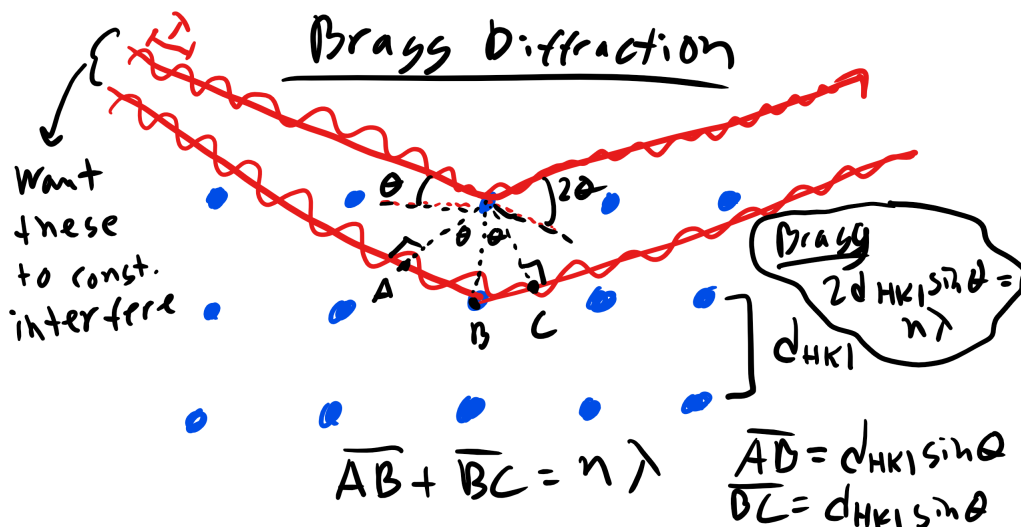


Figure 1-6: Bragg Diffraction

We again have two incident beams that will interact with two planes of atoms each at an angle of incidence θ_B which is the Bragg angle or the condition for diffraction [2]. So what is the condition for diffraction in the example? Well **we have to have constructive interference** so the extra path length traveled by the lower incident wave must be equal to an integer number of wavelengths as the upper incident wave and that equivalence gives us **Bragg's Law**

$$n\lambda = 2d_{hkl} \sin \theta_B \quad (1.1)$$

where n is an integer number which denotes the order of reflection, λ is the wavelength, θ_B is the Bragg angle, and d_{hkl} is the interplanar spacing. [2]

The interplanar spacing for cubic materials is defined as

$$d_{hkl} = \frac{a}{\sqrt{h^2 + k^2 + l^2}} \quad (1.2)$$

where a is the lattice parameter of the unit cell, and h, k , and l are the miller indices [2]. More

on these much later in the Structure Lecture.

Let's do a quick example

Ex. 1: I want to measure the 110 plane (miller indices hkl) of iron. I am using the typical Cu- K_α radiation. The readout from my diffractometer shows a very strong peak at 44.7° . Calculate the lattice parameter.

But now back to electrons... Electrons are described by quantum numbers, specifically **4 quantum numbers**. The **principal quantum number, n**, specifies the **electron shell** which takes on integer values, sometimes designed by K, L, M, N, O which corresponds to $n = 1, 2, 3, 4, 5 \dots$ [1]. Remember back to chemistry that these shells correspond to the Bohr atomic model where electrons revolve around discrete orbitals and that the electrons are quantized in discrete energy states[1]. In reality it is not a discrete orbital but instead electrons reside within some cloud according to a probability distribution. The second quantum number sometimes referred to as the **azimuthal quantum number, l**, designates the **subshell** [1]. **l is an integer value** as well and defined as $l = 0$ to $l = (n - 1)$. The letter designation is **s, p, d, and f** respectively. The orbital shapes depends on l [1].

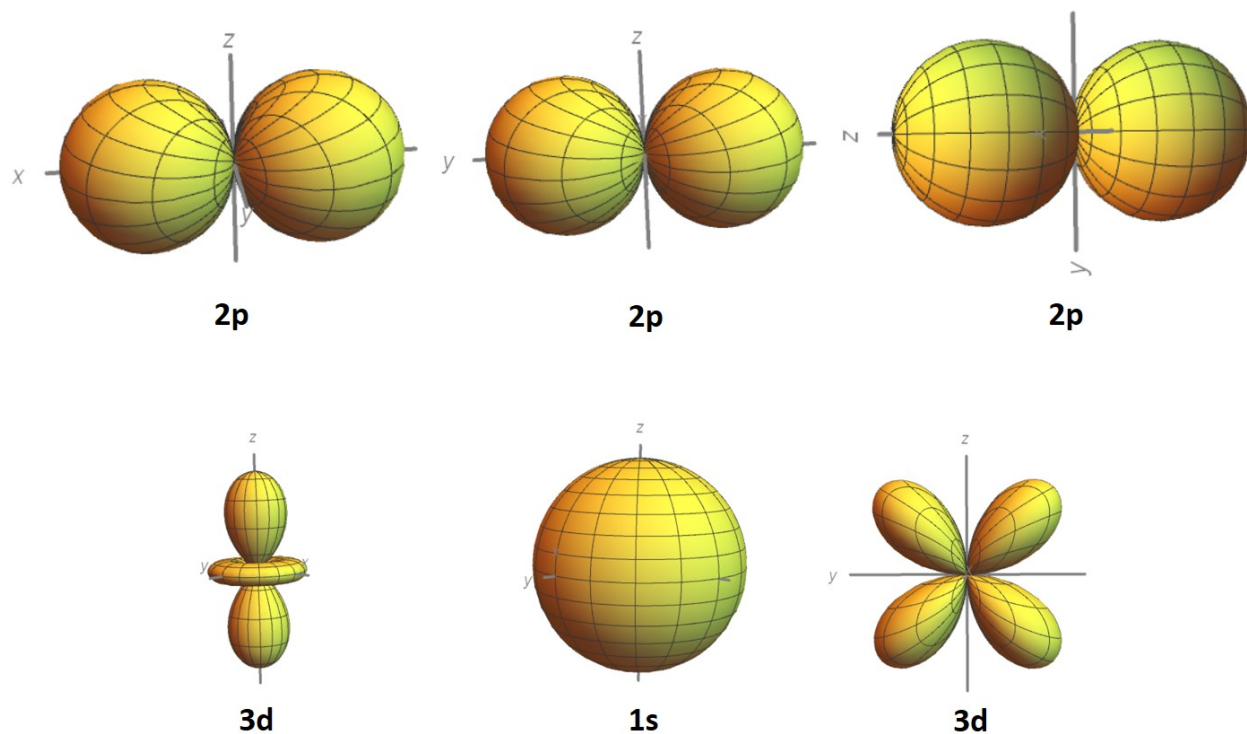


Figure 1-7: Electron orbitals.

The **number of electron orbitals for each subshell** is determined by the **third quantum number** sometimes called the **magnetic quantum number, m_l** . m_l can take on **integer values between -l and +l** [1]. Additionally with each electron there is a **spin moment** which must be **oriented either up or down** and this is captured by the **fourth and final quantum number**

m_s .

We fill electron orbitals or states using the **Pauli exclusion principle**, each electron state can hold **no more than two electrons and just have opposite spins** [1]. When electrons are occupying states such that the **energy is minimized they are in the ground states** but there are times when the electrons can become excited and **transition to higher states** but we will talk about that more in the Electrical, Optical, and Magnetic Properties section.

Ex. 2 Draw the electronic configuration for Chlorine? Identify each Quantum number. What quantum number determines shape?

$$1s^2 2s^2 2p^6 3s^2 3p^5 \quad (1.3)$$

1.4 Types of Bonding: Covalent, Ionic, Metallic, and Van Der Waals

Elements that have **no valence electrons** or that have a completely filled outer shell are called the **inert or noble gases**. All other elements which do not have a completely filled outer shell have **valence electrons** and these electrons are the ones of **import when it comes to bonding** [1].

Bonding is critically important as **most of the structural, physical, and chemical properties are influenced or determined by the interatomic bonding**. And typically we are concerned with four types of bonds[2]

1. **Covalent (5eV or about 200 kT)**
2. **Ionic (1-3eV or 80kT)**
3. **Metallic (0.5eV or 20kT)**
4. **Van Der Waals (0.001-0.1eV or 0.2kT)**

First question why do we even need bonding? Or a better question why does bonding occur?

Well it all goes back to Gibbs, the energy of the set of bonded atoms is lower than the isolated atoms. There are forces of attraction and repulsion between electrons and protons. And we remember that the force (F) is related to the potential energy (U) by $F = -\nabla U$. Remember that ∇ is the gradient mathematical operator and will take the partial derivative of the function with respect to the dimensionality of the problem. Now there are many different equations or potentials that describe the interactions between atoms i.e. Morse, Born-Mayer, Van Der Waals, etc. Let's take a look at one of these potentials, the **Lennard-Jones (LJ) Potential** which approximates the **interaction between a pair of neutral atoms** (it is popular due to the computational simplicity) [2]

$$V_{LJ} = 4\epsilon \left[\left(\frac{\sigma}{r} \right)^{12} - \left(\frac{\sigma}{r} \right)^6 \right] = \epsilon \left[\left(\frac{r_o}{r} \right)^{12} - 2 \left(\frac{r_m}{r} \right)^6 \right] \quad (1.4)$$

where ϵ is the depth of the potential well, σ is the distance at which the inter-particle potential is zero, r is the distance between particles, and r_m is the distance where the potential is minimized [2].

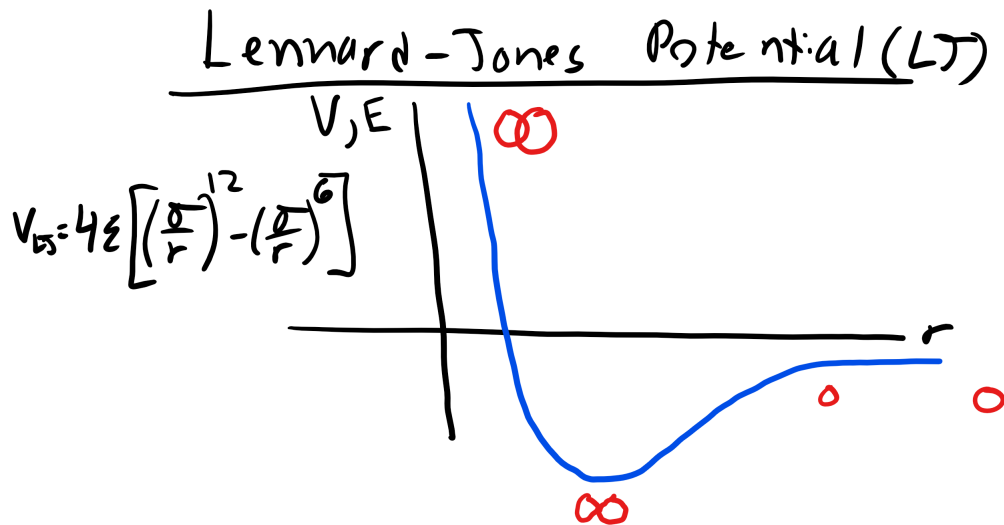


Figure 1-8: Lennard-Jones Potential

1.4.1 Distinguishing Between Types of Bonding By Electronegativity

However, again the **key to determining which type of bonding occurs is the valence electrons. Specifically if they are gained, lost or shared.**

For **Van der Waals** interactions there is **no charge transfer**. Instead we have **induced electric dipoles or permanent dipoles from weak attractive bonds**. With **covalent** bonds there are **valence electrons that are shared between adjacent atoms**, which results in a **pairing of electrons into localized orbitals and concentrating the negative charge between the positive nuclei** [2].

Now when atoms have a different affinity for electrons, different **electronegativities**, a **net transfer of charge** can occur forming **positively** and **negatively charged ions** [2]. These ions can form **networks of ionic bonds** held together by **long-range coulombic interactions**.

When the electronegativity is similar or the same between atoms the valence electrons are shared equally and the bond is purely covalent.

When the electronegativity is very different the more electronegative atom withdraws nearly all the valence electrons and the bond is purely ionic. cite Thus electronegativity is how we distinguish between Covalent and Ionic interactions!

Now you might ask what happens in the intermediate case of electronegativity differences. Well then you will have bonds that have **both covalent and ionic characteristics**. We call these bonds **polar covalent** and one atom will have a partial positive and negative charge, as in HCl [2]. While there is no universally agreed upon cutoff values **in this class we will define an electronegativity difference of 0-0.4 to be non-polar covalent, 0.5-1.7 to be polar covalent, and greater than 1.7 to be ionic.** [2]

In the case of **metallic bonds**, all atoms share their valence electrons and the nuclei form a **positively charged array in a sea of delocalized electrons** [2]. Van der Waals form **between covalently bonded molecules which have net or induced dipoles**. These are **very short-range force bonds** and therefore **localized** between neighboring molecules [2]. While these bonds are typically very weak and short range these interactions are critical to a number of unique phenomenon, in particular Gecko pads, graphite sheets, water, polymers, and proteins.

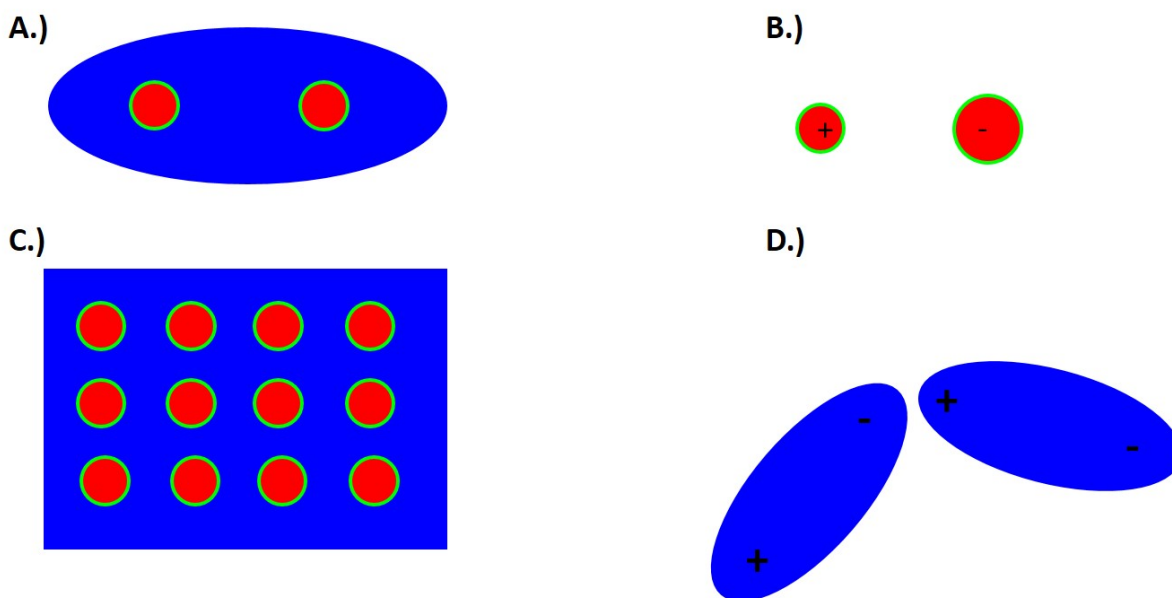


Figure 1-9: Bonding Schematic: A.) Covalent B.) Ionic C.) Metallic D.) Van der Waals. Blue is the share electrons, green is the core electrons, and red is the nucleus.
[2]

There are also secondary bonding which includes Van der Waals, hydrogen bonding, and dipoles. We will come back to these a bit later on.

1.4.2 Covalent Bonding: Hybridization

We should note here that **covalent bonding is directional** whereas **ionic bonding is nondirectional**. Additionally, covalent bonding typically involves **hybridization**, or the mixing or combining of two or more atomic orbitals during bonding which causes more orbital overlap. One of the most ubiquitous examples being **sp^3 hybridization** for Carbon.[1]

Here one electron is promoted from 2s to 2p and then the remaining 2s orbital is mixed with the other 2p orbitals. Thus we will have 4 sp^3 orbitals for carbon.[1]

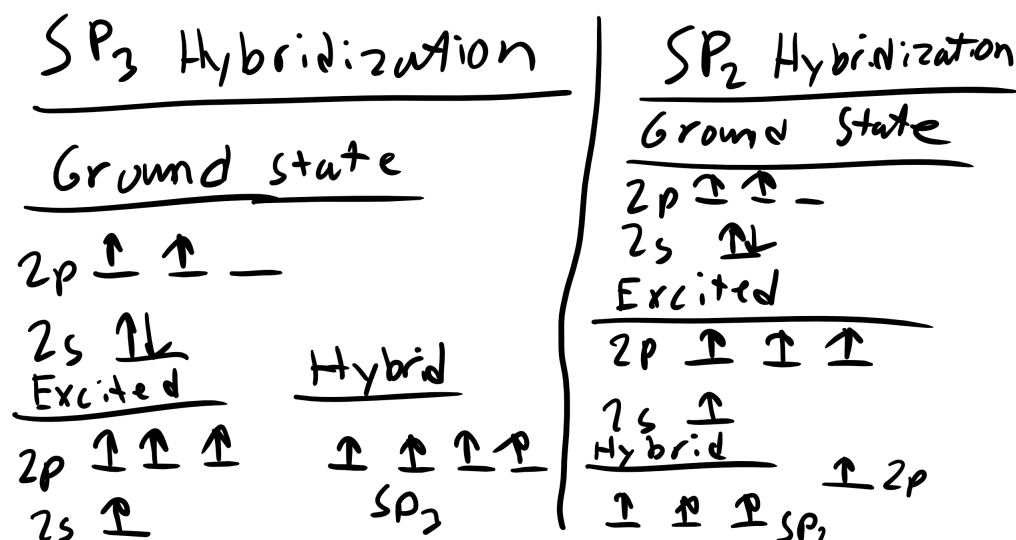


Figure 1-10: Covalent Hybridization.

There are also **sp² hybridization** as well where a 2s electron is promoted to the 2p orbital and mixes with two of the p orbitals. The remaining p orbital remains unhybridized, denoted as p_z. The sp² orbitals form a trigonal planar structure as opposed to the tetrahedral sp³ structure.[1]

1.4.3 Structural Descriptors of Bonding

We also have structural descriptors of bonded materials particularly **bond length, bond angles, and the size of atoms or ions** [2]. The **bond length** is simply the distance between two bonds. The distance between a Carbon-Carbon bonds is 1.54Å for reference. Bond length can change depending on whether the bond is covalent or ionic [2]. **Bond angles** are defined by the relative location of three atoms. In CO₂, this molecule is **planar** so the angle is 180° [2]. For **triagonal planar** molecules like BF₃ the bond angle is 120°. What is the bond angle for our Materials Tetrahedra? It is 109.28° [2].

The **size of an atom** is determined by the distance the electron distribution extends from the nucleus. However, this definition is problematic as the type of bonding and bonding in general will change the shape of the electron distribution. **So the better value to look for is the covalent, ionic, metallic, and van der Waals radii of the atom.** For metals we simply use metallic radii [2]. **Covalent radii is one half the covalent bond length. Ionic radii can vary an depends on how many electrons are transferred and the electronegativity difference.** The **van der Waals radii is the distance of closest approach or approximately the nearest neighbor distance** [2]. We will be talking a lot more about the nearest neighbor distances in the next lecture.

The 3D shapes of molecules can be predicted using **electron-domain theory** which focuses on the 3D distribution of the outermost electrons about a given atom and how these electrons will pair with other electrons from bonding atoms [2]. This theory distinguishes between bonding and non-bonding domains. The bonding domain is the shared electrons and the non-bonding domain belongs to a particular atom. Nonbonding domains occupies a larger space than the bonding domains [2]. This leads to preferred angles for example for two domains they will be 180° apart, for 3 it will be 120° , and for 4 it will be 109.28° .

1.4.4 Isomeric States:

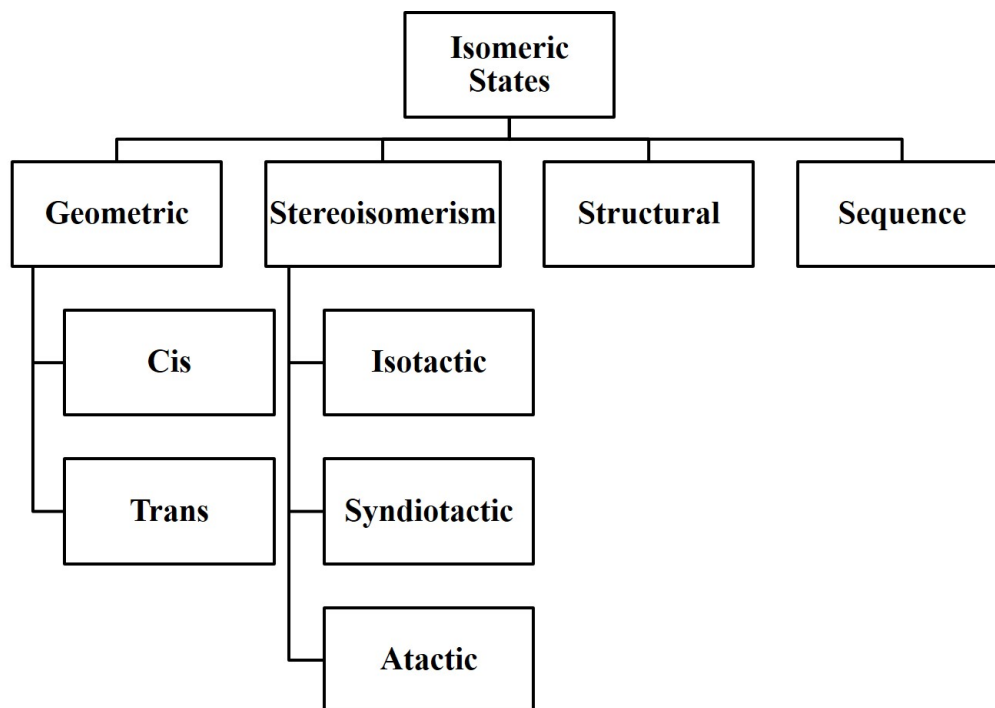


Figure 1-11: Structural, Geometric, Sequence, and Stereoisomerism

Molecules are typically held together by strong covalent bonds with many conformations available via *rotational isomeric states*. In other words, conformations are accessible due to the rotation of atoms around these intramolecular bonds. **Isomers/Isomeric States** are molecules which are **compositionally identical but structurally distinct**. **Conformers/Conformational Isomers** are related by **rotations around single bonds**. Note that **at room temperature thermal rotation around a double or triple bond is essentially zero**. There are **structural isomers, stereoisomers, geometric/configurational, and sequence isomers**. **Structural isomers** occur when certain bonds prohibit rotoconversion of two conformationally distinct states. Let's take a look at an example.

Dichlorethene is a structural isomer or a geometric isomer. We can see the **cis** and **trans** conformations in the figure. Here the **double bond** prevents rotational so they are **struc-**

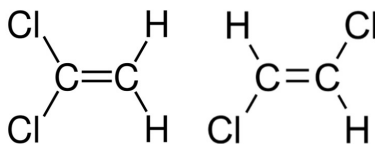


Figure 1-12: Dichloroethene

turally distinct. It is a **structural isomer not a conformer**.

Stereoisomers have an **ordered sequence** of linked units but the **substituents pendant to the main backbone of covalent bonds have different arrangements or tacticity**. Specifically they can be **atactic, isotactic, or syndiotactic**.

Stereoisomers are found in many different types of **polymers** and we can see an example of atactic, isotactic, and syndiotactic below:

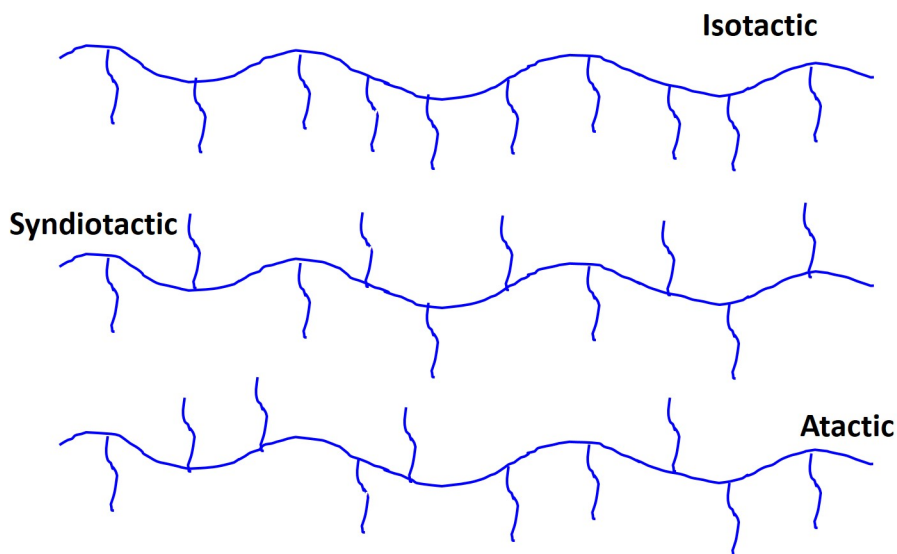


Figure 1-13: Stereoisomers: Isotactic, Syndiotactic, and Atactic

Isotactic stereoisomers will have all the side-chains on the **same side**. **Syndiotactic** will have some type of **repeated order** either top and bottom, or top-top, bottom-bottom, etc. **Atactic** is **completely random**.

A **geometric/configurational/cis-trans isomer** has the same chemical formula but typically the arrangements of the side groups are on different sides of an unsaturated carbon backbone bond. Specifically there will be **cis** and **trans** configurations.

Sequence isomers have many linked units like in a polymer but can have a variable sequence. For example think about block co-polymers which can be designed to be ABABABAB or AAAABBBB.

One example of a **conformer** is dichloroethane. This molecule has a single C-C bond so there are several different rotational states that can be accessed. We can actually plot the conformational

energies of these different states as a function of the C-C bond torsion angle.

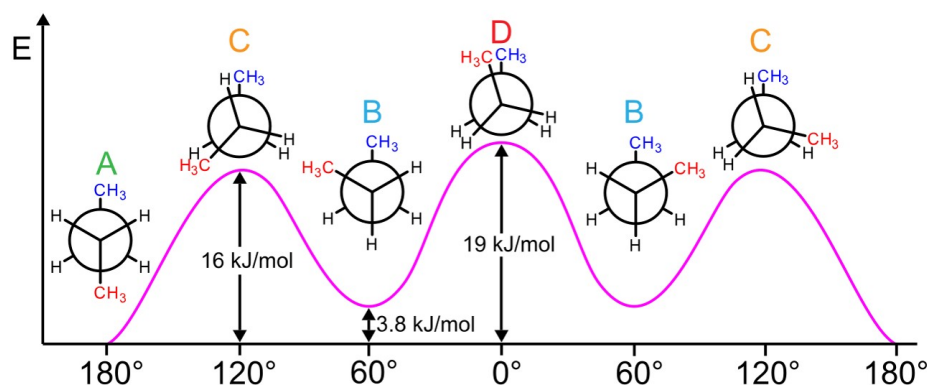


Figure 1-14: Rotational Isomeric States
[3]

In the figure we can identify some critical states. The lowest energy states, *A*, is the trans conformation as the methyl groups are the furthest distance apart from each other. The highest energy state, *D*, is the cis conformation and the energy is the largest because the methyl groups are the shortest distance from one another. The other two lower energy states, *B*, are termed **gauche** \pm conformations where there is larger amount of distance between the methyl group than in the cis conformation or the final conformation which is called the **eclipsed conformation**. The eclipsed conformation, *C*, where the methyl group is eclipsed by one of the side hydrogens. **Molecules like butane can change conformations up to $10^{10} \times$ depending on the temperature.**

1.4.5 Coordination Number (CN)

The **coordination number (CN)** is the number of nearest neighbors (NN). There are a number of coordination shells like the nearest neighbors and the **next nearest neighbors (NNN)**. For liquids and amorphous materials it will typically be an average number of nearest neighbors in a predefined shell of a particular distance or length or Voronoi Tessalation. We will also define and discuss the packing fraction V_v which is the ratio of the total occupied volume to the total volume. For gases this should be very low, almost zero. Fluids or glasses should be about 0.5 and we will see this is much higher for metals and ceramics.

THIS PAGE INTENTIONALLY LEFT BLANK

CHAPTER 2

STRUCTURE: STRUCTURE: CRYSTALLINE, AMORPHOUS, NON-CRYSTALLINE, AND LIQUID CRYSTAL MATERIALS

2.1 Crystal Structures:

We will eventually talk about **crystalline materials**, **amorphous materials**, **liquid crystals**, **short range order**, **long range order**, etc. But to start we are going to deal with the most ideal case of perfect crystalline materials.

Do we ever have a perfect crystal? **No!** Why? Well maybe at 0K but even then still probably not. **There are always defects in materials** but let's start with the simple case where we assume everything is perfect.

A crystal structure is a periodic array of atoms that repeats over large distances. [2] **There is long-range periodic order both long range translational and orientational order in addition to short range order.** So before we start to run off and analyze crystal structures we have to first start off with a **primitive lattice**, **lattice constants**, **interaxial angles**, **symmetries**, **point groups**, **Bravais lattices....**[2]

2.2 Lattice, Primitive Unit Cell, Basis Vectors, Lattice Constants

A **lattice** is a periodic array of points (atoms) in 1,2 or 3D. Those points are lattice points. Let's start with the 2D case[2]. A 2D lattice can be described by a primitive or unit cell which in turn is described by **two lattice constants** (a,b), two **basis vectors** (a_1 and a_2), and **an interaxial angle** γ [2]. Once we have defined this we can pick any point in our 2D lattice as an origin and we can describe any point in our lattice with the previous values. That is the beauty of crystallography!

Now when we pick our basis vectors we pick the shortest lattice translation as a_1 and the second to shortest translation is a_2 [2]. The lattice constants are the just given by $a = |a_1|$ and $b = |a_2|$. The interaxial angle γ is then simply defined. This also defines our primitive cell which will only contain a single lattice point[2]. **Let's do a couple of examples looking at the parallelogram cell below:**

How about a Rectangular lattice?

Associated with crystallography is a myraid of **symmetry operations** and we have actually just dealt with **translational symmetry just now**[2]. There are also reflection or **mirror symmetry**, **glide symmetry**, **rotational symmetry**, etc[2]. These topics are all important but we are not a crystallography class so we will not be covering this in detail but you should know these concepts exist. **There are also 230 space groups, 32 crystallographic point groups, 14 Bravais lattices** (we will discuss these), and **6 crystal systems** (will discuss these as well). [2]

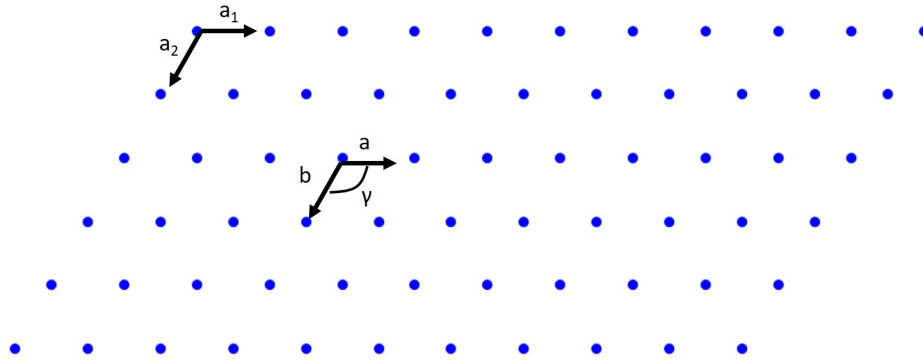


Figure 2-1: Lattice with Parallelogram Cell

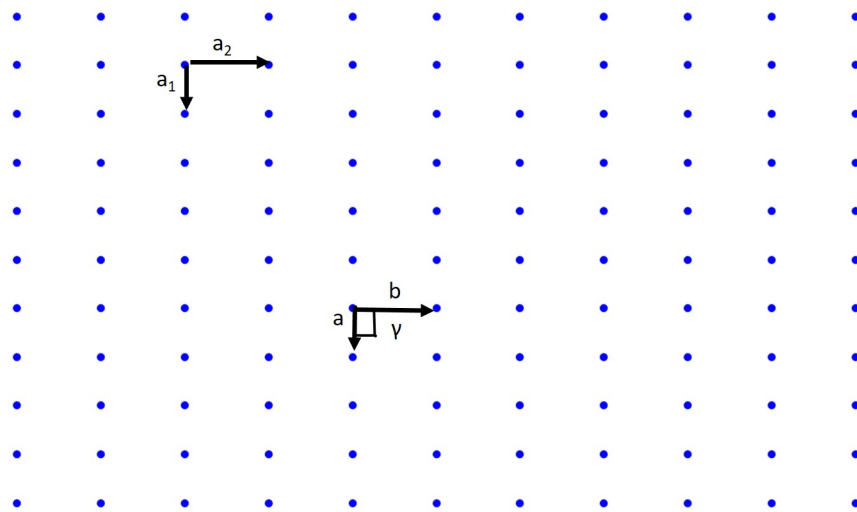


Figure 2-2: Lattice with Rectangular Cell

2.3 Crystal Systems: Simple Cubic, BCC, FCC, HCP

We are going to focus on the 6 crystal systems: **triclinic**, **monoclinic**, **orthorhombic**, **tetragonal**, **hexagonal**, and **cubic** and how to describe the unit cell, the primitive lattice vectors, and interaxial angles[2]. Before we start we can take a look at them and visualize many of them in Mathematica as well.

How about a Rectangular lattice?

You can see all the rules and relationships between the lattice constants and the interaxial angles on the lecture slides.

2.3.1 Crystallographic Directions:

When discussing crystals we will also have to specify crystallographic directions and planes[2]. In order to refer to specific crystallographic planes or direction we need a labeling system to index

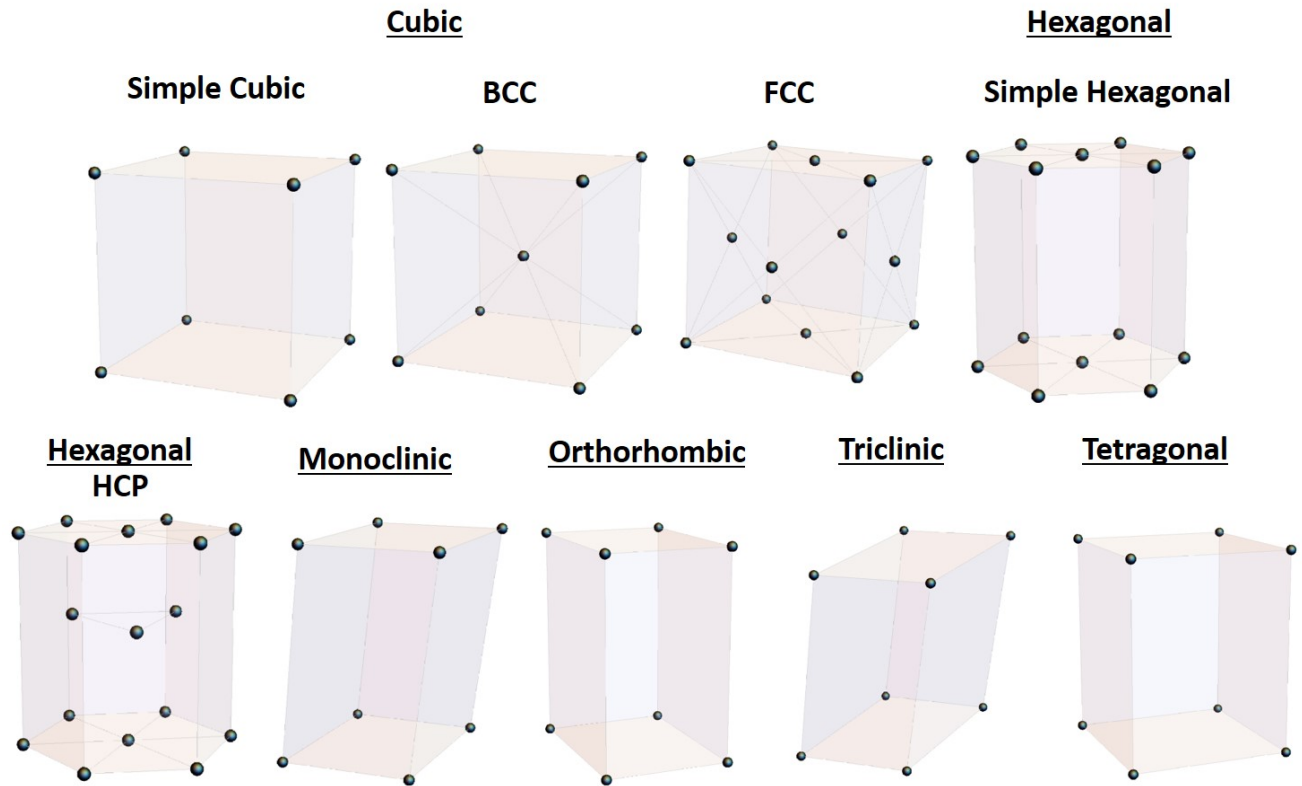


Figure 2-3: 6 Crystal Lattice Systems

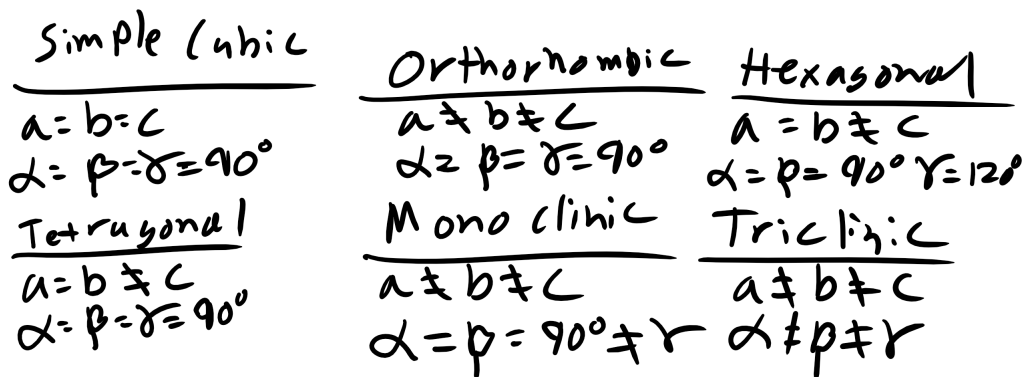


Figure 2-4: 6 Crystal Systems.

these directions or planes. Luckily such an index has already been developed, **Miller indices**[2]. A crystallographic direction is a vector denoted by $[uvw]$. u , v , and w are integers which correspond to the reduced projections along the x , y , and z axes, respectively[2]. Note we will always use $[\]$ for

vectors. Let's do a couple of examples.

Let start simple and draw the $[100]$ direction.

To draw the direction of a vector it is pretty straight forward. Pick an origin for the vector tail (side without arrow) then pick the ending point for the vector (arrow) and subtract the arrow point from the tail point and the resultant vector must coincide with the direction that you are trying to draw. Typically try to pick the origin as your origin.

How about the $[111]$ direction?

What about $[100]$?

Little more complicated what about $[1\bar{1}0]$?

What about drawing $[222]$?

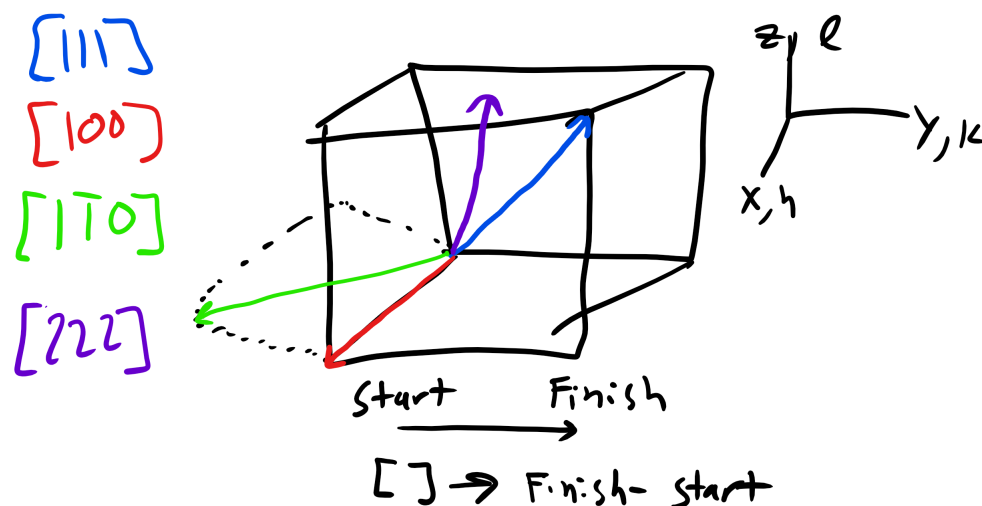


Figure 2-5: $[111]$, $[100]$, $[1\bar{1}0]$, and $[222]$ directions.

Now a little more complicated what is the vector I am drawing below?

Now for a number of crystal structures there are **several nonparallel directions** with different indices that are **crystallographically equivalent**[2]. **This means that the spacing and number of atoms along each direction is the same!** In cubic crystals $[100]$, $[\bar{1}00]$, $[010]$, $[0\bar{1}0]$, $[001]$, and $[00\bar{1}]$ are all crystallographically equivalent so we group them in a family which is denoted by angled brackets $\langle 100 \rangle$ [2].

Now you can see that we will run into a problem when we work with HCP materials. We have to use a 4 axis or Miller-Bravais coordinate system[2]. Our typical a_1 , a_2 , and a_3 are all contained in a single basal plane and are 120° apart from one another and the z-axis is perpendicular to the basal plane so we convert from

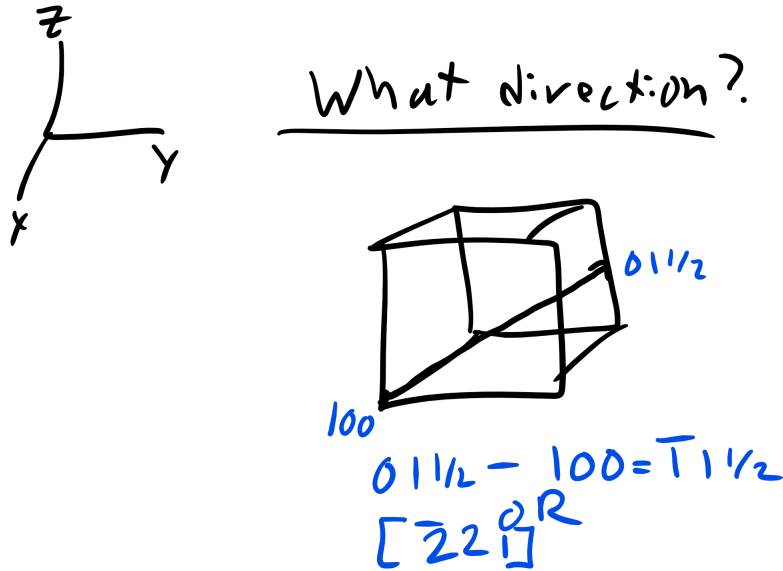


Figure 2-6: What Direction is this?

$$[u'v'w'] \rightarrow [uvw] \quad (2.1)$$

$$u = \frac{2u' - v'}{3} \quad (2.2)$$

$$v = \frac{2v'}{3} \quad (2.3)$$

$$t = -(u + v) \quad (2.4)$$

$$w = w' \quad (2.5)$$

We will not be talking about this much but this is crucial knowledge if you want to work with Titanium or Zirconium, or any HCP material[2].

2.3.2 Crystallographic Planes:

Now for crystallographic planes we utilize the Miller indices (hkl) which corresponds to the x, y , and z axes respectively[2]. Notice again that we use $()$ for planes and $[\]$ for directions[2]. $\langle \rangle$ is for family of directions. We will denote families of planes in $[2]$.

Now the question becomes how do we draw planes. Well we first must determine if the intercepts. The intercepts will be the inverse of the Miller indices. Let's take a look at a relatively straightforward example of the (111) .

Now what happens in the case of (110) for example. Well if you run into this problem an inverse that gives you an infinite number means that the plane will not intersect that coordinate axes and will instead be parallel to that axis. So the plane should look like this:

How about another tricky problem like below when we have the plane passing through our

(111) Plane
 Intercepts $\rightarrow x = 1 \ y = 1 \ z = 1$

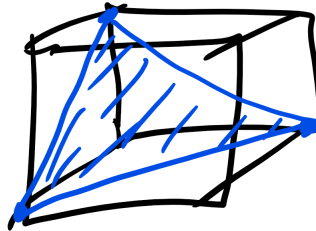


Figure 2-7: What Plane is this?

(110) Plane
 Intercepts $\rightarrow x = 1 \ y = 1 \ z = \frac{1}{0} = \infty$
 Parallel!!

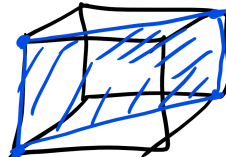


Figure 2-8: What Plane is this?

origin?

Here all the axes appear to be intersected, there are no parallel planes. True but this is actually misleading. When you have a plane that intersects the origin you need to choose a different origin and go through the same procedure to determine where the plane intercepts and then we can find the Miller indices of the plane.

The plane intercepts are again the inverse of the Miller indices and families of planes are denoted in curly brackets $\{hkl\}$.

Here is a nice demonstration to visualize the Crystallographic Planes:

<https://demonstrations.wolfram.com/CrystallographicPlanesForCubicLattices/>

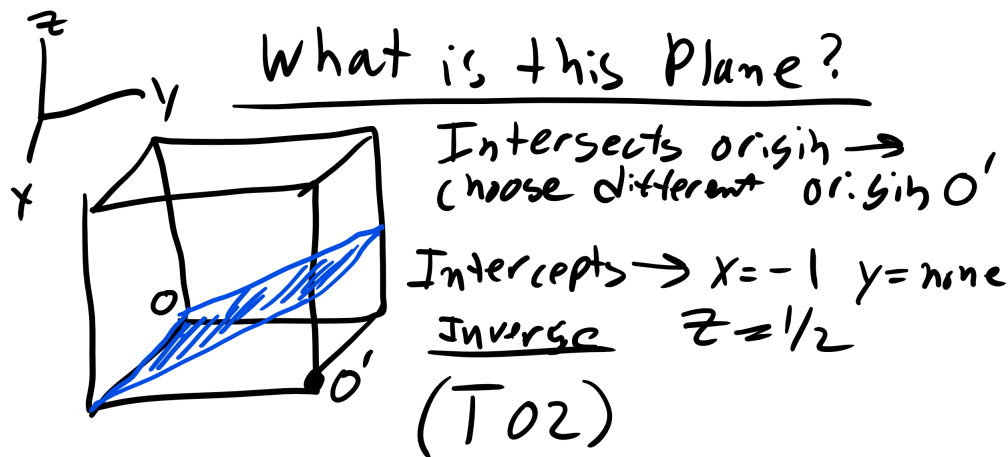


Figure 2-9: What Plane is this?

2.3.3 Anisotropy

Now it's important to mention that we have been assuming until now that material properties are the same in every direction however this is not actually the case. Often many materials are **anisotropic**, meaning that some materials properties (mechanical, optical, kinetic, etc.) are different depending on the crystallographic direction you are investigating[2]. For example titanium exhibits a larger modulus along the z-axis in the HCP structure than in the basal plane. This presents a significant problem when trying to superplastically form very thin foil made of titanium. A similar issue arises with magnetic properties of HCP materials as well. You should always remember as well that materials are not one perfect single crystal instead they are made of multiple crystalline grains, i.e. they are polycrystalline[2].

2.4 Simple Cubic

So let's start **simple with the simple cubic** to begin. So the simple cubic (SC) is also sometimes called primitive cubic and it is the crystal structure for Oxygen, Fluorine, etc[2]. **As you can see below it is described by the primitive lattice vectors a_1 , a_2 , and a_3 and interaxial angles α (angle between a_2 and a_3), β (angle between a_1 and a_3), and γ (angle between a_1 and a_2)**[2].

Notice the figure on the right is how the structure actually looks with the atoms touching. **Here $\alpha = \beta = \gamma = 90^\circ$. For simple cubic structures $a_1 = a[100]$, $a_2 = a[010]$, and $a_3 = a[001]$.** Right now I want to point that this is going to be the vector notation we use to signify a direction in a crystal lattice, more on this a bit later. **And for this case the lattice constants are all equal $a = b = c = a = 2R$ where R is the atomic radius of our element.**[2]

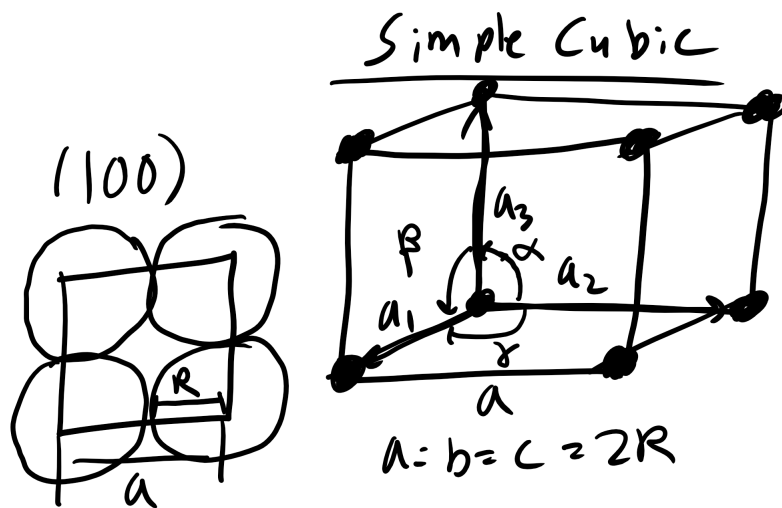


Figure 2-10: Simple Cubic

How many atoms are contained in our simple cubic cell?

Well it is simply 1 because the all the corner atoms are shared by 8 other unit cells so $\frac{1}{8} \times 8 = 1$.

How many nearest neighbors (NN) does each atom have?

6. Look at the Mathematica Notebook for this lecture for a neat visualization and possible project idea!!

How many second nearest neighbors?

12.

What is the NN distance?

$2R$

What about the NNN distance?

$2R\sqrt{2}$.

What about the atomic packing factor?

To calculate this we must calculate the volume of atoms in a unit cell by the total unit cell volume. Well for simple cubic we know that the volume of our conventional unit cell is a^3 . Additionally with the simple cubic lattice we only have 1 atom so that volume is simply $\frac{4}{3}\pi R^3$ so plugging and chugging we get.

It is $\frac{\pi}{6}$.

2.5 Body Center Cubic (BCC)

Let's look at a little more complicated cubic structure, **body centered cubic (BCC)**. BCC is the structure for Li, Fe, V, Mo[2].

and it is described by the primitive lattice vectors $a_1 = \frac{a}{2}[1-11]$, $a_2 = \frac{a}{2}[11-1]$, and $a_3 = \frac{a}{2}[-111]$

Atomic Packing Factor (APF)

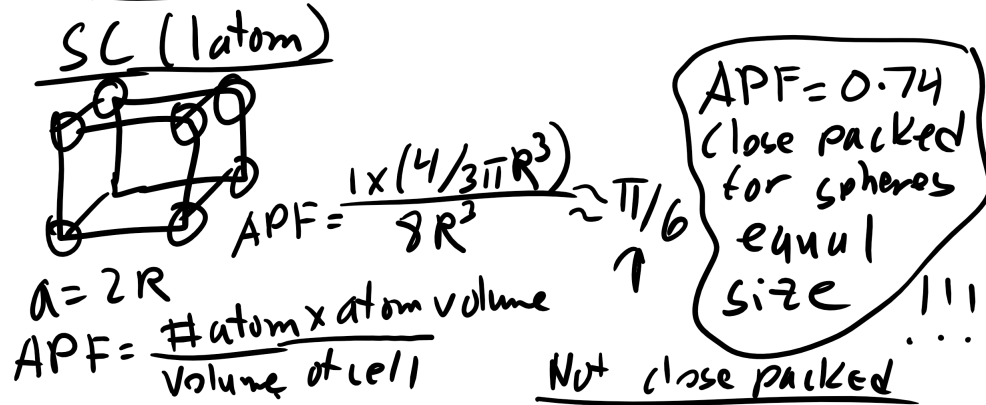


Figure 2-11: SC APF

Body-Centered Cubic (BCC)

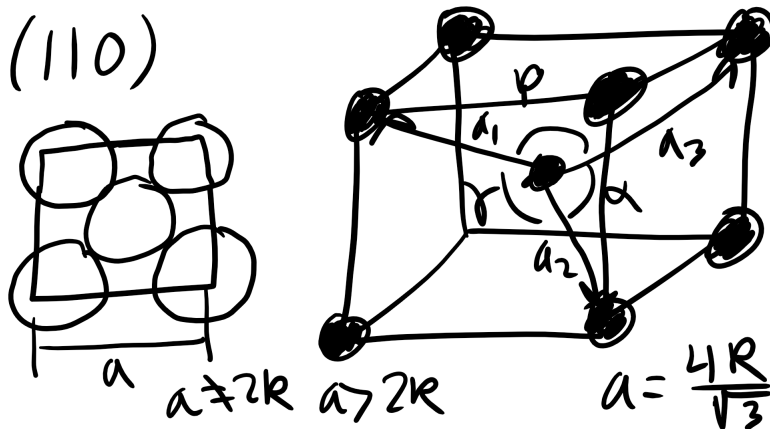


Figure 2-12: Body Centered Cubic

and $\alpha = \beta = \gamma = 90^\circ$ [2].

What is a now? Is it still $2R$? No it is not!!

Now $a = \frac{4R}{\sqrt{3}}$ where again R is the atomic radius which can be solved using a little bit of geometry.

How many atoms in a BCC conventional unit cell?

It is 2 atoms this time one in the interior and then 8 shared atoms so 2 total.

How many NN?

8.

How many NNN?

6.

What is the NN distance?

2R.

What about the second nearest neighbor distance?

It is simply $\frac{4R}{\sqrt{3}}$.

What about the atomic packing factor?

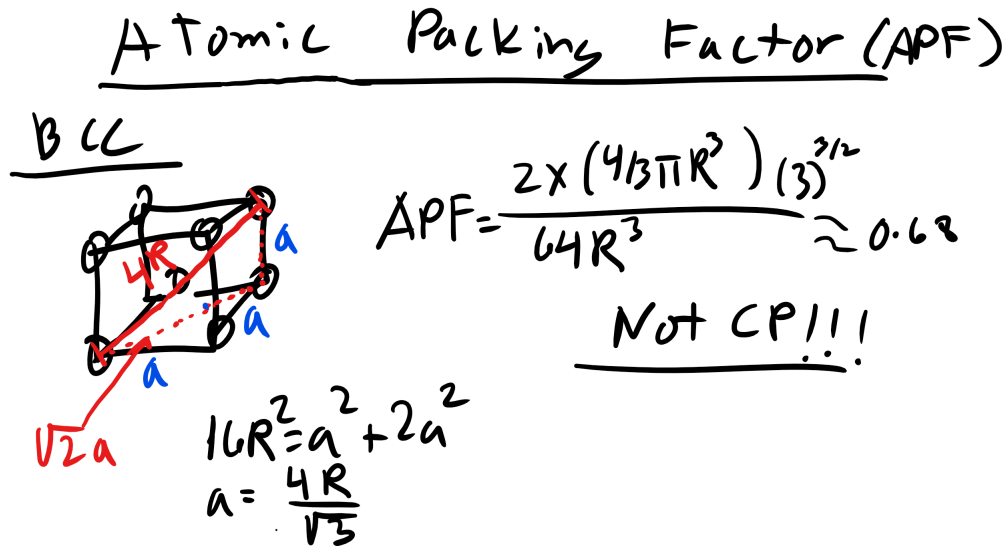


Figure 2-13: BCC APF

It is 0.68.

How did we get that? Well again how many atoms in a conventional BCC unit cell? 2 atoms. We also know the volume of our unit cell now since we found a . Double check!

2.6 Face Centered Cubic (FCC)

Next is face centered cubic (FCC). FCC is the structure for Ni, Cu, Ca and it is described by the primitive lattice vectors $a_1 = \frac{a}{2}[011]$, $a_2 = \frac{a}{2}[101]$, and $a_3 = \frac{a}{2}[110]$ and $\alpha = \beta = \gamma = 90^\circ$. Here $a = 2\sqrt{2}R$ where again R is the atomic radius. Remember that the primitive unit cell will have only a single atom but a conventional cell may not.

How many atoms in a FCC unit cell?

It is 4 atoms this time 8 share on the edges and 6 shared on the faces.

How many NN? 12.

How many NNN? 6.

What is the NN distance? 2R.

What about the second nearest neighbor distance? It is simply $2\sqrt{2}R$.

Face-Centered Cubic (FCC)

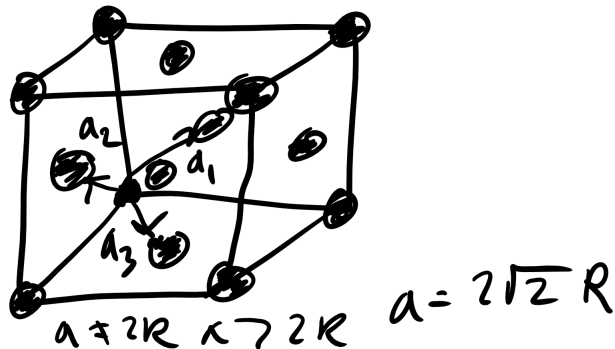
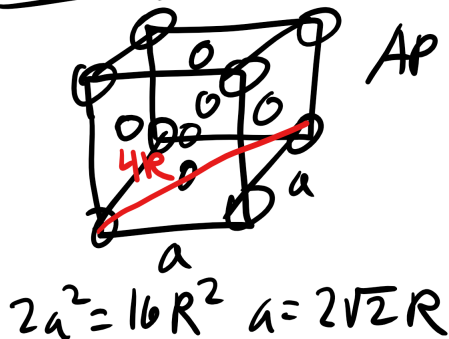


Figure 2-14: Face Centered Cubic

What about the atomic packing factor?

Atomic Packing Factor (APF)

FCC 4 atoms



$$APF = \frac{4 \times \left(\frac{4}{3}\pi R^3\right)}{(2\sqrt{2})^3 R^3} \approx$$

0.74
CP!!!

Figure 2-15: Face Centered Cubic APF

It is 0.74.

This is the maximum possible packing factor for spheres having all the same diameter.

2.7 Hexagonal Close Packed (HCP)

Finally hexagonal close packed (HCP). HCP is the structure for Ti, Zr, Y. It is actually not a Bravais lattice because we can't do our usual trick of describing the lattice in terms of basis vectors and then translating the entire crystal[2]. This can be done for Hexagonal Lattices and it is and it is described by the primitive lattice vectors $a_1 = \frac{a}{2}[1 - \sqrt{3}0]$, $a_2 = \frac{a}{2}[1\sqrt{3}0]$, and $a_3 = c[001]$, $\alpha = \beta = 90^\circ$, $\gamma = 120^\circ$, and $a = b \neq c$ [2].

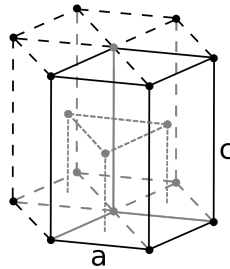


Figure 2-16: Hexagonal Close Packed
[4]

Here $a = \frac{4R}{\sqrt{2}}$ where again R is the atomic radius.

How many atoms in a HCP unit cell?

It is 6 atoms this time 12 share on the edges and 2 shared on the faces and 3 are in the interior.

How many NN?

12.

How many NNN?

6.

What is the NN distance?

2R.

What about the second nearest neighbor distance?

It is simply $\frac{4R}{\sqrt{2}}$.

What about the atomic packing factor?

It is 0.74. This is the maximum possible packing factor for spheres having all the same diameter. Ideally the c/a ratio should be 1.6333 geometrically but there are a number of materials that exhibit a c/a ratio which differs[2].

2.8 Close-Packed Structures

It is very interesting that **HCP and FCC have the same packing fraction or atomic packing factor**. Both HCP and FCC are called **close packed structures**. A close packed structure is one one that achieves the maximum packing density of spheres in a volume i.e. 0.74[2]. These structures can also be distinguished by the stacking sequence. **FCC stacks ABCABC...** indefinitely and **HCP stacks as ABAB...** indefinitely we can see the distinction below

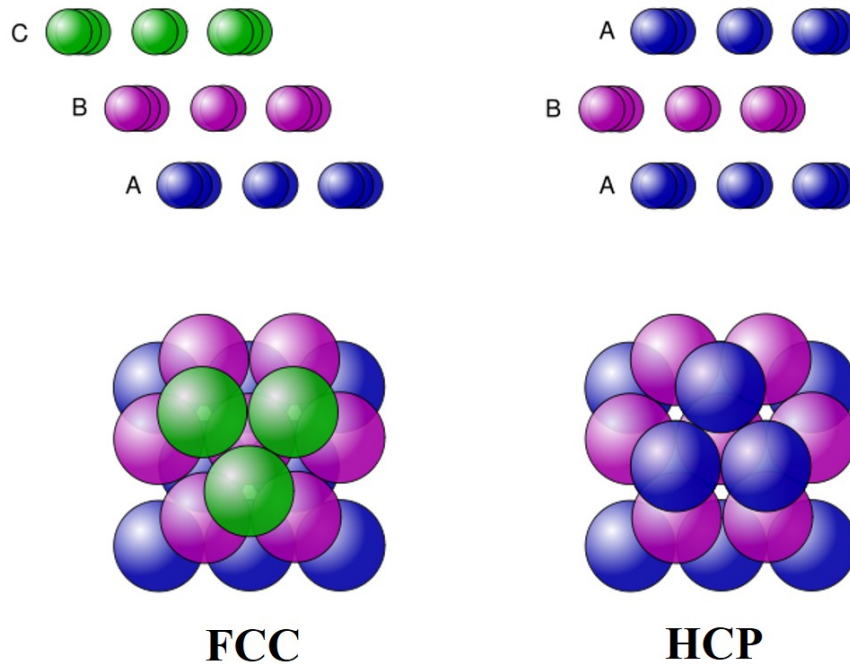


Figure 2-17: ABC or ABA Stacking
[5]

In these close packed structures there are two special interstitial sites: **tetrahedral and octahedral** sites[2]. The **tetrahedral sites** are equidistant from **four neighboring atoms** and **octahedral sites** are equidistant from **six neighboring atoms**. These sites are extremely important in ceramics and spinel structures but more on that a bit later[2]. We will note here as well that there are also **close-packed planes and close-packed directions**. **Close-packed directions** are directions along which the spheres are always touching, there are no gaps along the direction vector where the vector is not intersecting a sphere. Name some close packed directions in SC? What about BCC and FCC. What are some non-close packed directions?

A **close-packed plane** is defined as a plane with an **packing density of approximately 0.9069**.

What is the packing density for the (100) plane in SC?

What about the (110) plane in BCC?

What about the (111) plane in FCC?

Note that only close packed structures can have close packed planes but often we will be concerned (especially when we talk about diffusion, defects, and mechanics) about the **closest** packed plane in a crystal and that doesn't have to have a density of **0.9069**.

What are the close packed planes and directions for BCC, FCC, and HCP?

Close Packed Planes (CCP)

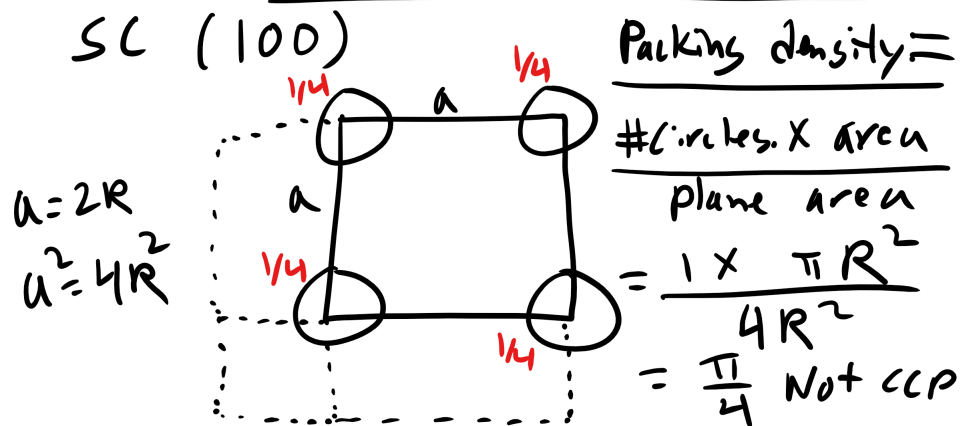


Figure 2-18: Planar Density

Close Packed Planes (CCP)

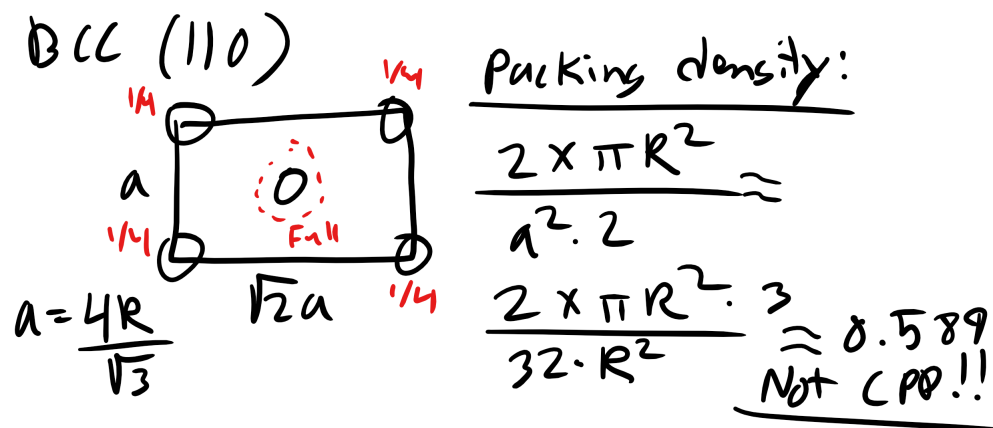


Figure 2-19: Planar Density

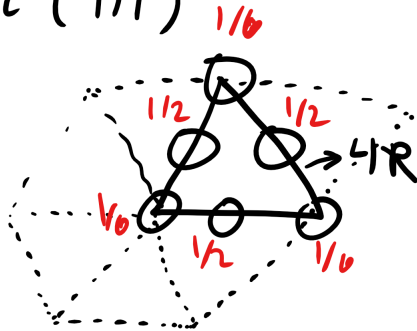
2.8.1 Polymorphism/Allotropy

Now when materials have more than one crystals structure they are polymorphic. In elemental solids this phenomenon is called **allotropy**[2]. You have encountered a number of polymorphic materials, some of you may be holding one in your hand. At least in the old days before tablets. It's carbon! Carbon can adopt a number of different structures i.e. diamond, graphite, fullerenes, graphene.) Iron (BCC and FCC) and Titanium (HCP and BCC) are also polymorphs[2]. We will also investigate lead titanate, a polymorph, in our XRD lab.



Close Packed Planes (CCP)

FCC (111)



Packing

$$\frac{2 \times \pi R^2}{\sqrt{3}/4 a^2} =$$

$$\frac{2 \pi R^2 \cdot 4}{\sqrt{3} 16 R^2} = \boxed{0.9069 \text{ (CPPI!)}}$$

Figure 2-20: Planar Density

2.9 Structure of Non-Crystalline Materials:

2.9.1 Polymers, Liquids, Glasses, Gas, and Liquid Crystals:

Now so far we have focused only on crystalline materials primarily because they are the simplest materials to characterize in terms of structure. However there are many more materials that do not adopt a simple crystalline structure with short range, long range translational, and long range orientational order. Specifically, polymers, liquids, gases, liquid crystals, glasses, and many others.

With crystalline materials we were able to translate a unit cell to essentially infinity. **That is because we had both short range order, long range translational order, and long range orientational order.** In polymers, glasses, and liquid crystals typically we will only have **short range order (SRO)** and perhaps **some degree of long range order either translational or orientational but typically not both** and not to the periodic nature of crystalline materials[2]. So how are we going to talk about structure in these non-crystalline materials which are often incorrectly called disordered materials. Well we are going to use a **dimensionless pair distribution function (PDF) or the radial distribution function (RDF)**, this is also called the **pair correlation function** as well I know very confusing, which is our key **descriptor** for quantifying the SRO present in a material[2].

The **PDF or RDF**, $g(r)$, is:

$$g(r) = \frac{1}{\langle \rho \rangle} \frac{dn(r, r+dr)}{dv(r, r+dr)} \quad (2.6)$$

where ρ is the average particle number density, dn is the number of particles counted in a small spherical shell sampling volume element of size dv at each distance r from a particle chosen as the origin. The number of particles in each shell is counted at each subsequent dr shell. This is shown

schematically below

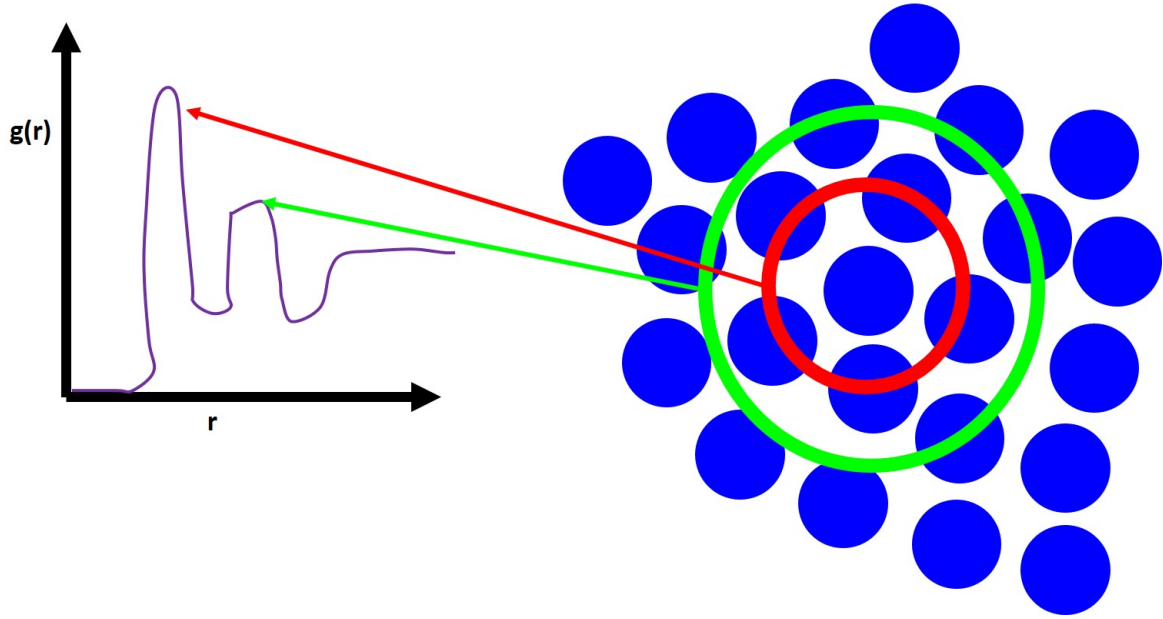


Figure 2-21: PDF/RDF

To get a smooth curve you want to pick a very small dr so that is **much smaller than the radius of the particle** and we must average this over multiple particles chosen as the origin. **For perfect crystals we will see the PDF exhibit a series of sharp and discrete peaks at precise values of interatomic spacings which will correspond to the particular crystal structure**[2]. Now for **liquids you will see a large peak and then some much smaller peaks**. This first peak corresponds to your number of nearest neighbors which can be derived by the following equation:

$$\langle NN \rangle = \langle \rho \rangle \int_{peak} g(r) 4\pi r^2 dr \quad (2.7)$$

We will also use PDF to quantify the SRO for glasses as well and let's take a look at silica glass as an example (this also holds for thermoset polymers as well)[2].

2.9.2 Silica

Pure silica glass is SiO_2 with each silicon bonding to four oxygen and the oxygen-silicon-oxygen bond angle is the tetrahedral bond angle 109.28° . A continuous random network forms through corner-to-corner connections of the SiO_4 tetrahedra to share oxygen ions to form -Si-O-Si- linkages with variable Si-O-Si bond angles between adjacent tetrahedra[2]. In this structure each oxygen anion should be linked to not more than two cations. The functionality of the central cation must be small. The oxygen polyhedra share corners, not edges or faces. At least three corners of each polyhedron should be shared. So in the ideal structure with each silicon ion bonded to four oxygen

PDF/RDF

what material is which?

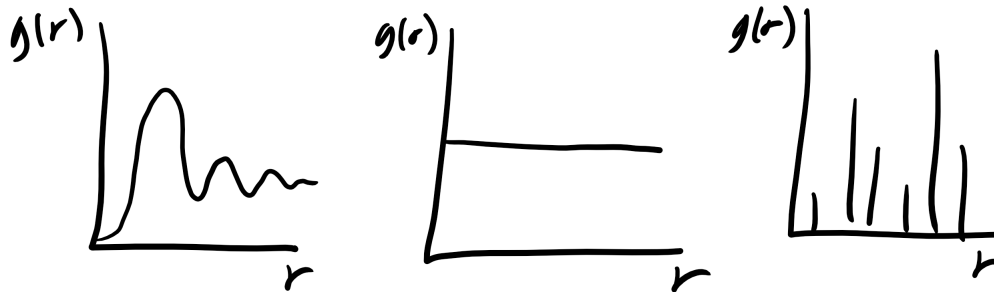


Figure 2-22: PDF/RDF

Metal PDF/RDF

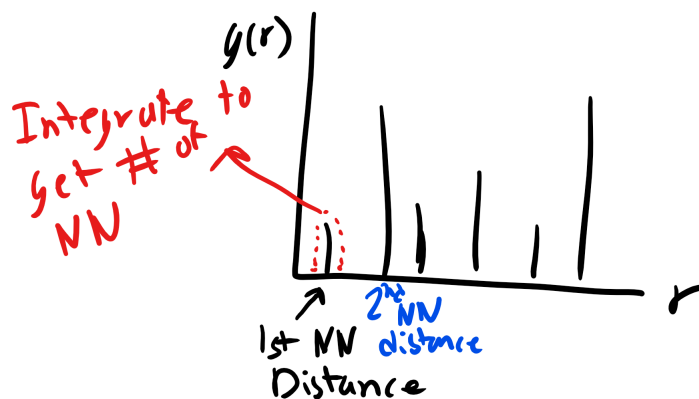


Figure 2-23: Metal RDF Interpretation

ions and each oxygen bonded to two silicon ions with no bonds left dangling leads to a very dense network structure and a very high glass transition temperature, T_g .

You can reduce the glass transition temperature by adding network modifiers to the glass which weakens the network structure. The network modifiers offer alternative bonding for the oxygen atoms and some become ionically bonded rather than forming the more rigid ionic-covalent bonding with the silicon atoms[2]. One network modifier is NaO_2 and the results is a more open structure and less covalent. However, the boron oxide anomaly is an interesting case study in glasses. In B_2O_3 the unit is a BO_3 triangle (3 sp^2) bonds which forms 2D network sheets. When small amounts

of NaO_2 is dissolve in borate glass the glass stiffens and at higher concentration the glass becomes less stiff. This is the boron anomaly and the explanation is that initially the addition of sodium ions converts the BO_3 triangles to BO_4 tetrahedra[2]. Further addition of sodium ions will cause the formation of NBO which once again weakens the continuous random structure.

2.9.3 Liquid Crystals:

Finally the last class of materials that we will discuss in terms of structure and order is Liquid Crystals (from LCDs in terms of applications and soapy water). **Liquid crystals exhibit short range order and some degree of long range orientational or positional order**[2]. There are number of different types of liquid crystals, specifically **Nematic, Twisted Nematic or Cholesteric, Schmectic, and Columnar**. Liquid crystals, from their namesake, exhibit characteristics of both the **liquid state**, SRO, and the **crystalline state** (long range orientational order)[2]. Additionally **Smectic and cholesteric** liquid crystals can exhibit **1D long range translational order**, and **columnar liquid crystals can exhibit 2D long range translational order**[2].

The liquid crystal structure is described using a **director**, n , which is the preferred axis along which molecules in a liquid crystals are oriented locally, and is specified by a **position dependent unit nonpolar vector**, p [2]. At a surface liquid crystals can be either **homogeneous**, the director lies parallel to the substrate, or **homoeotropic** where the director lies perpendicular to the substrate. When a force is applied to these materials they can splay, twist, or bend which will effect the optical properties of your LCD[2].

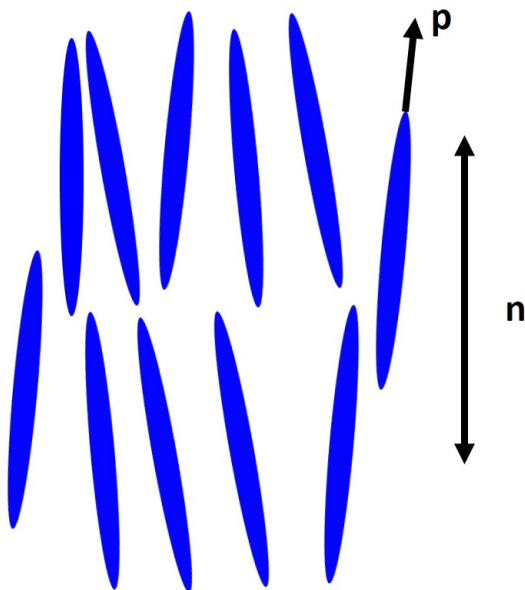


Figure 2-24: Liquid Crystal

Nematic phase, N, has short range-translational order and long-range uniaxial orientational order.[2]

Twisted nematic, N^* , or more commonly called the cholesteric LC. This phase is distinguished by a characteristic twist or helical nature of the director.[2]

Smectic, SM, LC have long range orientational order and long range 1D translational order.[2]

We also have a special version of our PDF descriptor for LC. In particular we have the **orientational order parameter**, S ,

$$S = \frac{3 \langle n \cdot p_i^2 \rangle_V - 1}{2} \quad (2.8)$$

and for a nematic liquid crystal the order parameter, S_N becomes

$$S_N = \frac{3 \langle \cos^2 \theta \rangle - 1}{2} \quad (2.9)$$

Where the θ is the time average angle between the director and each LC vector, p [2]. You can see that when the orientation is perfect, aligned with the director, $S_N = 1$ [2]. However, when the orientation is completely random the $S_N = 0$. Typically, you should expect experimental values of 0.6-0.8 until the temperature increases to a large enough values where the thermal energy is enough to overcome the long range orientational order[2].

THIS PAGE INTENTIONALLY LEFT BLANK

CHAPTER 3

DEFECTS IN CRYSTALLINE MATERIALS

**“Crystals are like people, it is the defects in them which tend to make them interesting!
- Professor Sir Colin Humphreys”**

A crystal is at a state of thermodynamic equilibrium when its free energy $G = H - TS$ is minimized. When are we (humans) at equilibrium?

We have two **knobs** that we can tune to lower the free energy of the system above and that is **entropy** and **enthalpy**. At low temperatures our entropy knob becomes negligible and energy is minimized by minimizing H . This is done via binding and forming the ordered structures that we discussed previously. At the limit of $T = 0$ that perfect crystal is the equilibrium configuration[2]. When temperature increases the free energy is minimized by adopting a less well-ordered atomic/molecular arrangement because that increases the entropy. Entropy increases when imperfections exist so when the temperature is not zero the **equilibrium state will most likely contain imperfections**. We can calculate the equilibrium concentration by looking at the change in free energy ΔG and the ΔS by adding imperfections and the enthalpic ΔH_f cost of forming those defects[2].

3.1 Crystalline Point Defects (0D)

3.1.1 Vacancies

A **vacancy** exists when a site that is normally occupied in the perfect crystal is **unoccupied**[2]. This can occur in many ways for example, forcing an atom onto an interstitial site, into a dislocation core, or to a grain boundary or free surface. You can see a couple of examples of a vacancy below

We can actually **calculate the equilibrium concentration of vacancies, n !** Consider a reference state of a **perfect crystal of N atoms** and a **continuous set of vacancies, n** [2]. The new state is a crystal containing a mixture of N atoms and vacancies. The total enthalpy change is then

$$\Delta H_f = n\Delta h_f \quad (3.1)$$

where Δh_f is the enthalpy of formation of a single vacancy. We can also get an idea about the change in configurational entropy from creating vacancies if we remember Boltmann's entropy equation (he had it carved on his tombstone...show off)

$$S = k \ln \Omega_m \quad (3.2)$$

where k is the Boltmann constant and Ω_m is the number of distinguishable ways you can arrange

0D Defects: Point Defects

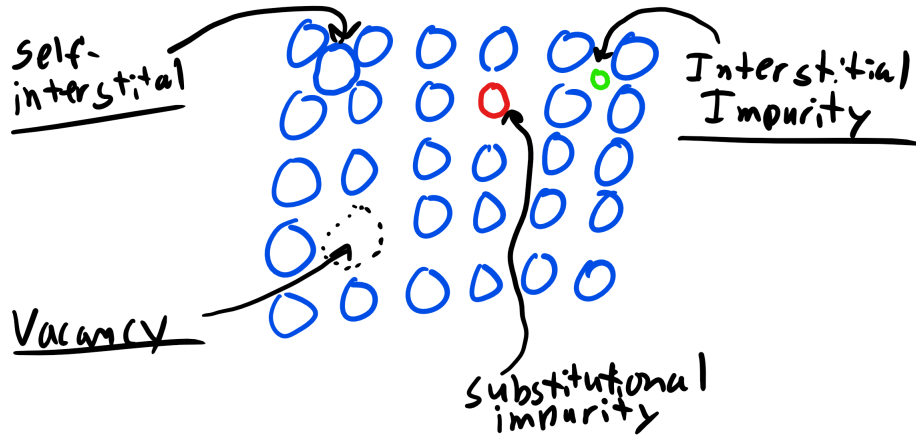


Figure 3-1: 0D Point Defects

the system[2]. The configurational entropy ΔS_c is then given by

$$\Delta S_c = S_{mix} - S_{ref} = k \ln \left(\frac{\Omega_m}{\Omega_{ref}} \right) = k \ln \Omega_m = k \ln \frac{(N+n)!}{N!n!} \quad (3.3)$$

where Ω_m is the number of distinguishable ways of arranging N atoms and n vacancies on $N+n$ sites and Ω_{ref} is the number of configurations in the ideal reference state, which is 1 since there are no defects[2]. So the total Gibbs energy change is

$$\Delta G = \Delta H - T\Delta S = n(\Delta h_f - T\Delta S_v) - kT[(N+n) \ln(N+n) - N \ln N - n \ln n] \quad (3.4)$$

where ΔS_v is the vibrational entropy of the atoms surrounding the vacancy and we used Sterling's approximation $\ln X! \approx X \ln X - X$ to get to the equation above[2]. Now how do we minimize Gibbs? Well we take the derivative and set it equal to zero:

$$\frac{\partial \Delta G}{\partial n} = \Delta h_f - T\Delta s_v + kT \ln \frac{n}{n+N} = 0 \quad (3.5)$$

We can now solve for the equilibrium fraction of vacant sites x_v

$$x_v = \frac{n}{n+N} = \exp \left(\frac{\Delta s_v}{k} \right) \exp \left(- \frac{\Delta h_f}{kT} \right) \quad (3.6)$$

You should notice in this equation that there is an **exponential temperature dependence**, known as **Arrhenius dependence** or **Arrhenius's law**[2]. This is critical because there are many behaviors in Materials Science which are Arrhenius (project idea???). Let's take a look at how strongly the concentration of vacancies varies with temperature by looking an example Arrhenius

plot below:

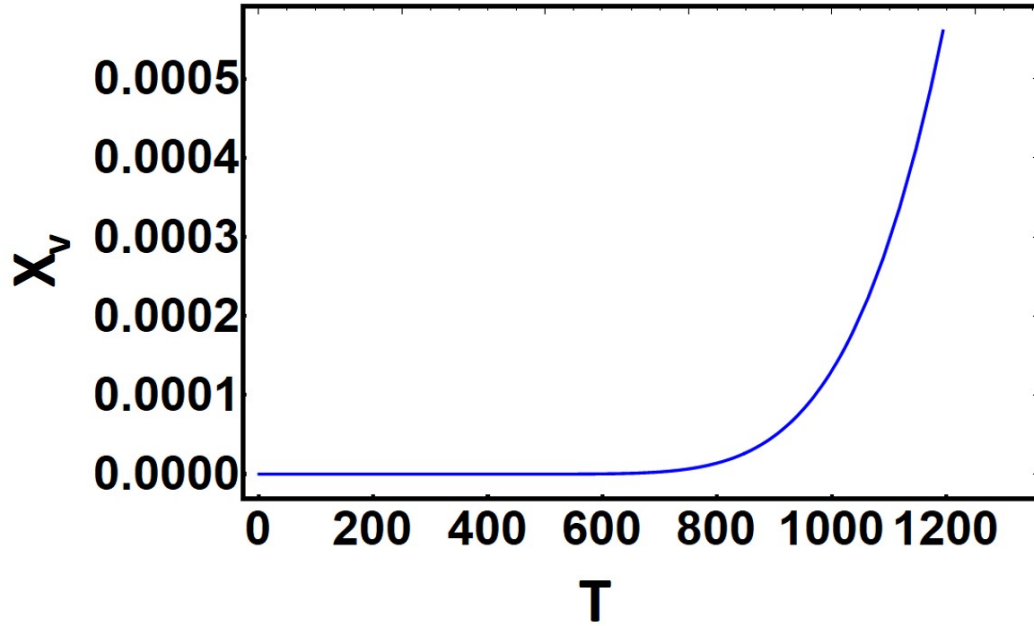


Figure 3-2: Arrhenius Plot of Equilibrium Vacancy Concentration in Gold

Now typically we can assume that the $\exp(\frac{\Delta S_v}{k}) \approx 1$. The **enthalpy of formation of vacancies for metals is typically on the order of 15-150kT** ($kT = 0.026$ eV) So we can clearly see that at room temperature the probability of forming vacancies will be pretty low already[2]. Is this supported by the graph?

This method is not the typical way Arrhenius graphs are presented. It is actually better to plot the Log of the equilibrium concentration of vacancies as a function of the reciprocal temperature $\frac{1}{T}$ [2]. That way we can extract the activation energy or energy of formation of the vacancy.

3.1.2 Interstitials

An **interstitial defect** occurs when an atom occupies an interior site which is not normally occupied. If the interstitial is of the same species in a single component crystal it is a **self-interstitial** and we have the following equation for the equilibrium number of self-interstitials

$$x_i = \frac{n}{n + N} = \exp\left(\frac{\Delta S_v}{k}\right) \exp\left(-\frac{\Delta h_f}{kT}\right) \quad (3.7)$$

however now the ΔS_v and Δh_f represent the enthalpy of formation and vibrational entropy for interstitial formation. As you might imagine the **energy of formation for interstitials is lower for more open and less densely packed structures**[2]. Obviously there are also **higher numbers of these 0D defects for nonequilibrium processes like quenching, irradiation, ion implantation, or cold working.**

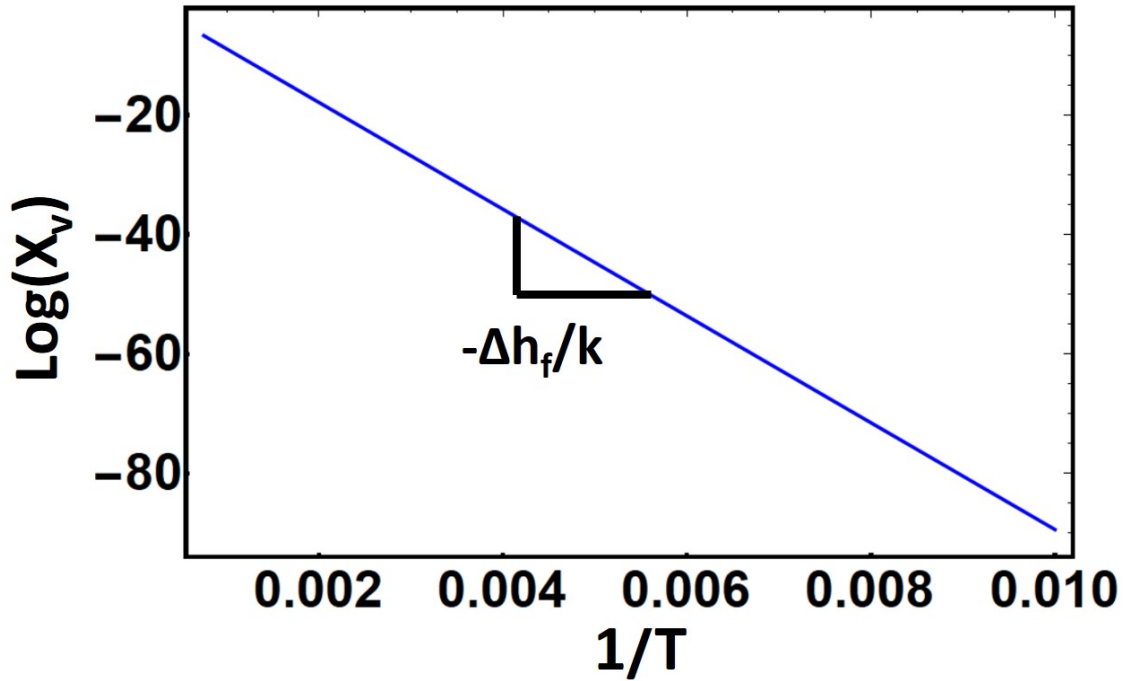


Figure 3-3: Arrhenius Plot of Equilibrium Vacancy Concentration in Gold

3.1.3 Alloys

An **alloy** is formed when one or more species is mixed to form a solid or liquid solution (brass, Ti-64, stainless steel, etc.) **The major component is the solvent and the minor component is the solute.**[1] When the solute occupies sites normally unoccupied by the solvent in the crystal then it is an **interstitial solid solution**[1]. If the solute occupies a site normally occupied by the solvent then the crystal is a **substitutional solid solution**.

Typically alloys should have

1. **Atomic radii differences of $\pm 15\%$**
2. **Same crystal structure**
3. **Maximum allowable concentration of interstitial impurities less than 10%.**

Just for definition's sake to calculate weight percent (wt%) it is simply

$$WT\% = \frac{m_A}{m_A + m_B} \times 100 \quad (3.8)$$

where m_A is the mass of component A and m_B is the mass of component B. And atomic percent (at%) is simply the number of moles of one element over the total number of moles in the alloy[1].

3.2 Point Defects, Kröger-Vink Notation, and Schottky and Frenkel Defects

Point defects in ionically bonded crystals typically have an associated **charge**[2]. Now the **net charge of a perfect crystal is zero**. **Cations** have lost one or more electrons and thus have a net positive charge. **Anions** have gained one or more electrons and thus have a net negative charge. A **cation vacancy** is created by removing a cation from a site in the crystal to a site on the surface. This vacant site then has a **net negative charge**[2]. An **anion vacancy** is created by removing an anion site in the crystal to a site on the surface and the **vacant site then has a net positive charge**[2].

Now the way we describe these point defects is by using **Kröger-Vink** notation and schematically it is represented by:

$$X_Y^Z \quad (3.9)$$

where **X represents what is on the site**: either V for a vacancy or if occupied by an element, the element symbol. **Y represents what type of site is occupied by X**, either i for interstitial or if normally occupied by an element the symbol for that element[2]. **Z represents the charge relative to the normal ion charge on the site Y** using **dots** to represent **positive** relative charges, **primes** to indicate **negative** relative charges, and **x** to indicate zero relative charge[2].

There are two idealized forms of charge-compensating point defects which are the **Schottky and Frenkel Defects**.

A **Schottky defect** consists of **charge-compensating anion and cation vacancies**[2]. Let's consider KCl for example. What is a Schottky defect? Well it would be

$$Null \leftrightarrow V_K' + V_{Cl} \quad (3.10)$$

What about TiO₂?

$$Null \leftrightarrow V_{Ti}'''' + 2V_{\ddot{O}} \quad (3.11)$$

A **Frenkel defect** is formed when an **ion moves from its normal site in the crystal into a nearby interstitial site, forming a Frenkel pair**[2]. Let's examine the **cation Frenkel pair** in Li₂O which is

$$Li_{Li}^x = Li_i' + V_{Li} \quad (3.12)$$

and the **anion Frenkel pair** would be

$$O_O^x = O_i'' + V_{\ddot{O}} \quad (3.13)$$

What about the cation and anion Frenkel pair in UO₂ respectively?

$$U_U^x = U_i^{\cdots} + V_U^{\prime\prime\prime} \quad (3.14)$$

$$O_O^x = O_i^{\prime\prime} + V_{\ddot{O}} \quad (3.15)$$

You need to have **charge and mass balance** in the above equations. **Charge balance** is attained when the sum of the charges on the right hand side equals the sum of charges on left hand side. **Mass balance** requires that the total number of ions or atoms of a given species is the same on both sides of the reaction[2]. **The equilibrium concentrations of charged Schottky defects and Frenkel defects** is:

$$x_{pairs} = \exp\left(-\frac{\Delta h_f}{2kT}\right) \quad (3.16)$$

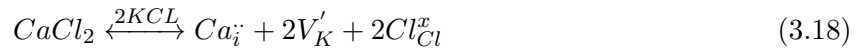
where the formation enthalpy is for a pair of ions either Schottky or Frenkel pair. Among the myriad of defects there will be a **dominant defect**, known as an **intrinsic defect** and typically it will be the one with the **lowest enthalpy of formation**[2].

3.3 Impurities in Kröger-Vink

We can also describe how impurities can induce formation of a variety of point defects using Kröger-Vink notation. Let's think about CaCl_2 impurities in KCl , specifically via incorporation of K into Ca sites[2]. We assume that the Cl sites can easily be integrated into the structure provided enough vacancies. So one type of impurity incorporation reaction could be:



Note that we write 2KCl for mass balance. Another defect could be

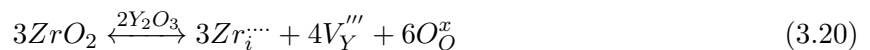


where we have Ca inserting into an interstitial site.

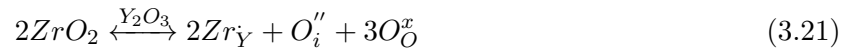
Let's practice with ZrO_2 (zirconia) impurities in Y_2O_3 (yttria), two very important ceramic materials, i.e. yttrium stabilized zirconium bio-engineering mechanical applications[2]. Let's look again at some possible impurity incorporation reactions



or another reaction



or yet another reaction



Yes you can expect many questions on this topic!

3.4 Dislocation Defects (1D)

Imperfections that are localized along a space curve passing through an ordered medium are **line imperfections**. A **dislocation** is one such defect. A **dislocation** is a linear or one dimensional line defect which involves translation of one part of a crystal with respect to another part[2]. A **disclination** involves rotation of one part with respect to another. We will deal with two types of dislocation in this class: **edge and screw dislocations**.

An **edge dislocation** is essentially an extra half plane of atoms that is inserted into the perfect crystal and it terminates within the crystal. You can see this below

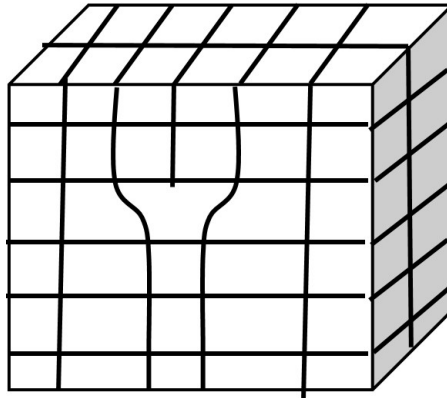


Figure 3-4: Edge Dislocation

Watch the Bragg Video and do demo.

A **screw dislocation** is a bit harder to visualize but you can imagine that a screw dislocation can be formed by an applied shear stress, seen below:

You can see that in this example some of the differences between edge and screw dislocations one begin that the **screw dislocation motion** will be **perpendicular** to the **applied force** but more on that in a little bit[2]. There are also **wedge and twist disclinations** as well.

Associated with each dislocation is a **dislocation core** which is where the largest displacements of atoms from the ideal sites occur and they are concentrated along a **dislocation line**. We describe dislocations via a **unit tangent vector**, t , and the **Burgers vector**, b . The tangent vector is a unit vector that is **tangential to the dislocation line at any given point**[2]. The **Burgers vector**, b , is defined in reference to the Burgers circuit. Now in this class we will use the **SF/RH** (start to finish, right-hand) **convention** to define the Burgers vector[2].

To define the Burgers vector:[2]

- Choose the **positive sense** of the **unit tangent vector** of the dislocation line

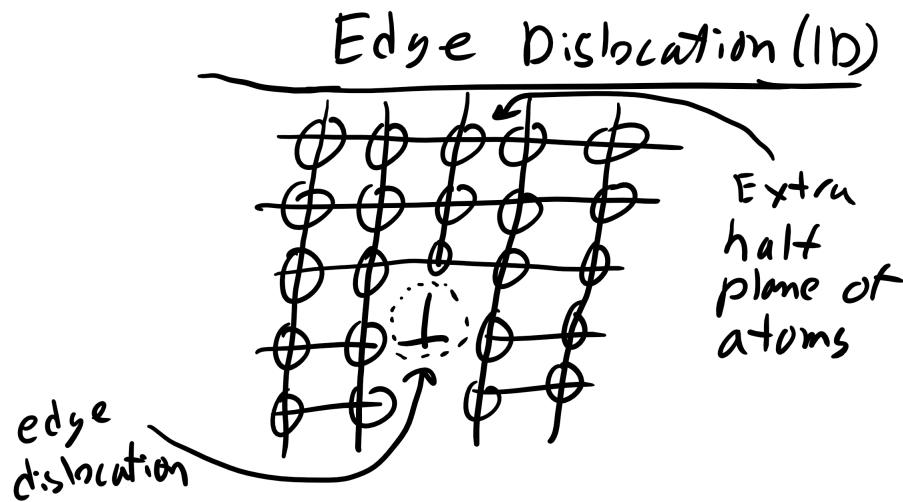


Figure 3-5: Edge Dislocation

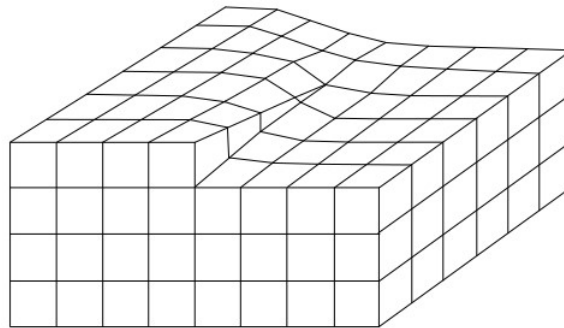


Figure 3-6: Screw Dislocation[6]

- By traveling along rows of lattice points make a **right hand circuit** in the crystal **containing the dislocation**. Define a Start Point, **S**, and Finish Point **F**.
- This circuit would be a **closed circuit in the perfect crystal** but in this instance the circuit is **only closed by the Burgers vector** which connects your **Start and Finish points**.

A couple of other quick notes about some of the properties of dislocations[2]

- It should be noted that the Burgers vector will be conserved and that for a given dislocation there is one constant Burgers vector, even as the tangent vector changes.
- A dislocation cannot end inside a crystal.
- A **pure edge dislocation** has b **perpendicular to t** everywhere along the dislocation curve and $t \times b$ **points toward the extra half plane of atoms**

- A pure screw dislocation is either parallel or antiparallel to t everywhere along the dislocation curve. A right-hand screw is parallel and a left-hand screw is anti-parallel.
- A dislocation that is neither pure edge or pure screw is a mixed dislocation and the vector component that is parallel to t is the screw component and the component that is perpendicular to t is called the edge component.
- Reversing the sense of t also reverses the sense of b .

Let's do an edge dislocation

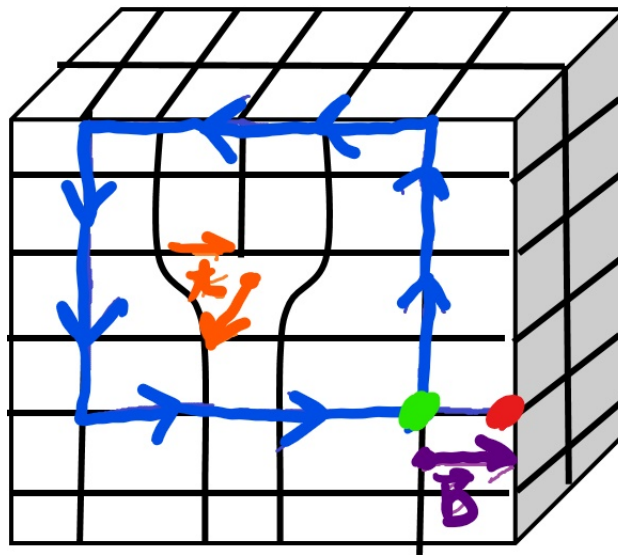


Figure 3-7: Edge Dislocation Burgers Circuit

Now how about a screw dislocation?

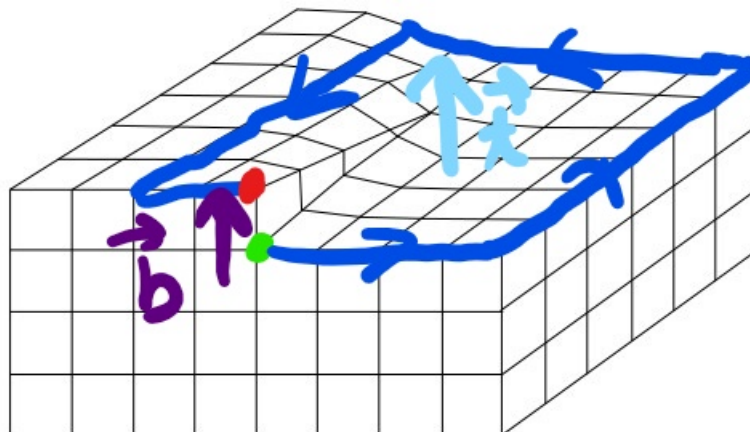


Figure 3-8: Right Handed Screw Dislocation Burgers Circuit

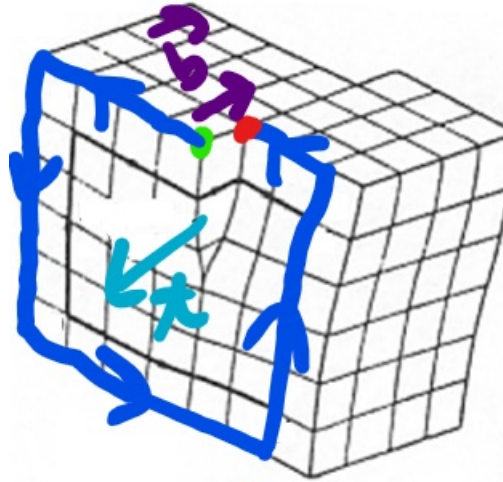


Figure 3-9: Left Handed Screw Dislocation Burgers Circuit [7]

How about another screw dislocation?

While we are speaking of dislocations one of the key material properties that you will come across is the dislocation density, ρ , which has units of m^{-2} . A **highly cold worked** material may have a **dislocation density of $10^{12}cm^{-2}$** whereas a **highly annealed material** can be as low as **10^5cm^{-2}** [2]. Dislocations are additional **motile** and they can move via **slip and climb**.

3.5 Grain Boundaries, External Surfaces, Phase Boundaries, Twin Boundaries, and Stacking Faults (2D)

Perhaps the most obvious 2D defect is just an **external surface** where the **bonds at the surface are not satisfied** which gives rise to an increase surface energy or surface tension[2].

Grain Boundaries are interfaces at which crystals of different orientations abut. There are special types of grain boundaries like low angle tilt and twist boundaries when the angle of misorientation of grains is not too large[2]. In fact they are considered simple periodic arrays of dislocations.

Phase boundaries exist in multiphase materials where a different phase exists on each side of the boundary[2].

A **twin boundary** is a special type of grain boundary across which there is a specific mirror lattice symmetry. The region of material between these boundaries is a twin[2]. Twins typically appear due to shear stresses or during annealing heat treatments after deformation. Annealing twins are more common in FCC crystals while mechanical twins are more common in BCC and HCP crystals[2].

Stacking faults are interfaces in crystals across which one part of the crystal is displaced relative to the other part by a displacement vector that is not a translational symmetry operation for that crystal. Remember that for FCC we had this ABCABC stacking and HCP we had ABABAB[2].

2D Defects: Grain Boundaries(GB)

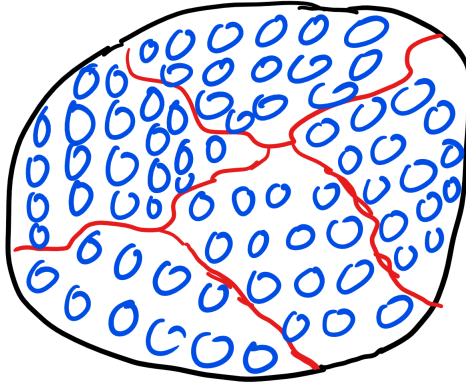


Figure 3-10: Grain Boundaries

A stacking fault in FCC would be ABCBCABCABC. If the fault is missing a layer that is an **intrinsic stacking fault** but if there is an **extra layer that is an extrinsic stacking fault**. Stacking fault energy has severe implications on the strain hardening behavior of materials[2].

There are also **antiphase/interphase boundaries** which are separate regions of the crystal by a relative translation that is not a symmetry operation of the crystal[2]. It is a special type of stacking fault, one that connects the crystallographically nonequivalent occupied sites in a perfect crystal[2]. They can be **coherent, semi-coherent, incoherent**.

3.6 Bulk or Volume Defects (3D)

Finally there are also bulk or volume defects which include pores, cracks, foreign inclusions, and other phases[2].

Part II

Kinetics

CHAPTER 4

KINETICS

Thermodynamics is the study of equilibrium states in which state variables of a system do not change with time [8]. **Kinetics** is the study of the rates at which systems that are out of equilibrium change under the influence of various forces[8].

4.1 Diffusion and Fick's First Law

Diffusion is the phenomenon of material transport by atomic motion. Diffusion typically involves **flux** of chemical components. This flux of material can arise from many different **driving forces**, i.e. electrostatic field, stress, thermal gradients, chemical potential, etc[8]. This last case of **flux in response to a chemical potential gradient** brings us to **Fick's First Law** which is:

$$\vec{J}_i = -D\nabla c_i = -D\frac{\partial c_i}{\partial x} \quad (4.1)$$

where D is the mass diffusivity, \vec{J}_i is the flux of chemical species, and ∇c_i is the gradient in concentration[8]. We should stop here and take a quick moment to appreciate the beauty of this equation.

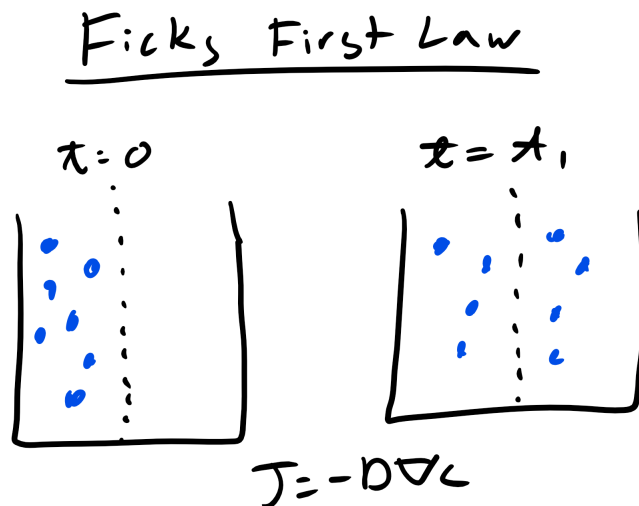


Figure 4-1: Schematic of Fickian Flux

Let's do a quick problem as well

You will see when you take heat transfer as a senior that heat flux has the following form:

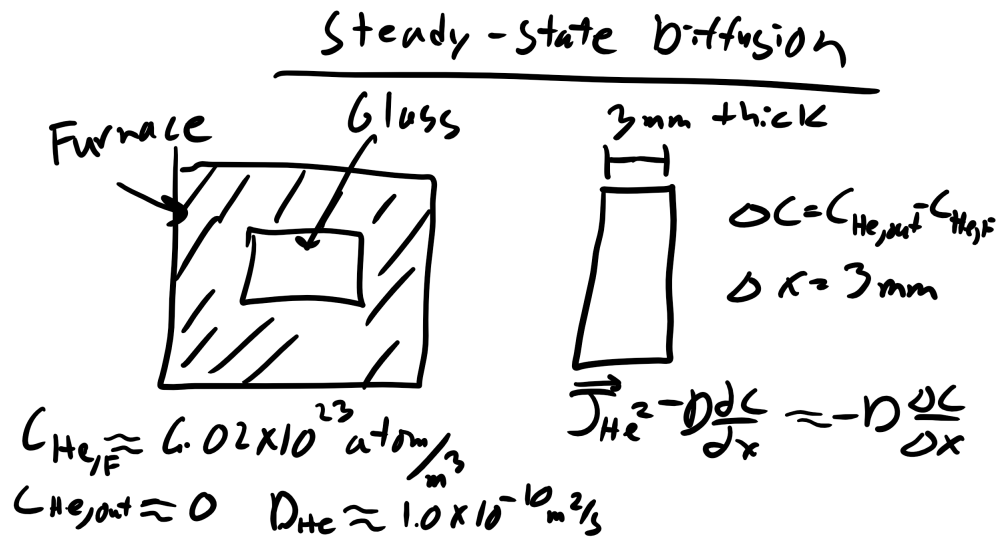


Figure 4-2: Steady-State Diffusion

$$\vec{J}_Q = -k \nabla T \quad (4.2)$$

where \vec{J}_Q is the heat flux, k is thermal conductivity in the material, and ∇T is the gradient in temperature[8]. Also the flux for charge is:

$$\vec{J}_q = -\nabla \phi \quad (4.3)$$

where \vec{J}_q is charge flux and $\nabla \phi$ is the gradient in electrical potential[8]. A similar form appears when you take fluids as well. We see a very similar form in all these different equations and it illustrates that we can relate a flux (\vec{J}) to a conjugate force ($-\nabla \Phi$). Remember that force is the negative gradient of a potential[8].

4.2 Kirkendall Effect

The simplest case of diffusion or diffusivity is just **self diffusion** in a chemically pure material and that diffusion is simply described by Fick's first law where D is the self diffusivity of the material[8]. A more complicated but fascinating case occurs when you have a diffusion couple of two different materials with different diffusivities and a phenomenon occurs which is called the Kirkendall effect[8].

The **Kirkendall effect** was observed in 1947 at Wayne State University, although he had initially observed the phenomenon as a graduate student, in a diffusion couple of brass with molybdenum wires (Mo is insoluble in brass). The wires were wrapped stretched across the length and then coated with a pure layer of copper. What he observed after annealing this material at 785°C

for 56 days was the the **wires started to move closer together**[8]. This was a startling revelation because previously diffusion was thought to occur via direct exchange mechanism or ring mechanism and this **implies that the atomic fluxes across an interface must be equal or equivalently that the velocity of that interface must be zero**[8].

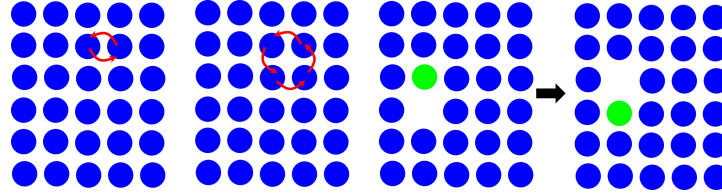


Figure 4-3: Direct Exchange, Ring, and Vacancy Diffusion Mechanisms

This experiment showed that the **interface velocity was not zero** and thus the **fluxes were not equal to zero**. Please make sure to read the article The Discovery and Acceptance of the Kirkendall Effect: The Result of a Short Research Career.

4.3 C-Frame:

So for the case of a **binary diffusion couple where the diffusivity of the two atoms are different** we need to rethink how we define the flux of atoms and the frame of reference that we will use. Let's define a **frame of reference** where we **place ourselves or some inert particle marker that is attached to a particular plane of atoms** and we will define this as the origin and we will call this our local C-frame[8]. Once we have our C-frame we also have the constraint that:

$$\vec{J}_1^C + \vec{J}_2^C + \vec{J}_V^C = 0 \quad (4.4)$$

This is an extremely important result. Why does the flux across our line of atoms or our plane of atoms have to be zero? Because of **conservation of matter** we are not creating any additional sites[8]. This also implies that there must be a continuous vacancy generation (**source**) on one side of our plane and the destruction of vacancies (**sink**) on the other side[8].

We also have a slightly different definition of our diffusivity which we will term the *intrinsic diffusivity*, D_1 , as you will see below:

$$\vec{J}_1^C = -D_1^* \left[1 + \frac{\partial \ln \gamma_1}{\partial \ln c_1} + \frac{\partial \ln \langle \Omega \rangle}{\partial \ln c_1} \right] \frac{\partial c_1}{\partial x} = -D_1 \frac{\partial c_1}{\partial x} \quad (4.5)$$

where γ_1 is the activity of component 1, c_1 is the concentration of component 1, $\langle \Omega \rangle$ is the average site volume, D_1^* is the self-diffusivity of component 1[8]. We can typically make a simplification and ignore the component that deals with changes in average site volume and get:

$$\vec{J}_1^C = -D_1^* \left[1 + \frac{\partial \ln \gamma_1}{\partial \ln c_1} \right] \frac{\partial c_1}{\partial x} = -D_1 \frac{\partial c_1}{\partial x} \quad (4.6)$$

The same equation holds for the second component (switching to the second index of course)[8]. We also see this nice relationship between the **self-diffusivity** and **intrinsic diffusivity**.

$$D_1 \approx \left[1 + \frac{\partial \ln \gamma_1}{\partial \ln c_1} \right] D_1^* \quad (4.7)$$

So we have just described the fluxes in the C frame using 2 different intrinsic diffusivities[8]. But these planes are constantly moving in a non-uniform manner so it is not the best method to describe diffusion throughout the specimen. Instead, if there is no change in volume, we want to describe diffusion in terms of a single diffusivity, the interdiffusivity, which is measured in a single reference frame[8]. The volume reference frame.

4.4 V-Frame

But we also want an equation for the **velocity of the marker particles**! For that we need to define a new reference frame, **the V-frame or the volume-fixed frame which assumes there is no overall change in specimen volume during diffusion**.

This gives us the following condition:

$$\Omega_1 \vec{J}_1^V + \Omega_2 \vec{J}_2^V = 0 \quad (4.8)$$

Where again remember that Ω is the atomic volume for components 1 and 2 and you can typically assume each are constant throughout the material[8]. This condition states that the flux of volume through any given plane is zero, hence the volume fixed frame. We then find the flux in the V-frame to be:

$$\vec{J}_1^V = - \left[c_1 \Omega_1 D_2 + c_2 \Omega_2 D_1 \right] \frac{\partial c_1}{\partial x} = -\tilde{D} \frac{\partial c_1}{\partial x} \quad (4.9)$$

where \tilde{D} is the **interdiffusivity** i.e. the diffusivity of component 1 in component 2 and vice versa. We can also make another approximation that typically $\Omega_1 = \Omega_2 = \langle \Omega \rangle$ and then the **interdiffusivity** becomes

$$\tilde{D} = X_1 D_2 + X_2 D_1 \quad (4.10)$$

The flux for component 2 also follows similarly[8]. The equation for the velocity of the markers in the C-frame with respect to the V-frame is:

$$v_c^V = (D_1 - D_2) \Omega_1 \frac{\partial c_1}{\partial x} \quad (4.11)$$

Thank you for staying with me through all that math. This is a very complex derivation and is done in Kinetics of Materials if you are interested. The key takeaways for you to have is what are the assumptions made and to know some of these key expressions. Now let's get back to what

is happening physically.

Now what does this mean physically in terms of the Kirkendall effect. Well let's go back to Kirkendall's experiment where he had a brass diffusion couple, placed Mo wires along the length, and then wrapped it in pure Cu foil and let the material anneal at high temperatures for long times[8]. Look at the example diffusion couple in the figure below with our reference plane indicated in green.

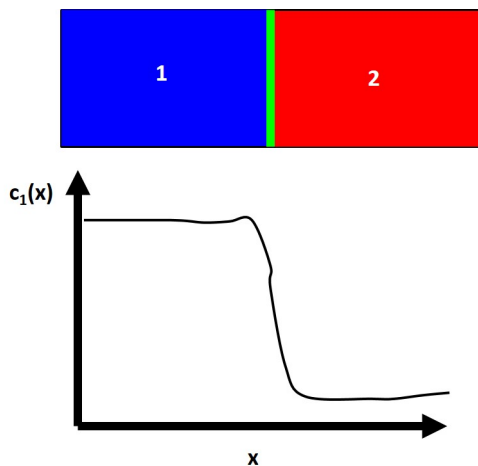


Figure 4-4: Diffusion Couple

As we previously described in the C-frame because these materials have different intrinsic diffusivities to conserve the number of sites must be conserved[8].

So if the fluxes of each component is not zero where will my marker move. Well let's say that in this alloy that the blue material is smaller, has a higher intrinsic diffusivity, and has a higher solubility in the red material than the red has for blue[8]. What is going to happen? Well if the intrinsic diffusivity is larger for blue than red more blue atoms are going to diffuse into the red so the flux of blue is larger than red[8]. That will result in a flux of vacancies toward the blue end. As more of the vacancies are consumed by blue particles on the red side the extra half planes of atoms will grow and cause expansion on the red side. On the blue side the vacancies will continue to flood in and destroy the extra half planes of atoms and cause that side to shrink. This will cause our original plane of atoms to move the blue side in the direction of vacancy flux.

Let's take Kirkendall's experiment as an example. The intrinsic diffusivity of zinc is larger than copper and thus the flux of zinc from the bar to the pure copper will be larger than the flux of copper from the pure copper into the brass bar[8]. Thus there will also be a flux of vacancies into the brass rod as well. Now when we have a flux of vacancies into the brass rod we are essentially destroying the extra half planes of dislocations via dislocation climb while we are completing the extra half planes in the pure copper foil. Thus on the copper foil side there is expansion and on the brass rod side there is contraction[8]. Thus the Mo foil will move towards the brass rod side or in the direction of the vacancy flux and that can be seen in the equation for the velocity of the plane of marker particles which determines the direction of the plane depending on the relative ratios of the intrinsic diffusivities of component 1 or 2.

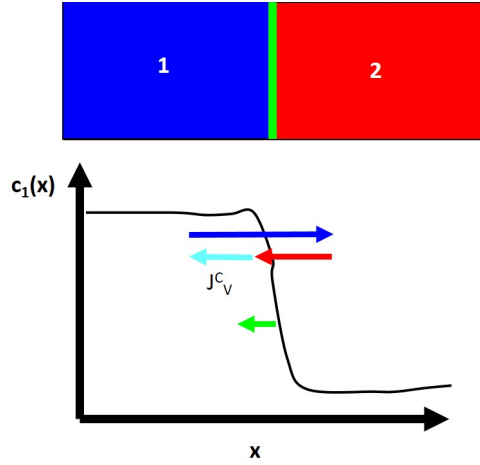


Figure 4-5: Kirkendall Effect

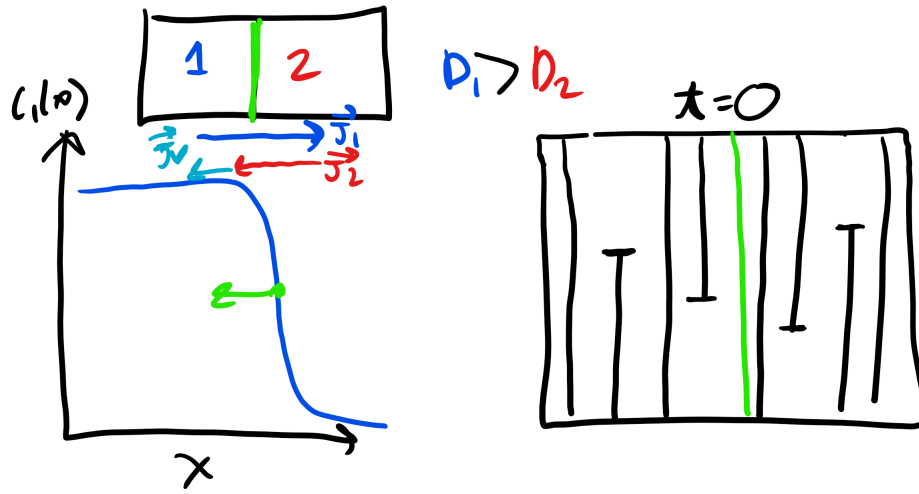


Figure 4-6: Kirkendall Creation and Destruction of Half Planes

4.5 Conjugate Forces to Drive Diffusion

Now there are a whole host of additional diffusion driving forces or conjugate forces as we mentioned in the beginning which can be summed up in the table below[8]:

Conjugate Force	Description
$\Phi_j = \mu_j$ or c_j	Chemical interactions
$\Phi_j = \mu_j + q_j \phi$	The diffusing species has change in electric field
$\Phi_j = \mu_j + \Omega_j P$	Diffusion in response to hydrostatic stress gradients
$\Phi_j = \mu_j + \gamma \kappa \Omega_j$	Surface diffusion in response to a curvature gradient
$\Phi_j = \mu_j + T$	Mass diffusion in a thermal gradient

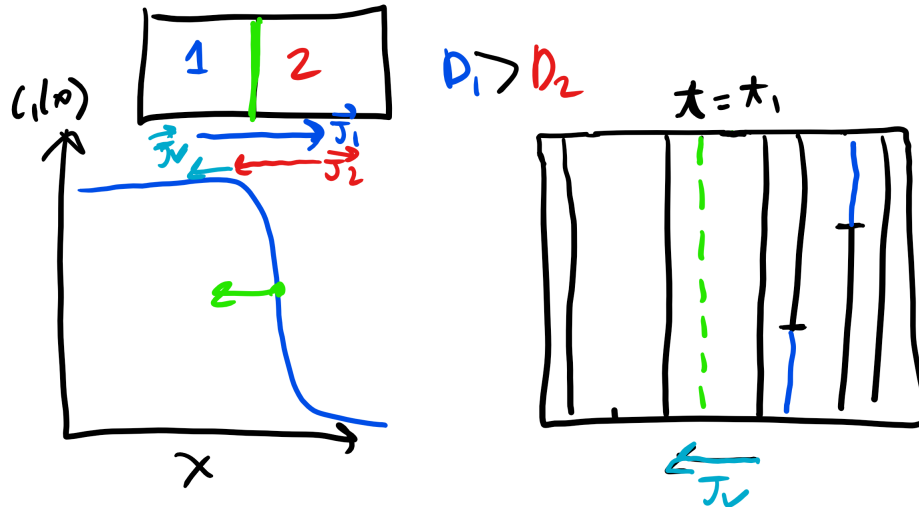


Figure 4-7: Kirkendall Creation and Destruction of Half Planes

4.5.1 Charged Species

We obviously do not have time to go through each of these scenarios but one example of charged chemical species in an electric field would be lithium ion batteries. What is interesting here is that you see you have effectively **two different diffusion contributions** one from the **chemical** gradients and one from the **electric field gradient**[8]. Now you can imagine that if you tune the electric field gradient you can **obtain a scenario where the flux is zero** when the two contributions are equal or you can actually **achieve uphill diffusion when the electric field component is larger!** The key thing is obviously the positively charged ions will diffuse towards the anode in this scenario[8].

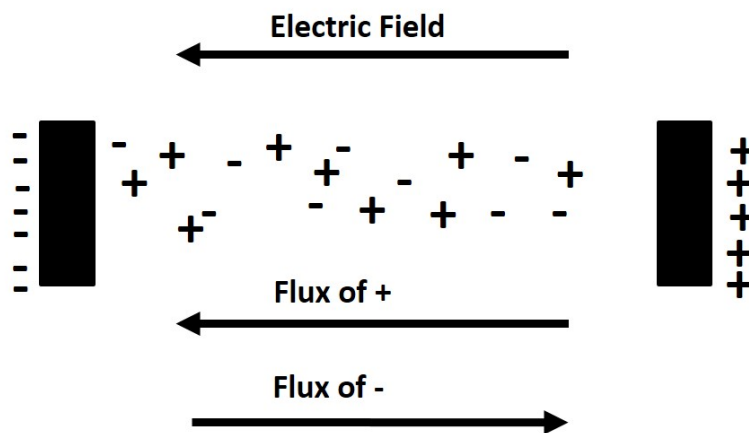


Figure 4-8: Electric Driven Diffusion

4.5.2 Temperature Gradient

For temperature and a chemical gradient the same scenario can be imagined and **typically atoms will migrate toward higher temperatures**[8].

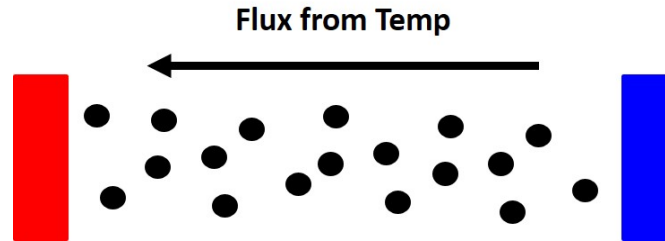


Figure 4-9: Temperature Driven Diffusion

4.5.3 Curvature

For curvature the flux will be from positive to negative curvature[8].

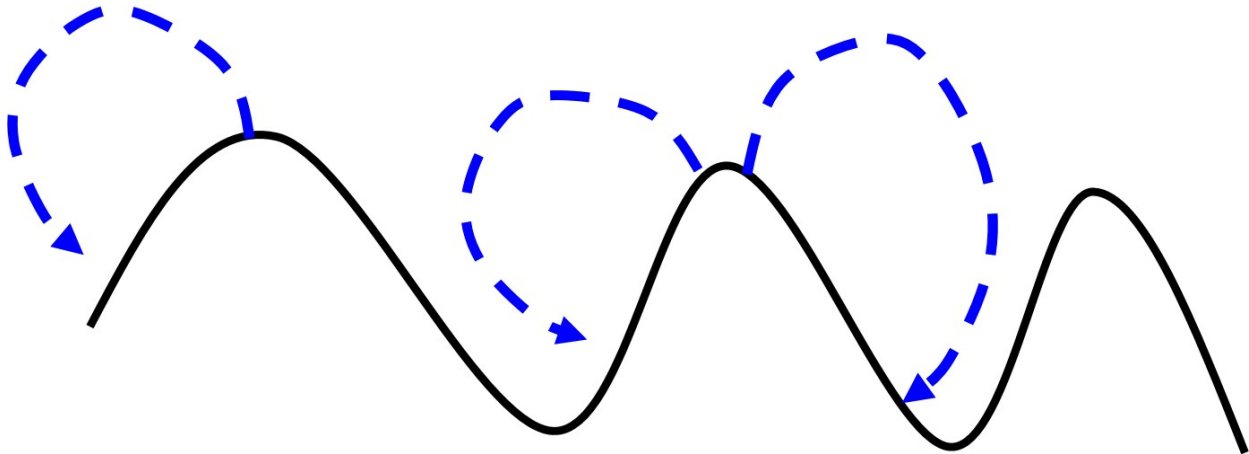


Figure 4-10: Curvature Driven Gradient

4.5.4 Stress

An interesting case occurs for atoms under hydrostatic stress or near a edge dislocation. Again for stress typically you observe migration from compressive regions toward the tensile region[8]. So for an edge dislocation is introduced into a region with a uniform interstitial concentration the solute atoms will immediately begin diffusing toward the tensile region[8]. Yet, the opposing concentration gradients will build up an eventually you will get to a steady-state solute atmosphere, known as a Cottrell atmosphere, which is when the concentration and stress conjugate forces cancel out. Look at Mathematica notebook/demonstration.

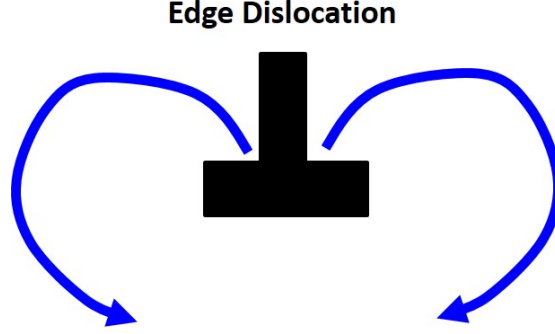


Figure 4-11: Stress Driven Diffusion

4.6 Fick's Second Law

We have hinted now several times about the time dependence or component associated with diffusion and now we will address this directly with **Fick's Second Law**[8]:

$$\frac{\partial c}{\partial t} = \dot{n} - \nabla \cdot \vec{J} \quad (4.12)$$

where \dot{n} is the rate of creation of new species (typically this is zero) and \vec{J} is the flux in the V frame so this equation then becomes

$$\frac{\partial c}{\partial t} = D(c) \nabla^2 c + \frac{dD(c)}{dc} (\nabla c)^2 \quad (4.13)$$

This equation hold for when D varies with the concentration, i.e. D is dependent on the concentration[8]. Typically (and much easier) D is independent of concentration and we get the following expression for Fick's Second Law:

$$\frac{\partial c}{\partial t} = D \nabla^2 c \quad (4.14)$$

Now we can solve how the concentration field or profile ($c(x,t)$) evolves under certain conditions and boundary-value diffusion problems[8]. Let's first look at a diffusion couple.

To solve this problem we are going to introduce the dimensionless variable η

$$\eta = \frac{x}{\sqrt{4Dt}} \quad (4.15)$$

Then we can convert Ficks Second Law from a PDE in x and t to an ODE in η . For this example we have 1D diffusion so:

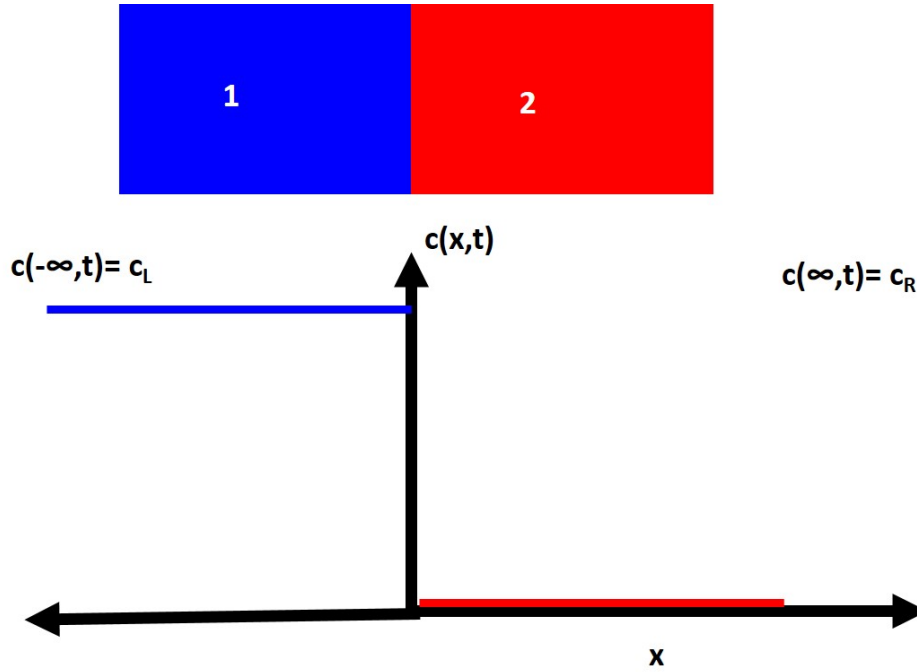


Figure 4-12: Diffusion Couple Concentration Evolution

$$\frac{\partial}{\partial t} = \frac{\partial \eta}{\partial t} \frac{\partial}{\partial \eta} \quad (4.16)$$

$$\frac{\partial}{\partial x} = \frac{\partial \eta}{\partial x} \frac{\partial}{\partial \eta} \quad (4.17)$$

where

$$\frac{\partial \eta}{\partial t} = \frac{-xD^{\frac{-1}{2}}t^{\frac{-3}{2}}}{4} \quad (4.18)$$

$$\frac{\partial \eta}{\partial x} = \frac{1}{2\sqrt{Dt}} \quad (4.19)$$

which can then be simplified to (remember back to chain rule)[8]:

$$-2\eta \frac{\partial c}{\partial \eta} = \frac{\partial^2 c}{\partial \eta^2} \quad (4.20)$$

For the step function example we need to re-write our boundary conditions in terms of:

$$q = \frac{dc}{d\eta} \quad (4.21)$$

$$-2\eta q = \frac{dq}{d\eta} \quad (4.22)$$

We can then integrate this to get

$$\frac{dc}{d\eta} = a_1 \exp^{-\zeta^2} \quad (4.23)$$

Then integrating again

$$c(\eta) - c(\eta_0) = a_1 \int_{\eta_0}^{\eta} \exp^{-\zeta^2} d\zeta \quad (4.24)$$

We can then plug in our boundary conditions which are $c(\eta = -\infty) = c^L$ and $c(\eta = \infty) = c^R$ and get

$$c(\eta) = c^L + \frac{a_1}{\sqrt{\pi}} \left(\int_{-\infty}^0 \exp^{-\zeta^2} d\eta + \int_0^{\eta} \exp^{-\zeta^2} d\zeta \right) \quad (4.25)$$

now you should recognize that

$$erf(z) = \frac{2}{\sqrt{\pi}} \int_0^z \exp^{-\eta^2} d\eta \quad (4.26)$$

And once we plug in and solve for our boundary condition we get our final expression[8]

$$c(x, t) = \frac{c_L + c_R}{2} + (c_R - c_L) erf\left(\frac{x}{\sqrt{4Dt}}\right) \quad (4.27)$$

We have our solution for a diffusion couple!!!! Look at the mathematica notebook to see how the solution evolves over time. Now that is a lot of disgusting math. I do not expect you to solve this problem by hand. We have a lot of cool math software and programs that can solve these ODE's. What I expect is for you to be able to deduce the boundary conditions and set them appropriately.

Let's do another example where we are considering diffusion of a species into semi-infinite solid where the surface concentration is held constant.

The boundary conditions for this problem are that at all times greater than zero

$$c(0, t) = C_s \quad (4.28)$$

$$c(\infty, t) = C_o \quad (4.29)$$

When can we make the semi-infinite approximation?

When the length, $l > 10\sqrt{Dt}$!

And we find that our expression for the semi-infinite solution for this problem to be

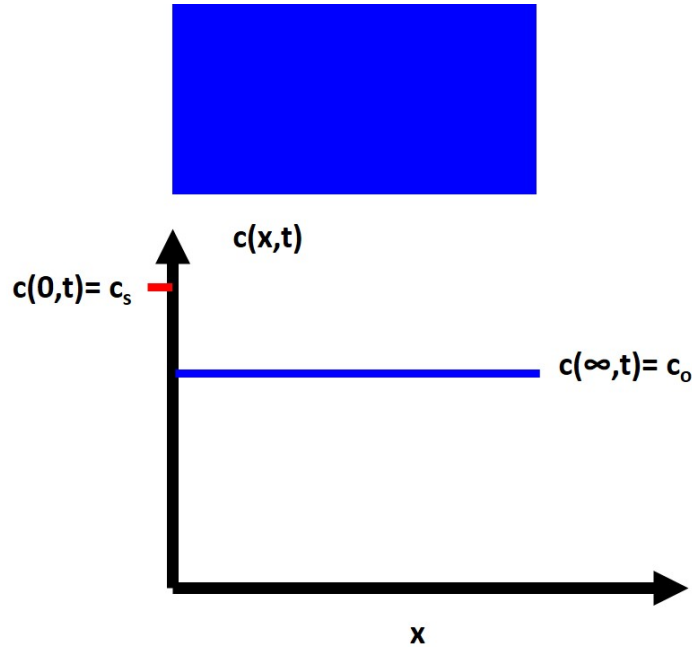


Figure 4-13: Semi-infinite Diffusion Solution

$$c(x, t) = C_s \left(1 - \operatorname{erf} \left(\frac{x}{\sqrt{4Dt}} \right) \right) + C_o \operatorname{erf} \left(\frac{x}{\sqrt{4Dt}} \right) \quad (4.30)$$

4.7 Engineering Approximation Diffusion Depth

You can solve a number of diffusion scenarios using this technique in conjunction with superposition principle but you can also solve many of these problems numerically as well[8]. There are also problems that are **steady-state diffusion** as well where there is **no time variation in composition**. There is also a very convenient **engineering approximation for estimating the diffusion depth**[8]. These engineering approximations are very handy and a lot of the time extremely accurate. As you see above many of the solutions to the composition profile adopt an **erf** like functional form. Now if you plug in a couple of values into the erf function you will see that about at value of **2** for x we see that the profile essentially becomes constant at that point, i.e. the diffusion is flat and there is no more diffusion[8]. You can solve for the diffusion depth, x , at that point if you know the time and D . So to estimate the diffusion depth use the following equation:

$$1 = \frac{x}{2\sqrt{Dt}} \quad (4.31)$$

4.8 Arrhenius Temperature Dependence of Diffusion and Anisotropy

So far we have been discussing the concentration dependence of D but you should also recognize that D also depends on temperature and it is also a tensor property which may or may not be anisotropic[8]. First let's talk about the **dependence of diffusivity with temperature**. The temperature dependence of diffusivity is

$$D = D_0 \exp\left(\frac{-Q_a}{kT}\right) \quad (4.32)$$

where Q_a is the activation energy for diffusion and D_0 is a constant. Again you can recognize that this is an **Arrhenius relationship**.

Let's do a practice problem where we can put this to work by looking at the graph below:

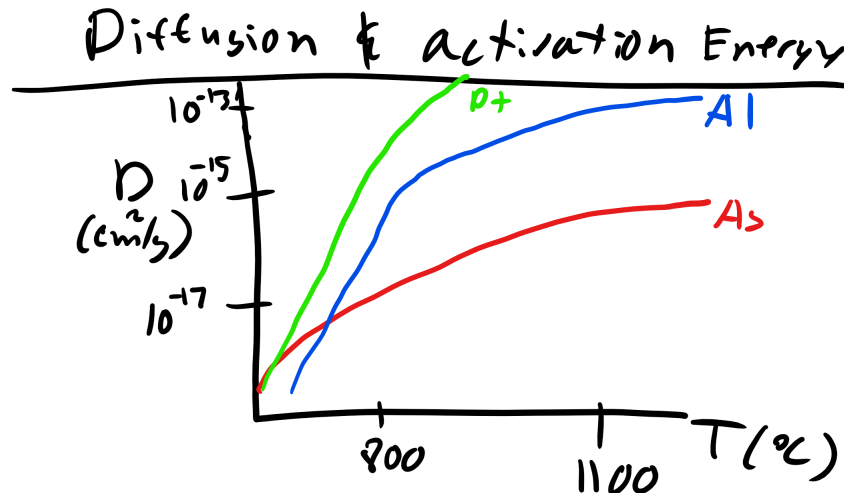


Figure 4-14: Diffusivity of Impurities in Silicon

What is the Diffusivity of Aluminum at 800°C?

What is the Diffusivity of Aluminum at 1100°C?

What is the activation energy for diffusion of aluminum?

What is D_0 ?

How long will it take for aluminum to diffuse 1 μm into silicon at 900°C?

Now you might think that diffusion is an isotropic property however it is actually highly anisotropic for certain materials[8]. Just a reminder anisotropy means that material properties will have different scalar values along different directions, typically crystallographic directions[8]. For cubic materials

$$\begin{bmatrix} D_{11} & 0 & 0 \\ 0 & D_{11} & 0 \\ 0 & 0 & D_{11} \end{bmatrix} \quad (4.33)$$

For tetragonal materials

$$\begin{bmatrix} D_{11} & 0 & 0 \\ 0 & D_{11} & 0 \\ 0 & 0 & D_{33} \end{bmatrix} \quad (4.34)$$

For hexagonal materials

$$\begin{bmatrix} D_{11} & 0 & 0 \\ 0 & D_{11} & 0 \\ 0 & 0 & D_{33} \end{bmatrix} \quad (4.35)$$

For orthorhombic materials

$$\begin{bmatrix} D_{11} & 0 & 0 \\ 0 & D_{22} & 0 \\ 0 & 0 & D_{33} \end{bmatrix} \quad (4.36)$$

For monoclinic materials

$$\begin{bmatrix} D_{11} & 0 & D_{13} \\ 0 & D_{22} & 0 \\ D_{31} & 0 & D_{33} \end{bmatrix} \quad (4.37)$$

For triclinic materials

$$\begin{bmatrix} D_{11} & D_{12} & D_{13} \\ D_{21} & D_{22} & D_{23} \\ D_{31} & D_{32} & D_{33} \end{bmatrix} \quad (4.38)$$

4.9 Diffusion as Random Walk

Another way that you can think about diffusion is a series of discrete jumps or hops in an idealized random walk and you can obtain the equation, after a lot of math (if you are interested again this derivation is in Kinetics of Materials),

$$D = \frac{\Gamma \langle r^2 \rangle f}{2d} \quad (4.39)$$

Where $\langle r^2 \rangle$ is the average mean squared displacement, d is the dimensionality of the diffusion, f is the correlation factor of the hops, and Γ is the hopping frequency described by [8]:

$$\Gamma = \nu \exp\left(\frac{-G^m}{kT}\right) \quad (4.40)$$

where again ν is a constant, G^m is the migration energy, and you see this is **Arrhenius again**.

Now the correlation factor f quantifies how **correlated** the jumps are. For a **perfect random walk**, i.e. no correlation $f = 1$. If **each jump is the each opposite of the previous jump** then $f=0$. Most **diffusion processes are closer to $f=1$** [8].

Now let's apply this to several different diffusion mechanisms. We have previously mentioned ring diffusion mechanism. However, **the predominant mechanism for self diffusion in metals (FCC, BCC, HCP) and many ionic crystals is the vacancy mechanism**[8].

Let's take the case of vacancy diffusion in an FCC lattice.

We can write the expression for diffusion. Let's assume $f=1$. Now for the jump rate $\Gamma = 12\Gamma'$. The jump rate is the same jump rate expression we described previously but it is multiplied by because there are 12 NN sites[8]. Additional r is the intersite jump distance which in this case is $r = \frac{a}{\sqrt{2}}$ which give us:

$$D = a^2 \nu \exp\left(\frac{S^m}{k}\right) \exp\left(\frac{-H^m}{kT}\right) \quad (4.41)$$

FCC Vacancy Diffusion

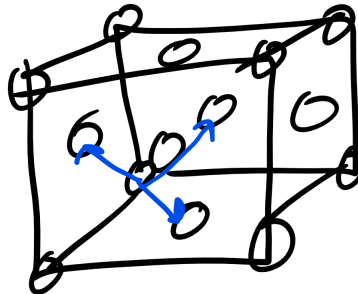


Figure 4-15: FCC Vacancy Diffusion

Interstitial diffusion mechanism is prominent for a **dilute solution of small interstitial components in a crystal of larger host atoms**. For **dilute solutions $f=1$** in this case.

Let's take the case of interstitial diffusion of carbon in BCC Fe where C resides in octahedral sites.

We can write the expression for diffusion. First we know that it is a dilute solution so assume $f=1$. Now for the jump rate $\Gamma = 4\Gamma'$. The jump rate is the same jump rate expression we described

previously but it is multiplied by because there are 4 NN C octahedral sites. Additional r is the intersite jump distance which in this case is $r = \frac{a}{2}$ which give us:

$$D = \frac{a^2}{6} \nu \exp\left(\frac{S^m}{k}\right) \exp\left(\frac{-H^m}{kT}\right) \quad (4.42)$$

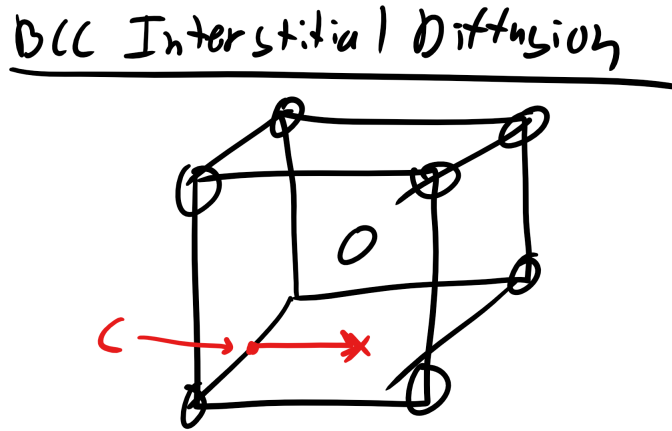


Figure 4-16: Interstitial Diffusion of Carbon Atoms in BCC

Also, interstitialcy mechanism involves a kickout process where two atoms move cooperatively or a dissociative mechanism.

4.10 Diffusion in Relation to Kroger-Vink

We can also now write the diffusion of elements in terms of the expression above and in our Kroger-Vink notation (Schottky and Frenkel defects). Let's take our old friend KCl and assume the dominant intrinsic defects are Schottky vacancies[8]

$$n_{\text{null}} = V_K' + V_{Cl} \quad (4.43)$$

We can write the equilibrium constant then as:

$$K_{eq} = K_S = [V_K'] [V_{Cl}] = \exp \frac{-G_S^f}{kT} \quad (4.44)$$

and electrical neutrality gives us the condition that

$$[V_K'] = [V_{Cl}] \quad (4.45)$$

which finally yields

$$[V'_K] = [V_{Cl}] = \exp \frac{-G_S^f}{2kT} \quad (4.46)$$

With this we can finally write the expression for diffusion as

$$D = a^2 \nu \exp \left(\frac{S^m + \frac{S_S^f}{2}}{k} \right) \exp \left(\frac{-H^m - \frac{H_S^f}{2}}{kT} \right) \quad (4.47)$$

The above expression for the vacancy populations is then entered into the expression for the self diffusivity of K and Cl[8]. We have to add not only the energy of migration but also this expression for the energy of formation of the Schottky defects[8].

We can also include an extrinsic defects where we incorporate CaCl_2 in the KCl crystal structure where we get



so now my total charge neutrality condition is

$$[V'_K] = [V_{Cl}] + [\text{Ca}_K'] \quad (4.49)$$

Now we can solve for the equilibrium concentration of K vacancies. Remember:

$$K_{eq} = K_S = [V'_K][V_{Cl}] = \exp \frac{-G_S^f}{kT} \quad (4.50)$$

This with our charge neutrality condition allows us to solve for $[V'_K]$ using quadratic formula get's us

$$[V'_K] = \frac{[\text{Ca}_K'] + \sqrt{[\text{Ca}_K']^2 - 4K_S}}{2} \quad (4.51)$$

In the **intrinsic case**, i.e. **low temperatures and very small concentrations of Ca**, we can plot the concentration and diffusivity vs temperature and in the extrinsic case, i.e. high temperatures and high concentrations of Ca[8].

These problems get even more interesting when we start having to also consider oxidation and reduction but you will have to wait for that discussion until the Electrochemistry Lecture.

4.11 Diffusion Depends on Local Environment

Now it's important to realize that diffusion will also be different for any material depending on the local environment i.e. if there are defects, dislocations, etc. However, we can make some predictions on the relative diffusivities in these different environments and we will specifically look at the **diffusivity along or within a dislocation core** (D^D), **diffusivity along a grain boundary** (D^B), **diffusivity along a free surface** (D^S), **diffusivity in the bulk crystal**

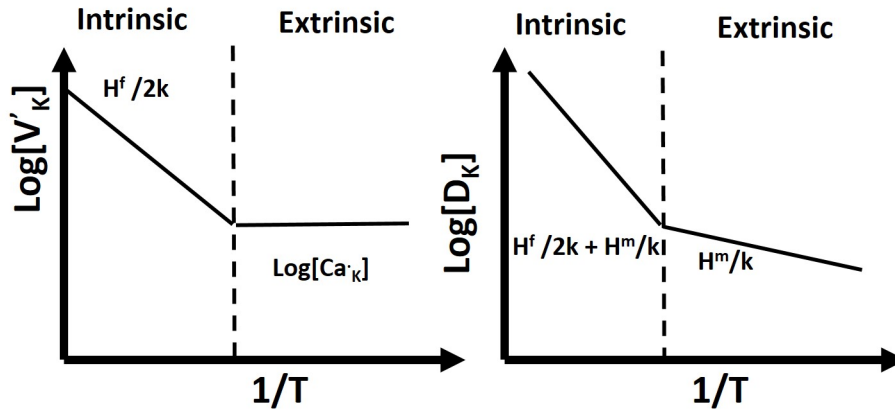


Figure 4-17: Concentration and Diffusion of Vacancies

free of line or planar defects (D^{XL}), and diffusivity in a liquid (D^L)[8].

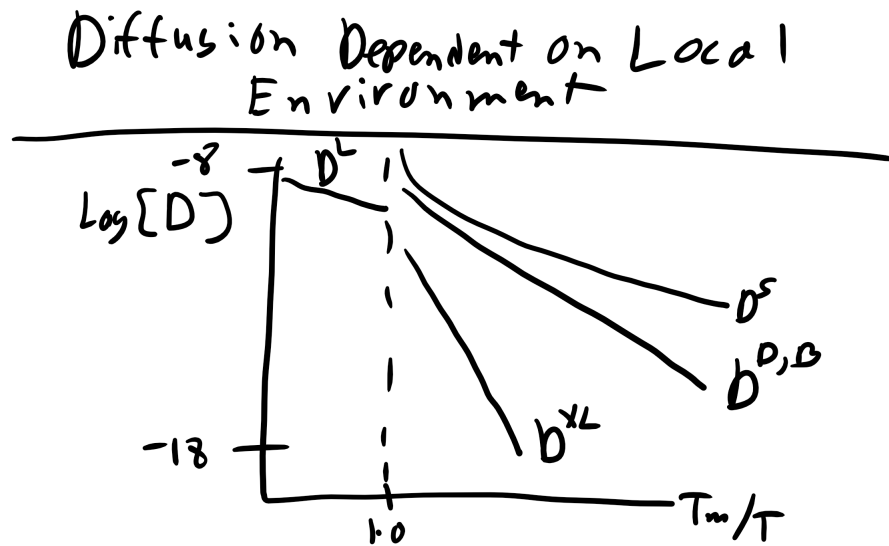


Figure 4-18: Diffusion in Different Environments

Taking a look at the plot and we can see the relative ranking of diffusivity in $D^L > D^S > D^D \approx D^B > D^{XL}$ [8]. And this should make sense because there is more **open space** in regions with more defects and thus the energy for particle or atom migration is much lower and that increases the diffusivity compared to in the pure bulk crystal that has little or no defects[8]. There you are surrounded by other atoms and must wait for atomic vibrations to open up enough room to squeeze and move between atoms.

Part III

Phase Diagrams and Microstructural Evolution

THIS PAGE INTENTIONALLY LEFT BLANK

CHAPTER 5

PHASE DIAGRAMS

5.1 Lowest Energy Wins!

Materials can exist as **different phases**, i.e. **solid, liquid, gas, vapor, plasma** and each of those phases are described by their own unique free energy curve [9]. **The thermodynamically stable phase is the one with the lowest free energy at any given temperature, pressure, composition, etc.** And **crossing points** in the free energy curves will **define the locations of phase transitions** [9]. We can see this schematically when considering a pure single component material going undergoing melting and we can plot the free energy as function of temperature and see the phase transition [9].

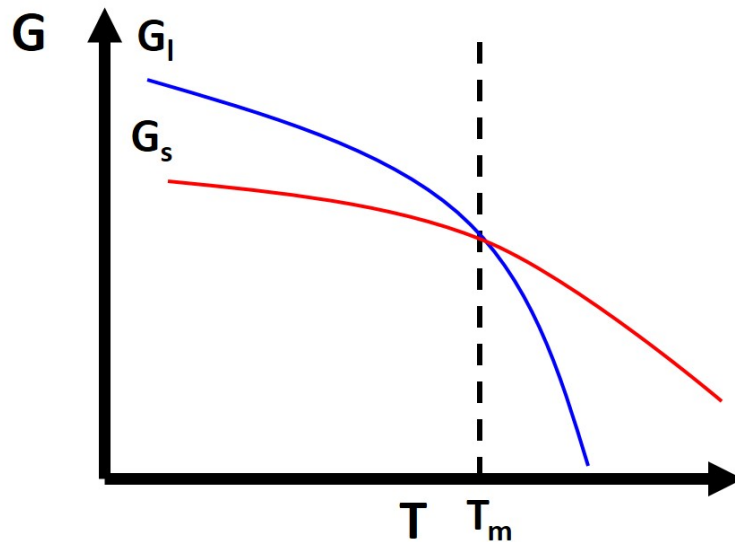


Figure 5-1: Free Energy Curve Melting Phase Transition

where \overline{G}_l is the molar Gibbs free energy of the liquid phase and \overline{G}_s is the molar Gibbs free energy of the solid phase. I will try to be as consistent as possible to keep liquid as blue color, like water.

We can also draw this out for the complete phase transition spectrum for a given material as the solid **melts**, the liquid **boils**, and the solid can **sublimate** directly to vapor [9].

However as we touched upon in structure materials can exhibit different crystalline forms in the solid state depending on the conditions of temperature and pressure.

What was the special name for these materials?

Polymorphs/allotropes.

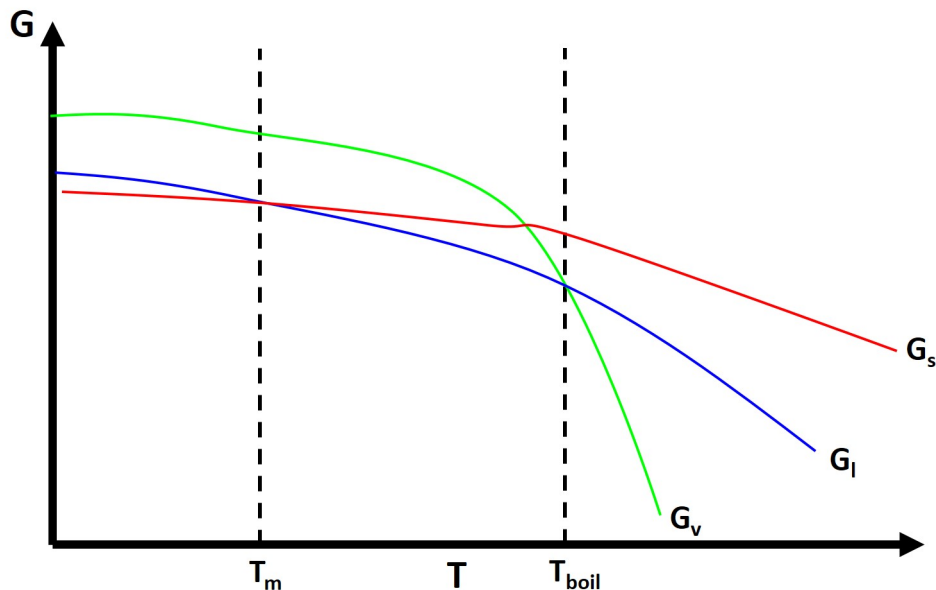


Figure 5-2: Free Energy Curve Melting and Vaporization

Wouldn't it be useful to have some type of diagram that would allow us to visualize these different phases....hmmm....!

5.2 Phase Diagrams of Single-Component Materials

Phase diagrams illustrate the phases of a system at equilibrium as a function of 2 or more thermodynamic variables.

Phase diagrams are also particularly useful because they **obey the laws of thermodynamics** and there are constraints on the structure of phase diagrams, particularly the **Gibbs Phase Rule**.

5.3 Gibbs Phase Rule

The **Gibbs Phase Rule** determines how many phases can be in equilibrium simultaneously and when those phases are stable along a field, line, or point in the phase diagram. There are **two criteria for phase equilibrium at a constant temperature and pressure** are that the **chemical potential of each component must be equal in each phase**:

$$\mu_1^\alpha = \mu_1^\beta = \mu_1^\gamma = \mu_1^P \dots \quad (5.1)$$

$$\mu_2^\alpha = \mu_2^\beta = \mu_2^\gamma = \mu_2^P \dots \quad (5.2)$$

$$\mu_C^\alpha = \mu_C^\beta = \mu_C^\gamma = \mu_C^P \dots \quad (5.3)$$

So we end up with $C(P-1)$ equations. And we also have the **second condition which is given by the Gibbs-Duhem equation** [9]

$$V^\alpha dP - S^\alpha dT - \sum_{i=1}^c n_i^\alpha d\mu_i^\alpha = 0 \quad (5.4)$$

$$V^\beta dP - S^\beta dT - \sum_{i=1}^c n_i^\beta d\mu_i^\beta = 0 \quad (5.5)$$

$$V^\gamma dP - S^\gamma dT - \sum_{i=1}^c n_i^\gamma d\mu_i^\gamma = 0 \quad (5.6)$$

So here we end up with **P equations**. So the **degrees of freedom (DOF)** is total number of variables - the total number of equations [9].

$$D = (CP + 2) - (C(P - 1) + P) \quad (5.7)$$

$$D = C - P + 2 \quad (5.8)$$

where D is the degrees of freedom, C is the number of components, P is the number of phases. The 2 comes from T and P as independent variables [9].

So let's do a couple of examples where we apply the Gibbs phase rule! Let's look at the single-component phase diagram below:

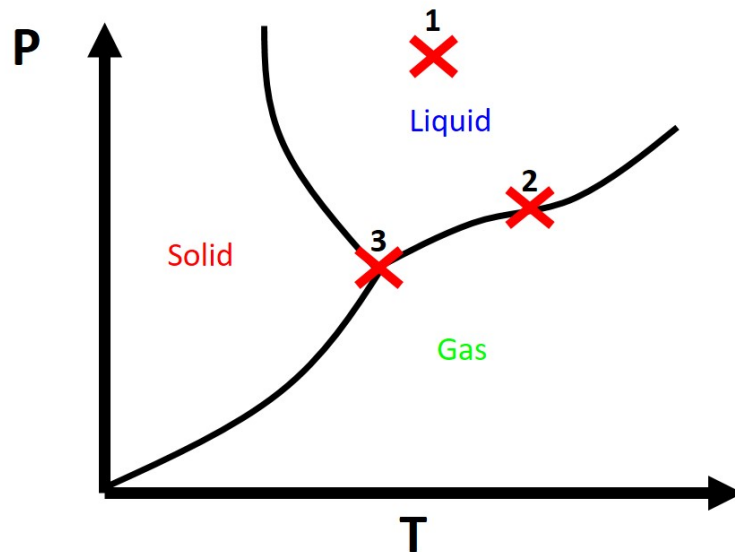


Figure 5-3: Single Component Phase Diagram

What is the DOF for the 1st X location?

The DOF is 2.

$$D + P = C + 2 \quad (5.9)$$

$$D + 1 = 1 + 2 \quad (5.10)$$

That means we can vary both T and P and still be in the liquid phase.

What is the DOF for the 2nd X location?

The DOF is 1. We can now only vary T or P freely the other is fixed.

What is the DOF for the 3rd X location?

The DOF is 0. We can not move anywhere. This is an **invariant or triple point**.

Now there is one unique point, an **invariant point**, called the **triple point** that can allow the 3 phases to co-exist, i.e. any change in the variables will cause the equilibrium to shift to either 1 or 2 phases in equilibrium. The slope of the 2-phase line on the P vs. T diagram is determined by the **Clausius-Clapeyron equation** evaluated at the coexistence curve:

$$\frac{dP}{dT} = \frac{\Delta \bar{S}^{S \rightarrow L}}{\Delta \bar{V}^{S \rightarrow L}} = \frac{\Delta \bar{S}_m}{\Delta \bar{V}_m} = \frac{\Delta \bar{H}_m}{T_m \Delta \bar{V}_m} \quad (5.11)$$

We know that typically the enthalpy of melting is positive so the slope of the P-T diagram for the solid-liquid coexistence curve should be positive [9]. Let's look at iron on the lecture slides. This seems to hold. What is happening between BCC and FCC?

5.4 Multi-Component Phase Diagrams

So far we have only dealt with phase diagrams of pure components but typically you will deal with either **binary, ternary, quaternary, etc. phase diagrams** [9].

Let's take a look at a relatively simple phase diagram, a **Binary Lens phase diagram** which holds for ideal solution scenarios.

(Side Note: When I say something is simple please do not interpret this as the concept being easy. These concepts are very difficult but what I mean by the problem is simple I want to encourage and show you that all these problems can be solved. When we say that this or that problem is really difficult that problem is given a special mystique and students might be wary about going about solving the problem or learning that concepts. By saying something is simple I want to remove that mystique.)

Note here that we are not varying pressure now because typically we are working in a **constant pressure environment**, although that is not necessarily always the case [9]. **Now this will change our Gibbs phase rule condition to:**

$$D + P = C + 1 \quad (5.12)$$

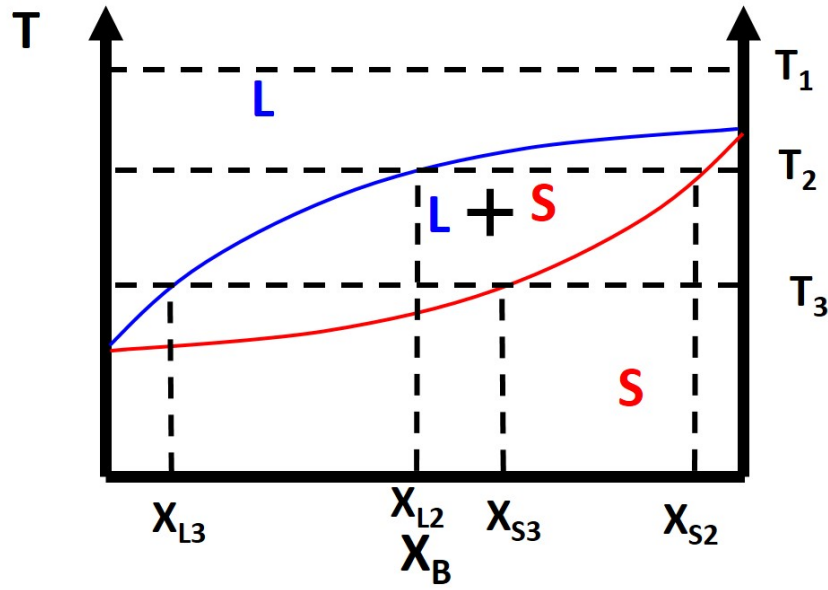


Figure 5-4: Binary Lens Phase Diagram

We can also take a look at the free energy diagrams as well to conceptualize the phase diagrams. At T_1 everything is as usual in terms of our free energy diagram with liquid phase being lower energy than the solid phase. Things start to get a little funky at T_2 where we have the two phase region of a solid and liquid. What happens here? Why does this occur? Well at compositions less than X_{L2} and greater than X_{S2} everything is normal. What happens is in between these compositions. You see that we can draw a common tangent line (purple). When you have a **common tangent** line the system can phase separate from a 1-component system (liquid) to a weighted mixture of two components (solid and liquid) which has a lower free energy than the starting 1-component phase. This is because the requirement for equilibrium as we previously mentioned is that the chemical potential of each component must be equal in all phases and we have the expression that the chemical potential μ is

$$\mu = \left(\frac{\partial G}{\partial n} \right)_{T,P} \quad (5.13)$$

So **common tangent rule** will allow us to find your equilibrium volume fraction of species in each phase via the **common tangents in free energy curves** and the slope is essential the chemical potential so when the slope is equal [9]. So between the common tangent points equilibrium will have the components in both phases, i.e. mixed as given below

$$\left(\frac{\partial G}{\partial X} \right)_{X=X^\alpha} = \left(\frac{\partial G}{\partial X} \right)_{X=X^\beta} \quad (5.14)$$

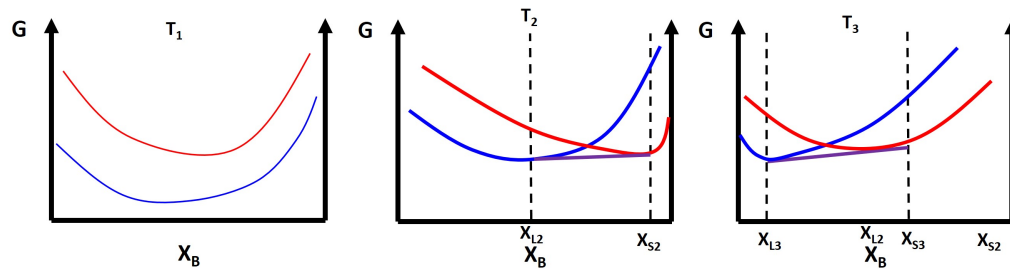


Figure 5-5: Binary Lens Phase Diagram

5.5 The Lever Rule:

Typically we are also interested in finding at a particular composition and temperature what will be the relative **fractions** of the **different phases of the material**, or in the case of a simple lens diagram, what fractions will be solid and liquid [9]. To calculate these **phase fractions** we will use the **lever rule**. Once you pick a temperature of interest, T_1 , and a composition, X_B^o then you draw a **horizontal isotherm** which connects or ties together the boundaries of a two phase regions. These horizontal isotherms are also called **tie lines** [9].

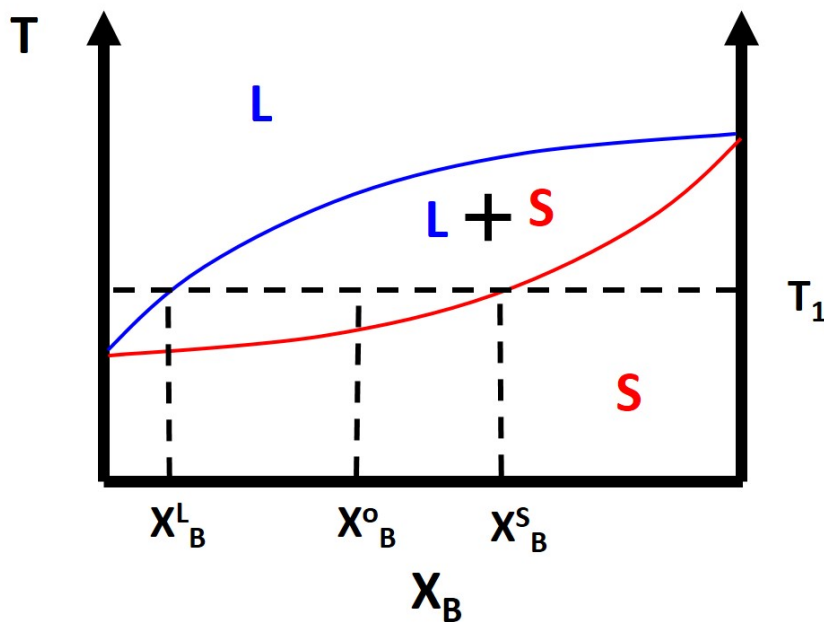


Figure 5-6: Lever Rule

The composition of the liquid and solid phases, X_B^L and X_B^S , respectively are simply where the tie line intersects the **liquidus** or **solidus** lines, again respectively [9]. The **liquidus** line defines the two phase coexistence between a liquid and a solid phase. The **solidus** line represent the two phase coexistence between a solid and another solid phase, for binary phase diagrams. We can also

calculate the fraction of phases that are present by using the lever rule. What you do is simply take the length of the tie line from the composition, X_B^o , to the phase boundary for the other phase and divide by the total tie line length [9]. For example:

$$f^S = \frac{X_B^o - X_B^L}{X_B^S - X_B^L} \quad (5.15)$$

$$f^L = \frac{X_B^S - X_B^o}{X_B^S - X_B^L} \quad (5.16)$$

where f^S and f^L are the phase fractions of solid and liquid respectively. This is typically the simplest type of phase diagram that you will find and it is actually the phase diagram for Cu-Ni. This also holds for ideal solution scenarios but typically most binary solutions or alloys will not be miscible at all compositions and temperatures. We know from structure that different materials have different crystal structures so those crystal structures might not always be compatible.

5.6 Phase Transitions Congruent vs Incongruent

A phase transition can occur **congruently** or **incongruently**. A **congruent** phase transition occurs when there is a complete transformation from one phase to another with no change in composition as seen in the examples below [9]. An **incongruent** phase transition is a partial transformation from one phase to another and there will be a change in composition like we just saw with the lens diagram [9].

5.7 Eutectic Phase Diagram

So far we have only discussed the **simple binary lens phase diagram** which only applied to several real experimental systems [9]. There is another relatively simple phase diagram that corresponds to many more experimental systems and that is the **binary eutectic phase diagram**.

The binary eutectic phase diagram has several distinctive features one being a **solid-solid phase mixture, limit of solubility at different temperatures, and an invariant point in the phase diagram, the eutectic point**.

The **solubility limit** is the maximum amount of solute that you can integrate into the structure (or phase) or the solvent to form a solid solution [9]. The solubility limit is a function of temperature and must be defined at a given temperature [9].

What is the solubility limit of B into A at T_1 ?

What about A into B?

Identify the Solidus Line

The **eutectic point** is an **invariant point**, $D = 0$, and it describes the constant composition transformation from a pure liquid phase to a two phase solid solution/mixture or alternatively [9]:

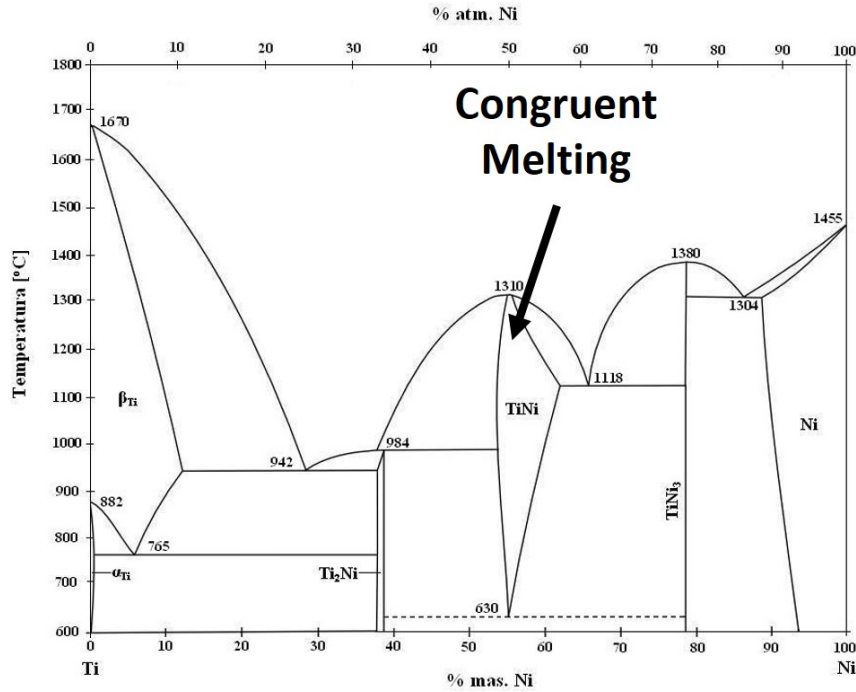


Figure 5-7: Congruent Melting

$$L\alpha + \beta \quad (5.17)$$

We know how the free energy will evolve as we cool from a purely liquid state for the lens and binary eutectic phase diagrams. But we can also see how the microstructure evolves [9]. We will get into why the microstructure adopts certain geometric structures when we get to our Nucleation and Growth Lecture next time.

There are also a number of different invariant points beyond the simple eutectic.

5.8 Eutectic, Eutectoid, Peritectic, Peritectoid, and Monotectic

We have already discussed one invariant point, the eutectic. There is also another invariant point called the **eutectoid** [9]. The **eutectoid** describes the constant composition transformation from a **pure solid phase** to **two phase solid solution/mixture** as described below

$$\gamma\alpha + \beta \quad (5.18)$$

This transformation is most notable in the iron carbon phase diagram where the **austenitic** phase can produce **ferrite** and **cementite**. This is obviously very similar to the eutectic but instead of liquid transforming into a two phase solid solution it is a solid undergoing this transformation.

There is also a **peritectic** invariant point [9]. The peritectic describes where a solid and liquid

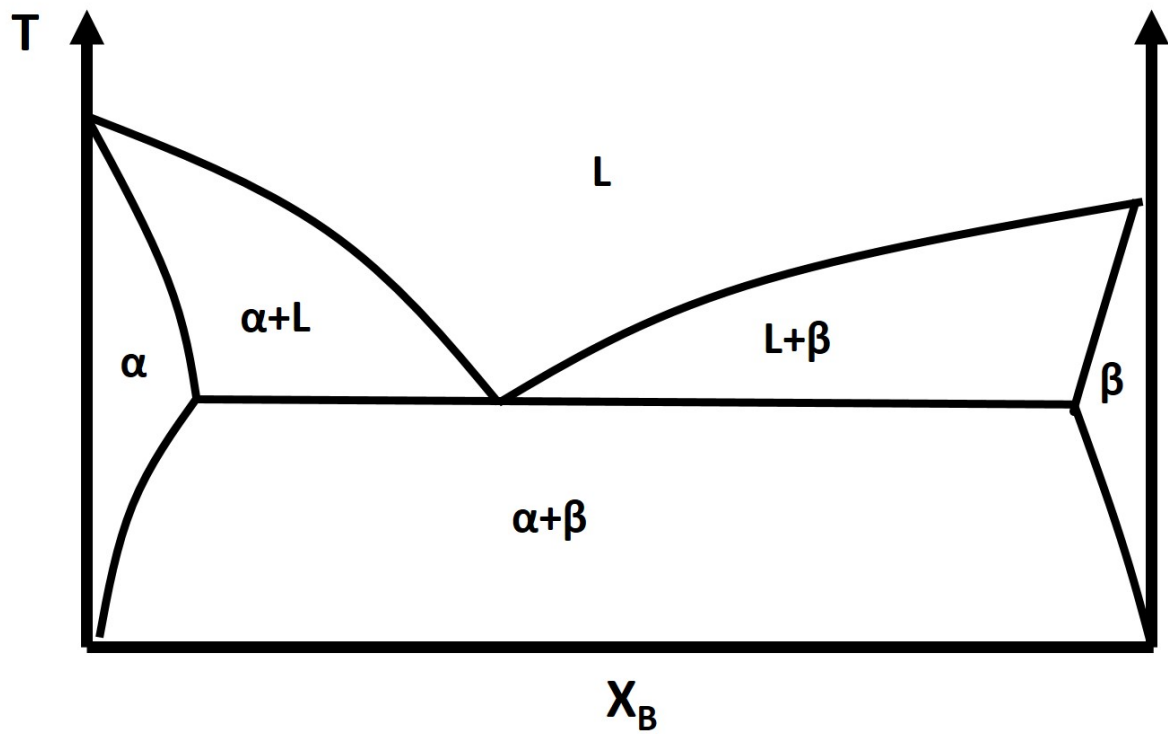


Figure 5-8: Binary Eutectic Phase Diagram

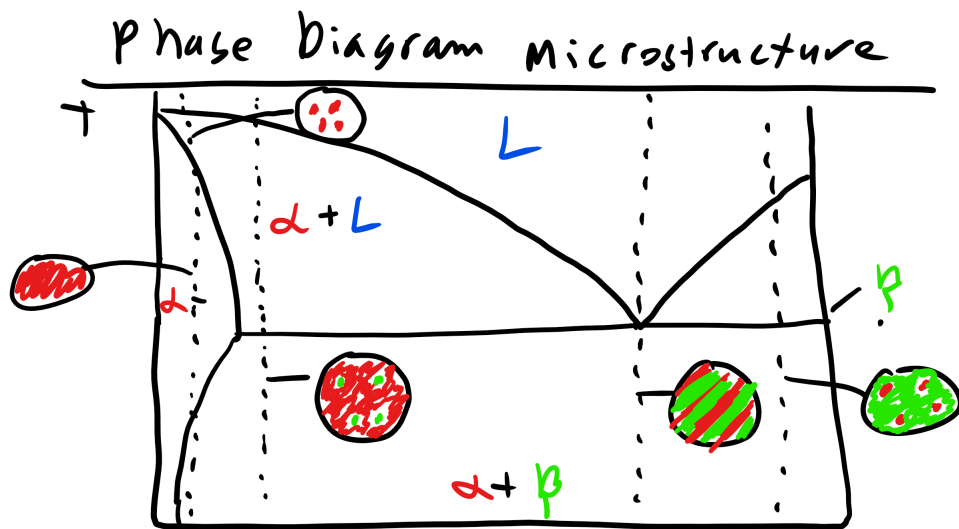


Figure 5-9: Binary Eutectic Microstructure Evolution

phase mixture will transform into a pure solid phase which is described by the equation below

$$L + \alpha\beta \quad (5.19)$$

This can also be seen in the iron phase diagram where the δ and liquid phase mixture transforms to pure austenite.

Finally the last invariant point is described by the **peritectoid** which is a transformation of two solid phases in a mixture to a single solid phase again described by the equation below [9]:

$$\gamma + \alpha\beta \quad (5.20)$$

There is also a **monotectic** invariant point that does not appear in too many phase diagrams but this invariant point describes the transformation from a pure liquid to another liquid and solid phase which is described by the equation below [9]:

$$L_1L_2 + \alpha \quad (5.21)$$

Let's do a couple of examples where we identify the invariant points in a couple of phase diagrams and calculate the fraction of phases at a given composition and temperature.

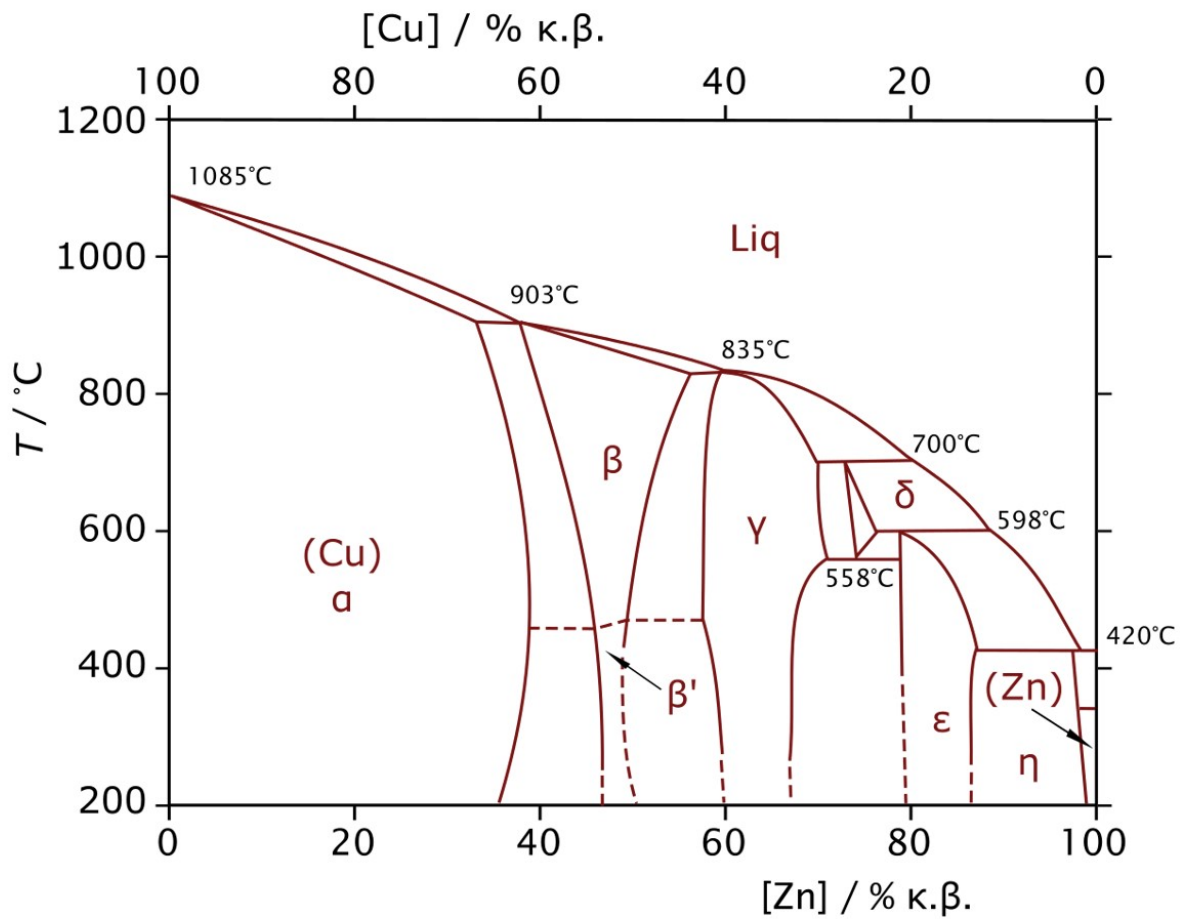


Figure 5-10: Identify the Invariant Points [?]

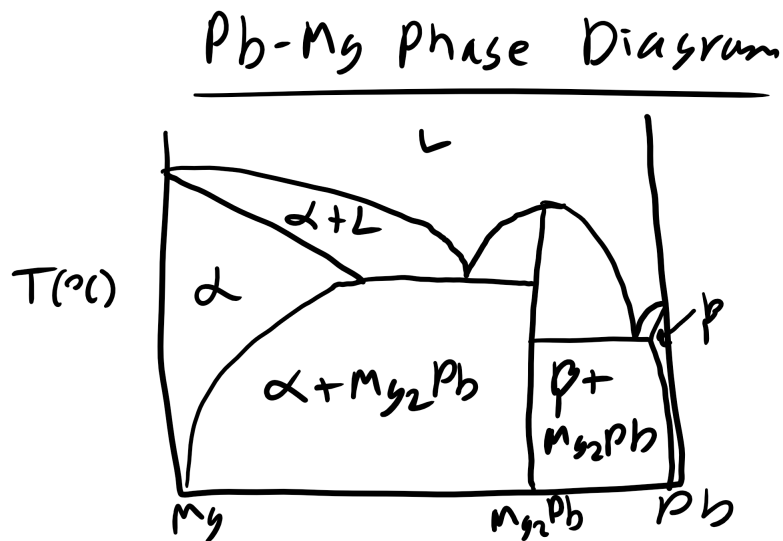


Figure 5-11: Identify the Invariant Points

5.8.1 Iron-Carbon Phase Diagram: A Must for Materials Science But Perhaps Not for Too Much Longer

The iron-carbon phase diagram is probably the most well known and studied phase diagram for obvious historical reasons. It is also a fantastic phase diagram to study because it includes many of the invariant points that we have discussed and there is probably no other phase diagram that has been studied more extensively so the kinetic and microstructure evolution at different temperatures and compositions is very well studied. Knowing this phase diagram front and back was once a must for any materials engineering student, particularly if you were to work in metallurgy [1]. However, as the field of materials science has evolved and really exploded to include polymers, biomaterials, magnetic materials, optical materials, acoustic metamaterials, etc. there is less emphasis on this phase diagram.

Nevertheless, we will study the phase diagram as seen below, note that we are only looking at a very small section of the phase diagram but this is relevant for steel [1]. **Pure iron** at room temperature has a **BCC** structure and is called **ferrite**, α , but upon heating it will undergo a **polymorphic** phase transformation **FCC** and is called **austenite**, γ at 912°C [1]. It will then revert back to **BCC** as δ -ferrite at 1394°C . Iron will finally **melt** at 1538°C [1].

5.8.2 Ternary and Quaternary Phase Diagrams

So far we have dealt with relatively simple binary phase diagrams however there are also much more complicated ternary and quaternary phase diagrams. These types of phase diagrams are crucial, particularly in the field of ceramics [1]. We can perform the same type of analysis on these diagrams but of course it becomes more complex.

5.9 Stable vs. Metastable Phase Boundaries: Cahn-Hilliard Spinodal Decomposition

We just touched upon the concept of stability and metastable with martensite. So let us define the **conditions for stability** [1]. For a closed system at constant temperature and pressure the **Gibbs free energy is minimized with respect to fluctuations in other extensive variables, particularly fluctuations in composition** [1]. To be stable against these fluctuations we have an additional condition on the second derivative of the free energy which is given by **Le Chatelier's principle**: A system perturbed by a **small fluctuation** will elicit a **thermodynamic driving force** to return to the **stable equilibrium state** [1]. Or in terms of fluctuations in composition the condition for stability is

$$\frac{\partial^2 G}{\partial X_B^2} > 0 \quad (5.22)$$

Let's take a look at this condition in the graph below:

We can clearly see here that we have several special points **binodals** and **spinodals**.

Binodals are defined by the following mathematical relations

$$\frac{\partial G}{\partial X_B} = 0 \quad (5.23)$$

$$\frac{\partial^2 G}{\partial X_B^2} > 0 \quad (5.24)$$

while **spinodals** are defined by

$$\frac{\partial^2 G}{\partial X_B^2} = 0 \quad (5.25)$$

We can also see a point in this diagram that is unstable where

$$\frac{\partial G}{\partial X_B} = 0 \quad (5.26)$$

$$\frac{\partial^2 G}{\partial X_B^2} < 0 \quad (5.27)$$

The **spinodal** points will define the **spinodal boundary** and the **binodal points** will define the **boundaries of the 2-phase regions** [1]. Systems that are initially unstable will undergo spinodal decomposition while systems that are initially stable or metastable will evolve via nucleation and mechanisms [1]. Spinodal decomposition is a homogeneous transformation while nucleation and growth is typically dominated by a heterogeneous process but more on that next lecture for Growth and Nucleation.

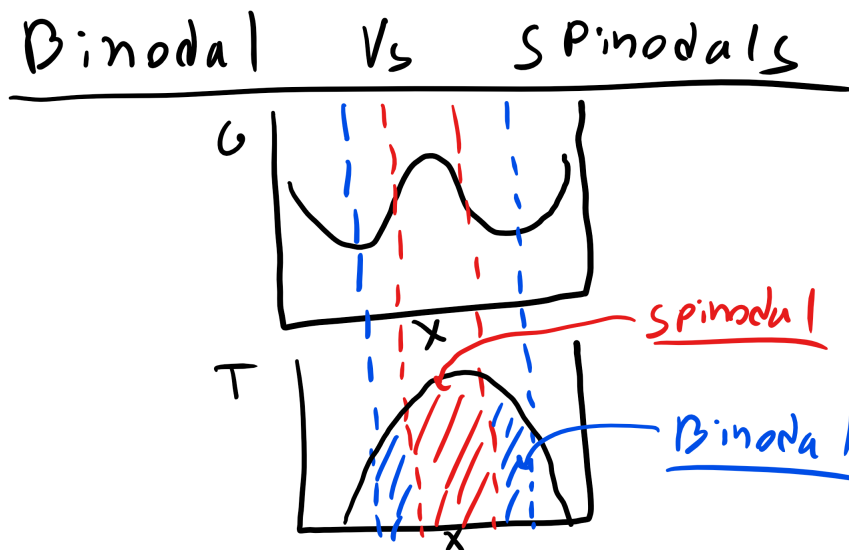


Figure 5-12: Stability Conditions

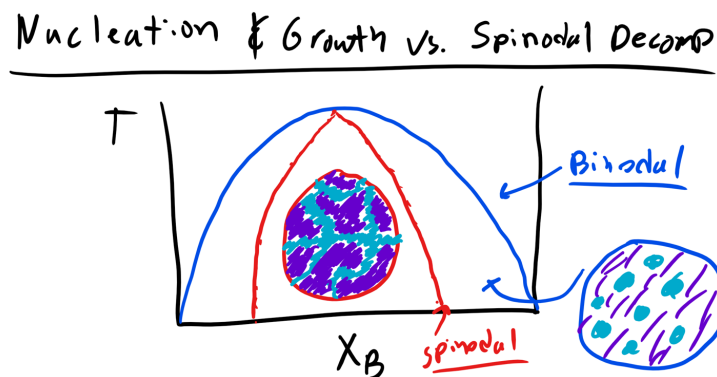


Figure 5-13: Nucleation and Growth Vs. Spinodal Decomposition

5.10 First Order vs Second Order Phase Transitions

This discussion brings us nicely to a discussion on the **order of phase transformations** [1]. So far we have really been focused on **first order phase transformations** like a crystal melting, water boiling, allotropes, etc, these are all first order phase transformations [1].

Why is that?

Well when we discuss order we are talking about whether the **transformation** is accompanied by a **discontinuity** in a **first, second, or higher order derivative** of Gibbs free energy [1].

The **second order transitions** are also called **continuous phase transitions** because the first derivative of Gibbs is continuous and it is not until there is a second order derivative that a discontinuity is observed [1]. Some examples of second order transitions are **ODT (Order-Disorder Transitions)**, glass transitions, superconducting transitions, ferromagnetic to

paramagnetic transitions.

We can see how these transitions look like by looking at Gibbs free energy.

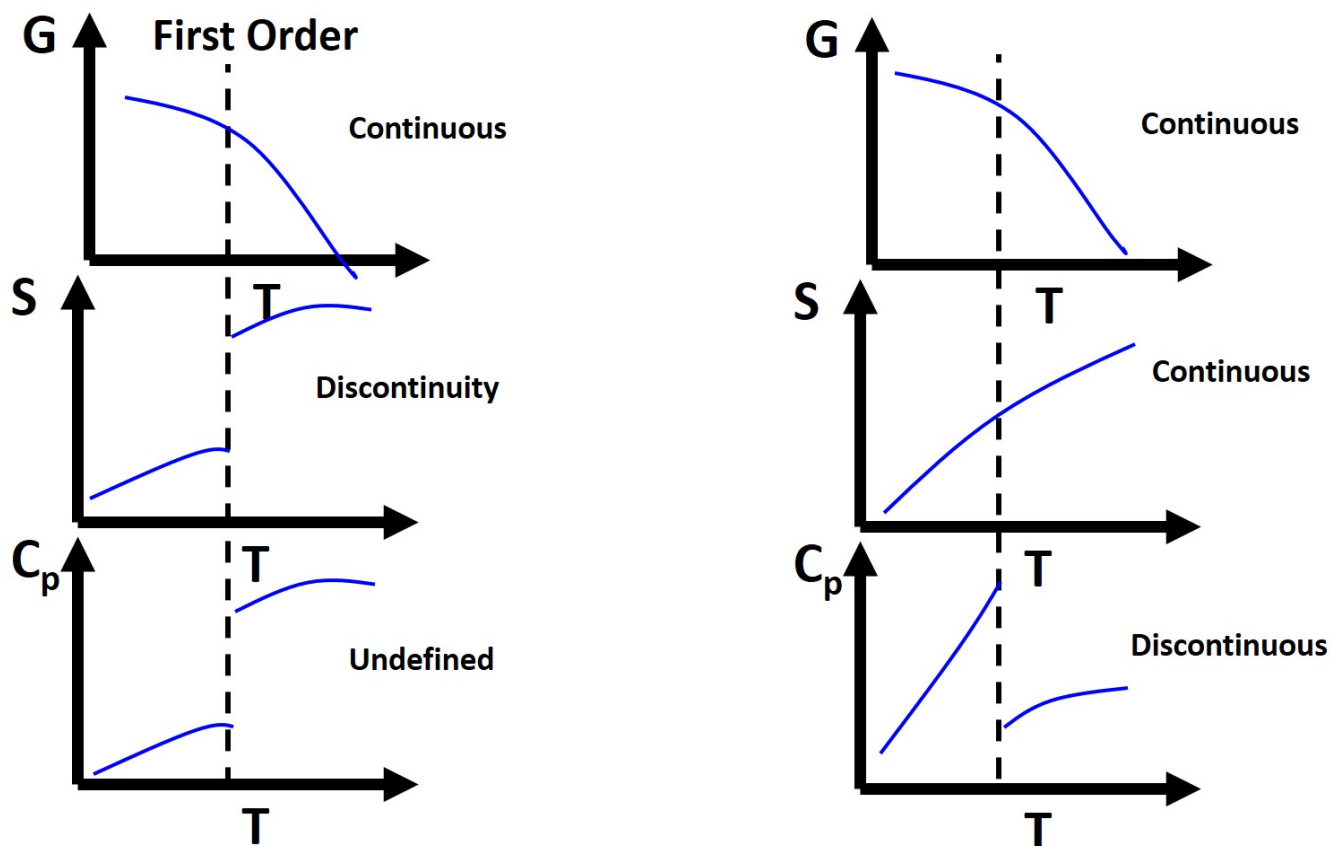


Figure 5-14: First and Second Order Phase Transitions

Remember from thermo that:

$$S = -\left(\frac{\partial G}{\partial T}\right)_{P,n} \quad (5.28)$$

$$C_p = -T\left(\frac{\partial^2 G}{\partial T^2}\right)_{P,n} \quad (5.29)$$

Can You Build The Phase Diagram From A Convolved and Self-Indulgent Story?

Your advisor is trying to submit a paper but needs help with the last figure an ReTi phase diagram. You have discussed it at length over the phone, office hours, etc. She asks you to label the diagram and submit the paper by 5:00PM tonight. However, when she updates the dropbox folder the file is corrupted. You try to get in touch with her but she is already off on sabbatical.

RE is HCP for all temperatures up to 3459K. Ti is hcp below 1155K, bcc between 115 and 1943K, and liquid above 1943K.

The system has one known intermediate compound at $\text{Ti}_5\text{Re}_{24}$. It appears at 3023K through a peritectic reaction from the liquid and hcp Re. It doesn't melt congruently. Another peritectic reaction occurs at 2298K which involves liquid, bcc Ti, and the aforementioned intermediate compound. At this peritectic temperature the bcc Ti-phase has a composition of about 50% Re. Addition of Re to Ti lowers the temperature at which the hcp Ti phase transforms to bcc.

Sketch the full phase diagram in the box below from 0 to 3500K.

THIS PAGE INTENTIONALLY LEFT BLANK

CHAPTER 6

NUCLEATION, GROWTH, AND OSWALD RIPENING

6.1 Surface Tension/Energy and Chemical Potential

Last lecture we actually already delved into a bit concerning the **kinetics of phase transformations**. However, here in this lecture we will delve more much deeply into these processes. To start typically when we have talked about phase transformations when we transform from a purely liquid state to a liquid and a solid mixture. In doing so we are essentially creating a **new surfaces** and this involves **work** so when we write out Gibbs Free Energy[?]

$$dG = VdP - SdT - \gamma dA \quad (6.1)$$

where γ is **surface tension or surface energy** and in a system at constant temperature and pressure with no additional work terms[?]

$$\gamma = \frac{\partial G}{\partial A}_{(T,P)} \quad (6.2)$$

this is **Surface Energy**[?]. Now the Gibbs free energy of a system will also typically depend on temperature and pressure, surface area, and the amount of moles added to the system which gives us

$$dG = -SdT + VdP + \gamma dA + \mu^P dn \quad (6.3)$$

So be careful here and notice that μ^P is not the chemical potential as typically defined below[?]:

$$\mu = \frac{\partial G}{\partial n}_{(T,P)} \quad (6.4)$$

instead it is

$$\mu^P = \frac{\partial G}{\partial n}_{(T,P,A)} \quad (6.5)$$

which is the work associated with the transfer of matter without changing the surface area. This distinction comes about from the fact that **dA** and **dn** are **not truly independent**[?]. You can't add matter to a system without changing the surface area. You can also think of μ^P as the chemical potential of a flat plate.

And in fact we can find a relationship between dA and dn for a simple case of a sphere we have[?]

$$dV = \bar{V} dn \quad (6.6)$$

where again \bar{V} is the molar volume. We know the derivative of the volume of a sphere to be

$$dV = 4\pi r^2 dr \quad (6.7)$$

and we also know that

$$dA = 8\pi r dr \quad (6.8)$$

with this we can find a relationship between dV and dA as seen below

$$dA = \frac{2}{r} dV \quad (6.9)$$

and by plugging back into 6.6 we get[?]

$$dA = \frac{2\bar{V}}{r} dn \quad (6.10)$$

We can also re-write our equation for Gibbs in terms of dn and eliminate dA

$$dG = -SdT + VdP + \left(\frac{2\gamma\bar{V}}{r} + \mu^P \right) dn \quad (6.11)$$

so we see that the total differential of G at constant T and P will yield the chemical potential of a sphere[?]

$$\mu_{sphere} = \frac{\partial G}{\partial n (T,P)} = \frac{2\gamma\bar{V}}{r} + \mu^P \quad (6.12)$$

6.2 Flux Across a Grain

We just calculated the chemical potential for spheres and talked about surfaces so let's delve in a little bit deeper into **curved grain boundaries** by looking at a scenario below where we have a curved boundary between two grains[?]. Now we can't talk about curves without talking about **curvature** and how to define whether the **curvature is positive to negative**[?]. In this class we define the curvature, K , of a circle or sphere as

$$K = \frac{1}{r_1} + \frac{1}{r_2} \quad (6.13)$$

where r_1 and r_2 are the principal radii of the curvature of a surface.

You can think of them as perpendicular tangents to the curvature and if they fall **inside** the material they are **positive** and if they lie **outside** of the material they are **negative**[?]. You can see that for material/grain 1 the curvature will be

$$K_1 = -\frac{2}{r} \quad (6.14)$$

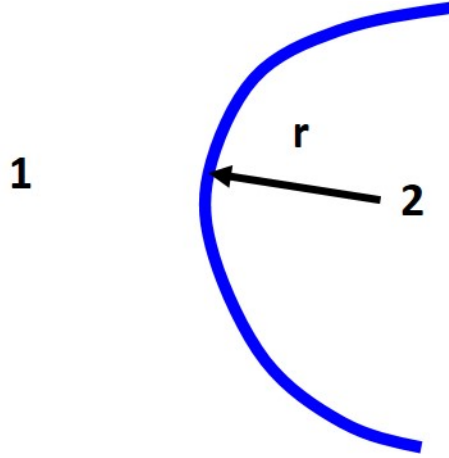


Figure 6-1: Curvature

and for material 2

$$K_2 = \frac{2}{r} \quad (6.15)$$

so we can write the **chemical potentials of material/grain 1 and 2** as

$$\mu_1 = \mu^P - \frac{2\gamma_{GB}\bar{V}}{r} \quad (6.16)$$

$$\mu_2 = \mu^P + \frac{2\gamma_{GB}\bar{V}}{r} \quad (6.17)$$

what is clear from this equation we see that the **chemical potential of grain 2 is greater than grain 1**[?]. This will lead to a **driving force** (work term) that will drive diffusion of material from Grain 2 to Grain 1[?]. This driving force for diffusion or Φ remember back to kinetics/diffusion is

$$\Delta\mu = \frac{-4\bar{V}\gamma_{GB}}{r} \quad (6.18)$$

So as this diffusion occurs **Grain 2 will shrink** and **Grain 1 will grow**. So the grain boundary will move some distance Δx towards the center of Grain 2[?].

We can then write the change in Gibbs for this process

$$\Delta G = \frac{-4\bar{V}\gamma_{GB}}{r} \left(\frac{A\Delta x}{\bar{V}} \right) \quad (6.19)$$

where **A** is the **area of the grain boundary** and the entire term in parenthesis represents the moles of materials moved[?]. We can reduce this equation and see that it has a familiar form

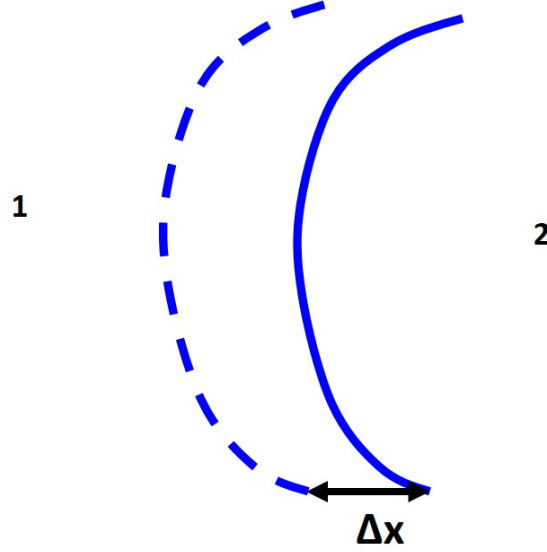


Figure 6-2: Grain Boundary Motion

$$\Delta G = 2\gamma_{GB} \left(\frac{2}{r} \right) A \Delta x \quad (6.20)$$

$$\Delta G = -F \Delta x \quad (6.21)$$

from this we can also derive an equation for stress

$$\sigma = 2\gamma_{GB}\kappa \quad (6.22)$$

This term states that there will essentially be a **stress acting towards the center of curvature** that will **pull the boundary**. **This is a profound equation as it means that a force will act on a boundary any time there is a Gibbs free energy difference between the grains.**[?] We can also use our knowledge of kinetics to determine an expression for the velocity at which the grain boundary moves.

Let's consider the flux of atoms from Grain 2 to 1.

$$J_{21} = A_1 \tau_2 n_2 \exp^{-\frac{\Delta \bar{G}_a}{kT}} \quad (6.23)$$

where τ_2 is the hopping frequency or vibrational frequency of atoms in Grain 2, n_2 is the number of atoms per unit area on Grain 2. We can also write the flux from from Grain 1 to 2[?].

$$J_{12} = A_1 \tau_2 n_2 \exp^{-\frac{\Delta \bar{G}_a + \Delta \bar{G}}{kT}} \quad (6.24)$$

clearly we see the fluxes are very similar except for the additional energy barrier for moving against the chemical potential gradient[?].

Figure 6-3: Energy Landscape for Diffusion

So the total flux across the grain boundary can be defined as

$$J_{GB} = J_{21} - J_{12} = A\tau n \exp^{-\frac{\Delta\bar{G}_a}{kT}} \left(1 - \exp^{-\frac{\Delta\bar{G}}{kT}} \right) \quad (6.25)$$

where we assumed that $A_1 \approx A_2 \approx A$, $\tau_1 \approx \tau_2 \approx \tau$, and $n_1 \approx n_2 \approx n$ [?]

The above equation becomes even simpler when $\frac{\Delta\bar{G}}{kT}$ is small we get

$$J_{GB} = A\tau n \exp^{-\frac{\Delta\bar{G}_a}{kT}} \left(\frac{\Delta\bar{G}}{kT} \right) \quad (6.26)$$

But remember we wanted to get an expression for the velocity of the grain boundary, so we just invoke the conservation of volume and we have that the flux across the grain boundary should also be [?]

$$J_{GB} = \frac{N_A v}{\bar{V}} \quad (6.27)$$

Now we just do a little bit of rearranging of terms and we will get that

$$v = \frac{A\tau n \bar{V}^2}{N_A kT} \exp^{-\frac{\Delta\bar{G}_A}{kT}} \frac{\Delta\bar{G}}{\bar{V}} \quad (6.28)$$

This equation reduces even more if we recognize that $\sigma = \frac{\Delta\bar{G}}{\bar{V}}$ and everything else is bundled into a proportionality constant, M, the mobility so we get [?]

$$v = M\sigma \quad (6.29)$$

where M is

$$M = \frac{A\tau n \bar{V}^2}{N_A kT} \exp^{-\frac{\Delta\bar{G}_A}{kT}} \quad (6.30)$$

6.3 Grain Growth:

So we have shown that grains will grow if there is a difference in chemical potential and the grain with positive curvature will shrink at the expense of the negative curvature grain and this will occur over time[?]. We can actually characterize the evolution of grain size as a function of time.

Remember that we have already derived that

$$\sigma = 2\gamma\kappa \quad (6.31)$$

and let's consider a simple case of two different grains at time $t = t_1$ and $t = t_2$ of different

grain sizes R_1 and R_2 with a radius of curvature r_1 and r_2 respectively[?]. The microstructure at these different times will differ only by scale so curvature will be inversely proportional to grain size so we can write

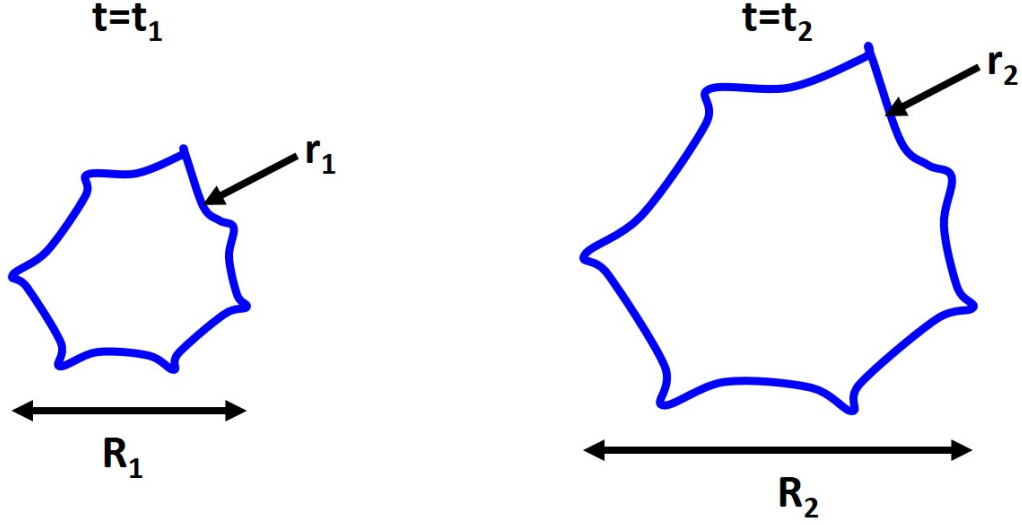


Figure 6-4: Two Grains after Growth for period of time.

$$\frac{r_1}{R_1} = \frac{r_2}{R_2} = 2K \quad (6.32)$$

where K is a constant that is related to grain topology[?]. We can then write that

$$\sigma_{avg} = \frac{2\gamma_{GB}}{K\bar{R}} \quad (6.33)$$

So if we want to write the rate of change in the grain size it is simply

$$\frac{d\bar{R}}{dt} = 2v = 2M\sigma \quad (6.34)$$

$$\frac{d\bar{R}}{dt} = \frac{4\gamma_{GB}M}{K\bar{R}} \quad (6.35)$$

$$\bar{R}^2 - \bar{R}_0^2 = \frac{8\gamma_{GB}Mt}{K} \quad (6.36)$$

For the first equation it is twice the velocity because of the opposing boundaries on a grain. So here we see that the **grain size should scale as $\bar{R} \approx t^{\frac{1}{2}}$** . [?] This scaling behavior is critically important. Being able to do this derivation would be amazing but for real engineering application this scaling behavior is more relevant and important.

6.4 Oswald Ripening and Coarsening

So we just covered how grains will grow and evolve in time now let us take a look at a similar scenario but now look at sea of particles with a distribution of sizes. Remember that we have just shown that whether a grain or particle grows will depend on the chemical potential difference between the two materials/grains[?]. Also **curvature is inversely proportional to grain size** so **smaller particles** will have a **higher chemical potential** than **larger particles**. [?] Thus the larger particles will grow at the expense of smaller particles. So the question then becomes in a sea of particles with a distribution of sizes what particles will grow, what particles will shrink, and at what rate?

Let's think about particle of Material A sitting in a liquid of Material B. Remember that we have previously defined the chemical potential of a particle of radius, a , as

$$\mu_A = \mu_A^P + \frac{2\bar{V}\gamma_{sl}}{a} \quad (6.37)$$

where γ_{sl} is the solid liquid interface surface energy. So let's start simple and assume that A forms an ideal solution and the chemical potential will then be [?]

$$\mu_A = \mu_o + RT \ln(x_A)_a = \mu_A^P + \frac{2\bar{V}\gamma_{sl}}{a} \quad (6.38)$$

This equation gives us the following relation for μ_A^P

$$\mu_A^P = \mu_o + RT \ln(x_A)_P \quad (6.39)$$

We can then solve for the molar fraction of A in solution with curved particles

$$(x_A)_a = (x_A)_P \exp\left(\frac{2\bar{V}\gamma_{sl}}{RTa}\right) \quad (6.40)$$

which if the exponent is small can be approximated to

$$(x_A)_a = (x_A)_P \left(1 + \exp \frac{2\bar{V}\gamma_{sl}}{RTa}\right) \quad (6.41)$$

or concentration is similarly [?]

$$(c_A)_a = c_o \left(1 + \exp \frac{2\bar{V}\gamma_{sl}}{RTa}\right) \quad (6.42)$$

what this equation is telling us is that concentration will vary as a function of the size of the particles! Particles that are small will be surrounded by A rich liquid while large particles are surrounded by liquid poor A[?]. However at steady-state conditions away from the particle surface the concentration profile of A is constant[?]. This means we can use Fick's 1st law to describe the diffusion and we have the constraint that

$$J_r A_r = \text{const} \quad (6.43)$$

where J_r is the flux through an arbitrary sphere are r and A_r is the surface area of the sphere[?]. Now we want an equation that will give us the flux at the surface of the particle so

$$J_a 4\pi a^2 = -D \frac{\partial c_A}{\partial r} 4\pi r^2 \quad (6.44)$$

where J_a is the flux at the surface of the particle[?]. We can reduce this equation to get

$$\frac{\partial c_A}{\partial r} = -\frac{a^2 J_a}{Dr^2} \quad (6.45)$$

We also have the boundary conditions that at

$$c_A = c_{A,a} @ r = a \quad (6.46)$$

$$c_A = \bar{c}_A @ r = \infty \quad (6.47)$$

where \bar{c}_A is the concentration in equilibrium with the average particle size[?]. We plug in these boundary conditions and integrate to get that

$$\bar{c}_A - c_{A,a} = -\frac{J_a a}{D} \quad (6.48)$$

Now the flux is related in or out of a particle is related to a change in volume which is related to a change in area

$$dV = A_P da \quad (6.49)$$

and the rate of volume change is

$$\frac{dV}{dt} = 4\pi a^2 \frac{da}{dt} \quad (6.50)$$

The flux is then related to the change in volume by

$$-J_a A_P = \frac{dV}{dt} \frac{1}{V} \quad (6.51)$$

which is reduced to

$$\frac{da}{dt} = -\bar{V} \frac{D}{a} (c_{A,a} - \bar{c}_A) \quad (6.52)$$

and if we remember back to previously[?]

$$c_{A,a} - \bar{c}_A \approx \frac{2\bar{V}\gamma_{sl}}{RT} c_o \left(\frac{1}{a} - \frac{1}{\bar{a}} \right) \quad (6.53)$$

when we substitute this in we finally reach our fundamental equation for how particle size varies in time

$$\frac{da}{dt} = -\frac{2coD\bar{V}^2\gamma_{sl}}{RTa} \left(\frac{1}{a} - \frac{1}{\bar{a}} \right) \quad (6.54)$$

This the fundamental equation for Oswald Ripening! We can see from this equation that particles that are smaller than the average particle size, \bar{a} , will shrink since $\frac{da}{dt} < 0$ [?]. Conversely, for particles that are larger than the average particle size will grow. You can see this curve below

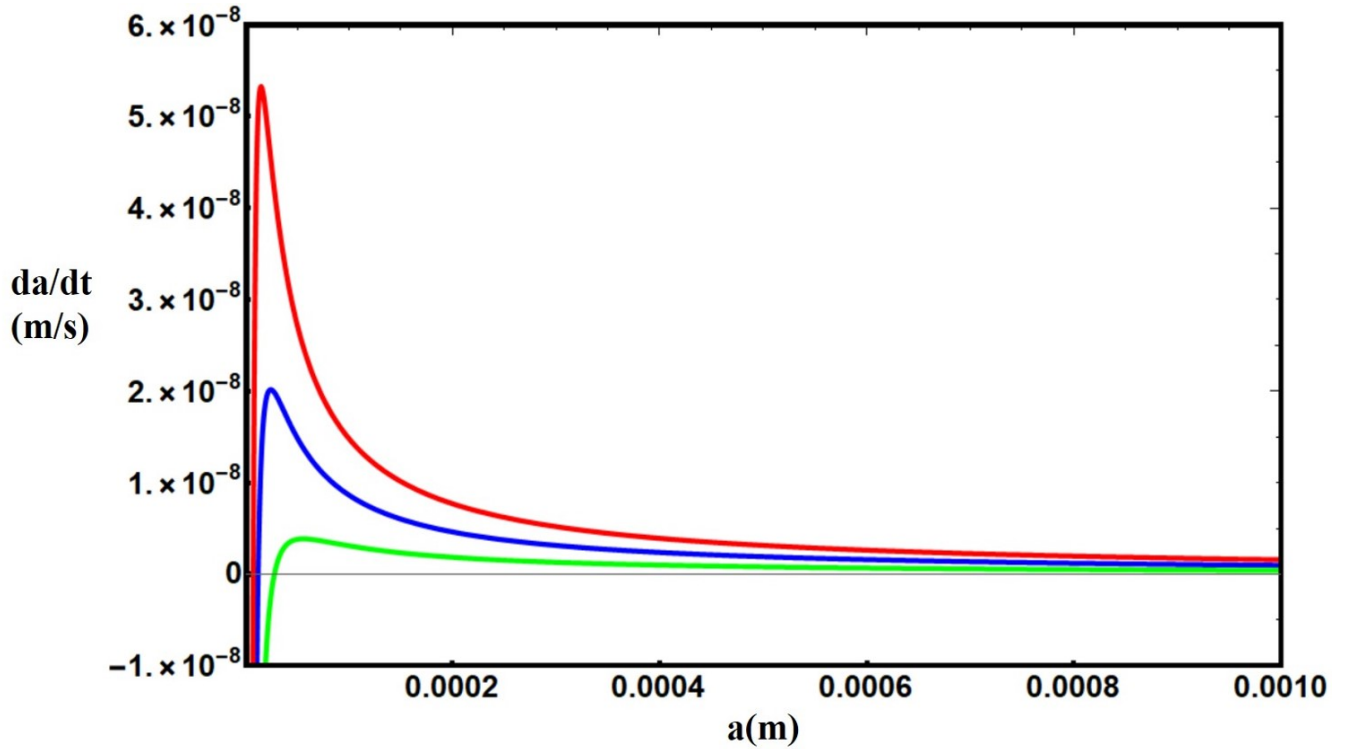


Figure 6-5: Oswald Ripening.

We can also find the particle size which exhibits a maximum growth rate by taking the derivative and setting it equal to zero and solve for a

$$\frac{\partial}{\partial a} \frac{\partial a}{\partial t} = 0 \quad (6.55)$$

As you can see in the Mathematica notebook the maximum growth rate occurs for particles with $a = 2\bar{a}$ [?]. We can also solve see how the average particle size will vary in time by first looking at how the particles which grow the fastest, $a_{max} = 2\bar{a}$, vary in time[?]

$$\frac{\partial a_{max}}{\partial t} \frac{1}{2} = \frac{\partial \bar{a}}{\partial t} \quad (6.56)$$

where

$$\frac{\partial a_{max}}{\partial t} = -\frac{2coD\bar{V}^2\gamma_{sl}}{RT2\bar{a}} \left(\frac{1}{2\bar{a}} - \frac{1}{\bar{a}} \right) \quad (6.57)$$

We can then substitute in for a_{max} to see how the average particle size varies in time as seen below[?]

$$\frac{\partial \bar{a}}{\partial t} = -\frac{coD\bar{V}^2\gamma_{sl}}{4RT\bar{a}^2} \quad (6.58)$$

and remember the initial conditions for this problem was that at time $t = 0$ the average particle size was $\bar{a} = a_0$ and we get

$$\frac{\bar{a}^3 - \bar{a}_o^3}{3} = \frac{c_oD\bar{V}^2\gamma_{sl}t}{4RT} \quad (6.59)$$

So the average particle size will grow with the cube root of time[?].

6.5 Homogeneous Nucleation

We just talked about how solid particles grow from a liquid but how does this process begin? Well let's think about a single component system in a liquid state, when will solids start to nucleate? Once the temperature falls below the melting temperature, T_m [?]. The amount that a system is **undercooled** is defined by

$$\Delta T = T_m - T \quad (6.60)$$

where T is the temperature that we are at currently. Look closely at this equation and see that undercooling is positive when we are below the melting temperature[?]. Think of the magnitude of undercooling as the driving force for growth. So once the system is undercooled we have the following change in our system:

Now the free energy of system 1 will be, with the assumption that there is no change in volume upon freezing:

$$G_1 = (V_L + V_S)G_V^L \quad (6.61)$$

and the free energy of state 2 is

$$G_2 = V_L G_V^L + V_S G_V^S + A_{SL}\gamma_{SL} \quad (6.62)$$

where V_L and V_S are the volumes of liquid and solid respectively and G_V^L and G_V^S are the volumetric Gibbs energies of liquid and solid[?] and $\Delta G_V = \frac{\Delta H_f \Delta T}{T_m}$. So the change in Gibbs Free energy is simply

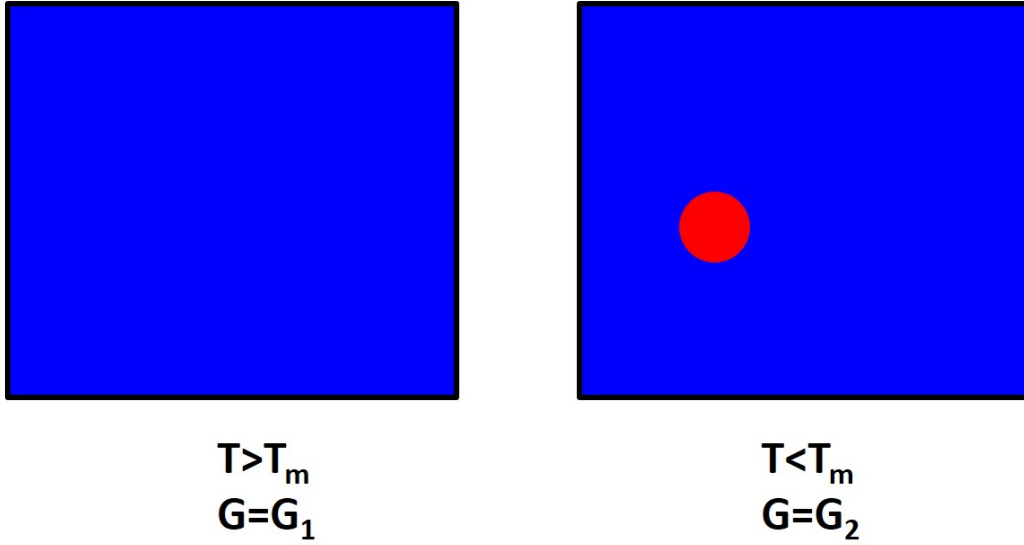


Figure 6-6: System before and after undercooling.

$$\Delta G = V_s(G_V^S - G_V^L) + A_S\gamma_{SL} = -\Delta G_V V_S + A_S\gamma_{SL} \quad (6.63)$$

where $\Delta G_V = G_V^L - G_V^S$ is the volumetric change in free energy upon melting[?]. This can be seen schematically below

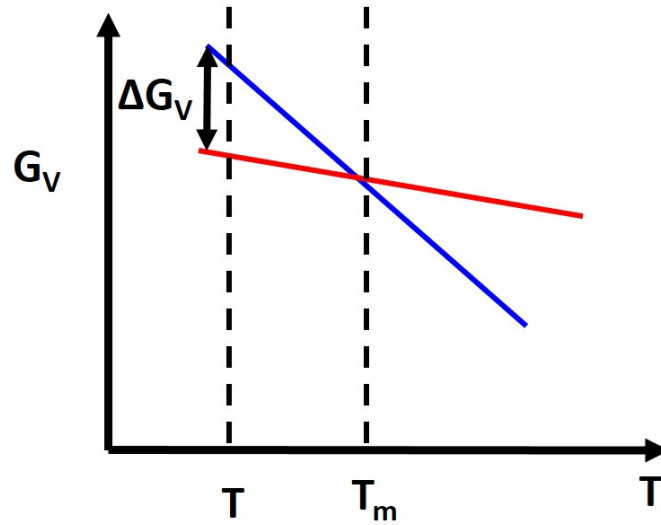


Figure 6-7: Free energy change upon undercooling.

Now for a solid spherical particle we can re-write the change in energy as function of r

$$\Delta G_r = -\frac{4}{3}\pi r^3 \Delta G_V + 4\pi r^2 \gamma_{SL} \quad (6.64)$$

now let us look at curve below:

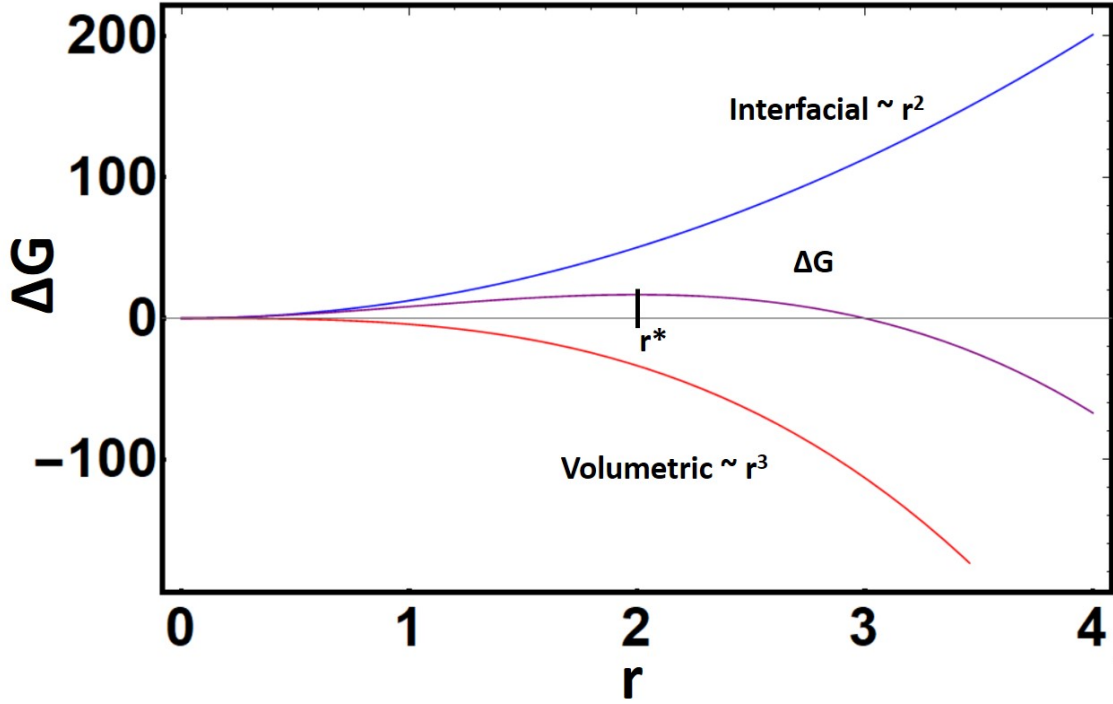


Figure 6-8: Interfacial energy vs. Volumetric energy Competition.

There are a couple of important points here. Notice that a small particles sizes the interfacial term dominates while at larger particles the volumetric term dominates. Additionally we see there is a maximum in the resultant purple change in free energy curve[?]. This maximum will define our critical radius r^* . This critical radius determines whether a particle will grow or shrink[?]. When $r > r^*$ the free energy decreases but if $r < r^*$ grows the free energy instead will increase. We can calculate the critical radius by once again taking the derivative and setting it equal to zero

$$\frac{\partial \Delta G_r}{\partial r} = 0 \quad (6.65)$$

we find that

$$r^* = \frac{2\gamma_{SL}}{\Delta G_V} \quad (6.66)$$

Moreover we remember that we have the relationship that

$$\Delta G_V = \frac{\Delta H_f \Delta T}{T_m} \quad (6.67)$$

so we can see the relationship between the critical radius and undercooling, when undercooling is large the critical radius decreases which should make intuitive sense[?].

We can also calculate the concentration of clusters as we have done previously

$$n_r = n_o \exp \left(- \frac{\Delta G_r}{kT} \right) \quad (6.68)$$

So this is great but this undercooling driving force is not the only component of nucleation. The atoms must cluster via diffusion mechanisms so diffusion is also a critical component[?]. We can calculate the steady-state nucleation rate, I , which is simply the number of atoms that successfully diffuse to the surface of the cluster multiplied by the concentration of clusters with a critical cluster size.

$$I \approx n_o \exp \left(- \frac{\Delta G_r}{kT} \right) \Gamma \quad (6.69)$$

where Γ is the frequency of jumps or diffusion which is

$$\Gamma = \nu \exp \left(- \frac{\Delta G_{diff}}{kT} \right) \quad (6.70)$$

so we end up with the following equation

$$I \approx n_o \nu \exp \left(- \frac{\Delta G_r + \Delta G_{diff}}{kT} \right) \quad (6.71)$$

We see here two energy competitors, ΔG_r and ΔG_{diff} . Now at low temperatures, large undercooling, we have a large driving force for nucleation and growth so you might expect the nucleation rate to be high[?]. However, at low temperatures the diffusion is extremely low so that effectively kills the energy term for undercooling. Conversely at large temperatures, low undercooling, we have a lot of diffusion but we don't have a large driving force for nucleation. It is only in this middle ground as seen below do we maximize the nucleation rate[?]. In the high temperature region this is essentially considered the growth regime. In this middle regime is where you want to nucleate.

6.6 Heterogeneous Nucleation

In real-life scenarios the activation energy for nucleation is typically much lower than previously calculated for homogeneous nucleation. The reason being that typically the activation energy for nucleation is lowered when nuclei form on pre-existing surfaces[?]. This type of nucleation is **heterogeneous nucleation** and we can see in the derivation below why the activation energy is reduced.

The nuclei/cluster wets the surface and will form a spherical cap with a radius of curvature r [?]. We can also see in the figure that γ_{SC} is the substrate-cluster interfacial energy, γ_{LC} is the liquid-cluster interfacial energy, and γ_{SL} is the substrate-liquid interfacial energy[?]. We also have the equilibrium conditions that dictate that:

$$\gamma_{SL} = \gamma_{SC} + \gamma_{LC} \cos \theta \quad (6.72)$$

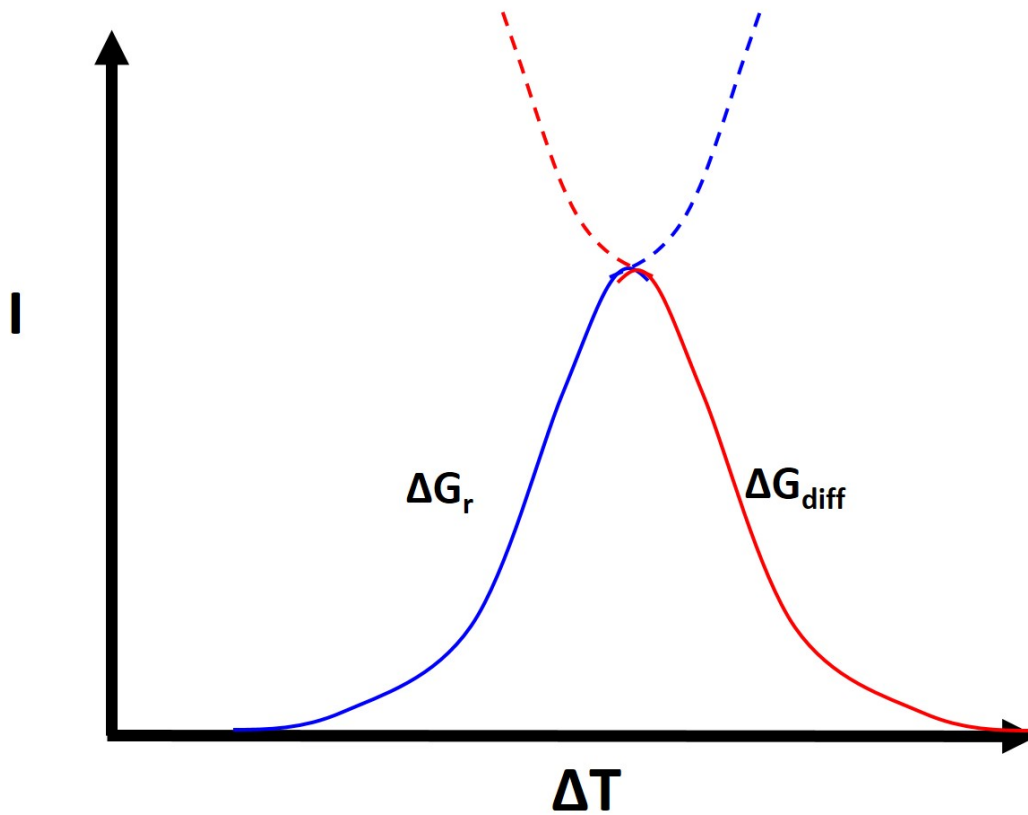


Figure 6-9: Nucleation Rate Curve.

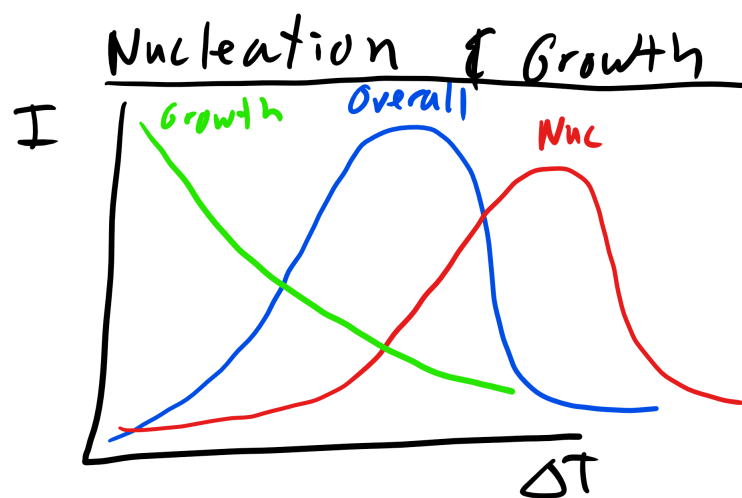


Figure 6-10: Nucleation Rate Curve.

Heterogeneous Nucleation

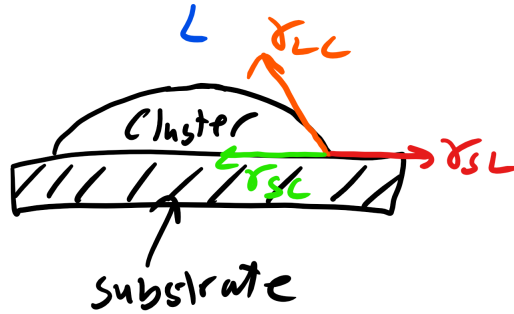


Figure 6-11: Nucleation on a Surface.

We also have some free energy associated with forming this spherical cluster, forming the liquid and substrate interface with the cluster and removing liquid-substrate interface which is the same amount as the area of interface between the substrate and cluster interface or shown mathematically below

$$\Delta G = -V_S \Delta G_V + A_{LC} \gamma_{LC} + A_{SC} \gamma_{SC} - A_{SC} \gamma_{SL} \quad (6.73)$$

where V_S is the volume of the cluster cap[?]. And for a spherical cap

$$A_{LC} = 2\pi r^2 (1 - \cos \theta) \quad (6.74)$$

$$A_{SC} = \pi r^2 \sin^2 \theta \quad (6.75)$$

$$V_S = \frac{\pi r^3}{3} (2 + \cos \theta) (1 - \cos \theta)^2 \quad (6.76)$$

and we can substitute this in and solve to find

$$\Delta G = \left(-\frac{4}{3} \pi r^3 \Delta G_V + 4\pi r^2 \gamma_{SL} \right) S(\theta) \quad (6.77)$$

where

$$S(\theta) = \frac{1}{4} (2 + \cos \theta) (1 - \cos^2 \theta)^2 \quad (6.78)$$

Now if you differentiate with respect to r and set to zero you will find that the critical radius for nucleation remains unchanged[?]. However, if you then substitute the critical radius back into the ΔG equation you get

$$\Delta G = \frac{16\pi\gamma_{LC}^3}{3\Delta G_V^2} S(\theta) \quad (6.79)$$

So the homogeneous nucleation energy barrier is modified by our θ term and we know that $S(\theta)$ is less than 1 for all values less than 180° [?]. So the presence of a surface will increase the rate of nucleation as the energy barrier is lower.

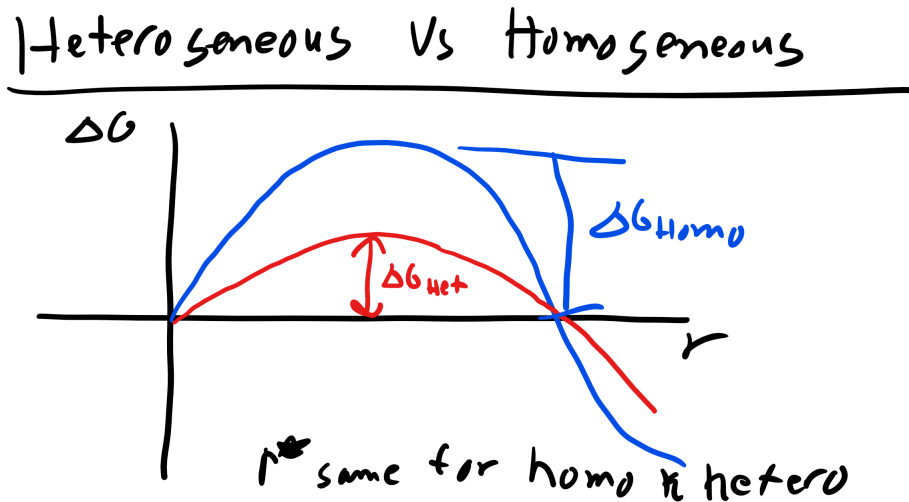


Figure 6-12: Heterogeneous nucleation lowers energy barrier.

This will then in turn change the amount of undercooling required for the highest nucleation rate as seen below [?]:

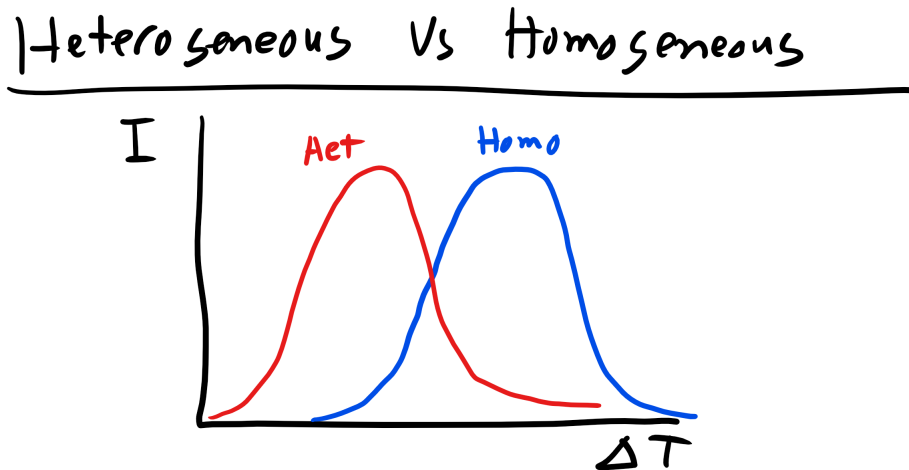


Figure 6-13: Heterogeneous nucleation lowers amount of undercooling for optimal nucleation rate.

6.7 Time-Temperature-Transformation Diagrams

We can visualize this process of transformation rates in Time-Temperature-Transformation diagrams below where we isothermally transform a material at a specific temperature and time.

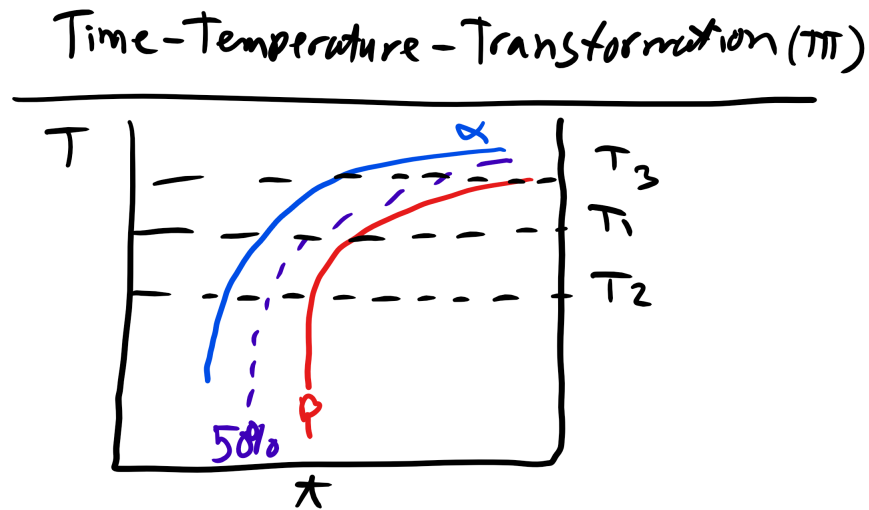


Figure 6-14: Time Temperature Transformation Diagram.

Part IV

Mechanical Behavior of Materials

CHAPTER 7

MECHANICAL BEHAVIOR OF MATERIALS

This is probably the section of the class that all of the Mechanical and Civil Engineers have been waiting for and it is where we will finally start talking about breaking things, fracture!

7.1 Sign Conventions:

To begin let's talk about **units and sign conventions**. We will define any forces, stresses, or strain in **tension** as **positive** and any forces, stresses, or strain under **compression** will be **considered negative**[10]. Additionally we will consider moments that are **counter clockwise** as **positive** and **clockwise** as **negative**[10].

7.2 Stress-Strain Curve:

When a material is placed under a stress state we will typically plot a stress-strain curve and that curve typically will have 3 distinct regions: **I) Elastic, II) Plastic, III) Fracture**[10].

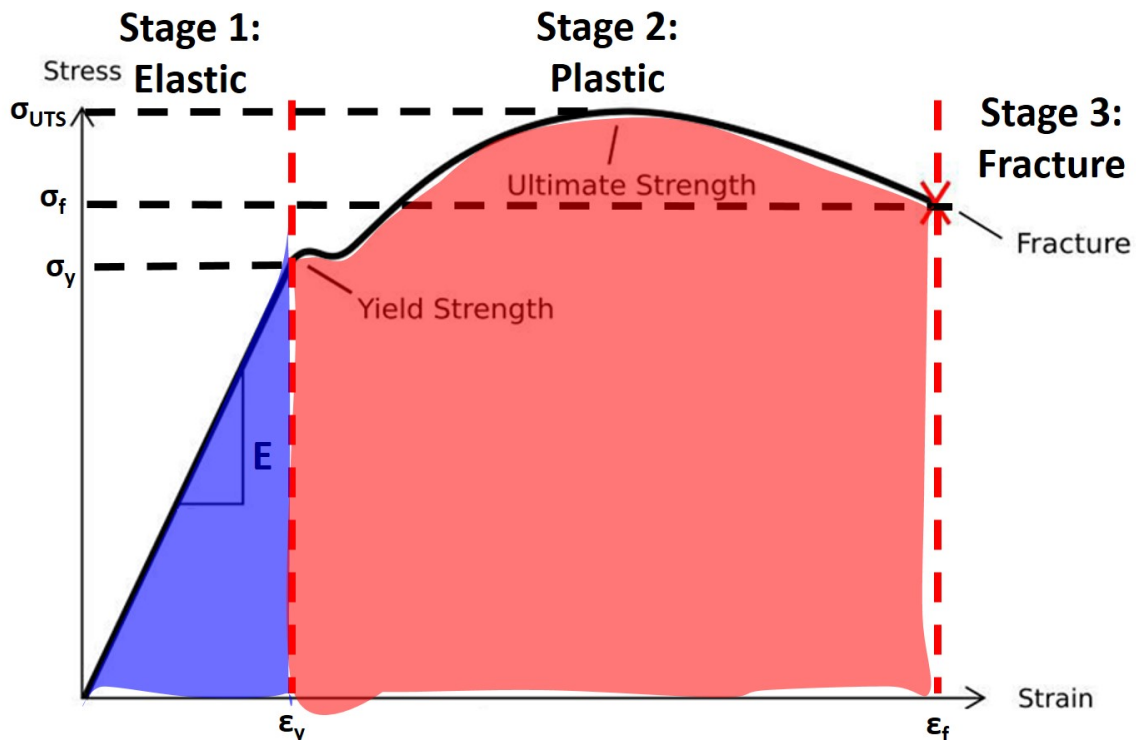


Figure 7-1: Stress Strain Curve.

I) Elastic Regime:

In the **elastic regime** the stress strain response is linear and defined by the expression below which should be familiar (Hooke's Law)[10]:

$$\sigma = E\epsilon \quad (7.1)$$

where E, sometimes Y, is defined as the **Young's Modulus**. It describes the stiffness of the material and is a material constant. **Metals** are typically in the **100s of GPa**, **ceramics** are high **200's and 300's of GPa**, **polymers** are closer to on the order of **1 GPa**. In the elastic region the strain is **completely reversible**, i.e. **there is no permanent or plastic deformation**[10]. You are just **pulling on the bonds not breaking any bonds**.

II) Plastic Regime:

Here you are **plastically** deforming the material and this is signified microstructurally by the **breaking of bonds** and the **movement of dislocations**[10]. Additionally with **plastic dislocation the strain is not reversible**, if you remove the force the strain remains. It is signified to begin on the stress strain curve by σ_y which is the **yield stress** and ϵ_y the **yield strain**[10]. The σ_{UTS} is the **ultimate tensile strength** and it denotes the **onset of necking** which is where the instantaneous area is now smaller than the original area.

III) Fracture:

As the name denotes this is where the material catastrophically fractures and is denoted by σ_f which is the **fracture stress** and the ϵ_f is the **fracture strain**[10].

At this point we need to stop and make a clear point about the language that we have to use when discussing the material properties of materials. Word choice is critical here because they mean very different things. When we talk about the **stiffness** of materials we are talking about the **Young's modulus** of the material[10]. The higher the Young's modulus the stiffer the material. When we talk about **strength** we are talking about the **yield strength**, the **ultimate tensile strength**, or the **fracture stress or strength**[10]. We we are talking about how **ductile** a material is we are talking about the **strain at failure**[10]. We also often talk about material resilience and toughness as well.

We define **elastic strain energy (ESE)** which is defined as:

$$U_{ESE} = V \int_0^{\epsilon_y} \sigma_{11} d\epsilon_{11} \quad (7.2)$$

where V is the volume which gives us units of energy. This is the blue shaded portion. **Toughness** is defined as

$$U_T = V \int_0^{\epsilon_f} \sigma_{11} d\epsilon_{11} \quad (7.3)$$

If a material is not as stiff it is called **compliant**, if a material is not strong it is **weak**, and if a material is not **tough** it is termed **brittle**[10].

Let's look at a couple of stress strain curves...

7.3 1. Elastic Regime:

7.3.1 Stress

Stress, σ , is a force normalized by the area over which it acts and the force is perpendicular to the area:

$$\sigma = \frac{F}{A} = \frac{N}{m^2} = Pa \quad (7.4)$$

where F is force and A is the original area. This is the definition of the **engineering stress** the **true stress** would be **normalized** by the **instantaneous area**[10]. In this class we will use the engineering stress primarily in this class. **Shear stress**, τ , is a force normalized by the area over which it acts and the force is parallel to the area[10].

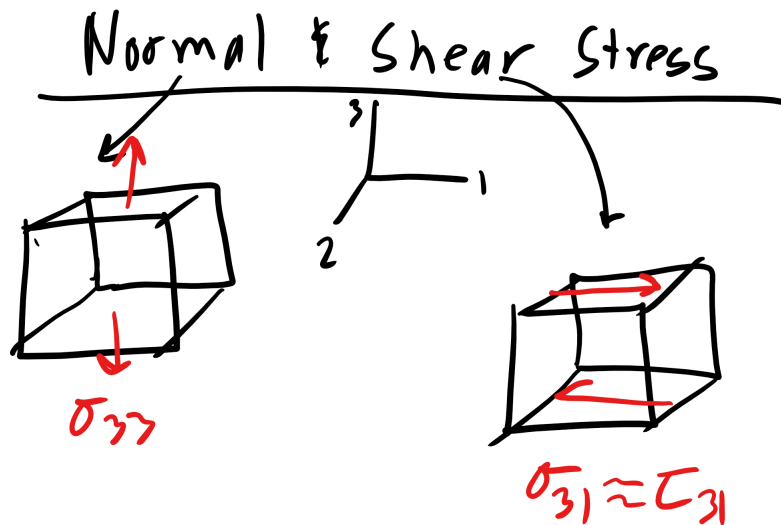


Figure 7-2: Normal and Shear Stress.

The shear stress is similarly defined as:

$$\tau = \frac{F}{A} \quad (7.5)$$

Now it should be noted here that stress is a second rank tensor, σ_{ij} , and so is strain, ϵ_{ij} [10]. For stress i denotes the **normal to the plane, on which the force is acting** and j is the **direction of the force**:

$$\sigma_{ij} = \frac{F_j}{A_i} \quad (7.6)$$

So our full stress tensor or our most generic stress state would be:

$$\sigma = \begin{bmatrix} \sigma_{11} & \sigma_{12} & \sigma_{13} \\ \sigma_{21} & \sigma_{22} & \sigma_{23} \\ \sigma_{31} & \sigma_{32} & \sigma_{33} \end{bmatrix} \quad (7.7)$$

Now this looks like a complex matrix with 9 independent components however they are not completely independent. If we assume that our cube volume element (**representative volume element (RVE)**) is in equilibrium (not rotating) then we have the condition that [10]

$$\sigma_{12} = \sigma_{21} \quad (7.8)$$

$$\sigma_{23} = \sigma_{32} \quad (7.9)$$

$$\sigma_{31} = \sigma_{13} \quad (7.10)$$

so our matrix reduces to 6 independent components for our RVE

$$\sigma = \begin{bmatrix} \sigma_{11} & \sigma_{12} & \sigma_{13} \\ \sigma_{12} & \sigma_{22} & \sigma_{23} \\ \sigma_{13} & \sigma_{23} & \sigma_{33} \end{bmatrix} \quad (7.11)$$

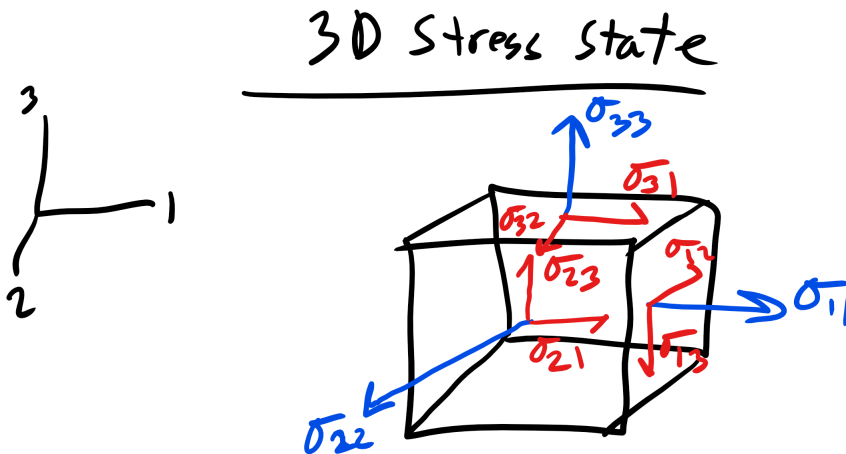


Figure 7-3: 3D Stress State.

Additionally we will encounter several special stress states like Uniaxial stress which gives the following stress state

$$\sigma = \begin{bmatrix} \sigma_{11} & 0 & 0 \\ 0 & 0 & 0 \\ 0 & 0 & 0 \end{bmatrix} \quad (7.12)$$

and Biaxial stress which gives us

$$\sigma = \begin{bmatrix} \sigma_{11} & \sigma_{12} & 0 \\ \sigma_{12} & \sigma_{22} & 0 \\ 0 & 0 & 0 \end{bmatrix} \quad (7.13)$$

but more on those a bit later. Additionally we define the **hydrostatic stress** as

$$P = \frac{1}{3}(\sigma_{11} + \sigma_{22} + \sigma_{33}) \quad (7.14)$$

7.3.2 Strain:

All machines, structural members, and materials will deform to some extent when externally loaded by a force or stress. That deformation results in a displacement or **strain**, ϵ [10]:

$$\epsilon = \frac{dL}{L} \quad (7.15)$$

$$\epsilon_t = \int_{L_1}^{L_2} \frac{dL}{L} = \ln \frac{L_2}{L_1} \quad (7.16)$$

where L_1 is the original length. This is the definition of **true strain**, ϵ_t but typically we work with a simpler form called the **engineering strain**[10], ϵ_e ,

$$\epsilon_e = \frac{L_2 - L_1}{L_1} = \frac{\Delta L}{L_1} \quad (7.17)$$

Typically engineers work with *microstrain* or parts per million. And the shear strain is[10]:

$$\gamma = \frac{dL}{L} = \tan \theta \quad (7.18)$$

Also for a material subjected to shear stresses we **observe a proportional relationship between shear stress and strain in the elastic regime**[10] which is defined as:

$$\tau = G\gamma \quad (7.19)$$

where G is the shear modulus (more on this later).

Now more formally we can define strain using **infinitesimal strain theory** (if you are interested please read in Chapter 5 of Young and Lovell Introduction to polymers)[10] gives us that

$$\epsilon_{ij} = \frac{1}{2} \left(\frac{\partial u_i}{\partial x_j} + \frac{\partial u_j}{\partial x_i} \right) \quad (7.20)$$

where x is an axis dimension and u is the displacement we also have from this theory that

$$\epsilon_{11} = \frac{\partial u_1}{\partial x_1} \quad (7.21)$$

$$\epsilon_{22} = \frac{\partial u_2}{\partial x_2} \quad (7.22)$$

$$\epsilon_{33} = \frac{\partial u_3}{\partial x_3} \quad (7.23)$$

$$\gamma_{12} = \gamma_{21} = \left(\frac{\partial u_1}{\partial x_2} + \frac{\partial u_2}{\partial x_1} \right) \quad (7.24)$$

$$\gamma_{23} = \gamma_{32} = \left(\frac{\partial u_2}{\partial x_3} + \frac{\partial u_3}{\partial x_2} \right) \quad (7.25)$$

$$\gamma_{31} = \gamma_{13} = \left(\frac{\partial u_3}{\partial x_1} + \frac{\partial u_1}{\partial x_3} \right) \quad (7.26)$$

with all this we can now create our strain matrix and seeing from the definitions above we know that $\epsilon_{12} = \epsilon_{21}$ and $\epsilon_{23} = \epsilon_{32}$ and finally $\epsilon_{13} = \epsilon_{31}$ [10] so that now our strain matrix has 6 independent components and can be written as

$$\epsilon = \begin{bmatrix} \epsilon_{11} & \epsilon_{12} & \epsilon_{13} \\ \epsilon_{12} & \epsilon_{22} & \epsilon_{23} \\ \epsilon_{13} & \epsilon_{23} & \epsilon_{33} \end{bmatrix} \quad (7.27)$$

or equivalently

$$\epsilon = \begin{bmatrix} \epsilon_{11} & \frac{\gamma_{12}}{2} & \frac{\gamma_{13}}{2} \\ \frac{\gamma_{12}}{2} & \epsilon_{22} & \frac{\gamma_{23}}{2} \\ \frac{\gamma_{13}}{2} & \frac{\gamma_{23}}{2} & \epsilon_{33} \end{bmatrix} \quad (7.28)$$

7.3.3 Poisson's Ratio:

Now what happens to the dimensions perpendicular to the direction of applied force when a the material is subjected to uniaxial tension? We know from experience that a **body begin pulled in tension will contract laterally**[10]. This **lateral strain** is described by the **Poisson's Ratio**[10]:

$$\nu = -\frac{\epsilon_L}{\epsilon_A} \quad (7.29)$$

where ϵ_L is the lateral strain and ϵ_A is the axial strain. Note the **negative sign which signifies a decrease in length**. The Poisson's ratio is typically around **0.3 for metals**, **0.5 for rubber**, **0.4-0.5 for polymeric materials or biomaterials**, and **0.2 for cork, cellular materials, or ceramics**[10].

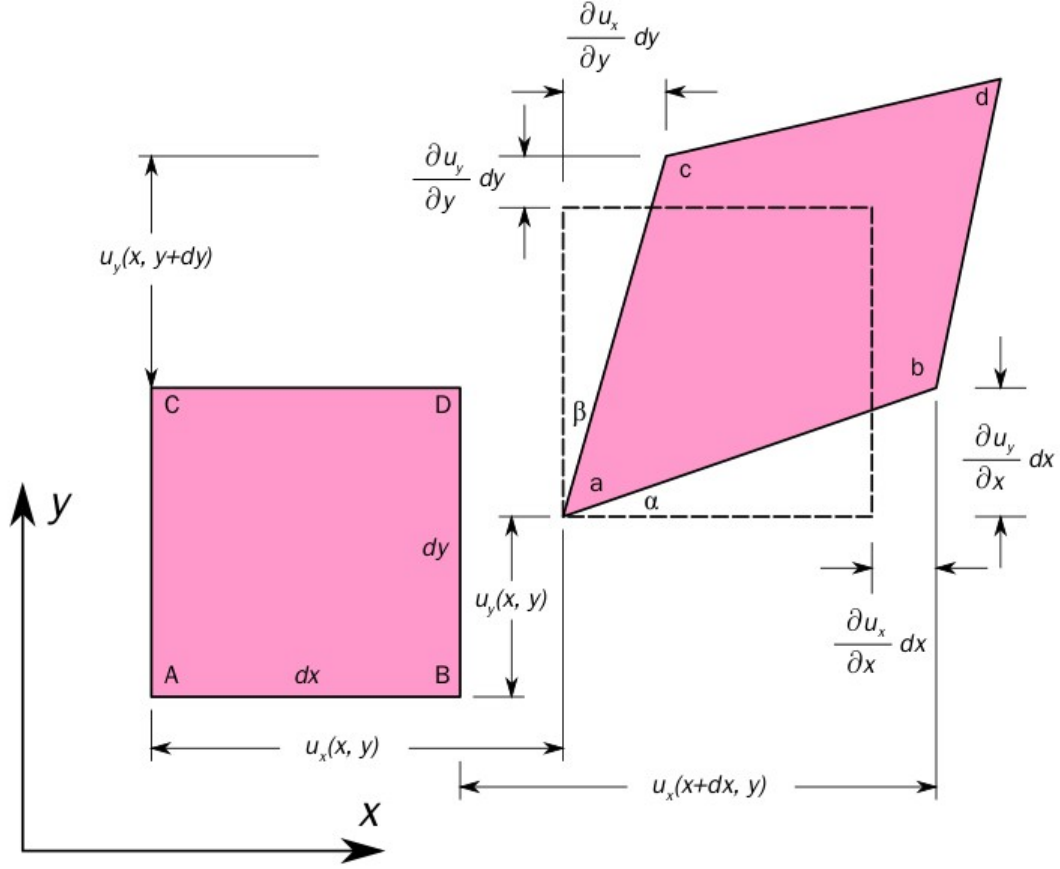


Figure 7-4: Infinitesimal Strain Theory[11].

7.3.4 Biaxial and Complex Stress States:

What happens when we have a **more complex stress state** and we are interested in the **stress state of a particular plane of orientation angle θ** ? Well we do this the same way we resolve force vectors onto a new axes of interest. Let's look at a case of **plane stress** which is a case when all the stress is contained in one plane[10].

So far we have been dealing with simple uniaxial stress along the principal testing direction however often materials can also be subjected to shear stress or strain.

With this information let us move on to more **complex stress states**, specifically one that typically exists on a **free**, not constrained, surface of a stressed material[10].

Consider the element which is initially stressed in the x direction by applying σ_x [10]. There will be a resultant strain:

$$\epsilon_x = \frac{\sigma_x}{E} \quad (7.30)$$

$$\epsilon_y = \frac{-\nu\sigma_x}{E} \quad (7.31)$$

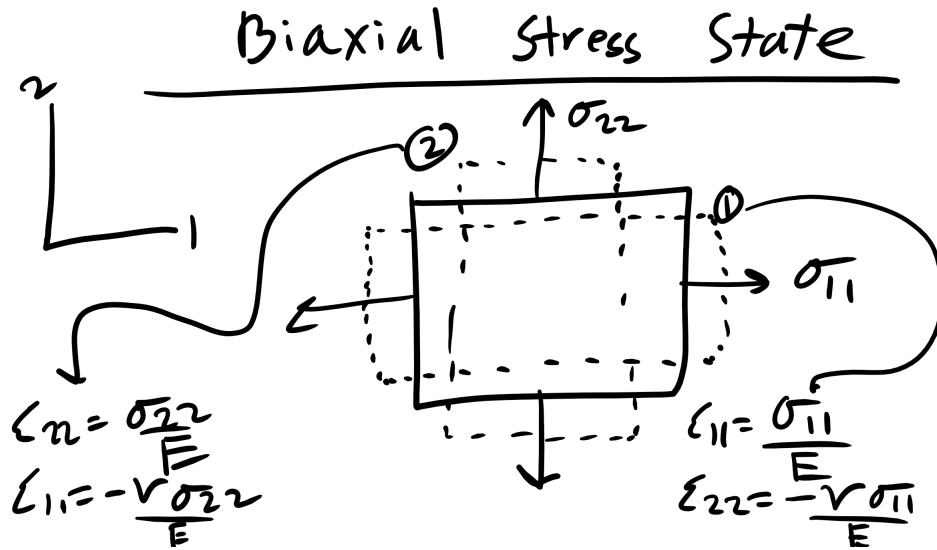


Figure 7-5: Biaxial stress condition

The element is **then stressed in the y direction** by applying σ_y . The resultant strain will be:

$$\epsilon_y = \frac{\sigma_y}{E} \quad (7.32)$$

$$\epsilon_x = \frac{-\nu \sigma_y}{E} \quad (7.33)$$

therefore the **total strain** in x and y directions will be:

$$\epsilon_x = \frac{\sigma_x - \nu \sigma_y}{E} \quad (7.34)$$

$$\epsilon_y = \frac{\sigma_y - \nu \sigma_x}{E} \quad (7.35)$$

We can solve these two equations (two unknowns and two equations) to find the **total stress** in the x and y directions[10]:

$$\sigma_x = \frac{E(\epsilon_x + \nu \epsilon_y)}{1 - \nu^2} \quad (7.36)$$

$$\sigma_y = \frac{E(\epsilon_y + \nu \epsilon_x)}{1 - \nu^2} \quad (7.37)$$

7.3.5 3D Stress State

We can extend this even further to find the total strain if there is another stress applied, σ_z , in the z direction[10]:

$$\epsilon_x = \frac{1}{E}[\sigma_x - \nu(\sigma_y + \sigma_z)] \quad (7.38)$$

$$\epsilon_y = \frac{1}{E}[\sigma_y - \nu(\sigma_z + \sigma_x)] \quad (7.39)$$

$$\epsilon_z = \frac{1}{E}[\sigma_z - \nu(\sigma_x + \sigma_y)] \quad (7.40)$$

We can similarly write the stress as well:

$$\sigma_x = \frac{E}{(1+\nu)(1-2\nu)} \left[(1-\nu)\epsilon_x + \nu(\epsilon_y + \epsilon_z) \right] \quad (7.41)$$

$$\sigma_y = \frac{E}{(1+\nu)(1-2\nu)} \left[(1-\nu)\epsilon_y + \nu(\epsilon_z + \epsilon_x) \right] \quad (7.42)$$

$$\sigma_z = \frac{E}{(1+\nu)(1-2\nu)} \left[(1-\nu)\epsilon_z + \nu(\epsilon_x + \epsilon_y) \right] \quad (7.43)$$

7.3.6 Anisotropic Linear Elasticity:

Now let's stop for just a second and look at these expressions. We have really been looking how to write expressions looking at matrices with primarily normal stresses but if both **stress** and **strain** are **second rank tensors** if we want a general relationship we need to introduce a **fourth rank tensor** to stand in for E in the Hooke's law expression[10]. So instead of our Hookes Law

$$\sigma = E\epsilon \quad (7.44)$$

We will have

$$\sigma_{ij} = C_{ijkl}\epsilon_{ij} \quad (7.45)$$

$$\epsilon_{ij} = S_{ijkl}\sigma_{ij} \quad (7.46)$$

where C is the stiffness matrix and S is the compliance matrix and we have the relationship that $S = C^{-1}$. As you can see this will get very, very messy quickly[10]. Instead of our nice and simple stress tensor that we were working with previously that we assumed to be isotropic and cubic and having only 6 independent components the full anisotropic fourth rank stiffness and compliance tensor has **81!** independent elastic components[10]. Now typically for almost every material this will not be the case there will be symmetries that reduce this number drastically and we can also reduce it further right now remembering the convenient relationships that reduced the number of

independent components in our stress and strain second rank tensors to 6[10]. Remembering this we can make a quick change in notation where we have

$$\sigma_{11} = \sigma_1 \quad (7.47)$$

$$\sigma_{22} = \sigma_2 \quad (7.48)$$

$$\sigma_{33} = \sigma_3 \quad (7.49)$$

$$\sigma_{23} = \sigma_4 \quad (7.50)$$

$$\sigma_{13} = \sigma_5 \quad (7.51)$$

$$\sigma_{12} = \sigma_6 \quad (7.52)$$

The same will hold for strain but remember the relationship for shear strain is $2\epsilon_4 = \gamma_{23}$ and the same follows for the other shear strains[10]. We can then re-write our expression as

$$\sigma_i = C_{ij}\epsilon_j \quad (7.53)$$

where now you should note that C_{ij} is 6×6 matrix not a tensor so we went from 81 to 36 components[10] as seen below

$$\begin{bmatrix} \sigma_1 \\ \sigma_2 \\ \sigma_3 \\ \sigma_4 \\ \sigma_5 \\ \sigma_6 \end{bmatrix} = \begin{bmatrix} C_{11} & C_{12} & C_{13} & C_{14} & C_{15} & C_{16} \\ C_{21} & C_{22} & C_{23} & C_{24} & C_{25} & C_{26} \\ C_{31} & C_{32} & C_{33} & C_{34} & C_{35} & C_{36} \\ C_{41} & C_{42} & C_{43} & C_{44} & C_{45} & C_{46} \\ C_{51} & C_{52} & C_{53} & C_{54} & C_{55} & C_{56} \\ C_{61} & C_{62} & C_{63} & C_{64} & C_{65} & C_{66} \end{bmatrix} \begin{bmatrix} \epsilon_1 \\ \epsilon_2 \\ \epsilon_3 \\ \epsilon_4 \\ \epsilon_5 \\ \epsilon_6 \end{bmatrix} \quad (7.54)$$

Here we see there are 36 components but we can reduce these components[10]. The strain energy density (area under stress strain curve in the elastic regime) does not depend on the direction of strain (compression or tension) so this implies that our stiffness, compliance, strain, and stress matrices must be symmetric, i.e. $C_{ij} = C_{ji}$ so this reduces our number of independent components to 21[10]. We are making progress!!!

But we can reduce this even more by invoking **Onsager's theorem**: which states that materials cannot exhibit properties of higher symmetry other than that of the material itself[10]. In other words, depending on the symmetry of the material some of these constants could disappear. Note: for a more complete discussion of Onsager read Sam Allen's Kinetics of Materials, best description that I have come across. For example:

- **Triclinic Materials:** Have all 21 independent coefficients
- **Monoclinic Materials:** Have 13 independent coefficients

- **Orthorhombic Materials:** Have 9 independent components, some examples of these are wood, composite laminate, polyethylene (semi-crystalline), etc.
- **Tetragonal Materials:** Have 7 independent components
- **Cubic Materials:** Have 3 independent components can be reduced to 2 if material is isotropic.

Remember for cubic materials ($a=b=c$ and $\alpha = \beta = \gamma = 90^\circ$ for cubic) you will find that there are only **3 independent elastic constants** C_{11} , C_{12} , and C_{44} and all others are 0 (proof beyond scope here)[10]. And if we assume elastically isotropic (same properties in all directions) then this reduces to just two where we have the relationship that

$$C_{44} = \frac{C_{11} - C_{12}}{2} \quad (7.55)$$

this proof is arduous and beyond the scope of the class. There is also a useful parameter called the Zener anisotropy ratio (same from light scattering)[10]

$$A = \frac{2C_{44}}{C_{11} - C_{12}} \quad (7.56)$$

A perfect isotropic material will have a value of 1 while materials that are more anisotropic will have larger values[10].

So the stiffness matrix for isotropic cubic linear elastic materials is thus

$$\begin{bmatrix} C_{11} & C_{12} & C_{12} & 0 & 0 & 0 \\ C_{12} & C_{11} & C_{12} & 0 & 0 & 0 \\ C_{12} & C_{12} & C_{11} & 0 & 0 & 0 \\ 0 & 0 & 0 & \frac{C_{11}-C_{12}}{2} & 0 & 0 \\ 0 & 0 & 0 & 0 & \frac{C_{11}-C_{12}}{2} & 0 \\ 0 & 0 & 0 & 0 & 0 & \frac{C_{11}-C_{12}}{2} \end{bmatrix} \quad (7.57)$$

and the compliance matrix is

$$\begin{bmatrix} S_{11} & S_{12} & S_{12} & 0 & 0 & 0 \\ S_{12} & S_{11} & S_{12} & 0 & 0 & 0 \\ S_{12} & S_{12} & S_{11} & 0 & 0 & 0 \\ 0 & 0 & 0 & 2(S_{11} - S_{12}) & 0 & 0 \\ 0 & 0 & 0 & 0 & 2(S_{11} - S_{12}) & 0 \\ 0 & 0 & 0 & 0 & 0 & 2(S_{11} - S_{12}) \end{bmatrix} \quad (7.58)$$

Do you understand how/why the value of S_{44} changed? Well remember we have the relationship that $C = S^{-1}$! Now this is good but again we want to put this in terms of material constants instead of these arbitrary compliance or stiffness notations[10]. Let's write out that first top line which gives us

$$\epsilon_1 = S_{11}\sigma_1 + S_{12}\sigma_2 + S_{12}\sigma_3 \quad (7.59)$$

Well we know previously we had an expression that looked very similar for strain in the 1 direction with only normal stress components right

$$\epsilon_1 = \frac{1}{E} \left[\sigma_1 - \nu(\sigma_2 + \sigma_3) \right] \quad (7.60)$$

Well with these two expression we can now begin to put these values in terms of what we already know the full matrix for only normal stresses will then be

$$\epsilon_1 = \frac{1}{E} \left[\sigma_1 - \nu(\sigma_2 + \sigma_3) \right] \quad (7.61)$$

$$\epsilon_2 = \frac{1}{E} \left[\sigma_2 - \nu(\sigma_1 + \sigma_3) \right] \quad (7.62)$$

$$\epsilon_3 = \frac{1}{E} \left[\sigma_3 - \nu(\sigma_1 + \sigma_2) \right] \quad (7.63)$$

So can you see any relationship pop up immediately? How about focus on S_{11} well we see that

$$S_{11} = \frac{1}{E} \quad (7.64)$$

and we can see for the other components that

$$S_{12} = -\frac{\nu}{E} \quad (7.65)$$

We can also introduce here a more general way to write strain where

$$\epsilon_{ij} = \frac{1}{E} \left[(1 + \nu)\sigma_{ij} - \nu\sigma_{kk}\delta_{ij} \right] \quad (7.66)$$

where δ_{ij} is the **Kronecker Delta** which will be 1 when $i = j$ and 0 when $i \neq j$ [10].

Let's keep this relationship in mind as we move on to the 4-6 rows of the compliance matrix. Well those equations are pretty straight forward

$$\epsilon_4 = 2(S_{11} - S_{12})\sigma_4 \quad (7.67)$$

$$\epsilon_5 = 2(S_{11} - S_{12})\sigma_5 \quad (7.68)$$

$$\epsilon_6 = 2(S_{11} - S_{12})\sigma_6 \quad (7.69)$$

We can alternatively write an expression for strain using the equation above and noting that the 4th row of our matrix we have only a shear stress component so we would have that

$$\epsilon_{12} = \frac{1 + \nu}{E} \sigma_{12} \quad (7.70)$$

$$\gamma_{12} = 2\epsilon_{12} \quad (7.71)$$

$$\gamma_{12} = \frac{2(1 + \nu)}{E} \sigma_{12} \quad (7.72)$$

$$(7.73)$$

now look at that last expression and remember that we had the general relationship for to relate shear stress and strain that

$$\tau = G\gamma \quad (7.74)$$

so now we can see that

$$G = \frac{E}{2(1 + \nu)} = \frac{1}{2(S_{11} - S_{12})} \quad (7.75)$$

We can find the **Poisson's ratio** as well since we know that in general

$$\nu_{ij} = -\frac{\epsilon_j}{\epsilon_i} \quad (7.76)$$

so we can find that for this system (assuming uniaxial tension only)

$$\nu_{12} = -\frac{S_{12}}{S_{11}} \quad (7.77)$$

with all these values now defined we can re-write our compliance matrix as

$$\begin{bmatrix} \epsilon_1 \\ \epsilon_2 \\ \epsilon_3 \\ \epsilon_4 \\ \epsilon_5 \\ \epsilon_6 \end{bmatrix} = \begin{bmatrix} \frac{1}{E} & -\frac{\nu}{E} & -\frac{\nu}{E} & 0 & 0 & 0 \\ -\frac{\nu}{E} & \frac{1}{E} & -\frac{\nu}{E} & 0 & 0 & 0 \\ -\frac{\nu}{E} & -\frac{\nu}{E} & \frac{1}{E} & 0 & 0 & 0 \\ 0 & 0 & 0 & \frac{1}{G} & 0 & 0 \\ 0 & 0 & 0 & 0 & \frac{1}{G} & 0 \\ 0 & 0 & 0 & 0 & 0 & \frac{1}{G} \end{bmatrix} \begin{bmatrix} \sigma_1 \\ \sigma_2 \\ \sigma_3 \\ \sigma_4 \\ \sigma_5 \\ \sigma_6 \end{bmatrix} \quad (7.78)$$

This is a very nice result and you can convince yourself why I neglected putting the notation on the Poisson's ratio. Now you will additionally see some further constants utilized to bundle these elastic constants like the **Lame's** constants[10]:

$$\mu = G \quad (7.79)$$

$$\lambda = C_{12} \quad (7.80)$$

This is just another way to represent the matrix seen above in another notation that is common.

7.3.7 Ex. Jewelry Maker: Strain Without Stress?

A jewelry maker creates a die to form a new cufflink made of steel. We need to know how much stress to apply to the metal slab to reduce the thickness to 3mm. The die is a simple channel that does not constrain the metal in the x-direction and the channel is well lubricated so that all frictional forces and stresses along the channel walls can be ignored[10].

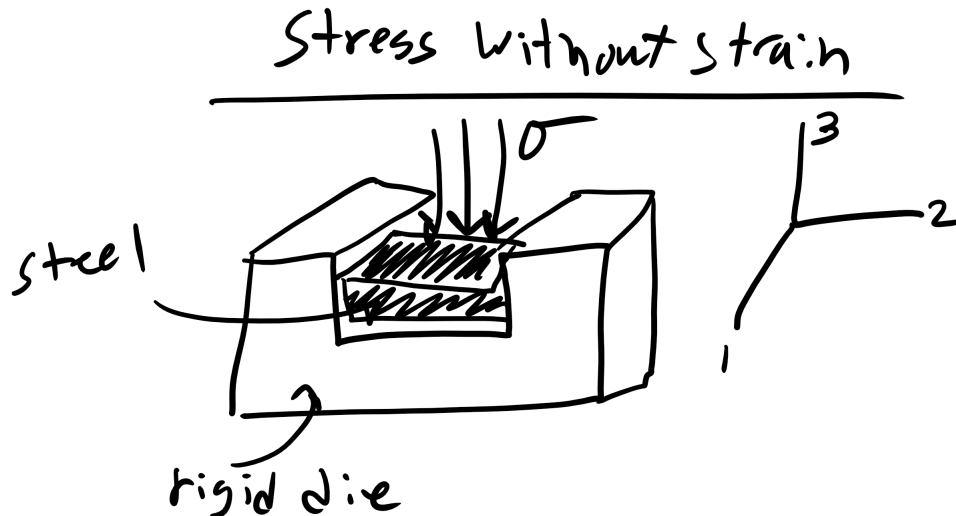


Figure 7-6: Die in which steel of initial thickness 6mm will be subjected to normal stress σ_{zz} .

a.) State all the components of the stress tensor under the applied stress.

Well there is clearly a stress in the z direction. What about x and y?

b.) Which normal strain components are zero and why?

c.) Use your answers in part a) and b) to express the relationship between the non-zero stresses in this system.

7.3.8 Pressure Vessels: A Special Stress State

Finally let's consider a very common scenario, a **thin walled pressure vessel**. The thin walled vessel has an applied **pressure difference** ΔP between the internal pressure and the environment[10]. The **wall thickness is sufficiently small** where we can say $t \ll R$ or that $\frac{R}{t} \geq 10$ [10]. **What is the stress state?** It is **plane stress state** due to symmetry considerations. Therefore we need to find σ_1 and σ_2 which we will accomplish by **drawing free body diagrams**[10].

Let us first **consider the longitudinal direction**. Remember that the **forces must sum to zero**.

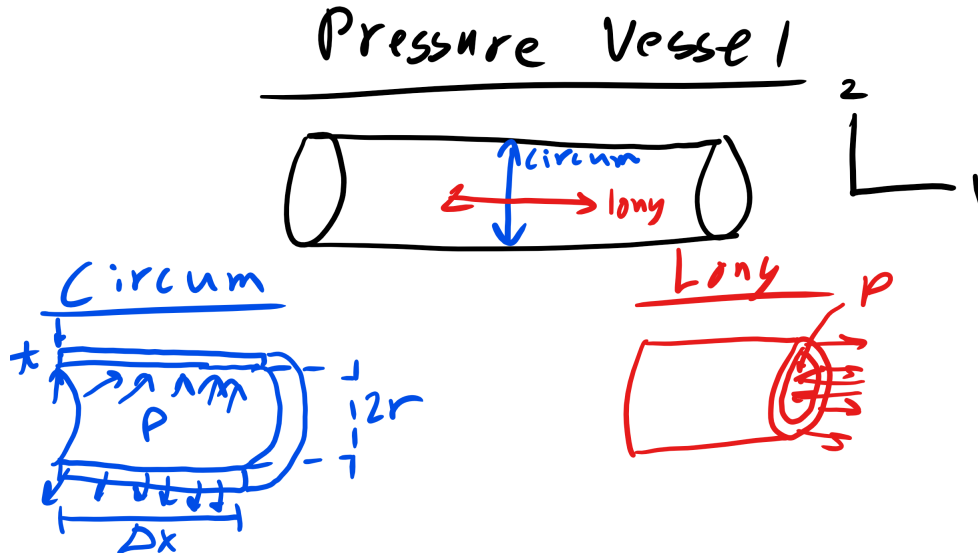


Figure 7-7: Pressure Vessel.

$$\sum F_1 = 0 = \Delta P \pi r^2 - \sigma_{11} 2\pi r t \quad (7.81)$$

$$\sigma_{11} = \sigma_{Longitudinal} = \frac{\Delta P r}{2t} \quad (7.82)$$

We have the longitudinal stress so now let us look at the other direction, **circumferential or hoop**, and again the forces must sum to equal zero:

$$\sum F_2 = 0 = -\Delta P \Delta x 2R + \sigma_{22} \Delta x t 2 \quad (7.83)$$

$$\sigma_{22} = \sigma_{Hoop} = \frac{\Delta P R}{t} \quad (7.84)$$

As you can see the **hoop stress is twice as large as the longitudinal stress** so you should expect the material to fail in such a manner, unless there are extenuating conditions, i.e. defects, corrosion, different processing, etc. The **strain ratio for hoop to longitudinal strain is nearly 4 : 1**. [10]

7.3.9 Resolving Stress on Plane of Interest:

First we must define a new coordinate system that aligns with the plane of interest, i.e. we must rotate our old coordinate axes (x, y) to align with our new coordinate axes (x', y') [10].

Then we balance out the forces assuming **static equilibrium** [10]:

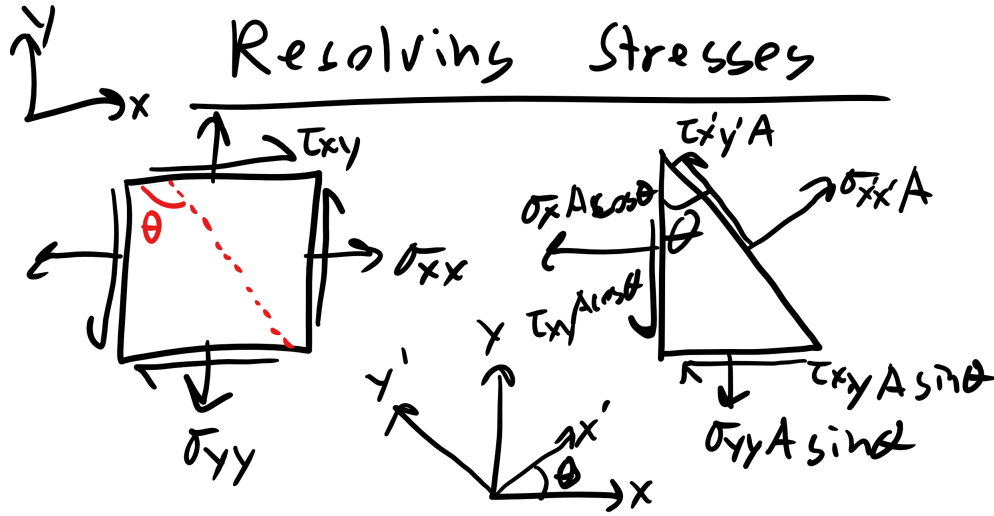


Figure 7-8: Biaxial stress condition and investigating stress state in an arbitrary plane.

$$\sum F_{x'} = 0 = \sigma_{x'x'}A' - (\tau_{xy}A' \sin \theta) \cos \theta - (\sigma_{yy}A' \sin \theta) \sin \theta - (\tau_{xy}A' \cos \theta) \sin \theta - (\sigma_{xx}A' \cos \theta) \cos \theta \quad (7.85)$$

After some rearranging and trig transformations:

$$\sigma_{x'x'}(\theta) = \frac{\sigma_{xx} + \sigma_{yy}}{2} + \frac{\sigma_{xx} - \sigma_{yy}}{2} \cos 2\theta + \tau_{xy} \sin 2\theta \quad (7.86)$$

$$\sigma_{y'y'}(\theta) = \frac{\sigma_{xx} + \sigma_{yy}}{2} - \frac{\sigma_{xx} - \sigma_{yy}}{2} \cos 2\theta - \tau_{xy} \sin 2\theta \quad (7.87)$$

$$\tau_{x'y'}(\theta) = -\left(\frac{\sigma_{xx} - \sigma_{yy}}{2}\right) \sin 2\theta + \tau_{xy} \cos 2\theta \quad (7.88)$$

We have successfully transformed the stress state to our new coordinate system! But as engineers we recognize that typically materials will **fail** at locations of **maximum stress**[10]. Typically **ceramics, brittle oxides, glassy polymers will fail at maximum normal stress** and **metals or composites will fail at maximum shear stress**[10]. In order to find the **maximum stress state** or **principal stress state** we simply **differentiate** with respect to θ and **set equal to zero** and find that[10]:

$$\tan 2\theta = \frac{\tau_{xy}}{\frac{\sigma_{xx} - \sigma_{yy}}{2}} \quad (7.89)$$

We can then substitute this back into the above equations and get:

$$\sigma_1 = \frac{\sigma_{xx} + \sigma_{yy}}{2} + \sqrt{\left(\frac{\sigma_{xx} - \sigma_{yy}}{2}\right)^2 + \tau_{xy}^2} \quad (7.90)$$

$$\sigma_2 = \frac{\sigma_{xx} + \sigma_{yy}}{2} - \sqrt{\left(\frac{\sigma_{xx} - \sigma_{yy}}{2}\right)^2 + \tau_{xy}^2} \quad (7.91)$$

σ_1 and σ_2 are the **principal maximum normal stresses** and you can see by definition that $\sigma_1 > \sigma_2$ [10]. We can do the same for the **maximum shear stress** and find that:

$$\tau_{xy,max} = \sqrt{\left(\frac{\sigma_{xx} - \sigma_{yy}}{2}\right)^2 + \tau_{xy}^2} \quad (7.92)$$

You can also do this transformation a bit easier using a transformation matrix T where

$$[T] = \begin{bmatrix} c^2 & s^2 & 2sc \\ s^2 & c^2 & -2sc \\ -sc & sc & c^2 - s^2 \end{bmatrix} \quad (7.93)$$

where $c = \cos \theta$ and $s = \sin \theta$.

So we now write that

$$\sigma' = T\sigma \quad (7.94)$$

or similarly

$$\begin{bmatrix} \sigma_{xx'} \\ \sigma_{yy'} \\ \tau_{xy'} \end{bmatrix} = \begin{bmatrix} c^2 & s^2 & 2sc \\ s^2 & c^2 & -2sc \\ -sc & sc & c^2 - s^2 \end{bmatrix} \begin{bmatrix} \sigma_{xx} \\ \sigma_{yy} \\ \tau_{xy} \end{bmatrix} \quad (7.95)$$

We can almost do the same for strain but for the following complication that we have the definition that $\epsilon_{xy} = \frac{1}{2}\gamma_{xy}$ so we have to account for this in our transformation specifically via the introduction of the **Reuter's Matrix**[10]

$$[R] = \begin{bmatrix} 1 & 0 & 0 \\ 0 & 1 & 0 \\ 0 & 0 & 2 \end{bmatrix} \quad (7.96)$$

So to transform to new coordinate systems for strain we have to do the following

$$\epsilon' = RTR^{-1}\epsilon \quad (7.97)$$

7.3.10 Mohr's Circle Construction

Otto Mohr, a German engineer in the 1800's, recognized that we can **represent the principal stress state graphically**[10]. We can re-write the equations above and sum the square of Eq.7.86 and Eq.7.88 to give us:

$$\left[\sigma_1 - \left(\frac{\sigma_{xx} + \sigma_{yy}}{2} \right) \right]^2 + \tau_{xy,max}^2 = \left(\frac{\sigma_{xx} - \sigma_{yy}}{2} \right)^2 + \tau_{xy}^2 \quad (7.98)$$

You should notice that this form has a similar form to the equation of a circle, i.e.

$$(x - c)^2 + y^2 = r^2 \quad (7.99)$$

where the center of the circle is $\frac{\sigma_{xx} + \sigma_{yy}}{2}$ and the radius of the circle is $\sqrt{\left(\frac{\sigma_{xx} - \sigma_{yy}}{2}\right)^2 + \tau_{xy}^2}$ [10]. We can **plot Mohr's circle for an arbitrary initial stress state**.

7.3.11 Ex. Plane Stress States

Consider a material initially under a strain state where $\sigma_{xx} = 22$ MPa, $\sigma_{yy} = 10$ MPa and $\tau_{xy} = 6$ MPa.

What is the stress state of a plane inclined at 30° CCW?

Draw Mohr's circle to find the principal stress state.

7.3.12 Linear Viscoelasticity (LVE):

So far we have dealt with **continuum isotropic linear elasticity** and **anisotropic linear elasticity**[10]. All these modes of deformation are **independent of time, rate, and temperature**[10]. However, today we will discuss linear viscoelasticity whose deformation is governed by time, rate, and temperature. **Linear viscoelasticity** is the deformation between that of an **elastic solid and a viscous fluid**. We can actually see this in the name linear viscoelasticity[10]. There is still a linear relationship between stress and strain for a given time and temperature. The **visco** term denotes a **time component** and **elasticity** denotes **reversibility**[10]. The elastic solid will again behave Hookean with the relationship

$$\sigma = E\epsilon \quad (7.100)$$

and the viscous fluid will be governed by this new equation

$$\sigma = \eta\dot{\epsilon} \quad (7.101)$$

Linear Viscoelasticity is typically used to describe the **mechanical response for polymers, glasses, tissues, and cells**[10].

When a **viscous fluid** is deformed under an applied shear stress there is **no recovery when the shear stress is removed** so our equation for shear stress becomes

$$\tau = \eta \dot{\gamma} \quad (7.102)$$

where η is the **fluid viscosity** (units of Pa s) and $\dot{\gamma}$ is the **shear strain rate** (units of inverse seconds)[10]. Again this is linear because there is a proportional increase in σ and ϵ for some time or temperature.

We can make a couple of linear viscoelastic (LVE) models which describe some LVE behavior phenomenologically as combinations of **springs and dashpots**[10].

7.3.13 Maxwell Model:

Let's take a look at the **Maxwell model** which is a combination of a **spring in series with a dashpot** that contains a Newtonian fluid.

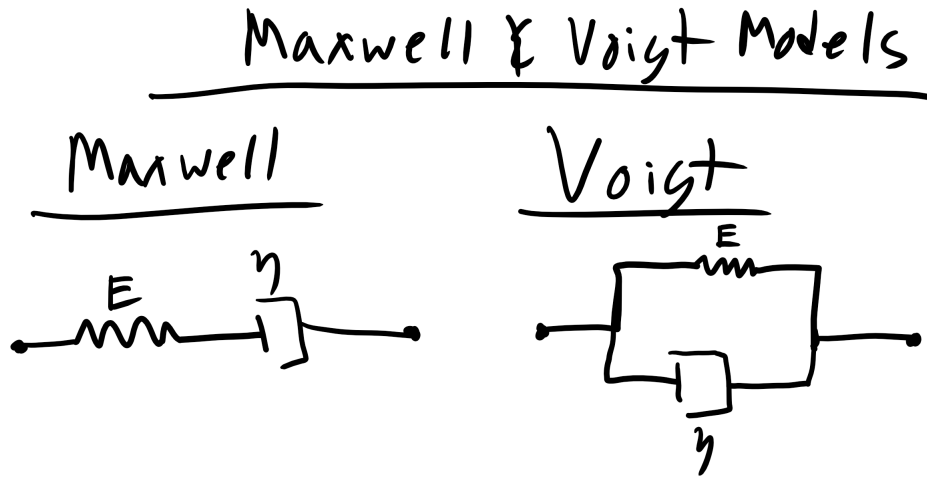


Figure 7-9: Maxwell and Kelvin-Voigt Model

The spring is described by the following equation:

$$\sigma_s = E_s \epsilon_s \quad (7.103)$$

where σ_s is the stress in the spring, E_s is the stiffness of the spring, and ϵ_s is the strain in the spring[10].

The dashpot is described by:

$$\sigma_d = \eta_d \dot{\epsilon}_d \quad (7.104)$$

where σ_d is the stress in the dashpot, η_d is the viscosity of the dashpot, and $\dot{\epsilon}_d$ is the strain rate of the dashpot[10].

Now let's say that I stress the system (this should be reminiscent of the composites pulled transverse to the fiber direction when we get to this) the **stresses should be the same for the spring and the dashpot** however the **strains in the dashpot and the spring will be different** which gives us the following equation[10]:

$$\sigma_M = \sigma_s = \sigma_d \quad (7.105)$$

$$\epsilon_M = \epsilon_s + \epsilon_d \quad (7.106)$$

$$\dot{\epsilon}_M = \dot{\epsilon}_s + \dot{\epsilon}_d \quad (7.107)$$

$$\dot{\epsilon}_M = \frac{\dot{\sigma}_M}{E} + \frac{\sigma_M}{\eta} \quad (7.108)$$

With this system we can do two types of experiments: **stress relaxation** ($\epsilon = \epsilon_0$ i.e. constant strain) and **creep** ($\sigma = \sigma_0$, i.e. constant stress).

For **stress relaxation** we can plug into our equation and solve for how the stress in our Maxwell model should vary over time[10]:

$$0 = \frac{1}{E} \frac{d\sigma}{dt} + \frac{\sigma}{\eta} \quad (7.109)$$

$$\int_{\sigma_0}^{\sigma} \frac{d\sigma}{\sigma} = \int_0^t \frac{-E}{\eta} dt \quad (7.110)$$

$$\sigma(t) = \sigma_0 \exp\left(\frac{-Et}{\eta}\right) \quad (7.111)$$

$$\sigma(t) = \sigma_0 \exp\left(\frac{-t}{\tau}\right) \quad (7.112)$$

where $\tau = \frac{E}{\eta}$ is the relaxation time. Similarly for **creep**:

$$\frac{d\epsilon}{dt} = 0 + \frac{\sigma_0}{\eta} \quad (7.113)$$

$$\int_{\epsilon_0}^{\epsilon} d\epsilon = \int_0^t \frac{\sigma_0}{\eta} dt \quad (7.114)$$

$$\epsilon(t) = \epsilon_0 + \frac{\sigma_0 t}{\eta} \quad (7.115)$$

7.3.14 Kelvin-Voigt Model:

There is also the **Kelvin-Voigt (KV) model** has the **spring and dashpot series in parallel**[10].

In this case now the **strain is the same** but now the **stresses are different** so we get[10]:

$$\epsilon_{KV} = \epsilon_s = \epsilon_d \quad (7.116)$$

$$\sigma_{KV} = \sigma_s + \sigma_d \quad (7.117)$$

$$\sigma_{KV} = E_s \epsilon_s + \eta_d \dot{\epsilon}_d \quad (7.118)$$

$$\epsilon_{\dot{KV}} = \frac{\sigma_{KV}}{\eta_d} - \frac{E_s}{\eta_d} \epsilon_{KV} \quad (7.119)$$

Now for **stress relaxation** we get the final equation for stress vs time as:

$$\sigma(t) = E\epsilon_0 \quad (7.120)$$

and for **creep** we get:

$$\epsilon(t) = \frac{\sigma_0}{E} \left(1 - \exp\left[-\frac{t}{\tau}\right] \right) \quad (7.121)$$

You can now build even more complex combinations to model viscoelastic properties like the Standard Linear Viscoelastic Solid Model[10]. Perhaps a more useful experimental measurement for viscoelastic behavior is accomplished by **Dynamic Mechanical Testing**.

7.3.15 Dynamic Mechanical Testing:

The more utilized characterization technique is typically some type of **dynamic mechanical testing** to probe the viscoelastic behavior of materials[10]. In this experiment the polymer is subjected of a sinusoidal loading at variable frequencies which can be described as such as

$$\sigma_{applied} = \sigma_o \sin \omega t \quad (7.122)$$

This is the applied stress but remember we are dealing with a viscoelastic material so there will be a phase lag, δ , in the strain behavior which will also be sinusoidal

$$\epsilon = \epsilon_o \sin \omega t \quad (7.123)$$

So what we will end up with is that the material will actually experience a stress that contains the phase lag as shown below

$$\sigma = \sigma_o \sin(\omega t + \delta) \quad (7.124)$$

$$\sigma = \sigma_o \sin \omega t \cos \delta + \sigma_o \cos \omega t \sin \delta \quad (7.125)$$

where in the equation above we just expanded our trig functions. Notice here that the first term represents the component that is in phase with the strain or the elastic response while the second term represents the out of phase behavior or the viscous response[10]. We can then define

two elastic moduli to describe the in-phase and out of phase behavior[10]. The **storage** or elastic modulus is the in-phase contribution and defined as

$$E' = \frac{\sigma_o \cos \delta}{\epsilon_o} \quad (7.126)$$

and the **loss** modulus is the out of phase component is

$$E'' = \frac{\sigma_o \sin \delta}{\epsilon_o} \quad (7.127)$$

We can now re-write our expression for the stress in the material as

$$\sigma = E' \sin \omega t + E'' \cos \omega t \quad (7.128)$$

then by definition we have that

$$\tan \delta = \frac{E''}{E'} \quad (7.129)$$

This is sometimes called the **loss tangent** and essentially represents the amount of energy lost over the energy stored[10]. You might also see these expressions written using complex variables like so

$$\epsilon = \epsilon_o \exp i\omega t \quad (7.130)$$

$$\sigma = \sigma \exp i\omega t + \delta \quad (7.131)$$

$$E = \frac{\sigma_o}{\epsilon_o} \exp i\delta = \frac{\sigma_o}{\epsilon_o} (\cos \delta + i \sin \delta) = E' + E'' \quad (7.132)$$

7.3.16 Analysis of DMA Experiments:

Typically you will find, at a fixed temperature that the **loss tangent** and the loss modulus are typically very small at very low and and very high frequencies and they will typically peak at intermediate frequencies[10]. The **storage modulus is high at high frequencies (short times)** which should make sense intuitively as polymers will typically behave **glassy or elastic at high frequencies and short times (strain rate is faster than relaxation time of polymer)** and at **low frequencies (long time longer than relaxation time) the polymer will behave more like a viscous fluid**[10].

More importantly from this analysis we can determine experimentally the **characteristic relaxation time** from the point where G' and G'' intersect. More often we will find that typical DMA experiments where G' , G'' , and $\tan \delta$ are plotted as a function of temperature. Here you will typically see larger peaks and changes in these parameters[10]. The amount of molecular motion and free volume will increase and this will affect these properties, particularly the loss tangent. So you will expect to see large changes at the glass transition temperature and melting temperature

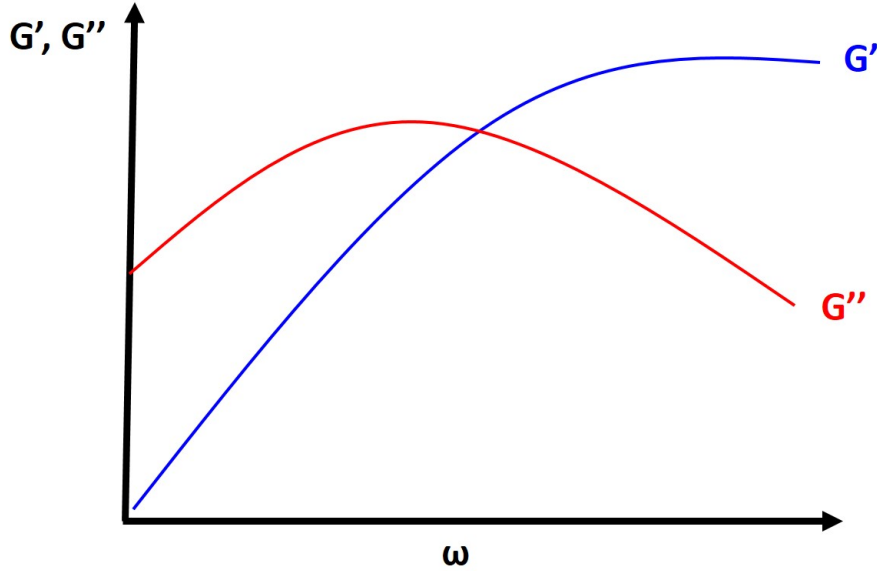


Figure 7-10: Storage and Loss Modulus as a Function of Frequency

but you also might expect to see other small peaks associated with **secondary transitions** (note this is not referring to second order thermodynamic transitions like T_g this is just referring to the magnitude of the peaks) associated with molecular motion of the polymer such as the temperature at which backbone side group rotation is accessible[10].

7.3.17 Composite Mechanics:

So far we have been talking about the mechanics of primarily metals but we haven't really touched on composite mechanics. **Composites materials are materials that contain typically more than one type of material combined**[10]. This typically involves a **material matrix** which is the **major component** in terms of **volume fraction**. This matrix material is reinforced by an additional material typically one that is **stiffer or tougher than matrix material**. The material that reinforces the matrix can be in **particle form, fibers, or precipitates**[10]. A composite can also be a porous material like metal foams, concrete, ECM, etc.

Let's take a look at a **particle reinforced composite** that is composed of a matrix which has some elastic modulus, E_m , and volume fraction, f_m [10]. There is also the particle reinforcement in this case which again has an associated elastic modulus, E_p , and volume fraction f_p [10]. Thus the **total composite modulus**, $E_{composite}$ is

$$E_{composite} = E_m f_m + E_p f_p \quad (7.133)$$

empirically there is typically a constant that is less than 1 for the particle reinforcement contribution but again that constant can only be found empirically.

Let's now look at a **fiber reinforced composite** that is pulled or stressed in the **transverse**

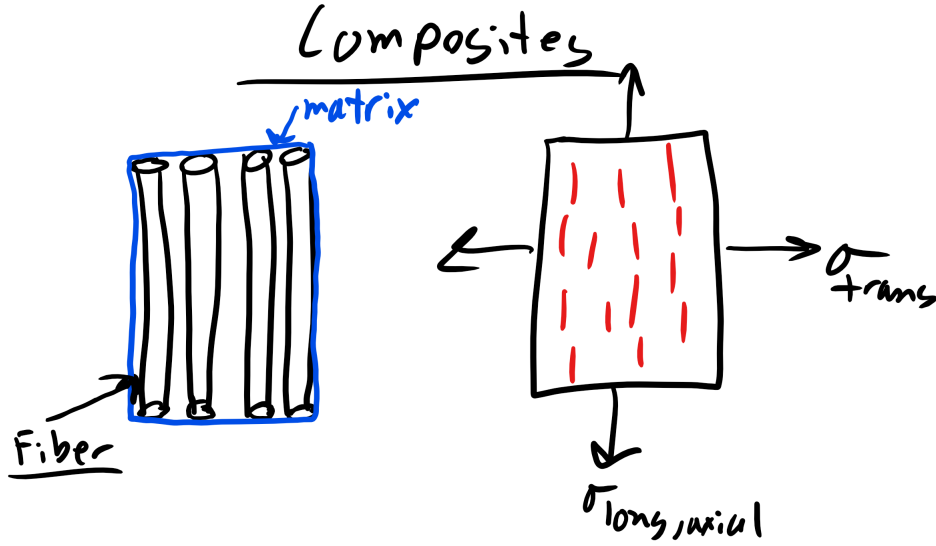


Figure 7-11: Composites pulled in the transverse or longitudinal/axial direction.

direction with respect the the **longitudinal or axial direction of the fibers**[10]. The **stresses are the same on the matrix and the fibers**. However the **strains of the fiber and matrix will be different**. With these constraints:

$$\sigma_m = \sigma_f = \sigma \quad (7.134)$$

$$\epsilon_c = \epsilon_m f_m + \epsilon_f f_f \quad (7.135)$$

$$\epsilon_c = \sigma \left(\frac{f_m}{E_m} + \frac{f_f}{E_f} \right) \quad (7.136)$$

$$\frac{1}{E_c} = \frac{f_f}{E_f} + \frac{f_m}{E_m} \quad (7.137)$$

If we instead **pull parallel to the fiber longitudinal or axial direction**. Here the **strain is the same** but now the **stresses will be different** for the fibers and the matrix[10]. So with those constraints we get

$$\sigma_c = \sigma_f f_f + \sigma_m f_m \quad (7.138)$$

$$\epsilon_c = \epsilon_m = \epsilon_f \quad (7.139)$$

$$\sigma_c = E_f \epsilon f_f + E_m \epsilon f_m \quad (7.140)$$

$$E_c = E_f f_f + E_m f_m \quad (7.141)$$

We can see the difference in the Young's modulus in both of these directions as function of volume fraction in the plot below:

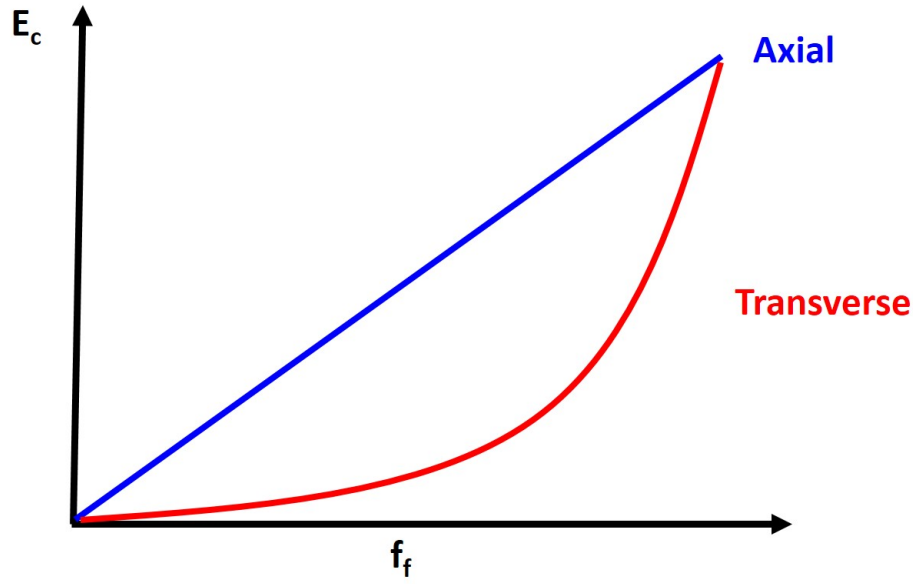


Figure 7-12: Composite modulus as a function of fiber fraction.

Composites are also useful tools to help blunt crack propagation.

7.4 2. Plastic Regime

7.4.1 Yielding Criterion:

So far we have just been talking about stress and strain up to the yield point. However what happens beyond the elastic limit of materials? Well we have already discussed that the **yield point** denotes that the deformation is now permanent or **plastic** and we have initiated **dislocation or defect motion**[10]. But as engineers perhaps the better or more useful question to ask is can we predict whether yielding will occur for materials that are not just simply loaded uniaxially. There are multiple yielding criterion that we will discuss, specifically: **Rankine, Tresca, and von Mises Yield Criterion**[10].

Rankine:

Rankine criterion also known as the **maximum normal stress** criterion states the a material will fail or yield when the maximal principal (normal) stress (σ_1) reaches the value where the material yields in uniaxial tension or compression so the material will yield when:

$$\sigma_1 \geq \sigma_y \quad (7.142)$$

Rankine doesn't accurately describe material yielding, it is **missing shear stress**.

Tresca:

So let's take a look at the **Tresca criterion** or the **max shear stress criterion** which states that the material yields when the $\tau_{max} = \frac{\sigma_1 - \sigma_3}{2} = \sigma_y$ reaches the value it does when material yields

under uniaxial loading which is described below:

$$\sigma_1 - \sigma_3 \geq \sigma_y \quad (7.143)$$

This is better, but in 1913 for WWI/WWII subs because they found that the Tresca criterion was a poor predictor for yielding[10].

Von Mises:

So we developed the **Von Mises criterion** is also called the **maximum shear deformation energy (SDE) criterion** and states the material will yield when the SDE reaches the yield stress value under uniaxial loading which is:

$$\sigma_{eff} = \sqrt{\frac{1}{2}[(\sigma_{11} - \sigma_{22})^2 + (\sigma_{22} - \sigma_{33})^2 + (\sigma_{33} - \sigma_{11})^2 + 6(\sigma_{23}^2 + \sigma_{31}^2 + \sigma_{12}^2)]} \geq \sigma_y \quad (7.144)$$

or in terms of the principal stresses:

$$\sigma_{eff} = \sqrt{\frac{1}{2}[(\sigma_1 - \sigma_2)^2 + (\sigma_2 - \sigma_3)^2 + (\sigma_3 - \sigma_1)^2]} \geq \sigma_y \quad (7.145)$$

You can see by drawing the yield loci of these different criterion that Rankine is the most conservative yield criterion[10].

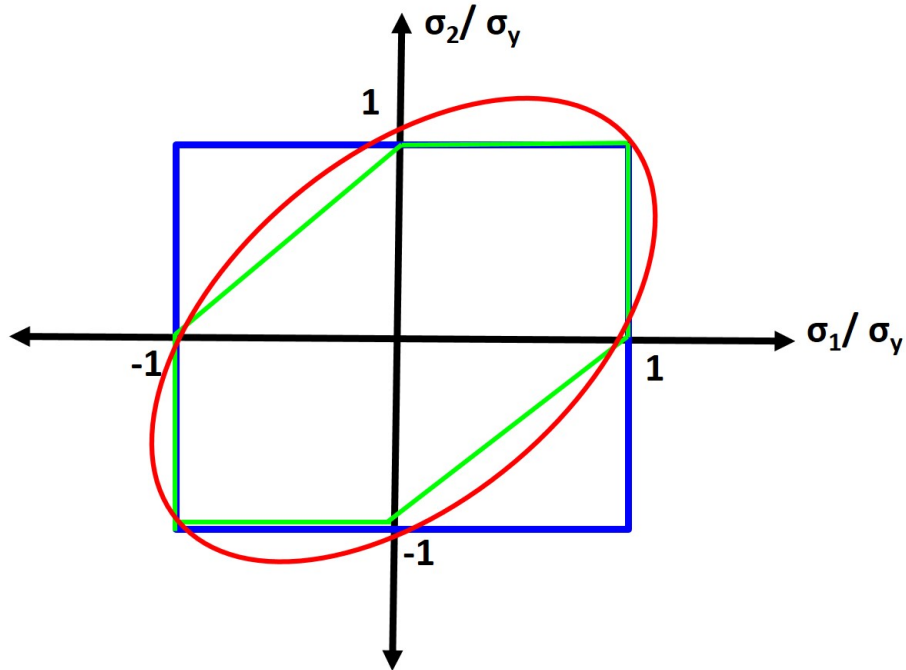


Figure 7-13: Yield Criterion. Rankine (blue), Tresca (green), Von Mises (red).

7.4.2 Yielding Mechanisms:

In a **perfect copper crystal** I can prove that the **yield stress should be approximately 20GPa** however the actual yield stress of copper is approximately **40MPa**[10]. **What can explain the 3 order of magnitude difference?** A nice approximation is that the theoretical yield stress is typically $\frac{G}{30}$ and the theoretical fracture strength is $\frac{E}{10}$ [10].

Well remembering back to structure real materials have **defects** that allow atomic motion and in **particular dislocation motion and slip a shear stress much lower than the theoretical prediction**[10]! We have talked quite a bit about the structure of dislocations but as of yet not too much about the **motion of dislocations**[10].

What direction of motion will contribute most to yielding and dislocation motion?

The direction that require the least amount of energy to move! And remembering back to structure this corresponds to the shortest distance in your cell, i.e. the **close paced planes and directions**[10]. So for **FCC the primary slip systems are the $\langle 110 \rangle$ directions and the 111 planes**. For **BCC it is the $\langle 111 \rangle$ directions and the 110 planes** even though these aren't close packed[10]. Remember as well that dislocations are also characterized by **dislocation density** which is again

$$\rho = \frac{N}{A} \quad (7.146)$$

where N is the number of dislocations in a given area A. A material that is **highly cold worked** with a high dislocation density would be 10^{14} dislocations per m^2 [10]. A **highly annealed material** would exhibit a dislocation density closer to 10^7 dislocations per m^2 [10]. You can also get a quick estimate of the distance between dislocations by the following relationship

$$\rho = \frac{1}{l^2} \quad (7.147)$$

where l is the distance between dislocations!

7.4.3 Strengthening Mechanisms:

Now we have talked quite a bit about material constants and how they are often not really a constant. They **vary depending on the material processing history!** Perhaps no other material constant varies more depending on the processing history than **yield stress**[10]. But as material scientists this gives us a fantastic knob to tune our materials for different applications. And the basic relationship to remember is that the **yield stress increases when it becomes harder for dislocations to move or propagate**[10]. So when there are **obstacles** to dislocation motion the **yield stress increases** and we can do this via 4 primary mechanisms:

- **Work Hardening (more dislocations)**
- **Solute Strengthening (more solute atoms)**

- Grain Size Strengthening (decrease grain size)
- Precipitate/Particle Strengthening (add precipitates or particles)

7.4.4 1. Work Hardening: Increase ρ via Plastic Deformation

$$\Delta\sigma_y = \alpha Gb\sqrt{\rho} \quad (7.148)$$

where G is the shear modulus, b is Burgers vector, and α is the materials constant (close to 1)[10]. During the work hardening process you plastically deform the material and initiate or create dislocations in the material. This is often done in rolling sheet metal via cold-rolling[10]. You create more dislocations which serve as obstacles for dislocation motion which then increases the yield strength as seen below.

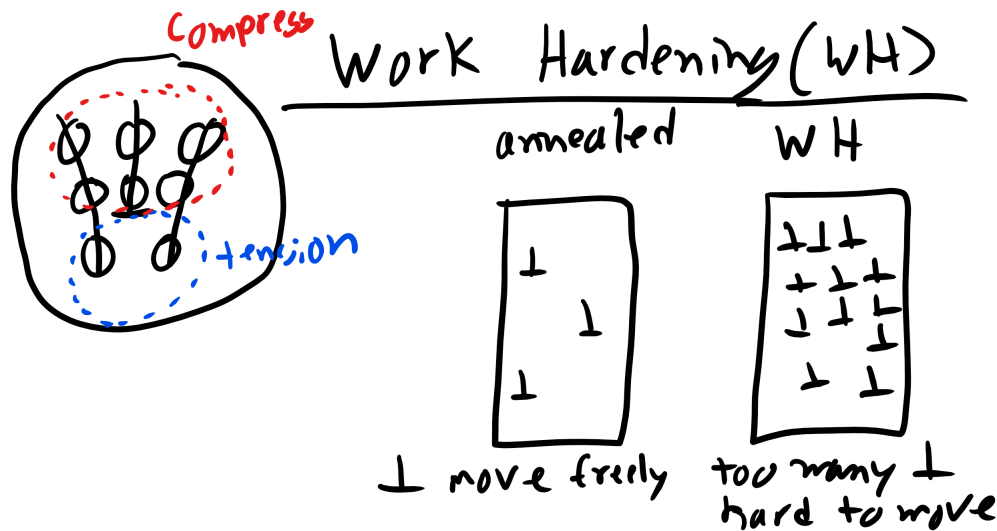


Figure 7-14: Work Hardening

7.4.5 2. Solute Strengthening

$$\Delta\sigma_y = Gb\sqrt{c_{sol}}\epsilon_{sol}^{\frac{3}{2}} \quad (7.149)$$

where c_{sol} is the concentration of the solute and ϵ_{sol} is the lattice strain due to any size mismatch[10]. We talked about this phenomenon a bit during structure. When you replace the a solvent atom with a larger solute atom you create a region with a localizes stress field that will interact with dislocation and again impede dislocation motion, causing yield stress to increase[10].

7.4.6 3. Grain Size Strengthening

$$\Delta\sigma_y = \frac{\kappa}{d_g} \quad (7.150)$$

Solute Strengthening

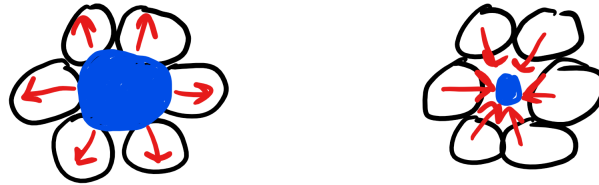


Figure 7-15: Solute Strengthening

where κ is a materials constant and d_g is the diameter of the grain. As you decrease the grain size there is less area for dislocation pile-up which is one method of reducing stress in your material[10]. Smaller grain sizes can only accommodate so many dislocations before the dislocations can no longer pile up and they must be removed from the grain. It should be noted here the the yield stress does not blow up to infinity as the grain size shrinks to zero[10]. Instead at about **less than 10nm** we see the yield stress begins to fall once again because now the grain is so small that only a single dislocation can fit inside a grain so you do not get enough dislocation pile-up.

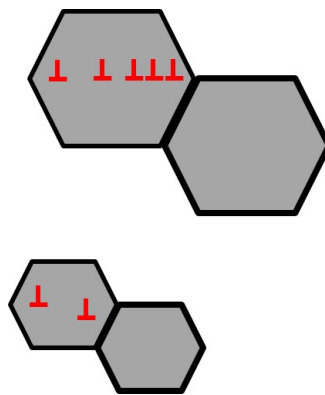


Figure 7-16: Grain Size Strengthening

7.4.7 4. Precipitate/Particle Strengthening

In this case the obstacle to dislocation motion is not a point defect, a dislocation, or a grain boundary, but instead we have a **new phase with a defined particle radius, spacing, and**

mechanical/structural properties[10]. So when the dislocation encounters a defect the dislocation can do one of two things: **1.) Cut the precipitate/particle or 2.) Bow around the precipitates/particle**. To cut through the particles we find the increase in yield stress to be:

$$\Delta\sigma_y = \frac{\gamma_{p-m}\pi r_p}{bl} = \kappa^3 \sqrt{r_p f_p} \quad (7.151)$$

where γ_{p-m} is the additional surface energy added when the particle is cut and thus is the surface energy of the particle/precipitate matrix, r_p is the radius of the particle, b is the burgers vector, l is the average particle spacing, κ is a materials constant, and f_p is the concentration or volume fraction of the particles[10].

To **bow around the precipitates/particle** the increase in yield stress is

$$\Delta\sigma_y = \frac{Gb}{l - 2r_p} \quad (7.152)$$

where G is the shear modulus, b is the burgers vector, l is the average distance between particles and r_p is the radius of the particle[10]. You can see energetically that at **very small particle diameters it is more energetically favorable to cut the particles** because the **energy penalty of creating an increased surface is less for smaller particles**[10]. As the particles become larger bowing is more energetically favorable, for the same volume fraction of particles. **As the volume fraction of particles or precipitates increases the critical radius for cutting vs. bowing decreases as you are now cutting even more particles which creates more surface area and an even larger energy penalty.**

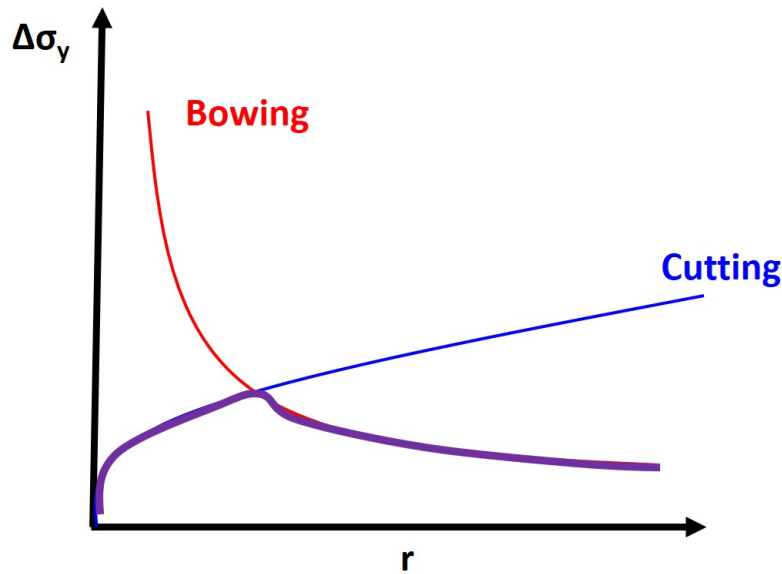


Figure 7-17: Bowling vs Cutting

7.4.8 Polymer Yielding: Shear Banding and Crazing

Shear Banding:

Are zones of material alignment that are **1000s of nm wide** and **nucleate at stresses** that are approximately $\frac{G}{10}$ and continue to grow as stress exceeds[10]. **Shear band deformation is highly nonuniform.** They are also not regions of high defect density but instead they are regions of **chain alignment**. Shear banding nucleation is also highly temperature dependent[10]. Typically for uniaxial tension **shear bands will form at 45° relative to the applied stress**(at locations of maximum shear stress).

Here is a good opportunity to talk about some asymmetry in yield criterion. Typically we find that the **yield stress for uniaxial compression is larger than the yield stress for uniaxial tension**[10]. In polymers this is particularly true as tensile stress will tend to open up more free volume which makes it easier for chains to align.

Craze formation:

Also regions of **highly localized deformation** and they are **distinct from a crack**. **Fibrils will span the craze**. Crazes will form **perpendicular to the loading axis** with fibrils aligned with the loading axis. Crazing will **not occur under compressive stress**[10]. You can **modify the von Mises criterion** when considering shear banding and Tresca when considering crazing.

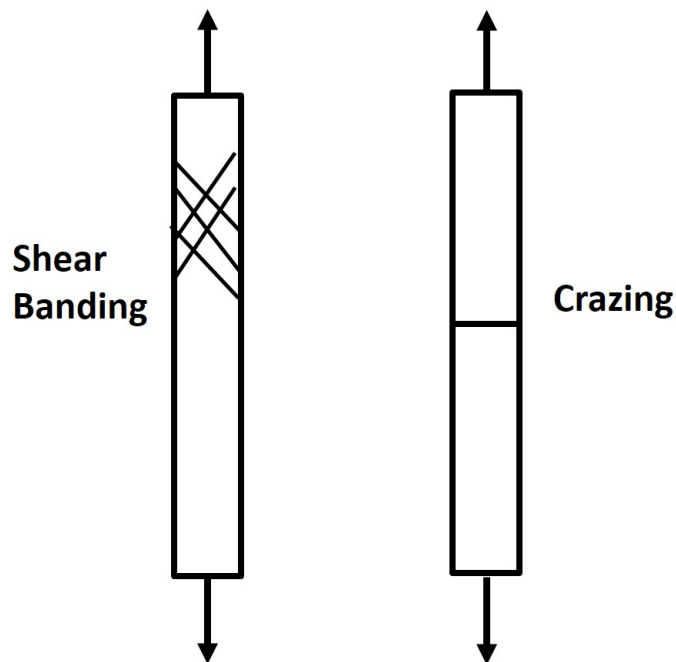


Figure 7-18: Shear Banding vs. Crazing

7.4.9 Time-Temperature Dependent Plasticity:

We have previously discussed creep in relation to polymer LVE. **Creep is time or temperature dependent plastic deformation in crystalline materials.** Creep is particularly insidious because like fatigue the **stress where creep or fatigue ensues is much much less than the reported or measured yield stress of a material**[10]. This is because there are new plastic deformation mechanisms accessed at high T, high stress, and long times.

There are three typical creep regimes:

- **Primary or Transient Creep**
- **Secondary or Steady State Creep**
- **Tertiary or Runaway Creep**

Again as materials scientists we want to focus on predicting the creep strain rate, $\dot{\epsilon}_c$,

$$\dot{\epsilon}_c = K_c \sigma^x d_g^y D_c = K_c \sigma^x d_g^y D_o \exp\left(\frac{-Q_c}{kT}\right) \quad (7.153)$$

where K_c is an empirical material specific creep constant, σ is the applied stress, d_g is the grain diameter, D_c is the creep diffusivity, and Q_c is the activation energy for that creep mechanism[10]. Now those diffusion mechanisms are diffusion of vacancies through the lattice or bulk diffusivity, diffusion of vacancies along grain boundaries, and diffusion of vacancies to dislocations[10].

7.4.10 Lattice/Volume/Bulk Diffusion: Nabarro-Herring Creep

We have our equation for Nabarro-Herring Creep below:

$$\dot{\epsilon}_{NH} = \frac{K_{NH} \sigma D_o \exp\left(\frac{-Q_L}{kT}\right)}{d_g^2} \quad (7.154)$$

the key things to see in this equation is the activation energy for lattice diffusion and the scaling behavior with the grain size[10].

7.4.11 Grain Boundary Diffusion: Coble Creep

Here the number of diffusive pathways increases as the grain size decreases and remember that the **activation energy for grain boundary diffusion is lower than for bulk**[10].

$$\dot{\epsilon}_{CC} = \frac{K_{CC} \sigma D_o \exp\left(\frac{-Q_{GB}}{kT}\right)}{d_g^3} \quad (7.155)$$

7.4.12 Dislocation Creep or Power Law Creep

Here the **net motion of dislocation cores moves in direction of applied stress**, i.e. macroscopic creep. The dependence on applied stress is critical as you can see the scaling behavior in the equation below. Additionally dislocation climb is the rate-limiting process[10].

$$\epsilon_{DLC} = K_{NH} \sigma^{4-6} D_o \exp\left(\frac{-Q_L}{kT}\right) \quad (7.156)$$

We can now take a look at some key aspects of creep and in particular the scaling behavior of creep:

Mechanism	Q	x	y
NH	Q_L	1	-2
CC	Q_{GB}	1	-3
DLC	Q_L	4-6	0

We can see that DLC will dominate at high temperatures and high stress and Coble creep will dominate at lower temperatures compared to NH[10].

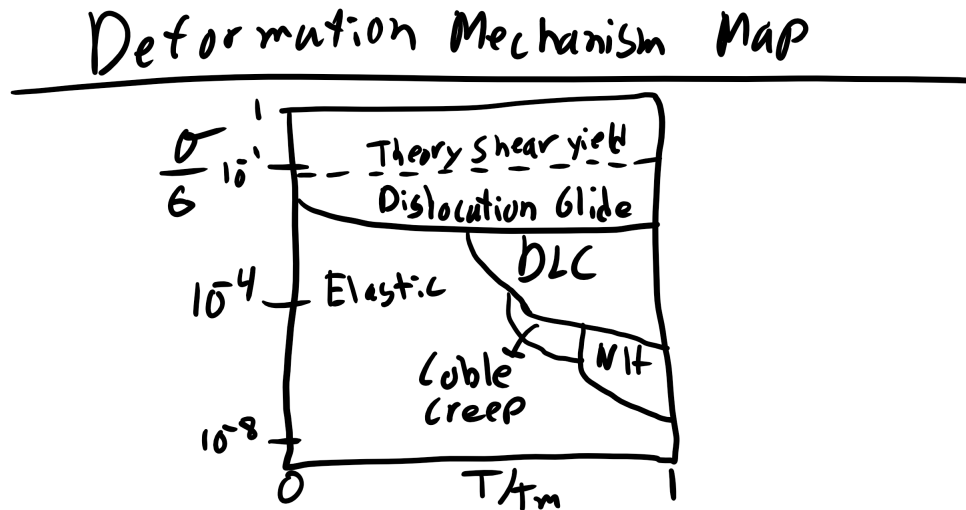


Figure 7-19: Deformation mechanism maps. Visualize and explain why certain mechanisms are predominant .

7.5 3. Fracture Regime

Fracture is the last resort for material deformation mechanisms when all **other elastic/plastic mechanisms are exhausted**. Energy is **dissipated by bond breaking**[10]. In uniaxial loading, the stress required to break the material in two pieces, at the stress fracture. Again as in the case

of yielding the theoretical stress required to fracture materials (Steel 4340 65GPa, Al 20GPa, Si 7GPa) is order of magnitudes lower than the actual stress required to fracture materials (Steel 4340-3GPa, Al .7GPa, Si .3GPa). This is because **real materials typically contains cracks** (inside, at surface, or at interfaces) and these **micro-cracks act as stress concentrators**[10]. And for an elliptical hole we can define the stress as a function of the distance from the stress concentrator

$$\sigma = \sigma_o \left(1 + 2\sqrt{\frac{a}{R}} \right) \quad (7.157)$$

and R at the tip of the crack is $\frac{b^2}{a}$ [10]. Brittle fracture occurs when the stress concentrates at a pre-existing crack tip is so high that the material will break catastrophically.

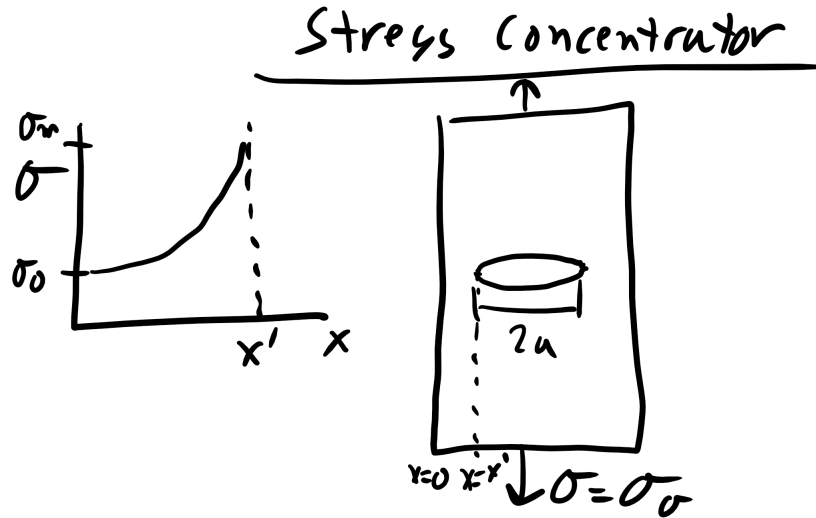


Figure 7-20: Stress Concentrator.

7.5.1 Griffith's Theory of Brittle Fracture:

We can develop an equation for brittle fracture from Griffith by considering the **surface area created** as the crack grows and **relieving stored elastic energy**[10].

Creating Surface Area as Crack Grows

To create the surface area of the crack as it grows we will have a change in the internal energy of the system

$$\Delta U_{surf} = 4at\gamma \quad (7.158)$$

Relieving Stored Elastic Energy

A similar change in internal energy will occur for the the relieved stored elastic energy

$$\Delta U_{el} = -\frac{\pi a^2 t \sigma^2}{2E} \quad (7.159)$$

The crack will reach critical length when we **minimize the total energy**

$$\Delta U_{tot} = \Delta U_{surf} + \Delta U_{el} = 0 \quad (7.160)$$

Giving us the critical crack length

$$\sigma_f = \sqrt{\frac{2\gamma E}{\pi a_{crit}}} \quad (7.161)$$

7.5.2 Orowan Theory of Ductile Fracture:

There are a number of materials, metals and polymers, which **won't fracture in a completely brittle manner** but instead from a **small plastic zone prior to each crack elongation**[10]. For these materials **Orowan** has a theory for ductile fracture which is:

$$\sigma_f = \sqrt{\frac{EG_c}{\pi a}} \quad (7.162)$$

where G_c is the strain energy release rate.

7.5.3 Fracture Toughness:

The final theory for **fracture toughness** considers when a material breaks when the **stress intensity factor** reaches a **critical factor**[10]. The **critical stress intensity factor** depends on the mode of fracture: I, II, and III.

$$K_c = f\sigma\sqrt{\pi a} \quad (7.163)$$

where f is a geometric constant factor and K_c is the fracture toughness and $K_{I,II,III}$ is the critical stress intensity factor under Mode I, II, or III loading.

When one looks at the impact energy or fracture toughness as a function of temperature for brittle materials (like BCC which doesn't have close packed slip planes) you will see a ductile to brittle fracture transition where the fracture toughness decreases dramatically as temperature decreases[10]. For ductile materials like FCC which has a number of slip planes you will not see this sharp transition.

7.5.4 Fatigue

Fatigue (cyclic) loading occurs at applied stresses that are much much less than the stress at fracture but again like creep can lead to **catastrophic failure** at these low applied stresses.

Fatigue failure: fracture due to crack growth every cycle of loading or the crack growth increment per loading cycle which is defined below

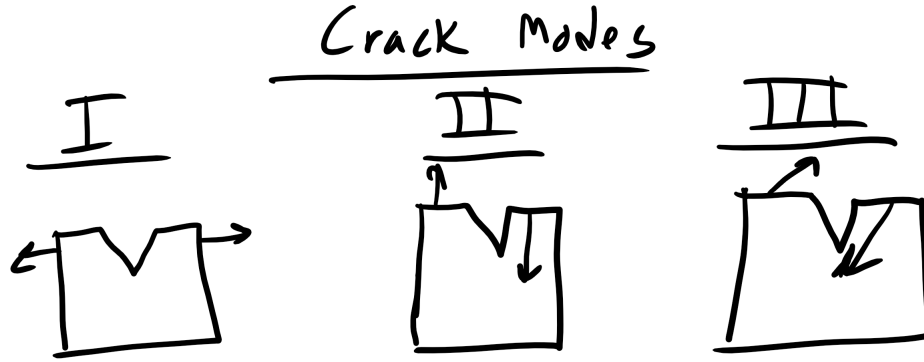


Figure 7-21: Modes of Cracking.

$$\frac{da}{dn} \quad (7.164)$$

where a is the crack length and n is the number of loading cycles[10].

We will deal with **Static Fatigue** and **Cyclic or Classical Fatigue**. **Static fatigue** occurs when a material is placed under a **static or constant load** and the crack faces of a material interacts with the environment, the **crack tip becomes embrittled** due to interaction with environment (stress corrosion cracking), the crack tip sharpens, the crack propagates, and the process repeats[10].

The more common fatigue scenario is **cyclic or classical fatigue** where a material is under a **cyclic load/stress**[10]. We need to define the cyclic applied stress specifically the frequency of the applied load, f , which is $\frac{1}{\tau}$ where τ is the period of the applied stress. We also want to quantify the **stress ratio, R**

$$R = \frac{\sigma_{min}}{\sigma_{max}} \quad (7.165)$$

As materials scientists we want to avoid catastrophic failure and for fatigue that involves trying to **estimate the number of cycles to failure, N_f** , which is the number of cycles to grow a crack from initial length, a_o , to the **critical or catastrophic crack length, a_c** [10].

There three distinct regimes of fatigue crack growth: **I) The Slow-Growth Rate or Near-Threshold Regime**, **II) Mid-Growth Rate or the Paris Regime**, and **III) High-Growth Rate Regime**

I) Slow-Growth Rate or Near-Threshold Regime

In the slow-growth rate regime the crack won't grow initially until the threshold stress intensity

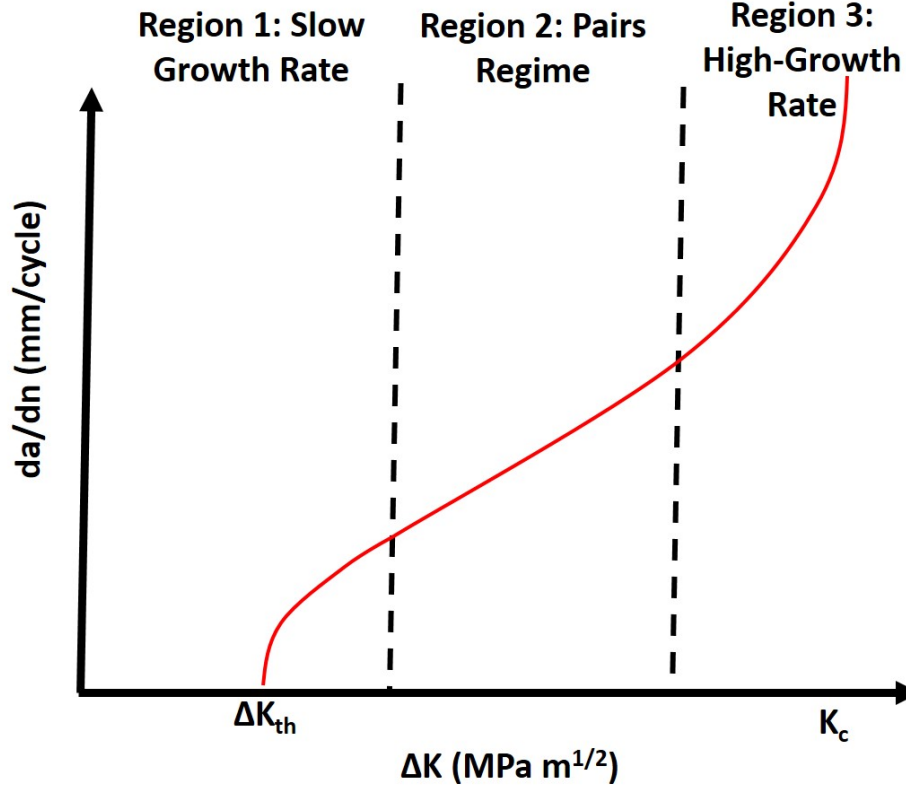


Figure 7-22: Fatigue Regimes.

factor, ΔK_{th} , is reached where

$$\Delta K = f \Delta \sigma \sqrt{\pi a} \quad (7.166)$$

Typically we say that **when the rate of crack growth is 10^{-8} mm/cycle or less the crack is dormant or growing at a near undetectable rate**. Once the threshold stress intensity factor is reached the crack growth rate will increase but still the **growth rate is extremely slow**, still below one lattice spacing per cycle until we reach the Mid-Growth Rate or the Pairs Regime[10].

II) Mid-Growth Rate or Paris Regime

In the **Mid-Growth Rate or Paris Regime** we actually have an equation or law to describe fatigue crack growth, aptly named the **Paris Law**:

$$\frac{da}{dN} = C \Delta K^m \quad (7.167)$$

where C and m are empirical constants which depend on the material, the applied stress, frequency, and R[10].

We can use Paris law to predict the number of cycles to failure, N_f

$$\int_0^{N_F} dN = \int_{a_o}^{a_c} \frac{da}{C(f\Delta\sigma\sqrt{\pi a})^m} \quad (7.168)$$

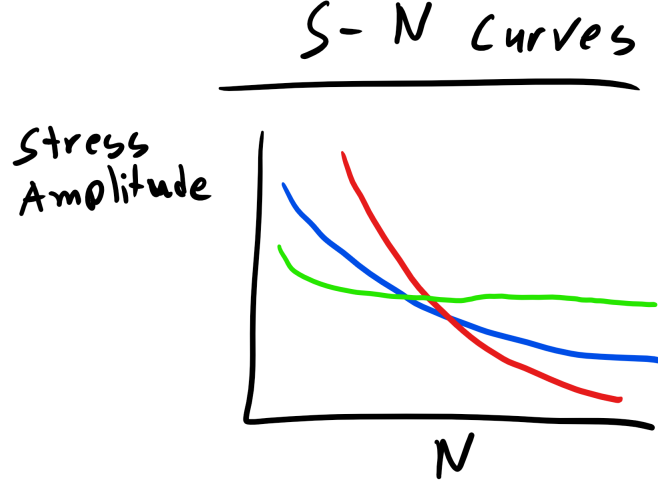


Figure 7-23: S-N Curve.

which leads to

$$N_f = \frac{1}{C(f\Delta\sigma\sqrt{\pi})^m} \left[\frac{a_c^{1-\frac{m}{2}} - a_o^{1-\frac{m}{2}}}{1-\frac{m}{2}} \right] \quad (7.169)$$

where a_o is the initial crack length and remember that a_c

$$a_c = \frac{1}{\pi} \left(\frac{K_{IC}}{\sigma_{max}} \right)^2 \quad (7.170)$$

Fatigue cracks are marked via striations on the fracture surface.

III) High-Growth Rate Regime

The last stage is the high-growth rate regime is characterized by **an orders of magnitude increase in the crack growth rate and additional cleavage in the material or microvoid coalescence**[10]. This is the end region where catastrophic crack failure will occur throughout the material. We need to take the material out of service before we reach this regime[10].

One way that we can try to predict the lifetime of materials is by looking at empirically determined S-N curves. S is the stress amplitude so the difference between the maximum and minimum applied stress. N is again the number of cycles. We can look at the curve and determine when the material will fail.

Part V

Electrochemistry

THIS PAGE INTENTIONALLY LEFT BLANK

CHAPTER 8

ELECTROCHEMISTRY

Over time eventually all materials will degrade. Polymers can be dissolved in organic solvents or crosslinks can be destroyed by UV radiation. Ceramics typically deteriorate in applications where they are utilized at very high temperatures or other extreme environments. And metals will typically undergo **corrosion**. Corrosion is often the unintentional attack typically at the surface. It is a very significant problem which we typically spend **5% of the GDP each year to prevent corrosion, perform maintenance, or deal with the catastrophic failures due to corrosion**[1]. So this is a very stable career choice for Materials Scientists and Mechanical Engineers and one that is very in-demand as the old guard of corrosion engineers are retiring.

What are some examples of corrosion that you have encountered?

There are multiple types of corrosion including[1]:

8.1 Types of Corrosion:

- **Uniform Attack**
 - Occurs uniformly over the entire exposed surface
- **Galvanic Corrosion**
 - Occurs when two different metals are electrically connected and exposed to conducting medium
- **Crevice Corrosion**
 - Concentration difference of ions builds up in the crevices between materials. Very localized corrosion
- **Pitting**
 - Localized corrosion occurring in small pits or holes
- **Intergranular Corrosion**
 - Occurs preferentially along grain boundaries
- **Erosion-Corrosion**
 - Combined chemical attack and mechanical wear
- **Stress Corrosion**

- Insidious form of corrosion associated with stress corrosion cracking (SCC). Corrosion of a material under applied or residual stress.

- **Hydrogen Embrittlement**

- Hydrogen induced cracking, H attack

We will cover most of these forms but all of these forms of corrosion are similar in the fact that they involve an **electrochemical** reaction whereby **electrons are lost and gained**[1]. These reactions are also called **redox** reactions which is an abbreviation of **reduction** and **oxidation** reactions[1].

8.2 Electrochemical Nature of Corrosion: Redox Reactions

Corrosion is an electrochemical process where by an element will either gain or lose electrons. During **oxidation** the element will **lose** it's valence **electrons**. During **reduction** electrons are **gained**[1].

Let's look at a couple of examples for **oxidation**:



Now how about **reduction**



8.3 Electrochemical Cell

These type of reactions which involve only half of the entire redox reaction process are called **half cell reactions**. [1] They are also called half-cell reactions because they are only describing one half of our typical electrochemical cell which can be seen below[1]:

A couple of key things to note about this diagram. The **cathode** is defined as **positive** because it is the electrode where **electrons flow in**[1]. The **anode** is defined as **negative** as it **gives up electrons**[1]. Additionally, you can see that **cathode** is where the **reduction** reaction occurs and that at the **anode** the **oxidation** reaction occurs[1]. In an electrochemical cell or in a redox reaction reduction cannot occur without corresponding oxidation from mass and charge balance consideration. We should also think about the sign of the potential that we measure. If the electrons actually do flow from the anode to the cathode as shown in the figure above the potential should

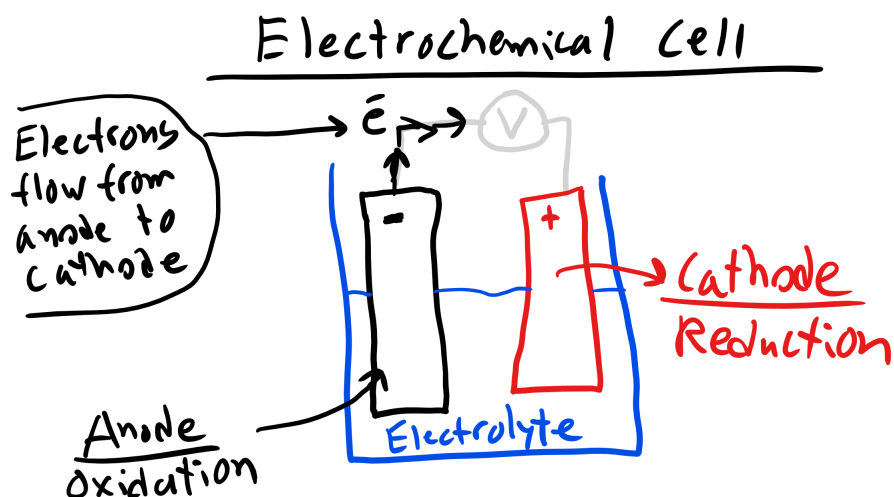


Figure 8-1: Electrochemical Cell.

be positive. If the electrons flow in the opposite direction from cathode to anode then we will measure a negative potential and we have mistakenly set up our cell and misidentified the cathode and anode materials.

Let's take a look at on typical electrochemical cell composed of iron as one of the electrodes and copper for the other[1]. The iron is immersed in a 1M solution containing Fe^{2+} ions and the copper is immersed in a 1M solution containing Cu^{2+} ions and it is separated by a membrane as seen below:

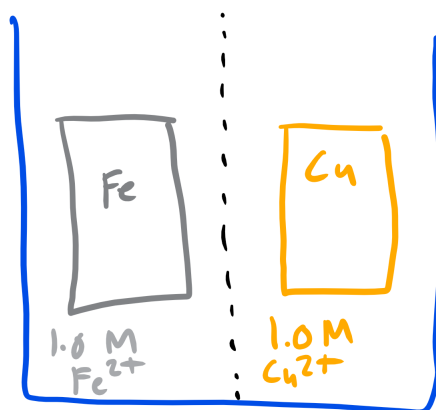


Figure 8-2: Cu-Fe Electrochemical Cell.

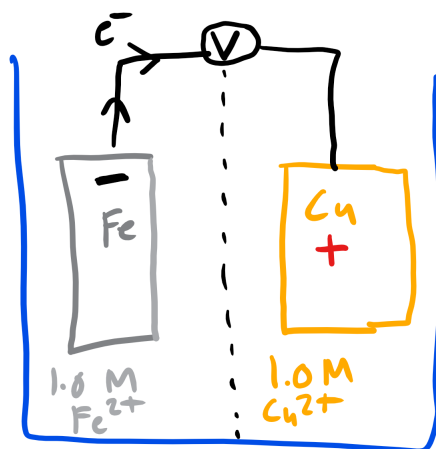


Figure 8-3: Cu-Fe Electrochemical Cell.

Let's start simple where will the electrons flow in this cell?

Well the only way that we can find that out is by actually measuring the potential but we can get some idea by looking at the **electronegativity** of each material[1]. The electronegativity of **Cu** is **1.9** and the electronegativity of **Fe** is **1.83**. Thus we should expect that Cu should pull electrons from Fe[1].

8.4 Standard emf Series:

We can also get an idea about the willingness of a material's affinity to either give up or gain electrons by looking at a **Standard emf Series** or a **Standard Electrode Potential Series**.

You can see that the potential that are at the top of the list are positive and they are materials that are increasingly inert or noble[1]. In other words these materials have a large electronegativity and want to grab electrons. Thus they are typically cathode materials where reduction will take place[1]. As you move down the list you see that the materials become less noble, more active, and these materials have a very low electronegativity. They want to give away electrons. Note above these are all reduction reactions so the values are assessing in a standard cell how well these materials would fair as cathode materials (positive good, negative bad cathodes should be anodes).

8.5 Half Cell and Full Cell Reactions:

So let's look back at our old friend the Cu-Fe cell. Let's assume that from our investigation into electronegativity and looking at the the Standard emf chart that we think that Cu is going to be the cathode where electrons will be gained and reduction will occur and the anode material will be



<u>Emf Series</u>		
	<u>Electrode Reaction</u>	<u>Standard Potential (V)</u>
Cathodic (inert)   Anodic (reactive)	$Au^{3+} + 3e^- \rightarrow Au$	1.42
	$Pt^{2+} + 2e^- \rightarrow Pt$	1.2
	$Ag^+ + e^- \rightarrow Ag$	0.8
	$Cu^{2+} + 2e^- \rightarrow Cu$	0.34
	$Pb^{2+} + 2e^- \rightarrow Pb$	-0.126
	$Ni^{2+} + 2e^- \rightarrow Ni$	-0.250
	$Fe^{2+} + 2e^- \rightarrow Fe$	-0.440
	$Zn^{2+} + 2e^- \rightarrow Zn$	-0.763

Figure 8-4: Standard Electrode Potential Series measured with reference to a standard hydrogen electrode which consists of an inert platinum electrode in a 1M solution of H^+ ions saturated with hydrogen gas.

iron where electrons are lost and oxidation occurs[1]. Let's write these two half cell reaction first at the cathode:



This half cell reaction will be referred to as the $E_{cathode}^o$.

Now for the anode:



This half cell reaction will be referred to as the E_{anode}^o . So the full cell reaction will be simple the cathode plus the anode reaction which gives us:



The overall potential of the cell will then be given as:

$$E_{cell}^o = E_{cathode}^o - E_{anode}^o \quad (8.8)$$

where in this case the values of $E_{cathode}^o = 0.340$ according to our table and the value of $E_{anode}^o = -0.440$. Notice the negative sign here because at the anode we don't have reduction we have an oxidation reaction. So the overall potential is 0.780V[1]. This value is positive and thus the reaction will proceed spontaneously. If you get a value that is negative then the reaction cannot proceed and you

8.6 What Material Corrodes in Galvanic Corrosion?

You have just done an experiment with a Galvanic electrochemical cell, two metals immersed in a conducting medium and electrically connected. But now you might be asking which material will corrode. Well let's look at what is happening at the cathode first[1]. Electrons are being pulled to copper and they are going to combine with the Cu^{2+} ions in the solution and electrodeposit Cu on the surface of the cathode. So the copper electrode will grow essentially[1]. Now on the other side at the anode the Fe is losing electrons and must dissociate and form Fe^{2+} ions in solution so the Fe anode will start to corrode! We can also tell which material in a standard cell configuration will corrode by simply looking at the Standard emf chart and seeing which is more anodic or active, that is the material that will corrode!

Let's do another example with Fe-Zn

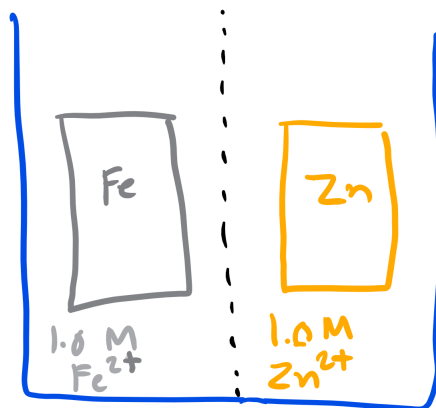


Figure 8-5: Fe-Zn Electrochemical Cell.

What is the electronegativity of each material?

Fe is 1.8 and Zn is 1.65.

Which is more noble and which is more active according to the Standard emf?

Fe is more noble and Zn is more active.

Write the half cell reactions



Write the full cell reactions

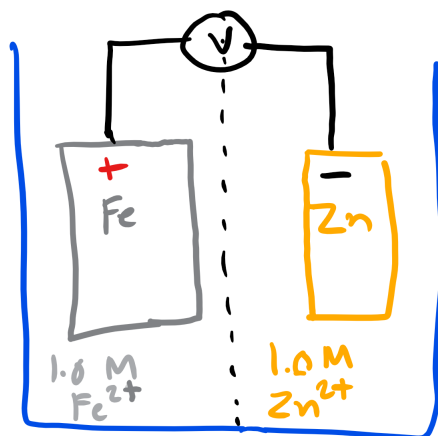


Figure 8-6: Fe-Zn Electrochemical Cell.



Calculate the overall potential

$$E_{cell}^o = E_{cathode}^o - E_{anode}^o = -0.440 + 0.763 = 0.323V \quad (8.12)$$

Which material will corrode? Which will electrodeposit?

Zn will corrode and Fe will electrodeposit.

8.7 Nernst Equation:

So far we have been dealing with a very idealized situation, we have always been at room temperature and at 1M solutions[1]. But this is often not the case as temperature and concentrations will typically deviate from this idealized scenario[1]. Luckily we can derive from thermodynamics an equation which describes this change in potential as a function of temperature and activity/concentration. The electrochemical work is defined as:

$$W = \Delta G = QE = -nFE \quad (8.13)$$

where Q is charge (Coulomb), n is the number of moles of electrons exchanged in a chemical reaction, F is the Faraday Constant ($F = N_{ave}$), and E is the cell voltage[1]. At standard conditions, the conditions we have been working with up to this point, the change in Gibbs free energy is

$$\Delta G^o = -nFE^o \quad (8.14)$$

Now in general we have the relation that the change in free energy for a chemical reaction is

$$\Delta G - \Delta G^o = RT \ln \frac{\Pi a_{products}}{\Pi a_{reactants}} \quad (8.15)$$

where $\Pi a_{products}$ are the arithmetic products and reactants. Or similarly

$$E - E^o = -\frac{RT}{nF} \ln \frac{\Pi a_{products}}{\Pi a_{reactants}} \quad (8.16)$$

or for our Cu-Fe example

$$E - E^o = -\frac{RT}{nF} \ln \frac{a_{Fe^{2+}}}{a_{Cu^{2+}}} \quad (8.17)$$

This is the Nernst equation which is a function of temperature and the activity/concentration.

8.8 Methods to Protect Against Galvanic Corrosion:

There are some relatively simple and straightforward methods to protect against corrosion which can include adding an insulating layer or a coating layer between two metals to break the metal or conducting contact[1]. Polymers are great materials for this. You should also avoid leaving any pockets or crevices uncoated as these are insidious sites for corrosion, specifically crevice corrosion to occur. One of the more creative ways to avoid this issue of corrosion is to provide **cathodic protection** using a **sacrificial anode**[1].

8.8.1 Cathodic Protection:

This mode of protection will be effective for every type of corrosion we previously discussed. Remember that corrosion will occur when the material gives up electrons so to avoid having our material of interest corrode we have to find another source to give up electrons[1]. This can be done using a **sacrificial anode** or using an **imposed current** to force electrons to flow in the desired direction. Let's talk about the sacrificial anode method first.

8.8.2 Sacrificial Anode

Let's consider an example of an electrochemical cell where we have Cu as the cathode, Fe as the anode which is also connected to Zn. What will happen in this cell? Well look at the electronegativities of Cu, Fe, and Zn. Cu is the most electronegative, then Fe, then Zn[1]. So Cu will pull electrons from Zn and Fe. Fe is going to give electrons to Cu but also pull electrons from Zn. And Zn will give electrons to both Cu and Fe. So the Cu will not corrode and will electrodeposit. While Fe will give up electrons to Cu it will also gain electrons from Zn so it will not electrodeposit[1]. Additionally remember reactions proceed in the direction where the energy barrier is the lowest so pulling electrons from Zn is easier than Fe.

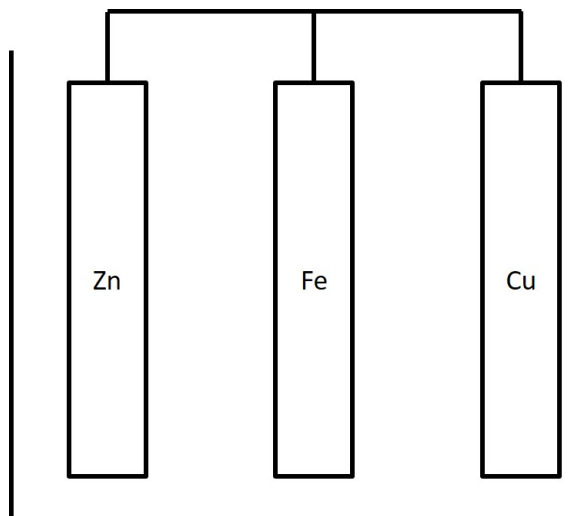


Figure 8-7: Sacrificial Anode.

Finally Zn will corrode as electrons are being pulled away by Fe and Cu. This is the sacrificial anode method of protecting against corrosion because we are adding an anode material that is more active than the material we are trying to protect against corroding and we are sacrificing this new material to die a corrosion death, but for a very good cause.

This technique is commonly done for ships and first discovered by Davy and Faraday in 1824 when they placed iron sacrificial anodes to the copper sheath of the hull below the waterline[1]. This technique is also used in pipelines as well.

8.8.3 Imposed Current

Another and often more costly methods is to apply a biased or imposed current on your system to prevent a material from corroding. What you do is insert a power supply into your circuit as seen below.

You can increase the applied voltage and bias the flow of electrons towards the material that you are trying to protect from corrosion.

8.9 Redox Reactions with Kroger Vink Notation:

We can also write these oxidation and reduction reactions using Kroger Vink notation[12]. The reaction for reduction written in Kroger Vink notation can be seen below

$$O_O^x = \frac{1}{2}O_2(g) + V_O^{\bullet} + 2e' \quad (8.18)$$

The way you want to think about this equation is that oxygen has been removed to the gas phase and left behind oxygen vacancies and the oxide has gained two electrons, thus reduction[12].

The equilibrium constant is then

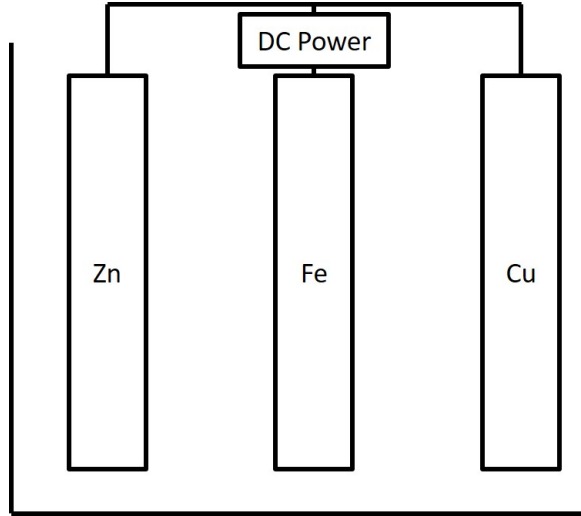


Figure 8-8: Imposed Current.

$$K_R = n^2[V\ddot{O}]P_{O_2}^{\frac{1}{2}} \quad (8.19)$$

where n refers to the electrons. We use this notation because n-p types semiconductors refer to electrons as n and holes as p[12]. The oxidation reaction would then be the consumption of oxygen vacancies



where h refers to the holes[12]. Oxygen vacancies were consumed, oxygen inserted into the oxide lattice, and two electrons were taken. Similarly the oxidation equilibrium constant is

$$K_O = \frac{p^2}{[V\ddot{O}]P_{O_2}^{\frac{1}{2}}} \quad (8.21)$$

where p refers to the holes here.

8.9.1 Brouwer Diagrams

Now we can look at even more complex defect reactions and determine at what temperatures and oxygen partial pressures a specific reaction is dominant[12].

When we are thinking about the possible reactions that can occur you should consider

- Schottky or Frenkel
- Electronic Defects
- Oxidation and Reduction

- Impurity Incorporation

Let's take a look at pure MgO and the dominant reactions at different ranges of partial pressures of oxygen[12]. In pure MgO we don't have to worry about impurity incorporation so we are left with the following reactions possible reactions

$$O_O^x = \frac{1}{2}O_2(g) + V_{\ddot{O}} + 2e' \quad (8.22)$$

$$null \rightarrow V_{Mg}'' + V_{\ddot{O}} \quad (8.23)$$

$$null \rightarrow e' + h \cdot \quad (8.24)$$

$$(8.25)$$

So with these equations we have the total electroneutrality equation below

$$n + 2[V_{Mg}''] = 2[V_{\ddot{O}}] + p \quad (8.26)$$

So we have four unknowns in the above equations: $V_{Mg}'', V_{\ddot{O}}, e', \text{ and } h \cdot$ and four equations so we can solve at this point but we can make life a little bitter easier by using a Brouwer approximation[12]. The Brouwer approximation considers conditions where one positive and negative sign dominate above all others which is usually the case due to the Arrhenius behavior with temperature and also partial pressure as well. So what are our potential Brouwer approximations? Well they are

$$2[V_{Mg}''] = p \quad (8.27)$$

$$n = 2[V_{\ddot{O}}] \quad (8.28)$$

$$2[V_{Mg}''] = 2[V_{\ddot{O}}] \quad (8.29)$$

$$n = p \quad (8.30)$$

We can make a further simplification if we know the electronic bandgap of MgO is very large so the concentration of Shockky defects will be much greater than the intrinsic electronic defects at high temperatures[12]. So now we have 3 Brouwer regimes one at high partial pressures of oxygen, one at low partial pressures of oxygen, and one intermediate range[12]. The high partial pressures of oxygen will be dominated by the first Brouwer approximation, the low partial pressure of oxygen range will be dominated by the second Brouwer approximation, and the intermediate case will be dominated by the 3rd Brouwer approximation[12]. So lets start at low partial pressure of oxygen we have our Brouwer approximation below

$$n = 2[V_{\ddot{O}}] \quad (8.31)$$

we can then use the rate relations for our other three interactions

$$K_s = [V_{Mg}''] [V\ddot{O}] \quad (8.32)$$

$$K_i = np \quad (8.33)$$

$$K_R = n^2 [V\ddot{O}] P_{O_2}^{\frac{1}{2}} \quad (8.34)$$

We can now write the expressions for the concentration of all our defects in this regime to get

$$n = (2K_R)^{\frac{1}{3}} P_{O_2}^{-\frac{1}{6}} \quad (8.35)$$

$$p = \frac{K_i}{n} \quad (8.36)$$

$$1[V_{Mg}''] = \frac{K_S}{[V\ddot{O}]} \quad (8.37)$$

$$1[V\ddot{O}] = \frac{1}{2} (2K_R)^{\frac{1}{3}} P_{O_2}^{-\frac{1}{6}} \quad (8.38)$$

$$(8.39)$$

The same can be done for the middle partial pressure regime which gives us our Brouwer approximation as

$$2[V_{Mg}''] = 2[V\ddot{O}] \quad (8.40)$$

We can once again write our expression for the concentration of all our defects in this regime

$$n = (K_R K^{\frac{-1}{2}})^{\frac{1}{2}} P_{O_2}^{-\frac{1}{4}} \quad (8.41)$$

$$p = \frac{K_i}{n} \quad (8.42)$$

$$1[V\ddot{O}] = K_S^{\frac{1}{2}} \quad (8.43)$$

$$1[V_{Mg}''] = K_S^{\frac{1}{2}} \quad (8.44)$$

$$(8.45)$$

Finally we have the final high partial pressure of oxygen regime which gives us our Brouwer approximation as

$$p = 2[V_{Mg}''] \quad (8.46)$$

We get our final concentrations for all the defects in this regime

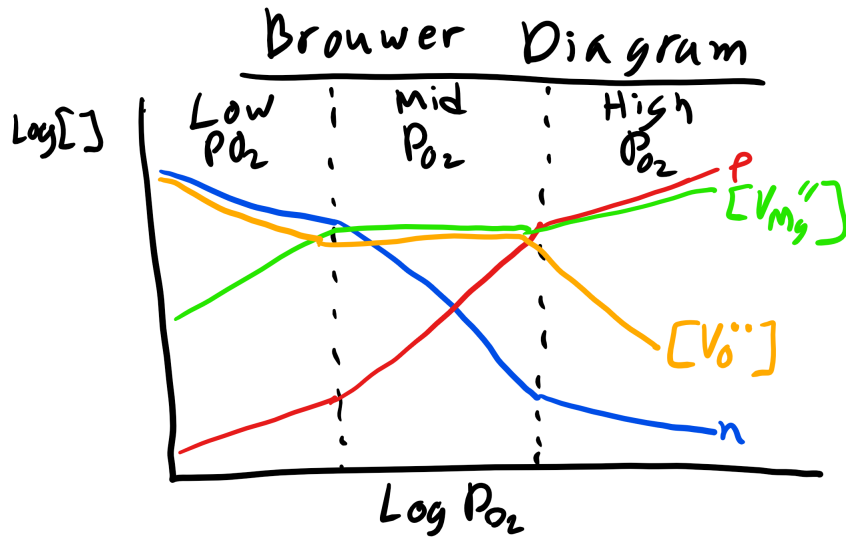


Figure 8-9: Brouwer Diagram MgO.

$$n = \left(\frac{K_i K_R}{2K_S} \right)^{\frac{1}{3}} P_{O_2}^{-\frac{1}{6}} \quad (8.47)$$

$$p = \frac{K_i}{n} \quad (8.48)$$

$$1[V_{\ddot{O}}] = \frac{K_R}{n^2 P_{O_2}^{\frac{1}{2}}} \quad (8.49)$$

$$1[V_{Mg}^{''}] = \frac{K_S}{[V_{\ddot{O}}]} \quad (8.50)$$

$$(8.51)$$

and what we finally end up with is a Brouwer diagram like the one below[12]

Part VI

Polymeric Electrical, Optical, and Magnetic Materials

CHAPTER 9

POLYMERS, SOFT MATTER, AND COMPOSITES

9.1 Soft Matter

Soft materials is a class of materials that includes **polymers, colloids, liquid crystals, nanoparticles, and hybrid organic-inorganic materials systems**[13, 14, 15]. We are primarily going to focus on polymers but the governing physics and foundation that we will develop will apply more broadly to soft materials and be particularly relevant to biological systems as well as most biological systems are composed primarily of soft materials[13, 14, 15].

The key to the interesting properties of soft matter is that most intermolecular interactions in soft matter systems have **energies (enthalpies) on the scale of approximately 1 kT**[13, 14, 15]. By comparison, most hard materials such as metals or ceramics are held together by much stronger covalent bonds, which have energetic interactions on the order of 10-100 kT. In other words, **soft matter is held together by very weak intermolecular interactions**, which leads to large fluctuations in thermodynamic quantities that determine the interesting physical behavior of polymer systems. In particular, this means that intermolecular bonds can be easily broken by applied stimuli, such as a pulling force[13, 14, 15]. One consequence of the prevalence of weak intermolecular bonds is that soft matter is highly **adaptive**, meaning that systems can undergo significant changes in response to stimuli. Adaptive behavior is particularly prominent in biological systems. For example, many proteins, such as transporters or receptors, rely on large conformational changes that are only possible in soft matter systems because bonding interactions are relatively weak[13, 14, 15]. That said, soft matter systems can still be strong and robust with respect to physical stimuli, since very strong properties can be built up from a very large number of weak interactions. For example, Kevlar, a prominent synthetic polymer, is used in bulletproof vests due to its ability to withstand impact, a property derived from a large number of weak interactions that are enhanced by the structure of the Kevlar backbone[13, 14, 15]. The physical consequences of these weak enthalpic interactions will become more apparent when we start discussing the thermodynamics of polymeric systems in future lectures. As we continue in the class we will also clarify the origin of different types of bonds, the impact of molecular geometry and structure, the role of fluctuations in position and conformation, and the interplay of enthalpy and entropy over several important length scales.

Throughout the study of soft matter, we will be interested in understanding polymeric behavior on different length scales, or equivalently, we will be interested in **hierarchical** behavior[13, 14, 15]. This is due to the multitude to length scales associated with soft matter systems. Typically, we can think of bonding behavior as relevant on the Angstrom or nanometer length scale, while self-assembled biological structures such as DNA, viruses, and cellular components have properties associated with the 10s to 100s of nanometers, or even up to the micrometer length scale[13, 14, 15].

What we will find, though, is that the properties of soft matter relies on the bridging of length scales - polymers that have widths on the order of nanometers, but lengths of up to meters[13, 14, 15]. It is a challenge to study systems across these length scales, and is unusual in the study of hard materials!

9.2 Polymer Chain Conformations:

We now know how to create polymers and we have discussed some of the unique characteristics of polymer chains (inter vs intramolecular bonding)[13, 14, 15]. We also have seen some of the different polymer architectures that we will encounter but we haven't really talked much about polymer conformations. I make a distinction here between **architecture** and **conformation**[13, 14, 15]. Polymer **architecture** has a connotation referring to the structure of the polymer whereas a polymer chain **conformation** has a connotation which refers to the **instantaneous state** of the polymer especially when subjected to an **external stimuli**[13, 14, 15].

In our discussion of polymer chain conformations we will start simple and build up from a simple **homopolymer** with a very high molecular weight. So this polymer architecture is **simply linear, flexible, chain** or if you like macroscopic analogies **spaghetti**. And the **flexibility** of the chain will be governed by the **intramolecular bonding of the repeat unit**, as well as other factors which we will get into in depth when we discuss the **glass transition temperature**[13, 14, 15]. One of the key ways that we can characterize a polymer chain conformation, just like we did with molar mass in the previous lecture, is by describing the **effective size** of a single polymer chain in solution. Now you might reasonably think that the **size of a linear polymer chain is simply the length of the monomer or repeat unit multiplied by the number of repeat units**[13, 14, 15]. However, this is not the case as we are interested in the **effective size** of the polymer which is the space occupied by the polymer. We will see in this lecture that depending on the **temperature, solvent, and local environment** even this **simple polymer chain** can adopted a **highly coiled collapsed structure, an highly elongated structure, or even in the most extreme circumstances a fully elongated structure**[13, 14, 15]. We also know from our supplemental thermodynamics notes that polymers can adopt a large number of possible conformation, microstates. The conformation and thus the effective size of the polymer can change rapidly. This means that we will also have to develop a metric to measure the size of the polymer which is probabilistic in nature.

You can see this in the embedded video in the PowerPoint slides.

We will describe in detail several different models which will describe the effective size of polymers with increasing complexity

- **Ideal/Freely Jointed Chain Model**
- **Mathematician's Ideal Chain**
- **Chemist's Chain in Solution and Melt Model**

- **Physicist's Ideal Chain**

We will examine the differences in each model and how the **scaling changes** depending on some of the factors mentioned above.

9.2.1 Characterizing Polymer Size: Mean-Squared-Displacement

We have just mentioned that describing the effective size of the polymer can be tricky and it is not just a matter of adding up the monomer lengths. This problem becomes even more complex when we are dealing with polymers with a more **complex architecture, i.e. branched, dendrimer, star polymers, syndiotactic, etc**[13, 14, 15]. How do we characterize the size of a polymer then? Well the tool that we will use is the **root mean squared end to end distance (RMSD)** which is shown below

$$\langle r^2 \rangle^{\frac{1}{2}} \quad (9.1)$$

where r is the vectorial position of the polymer at one end and the other end in 3D, seen in the image below

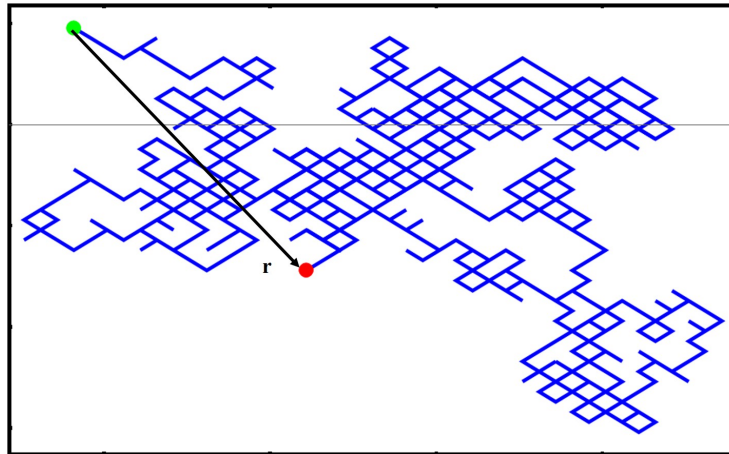


Figure 9-1: End-to-End Distance

We take the square because this will give us a quantity in units of length. Note as well that the $\langle \rangle$ indicates an average quantity as we will typically **average over many microstates and conformations**[13, 14, 15]. You can also see that by squaring the r we will never have negative values. Now there are many ways of calculating a mean square displacement. One method is simply **averaging the end-to-end displacement values of a single polymer chain as it moves and fluctuates over time** or you can **average one snapshot of identical polymer chains which are all under the same external stimuli/experimental conditions**[13, 14, 15].

To get started let's do a quick couple of extreme example of a linear rigid rod like polymer architecture that is stretched to the fully extended position. This polymer has a monomer length of l and the number of monomers is as always n . What is the MSD end-to-end distance?

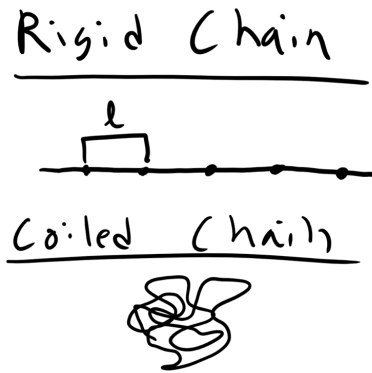


Figure 9-2: Rigid vs Coiled Polymer

Well let's start with the r vector?

It is nl ! So

$$\langle r^2 \rangle^{\frac{1}{2}} = nl = L \quad (9.2)$$

where L is the contour length of the polymer, the fully extended distance.

What would be the MSD end-to-end distance of polyethylene with a $D_{p,n}$ of 10000?

Approximately $1.5\mu\text{m}$.

9.2.2 Ideal/Freely Jointed Chain (FJC)/Gaussian Model

Now the above example is an **very extreme situation**, although an important one to consider. However, polymers are **not typically fully extended** and this is an **energetically unfavorable microstate**. To describe a more typical polymer conformation let's start with a simpler model[13, 14, 15]. Let's consider an **ideal polymer chain** where we assume that there are **no intramolecular steric interactions along the polymer chain**[13, 14, 15]. This means that the polymer can **intersect itself along the backbone without any penalty**. This is the **Ideal/FJC/Gaussian Chain Model**.

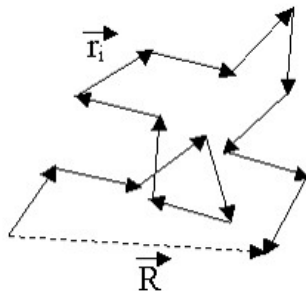


Figure 9-3: Ideal Chain Model [16]

So again here we have a polymer chain with a monomer length, l , and a number of monomers, n . We also assume that in **addition to the ability of chain to cross over itself** the **monomers can rotate in any dimension** with respect to one another[13, 14, 15]. We are essentially **ignoring the constraints that double or triple carbon bonds can place on polymer rotation, steric or repulsive interactions, or intermolecular interactions**. So with all of these assumptions we can describe the polymer as essentially performing a **random walk** through space in time. Or alternatively we can construct a polymer chain by **placing each monomer in a position in space using a stochastic or random algorithm** (Monte Carlo)[13, 14, 15]. In this random walk the step size would be fixed at l from the previous step/monomer and would continue until reaching n random steps. Thus the position of monomer i and $i + 1$ are completely **uncorrelated**.

9.2.3 Mathematician's Ideal Chain Derivation for Ideal Chain/FJC Model

We can derive the MSD of of the FJC Chain model without using a probabilistic perspective as well and this might be a little more intuitive for some people, at least it was for me. Again remember that in the random walk or ideal model we ignore bonding and it is really unphysical in most cases. The end-to-end distance of the Ideal Chain/FJC model can be derived using a different mathematical formalism, sometimes referred to as the **Mathematician's Ideal Chain**[13, 14, 15]. We again assume n monomers with a fixed monomer length l and which is represented as a vector in 3D space \vec{l}_i where this vector refers to monomer i .

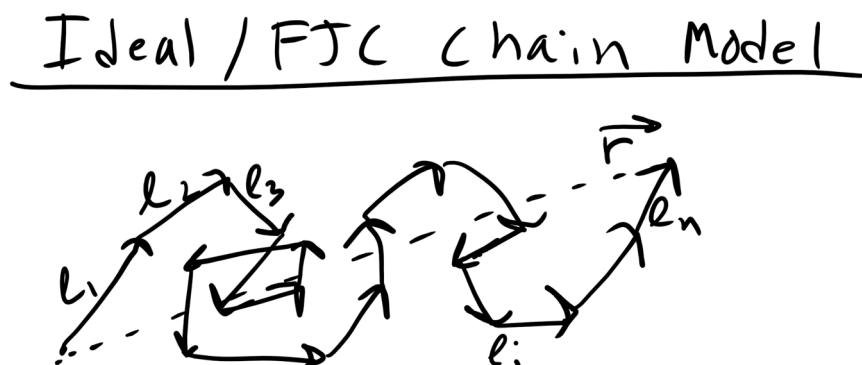


Figure 9-4: Mathematician's Ideal Chain Derivation

So the end to end distance vector is

$$\vec{r} = \vec{l}_1 + \vec{l}_2 + \dots + \vec{l}_n = \sum_{i=1}^n \vec{l}_i \quad (9.3)$$

On average what will be the value of $\langle \vec{r} \rangle$? Remember that for the ideal polymer chain each step

positive or negative is equally likely, these steps are **uncorrelated**[13, 14, 15]. So on average the value of $\langle \vec{r} \rangle = 0$.

The better question is what will be $\langle \vec{r}^2 \rangle$ and we can write this as the dot product

$$\langle \vec{r}_i \cdot \vec{r}_j \rangle = \left\langle \sum_{i=1}^n \vec{l}_i \cdot \sum_{j=1}^n \vec{l}_j \right\rangle \quad (9.4)$$

where i and j refer to monomer i and monomer j . Remember that the dot product is

$$\vec{l}_i \cdot \vec{l}_j = |l_i||l_j| \cos \theta_{ij} \quad (9.5)$$

We can show the MSD in matrix notation as well

$$\langle \vec{r}_i \cdot \vec{r}_j \rangle = \begin{bmatrix} \vec{l}_1 \cdot \vec{l}_1 & \vec{l}_1 \cdot \vec{l}_2 & \vec{l}_1 \cdot \vec{l}_3 & \dots & \vec{l}_1 \cdot \vec{l}_n \\ \vec{l}_2 \cdot \vec{l}_1 & \vec{l}_2 \cdot \vec{l}_2 & & & \\ \vdots & & & \ddots & \\ \vec{l}_n \cdot \vec{l}_1 & \dots & & & \vec{l}_n \cdot \vec{l}_n \end{bmatrix}$$

Now let's think about the value of the dot product on the diagonal component. The **magnitude** will simply be l^2 for every component but now we need to think about the $\cos \theta$ between the two vectors[13, 14, 15]. Well for the diagonal component they will always be pointing in the same direction so the angle will be 0° and then $\cos 0^\circ = 1$.

Now for the off diagonal components. Let's keep it simple and think about the 1D scenario. Well there the value of $\cos \theta = 1$ or $= -1$. But remember we are concerned about the averages so since both positive and negative steps are **equally probable (Markov/Monte Carlo) or uncorrelated** so on average the value of $\cos \theta = 0$ [13, 14, 15].

So the matrix reduces to

$$\langle \vec{r}_i \cdot \vec{r}_j \rangle = \begin{bmatrix} l^2 & 0 & 0 & \dots & 0 \\ 0 & l^2 & & & \\ \vdots & & & \ddots & \\ 0 & \dots & & & l^2 \end{bmatrix}$$

Thus the sum of this matrix becomes

$$\langle r^2 \rangle = nl^2 \quad (9.6)$$

just as we obtained previously with our other probabilistic method!

9.3 The Chemist's Polymer Chain Model

So far we have neglected a lot of detail in describing polymer chains that make the previous models a bit unphysical. We have neglected taking into account restrictions in bond angles to steric hindrance along the backbone chain as well as any solvent effect and how that may affect the end-to-end distance of the polymer chain[13, 14, 15].

Here, we will introduce two new **effective** parameters, C_∞ and α , that can be used to correct for problems in the simple random walk model end-to-end distance based on known bonding constraints and solvent considerations. Note that in a random walk, $C_\infty = \alpha = 1$. The parameter C_∞ is used to take into account restrictions due to bonding and steric hindrance from the polymer chain, while the parameter α takes into account effects from the solvent[13, 14, 15]. This improved model is referred to as the **Chemist's Polymer Chain in Solution and Melt** model. This model is more physically accurate as this model considers bond angle restrictions between adjacent atoms (or monomers) due to chemistry. This governing equation for the Chemist's model is

$$\langle r^2 \rangle = nl^2 C_\infty \alpha^2 \quad (9.7)$$

Let's figure where these new values come from starting with going back to the matrix that we developed in the FJC model. So in the **Chemist's Model** we assume that we have a fixed bond angle θ , makes sense thinking of polyethylene[13, 14, 15]. Now the dot product of monomer i and $i + 1$ will be

$$\vec{l}_i \cdot \vec{l}_{i+m} = l^2 (-\cos \theta)^m \quad (9.8)$$

where m is an integer denoting the number of monomers away from monomer i , the θ keeps getting multiplied because of the projection of the bond onto the next neighbor. You can see this model schematically here

Now we can adjust our previous matrix and get

$$\langle \vec{r}_i \cdot \vec{r}_j \rangle = \begin{bmatrix} l^2 & l^2(-\cos \theta) & l^2(\cos \theta)^2 & \dots & l^2(-\cos \theta)^{n-1} \\ l^2(-\cos \theta) & l^2 & \dots & & \\ \vdots & & & \ddots & \\ l^2(-\cos \theta)^{n-1} & \dots & & & l^2 \end{bmatrix}$$

And once you sum this matrix we find that

$$\langle r^2 \rangle = nl^2 \left(\frac{1 - \cos \theta}{1 + \cos \theta} \right) \quad (9.9)$$

This factor of $\frac{1 - \cos \theta}{1 + \cos \theta}$ is

Chemists Chain Model

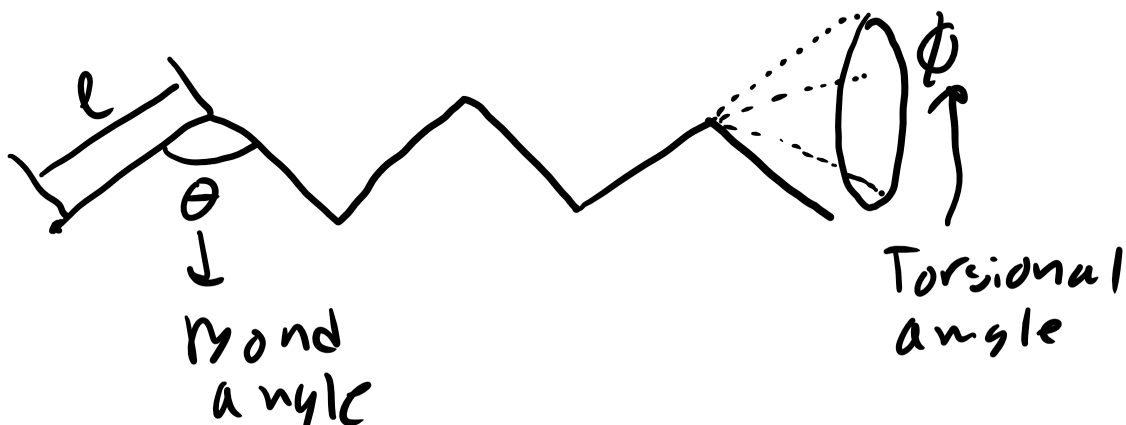


Figure 9-5: Chemist's Chain Model

$$C_{\infty} = \frac{1 - \cos \theta}{1 + \cos \theta} \quad (9.10)$$

so we now get that

$$\langle r^2 \rangle = nl^2 C_{\infty} \quad (9.11)$$

where C_{∞} is the **Flory characteristic ratio** can be thought of as a measure of the **stiffness of your monomer unit** or **how hard it is to rotate**[13, 14, 15]. You can look up this ratio for a number of different polymers and we should know that for C-C bonds $\theta = 109.5^\circ$. Much more on Flory to come.

9.3.1 Rotational Isomeric States

Now this is an improvement but we have missed something very important and it is related to our discussion of **conformers vs. isomers**[13, 14, 15]. We have previously briefly mentioned that there are certain molecules with different **isomeric states**, i.e. same chemical formula but distinct structures that can't be related via rotation around a bond. A conformer or conformational isomer can be related different structures via rotations around a single bond and these different rotational states are called **rotational isomeric states (RIS)**[13, 14, 15]. Additionally these different states will each have different potential energies and thus we will find these different RIS states according to the weighted probabilities determined by the rotational potential $V(\phi)$. We can see the different

RIS states of a conformer n-butane here

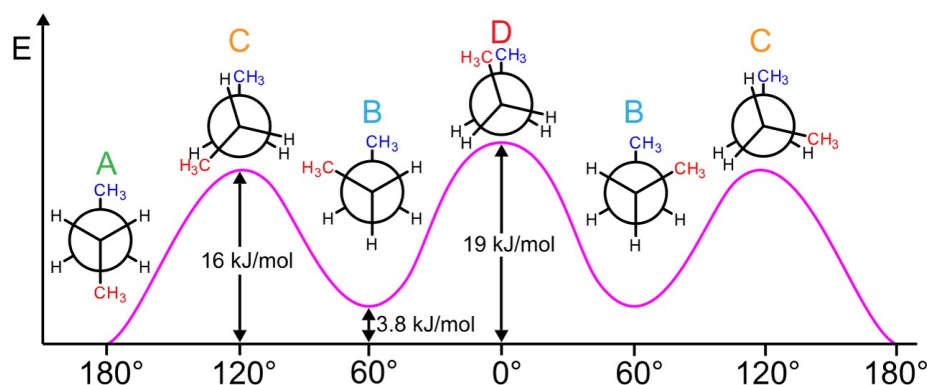


Figure 9-6: Butane RIS States [3]

Here there are clearly high energy states where the bulky methyl groups overlap with either a hydrogen or another methyl group. Then we have our lower energy conformation as seen denoted by **gauche** \pm and the lowest energy being the **trans** conformation[13, 14, 15]. I wanted to illustrate this example because we did not treat this case in our derivation of the Chemist's chain model so we need to take this into account. Luckily we can do so using a very similar train of logic as we did above but instead of simply just using a fixed $\cos\theta$ we need to take an **ensemble average** of the **RIS angles based on the number of microstates for each angle** so we will use

$$\langle \cos \phi \rangle = \frac{\int \cos \phi V(\phi) d\phi}{\int V(\phi) d\phi} \quad (9.12)$$

and we eventually end up with (skipping full derivation as it is very very very extremely difficult)

$$\langle r^2 \rangle = nl^2 \left[\left(\frac{1 - \cos \theta}{1 + \cos \theta} \right) \left(\frac{1 + \langle \cos \phi \rangle}{1 - \langle \cos \phi \rangle} \right) \right] \quad (9.13)$$

And now we have our new and improved Flory Characteristic Ratio C_∞ which is

$$C_\infty = \left(\frac{1 - \cos \theta}{1 + \cos \theta} \right) \left(\frac{1 + \langle \cos \phi \rangle}{1 - \langle \cos \phi \rangle} \right) \quad (9.14)$$

This derivation is beyond the scope of this course but you can look it up in **Statistical Mechanics of Chain Molecules** if you are interested, which is Flory's text again much more Flory to come[13, 14, 15]. Also some refer to this addition as the Hindered Rotation model.

Let's take a moment here to stop to appreciate what we have just done. By taking into account **bond angles and rotations** we get fairly accurate values of C_∞ compared to experimental measurements and usually this value **varies between 1-20**[13, 14, 15]. It's important to note that C_∞ **must always be at least 1** and this implies that the **FJC/ideal chain is the most coiled conformation**. This makes sense because by **restricting these bond rotations we are inherently expanding our polymer chain**, leading to a **more elongated polymer**[13, 14, 15].

However our work is not finished yet. We have taken into account bond angles and bond rotation

but what else must we consider? Well does this model make any distinction between polymers that might have a large or bulky side chain? No! For these polymers with large bulky side chains we should expect that C_∞ should increase as the rotations are more difficult due to steric interactions. So the increase is not due bonding interactions but due to **excluded volume effects**.

9.3.2 Excluded Volume

In order to capture these intramolecular steric interactions between monomers we have to talk about a somewhat initially obtuse concept of **excluded volume**. Excluded volume is the concept that monomers have **some volume around them that other molecules can't cross or move into this sphere**[13, 14, 15]. This takes care of the FJC ability of the chain to self-cross. These **excluded volume interactions usually occur between monomers far apart on the polymer chain** (because they must cross and intersect) and as you might imagine again like the bond angles and rotation this **excluded volume effect will increase the $\langle r^2 \rangle$ of the polymer chain**[13, 14, 15].

Now this may still be a bit obtuse but you can visualize this excluded volume as a hard, impenetrable sphere that surround a given molecule or monomer. The **size of the sphere must reflect the structure of the monomer**. So a monomer, like **polystyrene** with a large **bulky phenyl group** will have a **larger excluded volume** than **polyethylene** with it's **hydrogen groups and no side chain**[13, 14, 15]. This excluded volume interaction will also depend on the interactions of the monomer with **solvent interactions**. If the monomer **doesn't like to interact with the solvent then the polymer will want to coil and collapse to avoid these interactions and thus the excluded volume will decreases and vice versa**[13, 14, 15]. Remember that the solvent is the majority component and solute is the minority component.

9.4 Effect of Solvent on Polymer Chain MSD

Speaking of solvent effect...as we mentioned in our Polymerization lecture there are times when the polymer is immersed in some type of solvent (i.e. water, alcohol, organic solvent, etc.). This solvent can have serious consequences on the dimension of our polymer chain. In **good solvents**, i.e. **solvents were the polymer likes to interact with the solvent (favorable enthalpic intermolecular interactions)**, the polymer will **extend** in order to **maximize the number of interactions between monomer and solvent**. Conversely, if we are dealing with a **bad solvent** then the polymer **doesn't want to interact with the solvent** and the **polymer chain will fold in on itself** and **coil** in order to **minimize interactions** with the **solvent** and the end-to-end distance will decrease[13, 14, 15]. In the FJC/Ideal model we are in a very special condition with regards to solvent in that we are in a **θ condition** and thus in a **theta solvent**. In this condition you can imagine that upon mixing a polymer chain and a **solvent the enthalpy of mixing is 0** just like an **ideal solution**. Alternatively you can imagine that **excluded volume of the polymer chain does not change upon adding a θ solvent**.

The parameter that we use to quantify the effect of **solvent quality** is measured via a factor α [13, 14, 15]. Luckily α is a fairly simple quantity to measure and is simply the ratio of the MSD end-to-end distance of the real chain in solution vs the chain in a θ solvent

$$\alpha^2 = \frac{\langle r^2 \rangle}{\langle r^2 \rangle_\theta} \quad (9.15)$$

where $\langle r^2 \rangle_\theta$ is the MSD of the chain in a θ solvent. So let's define some values of α .

What will be the value of α in a good solvent?

Well $\alpha > 1$ for a good solvent.

What about a bad solvent?

$\alpha < 1$ for a bad solvent

What about a θ solvent?

$\alpha = 1$ for a θ solvent

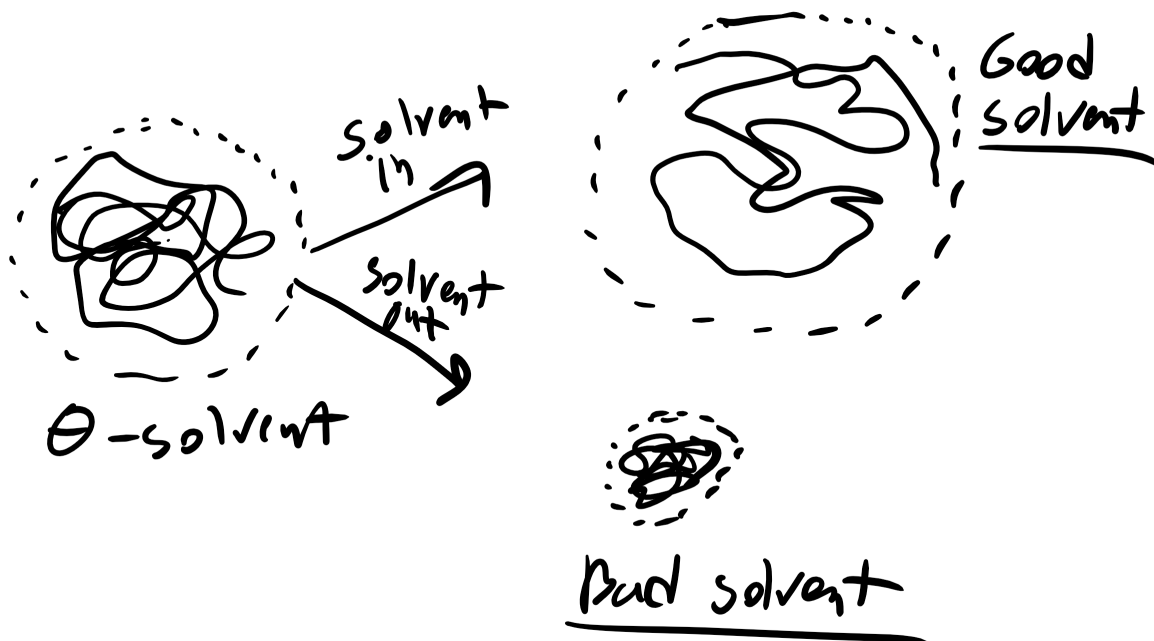


Figure 9-7: Solvent Quality

We will be talking much more about enthalpic interactions when we discuss Flory and whether **enthalpic interactions are good/favorable and whether they are bad/poor/unfavorable interactions**[13, 14, 15]. We will talk about **monomer-monomer interactions** (ϵ_{m-m}), **monomer-solvent interactions** (ϵ_{m-s}), and **solvent-solvent** (ϵ_{s-s}) interactions. Remember from the thermodynamic lecture that we always want lower or negative energies so **for a good solvent** ϵ_{m-s} should be the **lowest energetic interaction** and for **bad solvent** ϵ_{m-s} should be larger[13, 14, 15]. Much more on this when we get to Flory.

9.5 Physicist's Ideal Chain

The last model is the **Physicist's Ideal Chain**. Here we take a **coarse-grained approach** and approximate **larger chains as freely jointed chains**. We then change the values of n and l to N and b to reflect a larger length scale, where b is the **Kuhn length**[13, 14, 15]. This model holds for a chain in θ condition or in the **melt state**, where the polymer chain is not in solvent (again we will discuss this more in depth once we get to Flory)[13, 14, 15]. Essentially, all the work that we have just done in defining C_∞ is encapsulated in these terms as seen below

$$N = \frac{n}{C_\infty} \quad (9.16)$$

$$b = C_\infty l \quad (9.17)$$

Physicist's Ideal Chain

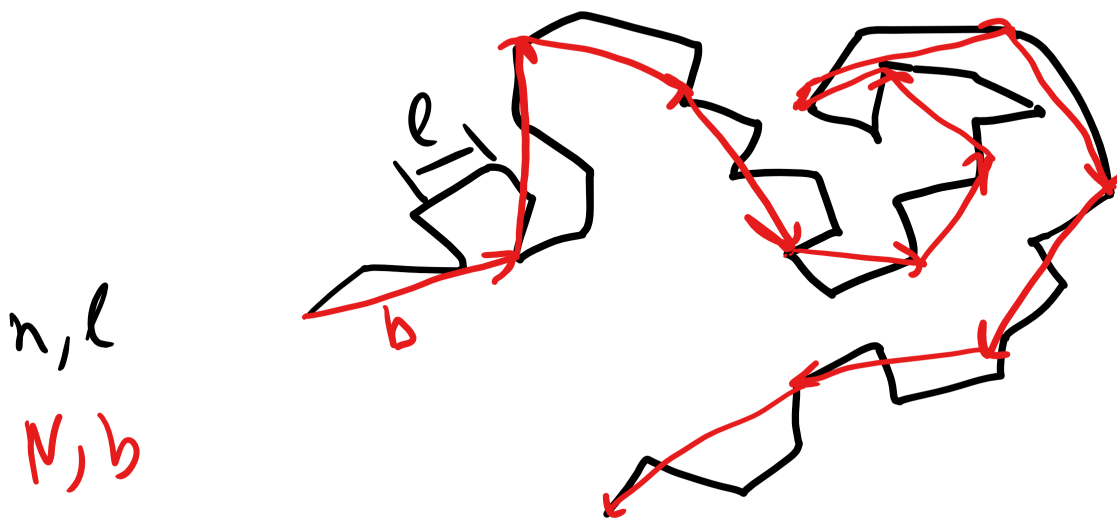


Figure 9-8: Physicist's Ideal Chain

9.5.1 Radius of Gyration

Now before we move we should consider that polymers are not all simple linear chains. We encounter **star, dendrimers, branched, and many other complex architectures** and it becomes much more complicated to measure the average mean squared end-to-end distance[13, 14, 15]. For these polymers we will typically calculate the **radius of gyration** which is

$$r_g^2 = \frac{1}{n} \sum_{i=1}^n (\vec{r}_i - r_{cm})^2 \quad (9.18)$$

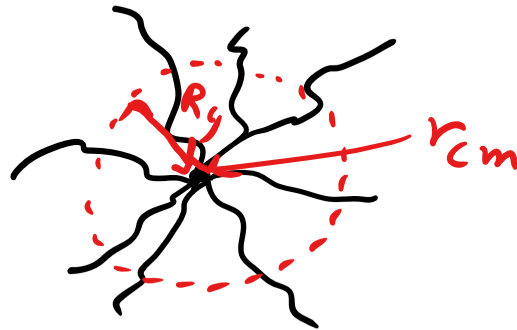
where r_{cm} is the center of mass of the polymer as seen below

$$\vec{r}_{cm} = \frac{\sum_{j=1}^n M_j \vec{r}_j}{\sum_{j=1}^n M_j} \quad (9.19)$$

Radius of Gyration



Random
Coil



Star Polymer/
Dendrimer

Figure 9-9: Radius of Gyration

but typically we know that the monomer mass M will be the same for all monomers so $M_j = M_o$ and we can re-write the position vector of the center of mass as

$$\vec{r}_{cm} = \frac{1}{n} \sum_{j=1}^n M_j \vec{r}_j \quad (9.20)$$

This is a very useful parameter because you can calculate this if the polymer is branched, crosslinked, or a comb as well[13, 14, 15]. The **radius of gyration is simply the mean squared end-to-end distance from the center of mass divided by the number of monomers**. This also gives us an idea of the mass density distribution of the polymer as well.

Now you can derive the radius of gyration for all of the polymer chain models that we will discuss in this lecture but one of the most important relationship is **relating the radius of gyration to the ideal linear chain model** which is

$$\langle r_g^2 \rangle = \frac{\langle r^2 \rangle}{6} \quad (9.21)$$

9.6 Real Polymer Chains : Swelling and Excluded Volume

We have just given a fairly hand-wavy description of the solvent quality parameter α but we have failed to capture the behavior of **real** chains. Specifically, the **interactions between monomers and between monomers and solvent molecules**[13, 14, 15]. We will now include these interactions and derive α explicitly using theory developed by **Paul Flory a polymer physicist and Nobel Prize winner**. We will also see our **first instance of our never ending battle between entropy and enthalpy**[13, 14, 15]. We will see the different contributions that effect α , learn how to control or modify α , and the effect it has on properties like viscosity or the end-to-end distance of the chain.

9.6.1 Contributions to Polymer Swelling: Entropic Spring and Excluded Volume

So before we jump into the factors that can cause polymer swelling or polymer coiling let's start from the the **initial unperturbed state where $\alpha = 1$** and move to it's **final swollen state where $\alpha > 1$** [13, 14, 15]. For most polymers we should expect that in reality the polymer end-to-end distance will always be larger than in the θ solvent case as typically the the monomer-monomer interactions should lead to some **mutual repulsion** (like-like interactions) and **increase the end-to-end distance** of the polymer chain[13, 14, 15].

When thinking about how to describe the contributions to polymer swelling we will typically have

1. **Entropic (Elastic) Contribution:** Chain wants to compress and coil to maximize number of configurations/microstates
2. **Enthalpic Contribution:** Monomer-monomer interactions (excluded volume) increases chain size, maximize enthalpy

Let's think about these two contributions starting with the **entropic contribution** which is sometimes referred to as the **entropic spring** or **entropic restoring force**[13, 14, 15]. When the polymer chain is extended via swelling or if you take it to the extreme and we pull and stretch a polymer chain we know that the end-to-end distance distribution of polymer chains follows a Gaussian distribution. By **pulling on the polymer chain or swelling a polymer chain we are biasing the distribution and the polymer will adopt much less probable larger end-to-end distances**[13, 14, 15]. Doing this **decreases the number of microstates** and thus **decreases the entropy of the system**. This is not energetically favorable we want to **always increase the entropy of the system**. So this induces an **entropic restoring force** to the

undeformed state. You can also call this an **entropic spring** because the functional form of his entropic restoring force will be very similar to Hooke's law. **So when we swell or pull on a polymer we pay a cost in entropy or pay an entropy energy penalty**[13, 14, 15].

So now what about the **enthalpy contribution**. When we have a polymer in a solvent the effective interactions between monomers is dependent on the interaction between monomers and the monomers with the solvent[13, 14, 15]. As we have mentioned previously in a **good solvent** the monomer-monomer interaction is less favorable (higher energy) than the monomer-solvent interactions and vice versa for the **poor solvent**[13, 14, 15]. In a **theta** solvent the monomer-solvent interaction counter acts the monomer-monomer interaction so that there is no net interaction, i.e. enthalpy of 0, ideal solution.

So with these two contributions we will have the total free energy as being composed of two contributions which sum

$$G = G_{entropic} + G_{enthalpic} \quad (9.22)$$

where G is the system free energy of the polymer and solvent, $G_{entropic}$ is the entropic spring contribution and $G_{enthalpic}$ is the enthalpic contribution. Let's derive these two contributions to free energy.

9.6.2 Entropic Spring

Let's start with the entropic spring contribution. We can remember that the probability distribution of an ideal chain is

$$P(r, n) = \left(\frac{1}{2\pi nl^2}\right)^{\frac{3}{2}} \exp\left(-\frac{3r^2}{2nl^2}\right) \quad (9.23)$$

We want to write an expression for the free energy contribution of the entropic spring, i.e. how the free energy will change as a function of the end-to-end distance of our polymer chain, r [13, 14, 15]. Well we know from our thermodynamics and statistical mechanics lecture that we can relate the number of possible configurations Ω to the entropy

$$S = k \ln \Omega \quad (9.24)$$

When we change the initial end-to-end distance of our initial ideal chain with an end-to-end distance of r_0 and a number of monomers n the entropy can be re-written as

$$S(n, r) = k \ln \Omega(n, r) \quad (9.25)$$

where you can see that both the entropy and number of possible configuration will change as a function of the number of monomers and end-to-end distance but typically in the problems that we will work on the **number of monomers will be fixed**, n , but the end-to-end distance will change[13, 14, 15].

Now we can write the probability that a polymer **assumes a given microstate or configuration for a given number of monomers and end-to-end distance** is just as we have described before in our supplementary lecture

$$P(n, r) = \frac{\Omega(n, r)}{\int \Omega(n, r) dr} \quad (9.26)$$

Again quick note that we are working on the assumption that **all configurations are equally probable** i.e. ideal chain[13, 14, 15]. Thus the probability is just the number of configurations with that particular microstate divided by the total number of configurations. So now we can do some math

$$S(n, r) = k \ln \Omega(n, r) \quad (9.27)$$

$$S(n, r) = k \ln \left[P(n, r) \int \Omega(n, r) dr \right] \quad (9.28)$$

$$S(n, r) = k \ln P(n, r) + k \ln \left[\int \Omega(n, r) dr \right] \quad (9.29)$$

$$S(n, r) = -\frac{3}{2}k \frac{r^2}{nl^2} + \frac{3}{2}k \ln \left(\frac{3}{2\pi nl^2} \right) + k \ln \left[\int \Omega(n, r) dr \right] \quad (9.30)$$

$$S(n, r) = -\frac{3}{2}k \frac{r^2}{r_0^2} + S(n) \quad (9.31)$$

We have our entropy expression which **varies as a function of the ratio between the actual end-to-end distance of the chain r vs the unperturbed or ideal chain distance r_0 which should be familiar $\frac{r^2}{r_0^2} = \alpha^2$** [13, 14, 15]. Now this last term is not a function of r and this will become important in just a bit because we always want to find the state of the system at equilibrium which will involve taking the derivative of the free energy with respect to r so this will eventually disappear. Now we can write

$$G_{entropic}(n, r) = H(n, r) - TS(n, r) = \frac{3}{2}kT \frac{r^2}{r_0^2} + S(n) \quad (9.32)$$

where remember we set **H to 0 as we are working on the ideal chain assumption**. Now you might be concerned about this ratio of distances and at this point we have to state **this expression is valid only in tension**, i.e. $r > r_0$ [13, 14, 15]. I won't go into the full derivation but we can modify this expression slightly to include compression and we obtain a more useful equation

$$G(r)_{entropic} = \frac{3kT}{2} \left(\frac{r^2}{nl^2} + \frac{nl^2}{r^2} \right) \quad (9.33)$$

Here we see that in **tension the first term is large** and the **second term goes to 0** and **vice versa for compression**[13, 14, 15]. This make sense as **any perturbation from ideal chain**

conditions will reduce the number of possible microstates and thus decrease entropy!

9.6.3 Enthalpic/Excluded Volume Interactions:

Now, we need to write an expression which considers the monomer-monomer interactions. Well to start we can remember back to ENGR045 to our LJ potential and treat the monomers as hard spheres and look at the potential between the spheres as shown below

$$V_{LJ} = 4\epsilon \left[\left(\frac{\sigma}{r} \right)^{12} - \left(\frac{\sigma}{r} \right)^6 \right] = \epsilon \left[\left(\frac{r_o}{r} \right)^{12} - 2 \left(\frac{r_m}{r} \right)^6 \right] \quad (9.34)$$

where ϵ is the depth of the potential well, σ is the distance at which the inter-particle potential is zero, r is the distance between particles, and r_m is the distance where the potential is minimized[13, 14, 15]. This is a very specific potential and this expression will change for different interactions but this is a starting point for what we will discuss.

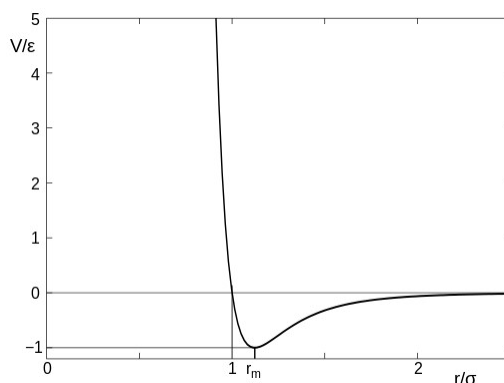


Figure 9-10: Lennard Jones Potential

At short distances the potential will increase (energetically unfavorable) due to **overlap of electron clouds**. At larger distance the potential will be slightly negative but will approach 0 as the monomers are too far away to interact[13, 14, 15]. At some **equilibrium distance** there will either be a well or a hill in the curve and this will depend on the **solvent quality**. Lower energy will always denote a more favorable interaction so in **poor solvents** where we know that the monomer-monomer interaction is more favorable we will see a well and most likely a deep well[13, 14, 15]. For good solvent this well will be much more shallow or even become positive and create an energy hill. The depth of the well or hill is given by ϵ .

Again we can also find the probability of finding two monomers separated by a given distance r is

$$P(r) = \exp \left(- \frac{U(r)}{k_b T} \right) \quad (9.35)$$

which you can see here and we can see that probability matches our discussion above. Note

that at very large values of r the energy goes to zero and thus the exponential of 0 is 1.

Now in order to find the excluded volume we have to utilize the **Mayer f-function**, a function that you will work with more often if you take a thermodynamic course which is

$$f(r) = \exp\left(-\frac{U(r)}{k_b T}\right) - 1 \quad (9.36)$$

All this function effectively does is subtract the probability at large r values[13, 14, 15]. What this function effectively does is describe the relative probability of finding two monomers close to one another versus no interaction at all. The excluded volume is then giving by the integral of this curve

$$v = - \int f(r) dr \quad (9.37)$$

which is also shown schematically here

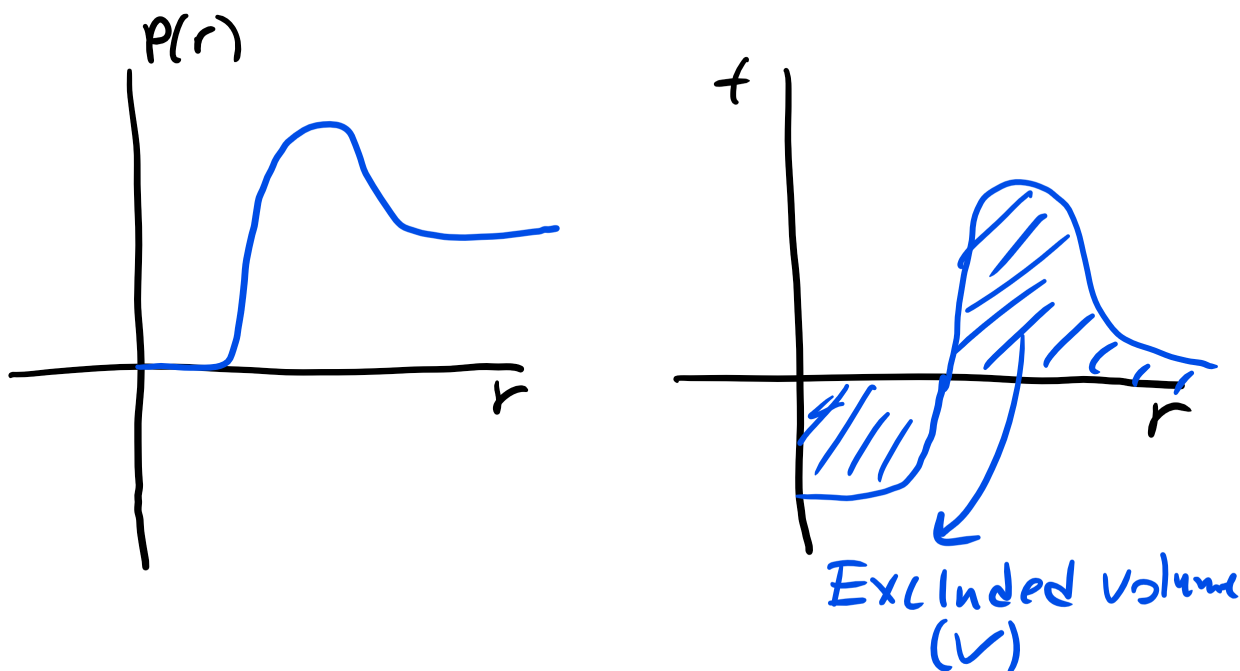


Figure 9-11: Excluded Volume

What this graph shows is that the **excluded volume** is related to the **net** probability of finding two monomers close to each other across all space, thus accounting for **net interactions between two monomers**. The **excluded volume** is the **effective** volume occupied by a monomer including interactions with solvent and other monomers as well[13, 14, 15]. We will have $v < 0$ for net attraction (poor solvent), $v = 0$ for no interaction (θ solvent), and $v > 0$ for net repulsion (good solvent).

Let's take a physical look at what this equation is telling us. Let's say think about what will

happen if the potential has an energy hill or only a repulsive component, no attraction like in the case for a very good solvent. Well then the excluded volume will only be positive and very large which leads to swelling as we might expect[13, 14, 15]. As the attraction between monomers increase the excluded volume will still be positive but with a smaller magnitude and less swelling. At some point the attractive part of the potential will be the same magnitude as the repulsive leading to an excluded volume of 0 which is θ conditions[13, 14, 15]. If the attraction increases further then the excluded volume will become negative the polymer will coil and collapse on itself.

Now that we have defined excluded volume as an interaction between monomers we can **derive an expression for the free energy between all the monomers in the chain**. Let's consider a single monomer in a polymer chain with an excluded volume v and n other monomers in the polymer chain[13, 14, 15]. Now remember what makes polymers and soft matter unique is that the **polymer chains interaction are on the order of kT and this produces fluctuations of the polymer chain**. So let's consider a scenario where **one of the monomers collides or attempts to occupy the excluded volume of another monomer**[13, 14, 15]. The **interaction energy** between these monomers **increases approximately by an amount of kT** . We can then approximate the total interaction based on the number of these collisions.

So let's keep it somewhat simple and say the probability of these interactions will clearly depend on the size of the excluded volume v and the number of monomers n [13, 14, 15]. We will also have to divide by the volume of the chain which we will approximate as $V \approx r^3$, as the larger the volume of the chain/end-to-end distance the less likely monomers will collide[13, 14, 15]. So this will give us the interaction for a single monomer but we have n monomers in our chain so we have to multiply again by n and divide by 2 to avoid overcounting.

So we can write the free energy density for the enthalpic contribution as

$$\frac{G_{enthalpic}(r)}{V} \approx \frac{kTv}{2} \frac{n^2}{r^6} \quad (9.38)$$

Additionally we can see that the concentration of polymer c as seen below

$$c = \frac{n}{r^3} \quad (9.39)$$

which allows us to write the expression below

$$\frac{G_{enthalpic}(r)}{V} \approx \frac{kTv}{2} c^2 \quad (9.40)$$

Note you can generalize this expression to include many body interactions

$$\frac{G_{enthalpic}}{V} \approx kT \left(\frac{vc^2}{2} + \frac{wc^3}{6} + \dots \right) \quad (9.41)$$

We can then simply multiply by volume to get our total free energy

$$G_{enthalpic} \approx kT \frac{vc^2 r^3}{2} \quad (9.42)$$

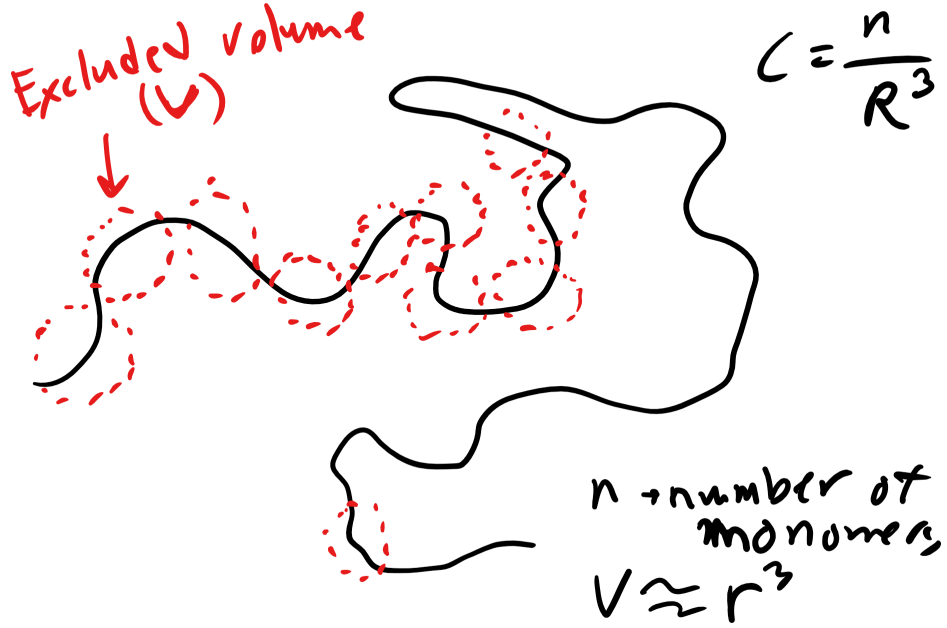


Figure 9-12: Enthalpic Picture

9.7 Flory Full Free Energy:

Finally we can now combine our two terms to obtain the full Flory Free Energy

$$G = G_{\text{entropic}} + G_{\text{enthalpic}} = kT \left(\frac{vc^2r^3}{2} + \frac{wc^3r^3}{6} + \dots \right) + \frac{3kT}{2} \left(\frac{r^2}{nl^2} + \frac{nl^2}{r^2} \right) \quad (9.43)$$

We can also re-write this a bit more simply **ignoring the prefactors that are on the order of 1** and we can **ignore interaction terms beyond 3 body interactions**

$$\frac{G}{kT} = vc^2r^3 + wc^3r^3 + \frac{r^2}{nl^2} + \frac{nl^2}{r^2} \quad (9.44)$$

Now we can use our relationship for concentration of polymers and substitute in

$$\frac{G}{kT} = \frac{vn^2}{r^3} + \frac{wn^3}{r^6} + \frac{r^2}{nl^2} + \frac{nl^2}{r^2} \quad (9.45)$$

To obtain free energy we have to take the derivative and set this equal to zero

$$\frac{\partial G/kT}{\partial r} = -\frac{3vn^2}{r^4} - \frac{6wn^3}{r^7} + \frac{2r}{nl^2} - \frac{2nl^2}{r^3} \quad (9.46)$$

$$\frac{\partial G/kT}{\partial r} = -3vn^2 - \frac{6wn^3}{r^3} + \frac{2r^5}{nl^2} - 2nl^2r \quad (9.47)$$

Again **ignoring prefactors on the order of 1** and dividing by $(nl^2)^{3/2}$

$$\frac{\partial G/kT}{\partial r} = -\frac{vn^2}{(nl^2)^{3/2}} - \frac{w}{l^6} \left(\frac{nl^2}{r^2}\right)^{3/2} + \left(\frac{r^2}{nl^2}\right)^{5/2} - \left(\frac{r^2}{nl^2}\right)^{1/2} \quad (9.48)$$

substituting in for α from the Chemists chain model i.e. $\alpha = \left(\frac{r^2}{nl^2}\right)^{1/2}$

$$\frac{\partial G/kT}{\partial r} = -\frac{vn^{1/2}}{l^3} - \frac{w}{l^6}\alpha^{-3} + \alpha^5 - \alpha = 0 \quad (9.49)$$

With this expression in hand we can now explicitly determine the scaling behavior of the end-to-end distance of polymer chains in different solvents[13, 14, 15].

9.8 Scaling Behavior in Solvents:

9.8.1 Good Solvents:

Let's first consider the Full Free energy expression for a good solvent where we know that $v \gg 0$ and $\alpha \gg 0$. In doing so we can rearrange our expression

$$\alpha^5 - \alpha = \frac{vn^{1/2}}{l^3} + \frac{w}{l^6}\alpha^{-3} \quad (9.50)$$

We can see in this expression that the α^{-3} term will be essentially 0 and that α^5 will be much greater than the α term so the expression reduces to

$$\alpha^5 = \frac{vn^{1/2}}{l^3} \quad (9.51)$$

We can then again use our Chemist's Chain model definition of α and obtain that

$$\langle r^2 \rangle^{\frac{1}{2}} \approx ln^{3/5} \quad (9.52)$$

This is our **essential finding!**[13, 14, 15] We **quantitatively** prove what we have been discussing for several weeks that the end-to-end distance will scale differently $n^{3/5}$ vs the ideal scenario $n^{1/2}$ and that the polymer will expand and swell[13, 14, 15]. This difference of $n^{1/10}$ may seem small but remember we have n values up to 100,000.

Now we made a lot of assumptions here but when you run computer simulations of **self avoiding random walks (SARW)** where lattice sites can only be occupied by one monomer the scaling exponent is 0.588 so Flory was pretty close, he didn't get a Nobel for no reason[13, 14, 15].

9.8.2 Poor Solvent

We can do the same analysis for a poor solvent knowing that $v < 0$ and $\alpha \ll 1$. The expression now reduces to

$$\frac{vn^{1/2}}{l^3} = -\frac{w}{l^6}\alpha^{-3} \quad (9.53)$$

and plugging in for again for α

$$\alpha^3 = \frac{w}{l^6} \frac{l^3}{vn^{1/2}} \quad (9.54)$$

$$\alpha = \left(\frac{w}{vn^{1/2}l^3} \right)^{1/3} \quad (9.55)$$

$$\frac{r}{n^{1/2}l} = \left(\frac{w}{vn^{1/2}l^3} \right)^{1/3} \quad (9.56)$$

$$\langle r^2 \rangle^{\frac{1}{2}} \approx \left(\frac{w}{v} \right)^{1/3} n^{1/3} \quad (9.57)$$

Here again we care about the scaling behavior so that pre-factor doesn't matter to use and we see that $\langle r^2 \rangle^{\frac{1}{2}} \approx n^{1/3}$ so this scaling is smaller than the ideal polymer chain so this polymer will be more coiled and collapsed and this all matches our intuition[13, 14, 15].

9.8.3 Theta Solvent

In a theta solvent we know that $v = 0$ and the three body parameter $w = 0$. This leads to an $\alpha = 1$ and we obtain our typical scaling for a theta solvent.

This concludes our analysis where we had two competing factors that we had to deal with to reach our thermodynamic state of equilibrium: a compressive elastic contribution that arises from an entropic spring restoring force and an expansive excluded volume effect from enthalpic interactions between polymer segments. Don't worry though we will do a similar analysis many more times in this class.

So to quickly summarize

1. **Mathematician's Ideal Random Walk/Ideal Chain Model** $\langle r^2 \rangle = nl^2$
 - Assumes freely jointed chain, no bond angles, polymer can cross itself, no RIS states, steric interactions, or solvent/excluded volume interactions. Captures behavior of θ solvent and melt state fairly well.
2. **Chemist's Chain Model In Solution and Melt** $\langle r^2 \rangle = nl^2 C_\infty \alpha^2$
 - θ Solvent or Melt $\langle r^2 \rangle \approx nl^2$
 - Good Solvent $\alpha > 1$ $\langle r^2 \rangle \approx n^{\frac{6}{5}}$
 - Poor Solvent $\alpha < 1$ $\langle r^2 \rangle \approx n^{2/3}$
 - Takes into account preferred bond angles, steric interactions, RIS states, solvent, and excluded volume interactions.
3. **Physicist's Universal Chain** $\langle r^2 \rangle = Nb^2$

- Simplifies previous the Chemist's chain by incorporating the Flory parameter into the Kuhn length b , accurate for θ solvent and melt.

9.9 Non-Crystalline/Amorphous Polymers:

Now that we have exhausted our discussion of semi-crystalline polymers we can move on to discussing **non-crystalline/amorphous polymers** which are polymers that do not undergo a melting transition but instead a **glass transition** when the temperature is lowered[13, 14, 15]. These polymers then form amorphous but solid structures that lack the long range orientational and translational order of crystals.

9.9.1 Short Range and Long Range Order

Non-crystalline materials are characterized as having short-range order (SRO) but not long range orientational or long range translational order (LRO)[13, 14, 15]. This means that the probability of locating another atom within some distance r is more probable at certain short distances of r than at long distances, where the probability essentially becomes constant. Short-range order (SRO) arises because atoms prefer to pack together is characteristic of liquids in general due to a combination of bonding interactions and weak non-specific bonding[13, 14, 15]. In polymers, SRO is due to local chemistry (such as polymer connectivity), excluded volume and the restricted conformational states due to the finite rotations of intramolecular covalent bonds. Long-range order arises in crystalline solids where the presence of translational symmetry (i.e. a well-defined unit cell) is due to highly specific, strong binding interactions (covalent bonds) or a strong non-specific intermolecular bonding[13, 14, 15]. Polymers that exhibit short-range order but not long-range order are called amorphous; **non-crystalline polymers are amorphous at all temperatures**, while **semi-crystalline polymers exhibit both amorphous regions and crystalline regions**.

9.9.2 Glass Transition Temperature:

We have just discussed how non-crystalline amorphous polymers can be distinguished from semi-crystalline polymers based on the presence of long range order. However, another critical parameter that is utilized to distinguish/describe amorphous polymers is the **glass transition temperature** (T_g [13, 14, 15]. Typically, non-crystalline polymers can be broadly classified as either **rubbery** or **glassy**, both of which exist as highly interpenetrated/entangled Gaussian coils at relatively high temperatures above the glass transition temperature[13, 14, 15]. When we say interpenetrated, the physical picture is of polymer coils that overlap with each other such that separate coils intertwine with each other. In this highly interpenetrated state, without solvent, the polymer acts as if it is unperturbed - that is, in the melt state the polymer is at the θ condition, and can be treated as an ideal chain[13, 14, 15]. You can think of melt polymers as essentially feeling some pressure due to surrounding polymers that overcomes excluded volume effects, yielding an ideal state. The ideal nature of polymers in the melt make them much easier to think about theoretically.

The *glass transition temperature* is the temperature at which a polymer transitions from its fluid-like state to a glassy state. When we say a glass, we mean a material with **only short-range order** but **lacking the translational fluctuations** associated with liquids[13, 14, 15]. Hence it is **like a solid, but with randomly positioned atoms rather than ordered ones as we expect in a crystal**. We can identify the physical origin of the glass transition temperature in two different ways - first, you can think of increasing the temperature from below the glass transition, or you can think of decreasing the temperature from above the glass transition temperature[13, 14, 15]. In either case, the **glass transition is a competition between the available thermal energy kT and the strength of intermolecular bonds ϵ_{ij}** .

If we think of **increasing temperature**, then the glass transition temperature is the point at which **thermal energy is sufficient to break local intermolecular bonds, enabling fluid-like motions** - that is, the point where $kT > \epsilon_{ij}$. If we think of **decreasing temperature**, then the glass transition temperature is the point at which the **viscosity of the polymer essentially becomes infinite, eliminating molecular motion**[13, 14, 15]. In either case, the key property of a glass is that the **rearrangement of atoms is hindered, limiting the ability of the system to relax to equilibrium when a stress/perturbation is applied**[13, 14, 15]. This is intimately related to the concept of a **characteristic relaxation time** which we will take a quick aside right now to discuss.

9.9.3 Relaxation Time τ^* :

The physical properties of amorphous polymers (and materials in general) are influenced by τ^* , the **characteristic relaxation time** of the polymer, and how large this relaxation time is relative to a relevant experimental time (or the interaction time) t [13, 14, 15]. The **relaxation time** is essentially a measure of how **long it takes for a material to return to equilibrium after the application of some perturbation**. The ratio between the relaxation time and experimental time is called the **Deborah number** - i.e. $De = \frac{\tau^*}{t}$ [13, 14, 15]. It is easiest to think of the importance of the relaxation time in terms of known material behavior.

Let's consider as an example a system consisting of some material in a container such that the material is magically attached to the container walls. We impose a perturbation on the system consisting of moving the walls of the container apart such that the material in the container is deformed/stretched[13, 14, 15]. First consider the case that the **relaxation time of a material is much smaller than the experimental time**, such that $\tau^* \ll t$ and $De \ll 1$ [13, 14, 15]. Because the relaxation time is so much lower than the experimental time, the material effectively relaxes instantaneously to the new system dimensions as the perturbation is applied; in other words, the **system adjusts to the new constraint by relaxing to equilibrium immediately**[13, 14, 15]. Physically, we could imagine this as the material rearranging its constituent molecules to instantaneously fill the new volume of the container - we would say that the material **flows**, and call the material in the container a liquid.

Now consider the opposite case, where the **relaxation time is much greater than the**

experimental time such that $\tau^* \gg t$ and $De \gg 1$ [13, 14, 15]. Now when we adjust the walls of the container, the material effectively **never relaxes to equilibrium as the perturbation occurs**, instead being driven very far from equilibrium into a high energy state. In our physical example, we would imagine the material in the container being stretched but being unable to adjust the positions of its atoms because the relaxation time is so long, so that the material instead **builds up a large amount of strain energy**; we would consider this an **elastic** response and call the material an elastic solid[13, 14, 15]. Note that the only distinction we are drawing here between the liquid and solid case is the experimental time - this implies that if we apply a stress/strain to a solid and wait long enough, it would appear to flow like a liquid (in the case of crystalline solids this would be due to the gradual movement of defects throughout the material to change the solid dimensions)[13, 14, 15]. In an intermediate regime where the **relaxation time is roughly the same as the experimental time**, the material will exhibit behavior consistent with both **viscous liquids and elastic solids**; we call these materials *viscoelastic* and will discuss their properties much more in future lectures.

We can gain some understanding of relaxation times from the molecular structure of a given material[13, 14, 15]. For example, for small molecules like water, the relatively free motion of water due to its small size would lead to a small relaxation time, and hence water is only solid at low temperatures. Polymers tend to exhibit a longer relaxation time due to the connectivity monomers, requiring collective motion to adjust to a perturbation. As we will discuss shortly, at lower temperatures the energetic cost for this motion is too great to allow the polymer to flow, leading to glassy behavior[13, 14, 15]. We might also imagine, then, that polymers with more rigid backbones have longer relaxation times due to the lessened flexibility of the chain.

Characterizing a polymer as a rubber, liquid, or solid (glass) is impossible without further information on the overall environment, as the response of the polymer depends on the **time scales** involved[13, 14, 15]. We will also see that the relaxation time in polymers is a function of temperature, yielding many of the characteristic mechanical properties which we will discuss in future lectures. To wrap up if the molecular motion is slow/hindered, the relaxation time of the polymer is very long and thus the polymer exhibits solid-like behavior.

9.9.4 Back to Glass Transition Temperatures:

A key point about the glass transition temperature is that it is not strictly a thermodynamic transition. The melting temperature, for example, results because there is some specific temperature for materials where the free energy of the liquid phase becomes lower than the free energy of the solid phase, leading to melting behavior (and more specifically there is an abrupt change in thermodynamic quantities reflecting a first-order phase transition)[13, 14, 15]. Hence, the melting point is thermodynamic in nature, resulting from the competition between the higher entropy liquid phase and lower enthalpy solid phase. The **glass transition is not strictly thermodynamic**, as a glass is **not a stable thermodynamic phase** but rather a **kinetically-trapped phase resulting** from the large energy barriers faced by a glass when it must adjust to a perturbation[13, 14, 15].

The glass transition thus reflects the kinetics and time scale of a system and as such the transition temperature is not easily defined - in fact, **the exact measurement depends on cooling rate** and typically a range of glass transition temperatures are reported for specific samples[13, 14, 15].

9.9.5 Free volume theory of T_g

An explanation for the origin of the glass transition temperature comes from **free volume theory**[13, 14, 15]. **Free volume** (not be confused with excluded volume) is the space in a polymer sample **in excess** of the volume present in a random, *densely packed* glass. Free volume is the **volume that monomers in a particular sample are able to access via thermal fluctuations**[13, 14, 15]. In a **liquid state**, we would imagine that the **free volume is high**, allowing large fluctuations and easy response to perturbations due to the availability of free volume through which monomers can move[13, 14, 15]. By contrast, in the **glassy state** the **free volume is very low** and as a result molecular motion is hindered by steric/excluded volume considerations.

The glass transition temperature is also dependent on the **rate of cooling** of the sample. The cooling rate dependence of the glass transition temperature can be explained by what's called **percolation**[13, 14, 15]. If we imagine the polymer sample superimposed on a lattice, and each lattice point can be thought of as either in the glassy state or fluid state, then the **network is percolated when a connected network of glassy points spans the entire lattice**. In other words, it is not necessary for the entire polymer sample to be glassy; it is **only necessary for connected regions that cross the network to be glassy**, since **these connections essentially cut off the fluid parts from each other**, leading to glassy behavior on the macroscale[13, 14, 15]. We can think of each lattice point as transitioning between fluid and glassy with some characteristic probability, and can also imagine some other characteristic probability for the point to transition from glassy back to fluid. **Physically, this reflects the ability of monomers to move through the available free volume**, and hence at **lower temperatures** we expect the probability of a fluid-to-glass transition to increase, and the **probability for a glass-to-fluid transition to decrease** as the **decreasing free volume favors the glassy state**. As we cool the sample, then, the probability of forming a glass progressively becomes higher, and the time taken for glass points to transition back to fluid takes progressively longer[13, 14, 15]. If we **cool at a very fast rate**, lattice points will have **sufficient time to transition from fluid to glass but not back** (since as we cool it takes longer and longer for the glass-to-fluid transition), **leading quickly to a percolated network at a high temperature** since glassy behavior will be observed as soon as connected glassy regions span the sample[13, 14, 15]. If we **cool at a slower rate**, a percolated network is more difficult to form because at **higher temperatures the relatively short time associated with the glass-to-fluid transition will disrupt the network** as it forms. This means that the glass transition will be observed at a lower overall temperature.

9.9.6 T_g and Chemical Structure of Monomers:

Trends in T_g can be explained by looking at the chemical structure of monomers due to the influence of monomer structure on both chain flexibility and free volume. Recall that T_g is determined by the onset of long range **cooperative molecular motion**, meaning the motion of 10-30 connected chain monomers at once. The cooperative motion requires both sufficient thermal energy to induce the movement of these monomers and sufficient free volume for the monomers to move into [13, 14, 15]. Both of these requirements are influenced by monomer structure. There are essentially 3 elements of monomer structure that can influence these motions:

1. **Chain interactions** - energetic interactions between monomers
2. **Ease of rotation about main chain bonds** - whether there is significant steric hindrance to rotation
3. **Amount of free volume available** - how densely the monomers pack

We can think of polymers as essentially divided into their backbone and sidechains coming from that backbone [13, 14, 15]. In polymers with flexible backbones, like polyethylene (lots of C-C single bonds) and PDMS (Si-O bonds, which are flexible due to the 4 electrons on the oxygen atoms in place of hydrogens), the hindrance to rotation is low and hence less thermal energy is necessary to induce molecular motion, leading to a low T_g [13, 14, 15]. On the other hand, polymers with phenyl molecules along the backbone (e.g. polycarbonate) tend to have a much higher T_g , since the bulky phenyl constituent greatly increases the amount of energy necessary for rotation (i.e. the rigidity). Note that we can generally relate C_∞ to the rigidity of a backbone, and hence expect T_g to increase with C_∞ [13, 14, 15].

Similarly, large bulky sidechains, such as phenyl groups, also oppose rotation due to steric hindrance, and in addition decrease the amount of free volume available since they occupy a greater excluded volume, leading to a higher glass transition temperature [13, 14, 15]. Finally, intermolecular interactions, such as hydrogen bonds or ionic interactions, which are typically seen between sidechains, will tend to greatly increase the glass transition temperature since thermal energy will also have to break these bonds to induce rotation [13, 14, 15]. The lecture notes provide some examples of polymers, sidechains, and the related T_g s. The main principles to keep in mind are that chain flexibility allows easier cooperative movement of monomers, decreasing the T_g , and increased free volume around the chain backbone lowers the barrier to cooperative movement and hence decreases the T_g [13, 14, 15].

We can also relate these observations back to the idea of crystallinity, as well, as the factors that influence the glass transition temperature will also influence the ability of polymers to crystallize [13, 14, 15]. In fact, there is a correlation between T_g and T_m for semi-crystalline polymers - typically T_g is about 0.5 to 0.8 T_m in Kelvin.

9.10 XRD Analysis:

We have talked about XRD analysis and have done our XRD lab which included a polymer. We know that the peaks observed in the diffractogram will be more broad than that for metals due to the lack of long range translational and orientational order for polymers[13, 14, 15]. However, we can obtain some key information from XRD analysis of polymers to allow us to deduce some information about the structure of polymers and how they might be arranged. Let's take for example the case of the family of polymethacrylates, specifically PMMA, PPMA, PEMA, and PBMA[13, 14, 15].

When we examine the XRD profile of these polymers we can see that there are some XRD peaks that do not shift for the entire family of polymers. Additionally, the peaks that appear to be consistent between the family are all located at large Bragg angles (2θ)[13, 14, 15]. At lower Bragg angles there appears a considerable amount of peak shifting and perhaps even some creation or destruction of peaks in the XRD curve. How can we explain what is happening here?

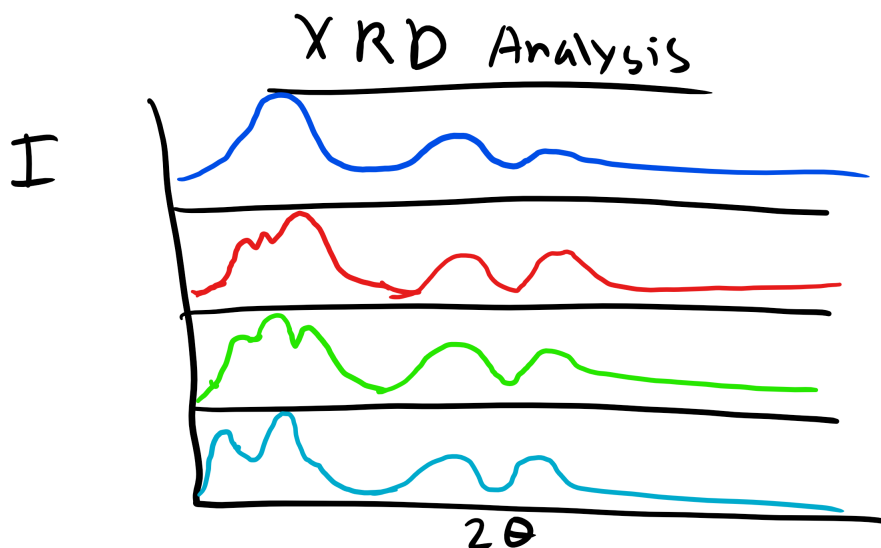


Figure 9-13: XRD Curves of Methacrylate Family.

Well again remember that we observe peaks in the XRD curves when there is constructive interference which occurs when at that particular incident angle there is some local order perhaps even long-range order of some type. We also know from Bragg's law that the Bragg Angle $\theta \propto \frac{1}{d}$ [13, 14, 15]. So the characteristic distance where this local order appears is inversely proportional to the incident angle. Let's think about the structure of these polymers at very short distances like the C-C bond distance or the distance between the methyl groups. This distance will not change depending on the polymer we are looking at in this family[13, 14, 15]. These small distances correspond to large angles and so this explains why the peaks are conserved for the different polymers.

Now what is happening for the other polymers. Well there are other characteristic distances for

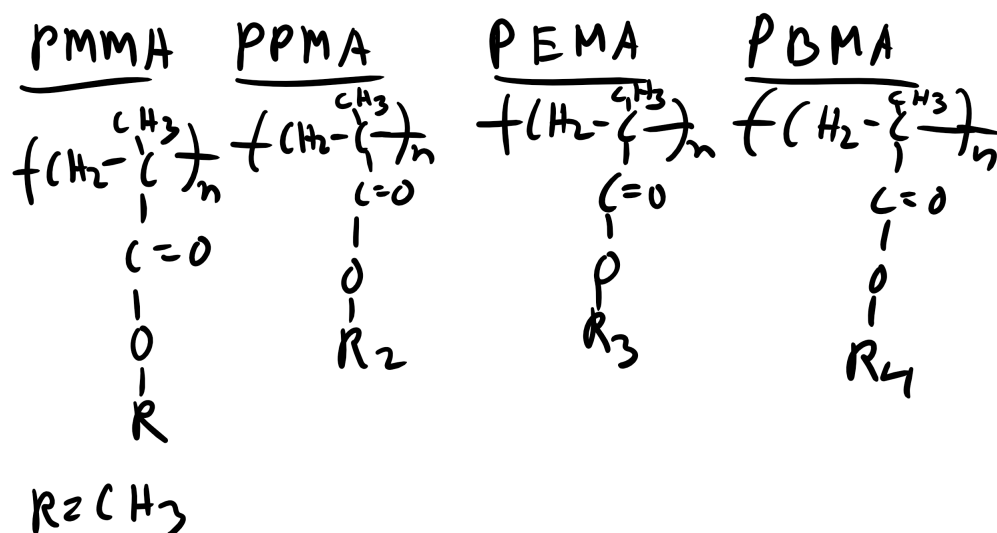


Figure 9-14: Methacrylate Family of Polymers

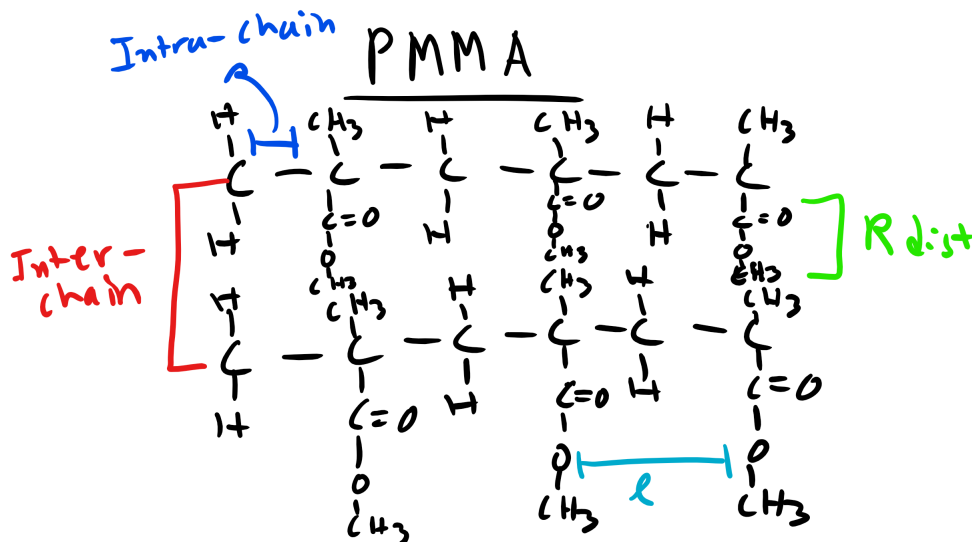


Figure 9-15: PMMA Chain Schematic.

these polymers. For example the distance from the chain backbone to the end of the R functional group. Or even the inter-chain distance within the polymer. These distances will change depending on whether the polymer is PMMA, PBMA, etc. If the distance changes there will be a corresponding shift in the location of the peaks[13, 14, 15]. And we see that on average as the side group R increases in length for these polymers the peaks tend to shift to the left which is consistent from what we know about diffraction! This is critical information as it gives us a schematic of the structural characteristics of an unknown polymer chain[13, 14, 15].

9.11 DSC Analysis:

Differential Scanning Calorimetry (DSC) is a thermal analysis technique useful for measuring thermodynamic properties of materials such as specific heat, melting point, boiling point, glass transition temperature (in amorphous/semi-crystalline materials), heat of fusion, reaction kinetics, etc. The technique measures the temperature and the heat flow, corresponding to the thermal performance of materials, both as a function of time and temperature.

Typically a DSC will utilize a heat flux type system in which the differential heat flux between a reference (e.g. sealed empty aluminum pan) and a sample (encapsulated in a similar pan) is measured. The reference and the sample pans are placed on separate, but identical, stages on a thermoelectric sensor platform surrounded by a furnace. As the temperature of the furnace is changed (usually by heating at a linear rate), heat is transferred to the sample and reference through the thermoelectric platform. The heat flow difference between the sample and the reference is then measured by measuring the temperature difference between them by using thermocouples attached to the respective stages. The DSC provides qualitative and quantitative information on endothermic heat absorption (e.g. melting) and exothermic heat release (e.g. solidification or fusion). These processes display sharp deviation from the steady state thermal profile, and exhibit peaks and valleys in a DSC thermogram (heat flow vs. temperature profile). The latent heat of melting or fusion can then be obtained from the area enclosed within the peak or valley.

DSC analysis is an extremely critical and useful tool in characterizing the thermodynamic quantities of polymer, specifically in identifying T_g and T_m as well as determining if a polymer is amorphous or crystalline.

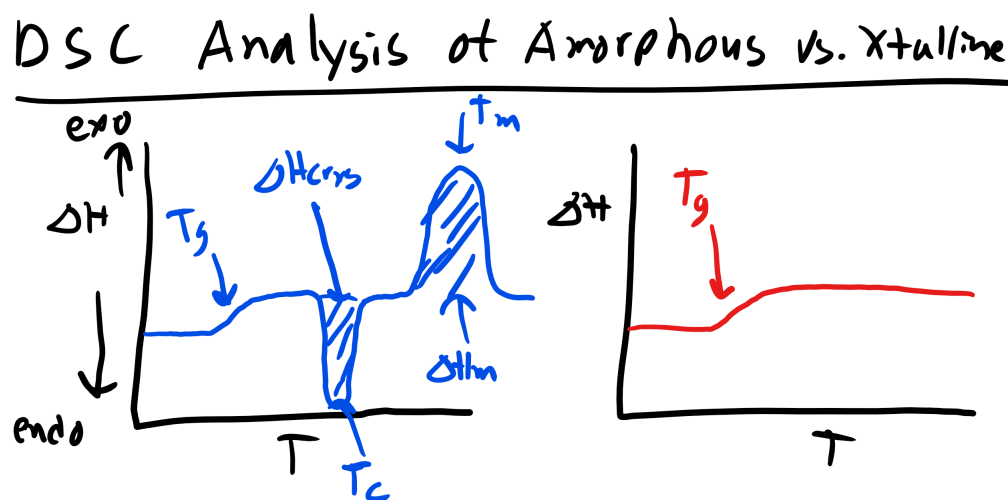


Figure 9-16: Amorphous Vs. Crystalline DSC Curves

As you can see below if we are working a polymer that is semi-crystalline we can typically observe 2 peaks in the DSC curve as well as a change in the slope of the curve of heat flow vs

DSC Analysis of Thermoplastic vs. Thermoset

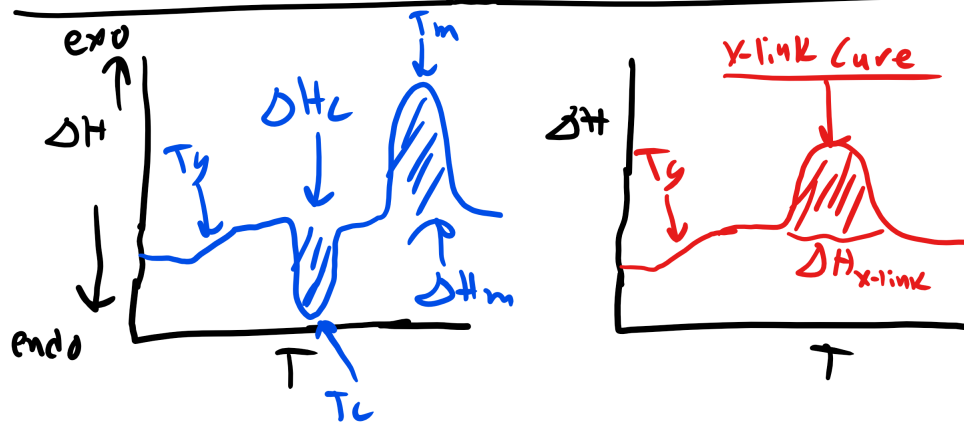


Figure 9-17: Thermoplastic Vs. Thermoset DSC Curves

temperature. Let's take this analysis step by step. If we remember back to Materials Science we know that a first order phase transition will result in a discontinuity in the first order derivative of the free energy as a function of temperature (at the temperature of the transition). Whereas second order transitions will exhibit a discontinuity in the second derivative of the free energy and will only exhibit a change in slope for the first derivative as a function of temperature. Now the plot that we are looking at is heat flow vs temperature which is essentially δH vs T so we are looking at a plot of the first derivative of free energy.

Now the first feature that we come across (increasing in temperature) is a change in slope. Well we know this must be a second order transition. Additionally we know that this transition occurred at fairly low temperatures. Since our sample is a polymer this transition most likely signifies the glass transition temperature, T_g . This should make sense as we know the T_g is a second order transition. Now the next feature that we see is an exothermic peak. Well we know that this peak indicates a first order transition and if this is an exothermic reaction this should signify some solidification or re-crystallization, T_c . This might at first seem counter-intuitive, why would increasing temperature cause the polymer to crystallize? Well it is because as we increase temperature we increase the mobility of the previously glass amorphous regions. With this increased mobility there is a higher likelihood of encountering other chains the enthalpic interactions accessed here might favor the formation of crystalline regions. This curve might not show up in every polymer. The last peak is an endothermic one and we will recognize this as the melting point, T_m . Now remember this does not break the carbon-carbon backbone bonds but instead the secondary intermolecular interactions.

How would this curve change for a purely amorphous polymer? Well we would simply see a change in the slope to indicate the glass transition and that would be it. Now what if you had a

thermoset polymer which has to cure and form crosslinks. Well, we would see a T_g as this is still a polymer. Now would you see a melting temperature? No a thermoset does not undergo melting due to the permanent crosslinks! They would exhibit an exothermic peak that would indicate the energy required to cure/crosslink the polymer!

CHAPTER 10

ELECTRICAL, OPTICAL, AND MAGNETIC PROPERTIES OF MATERIALS

10.1 Electrical, Optical, and Magnetic Materials

Electrical, Optical, and Magnetic properties are critical material properties which are critical to a myriad of applications from information storage, semi-conductors, optical fibers, and magnetic resonance imaging (MRI). Unfortunately the complete understanding of many of the phenomenon and properties that we will discuss require a through understanding of quantum mechanics, solving **Hamiltonians**, and **eigenvectors** and **eigenvalues**[17, 18, 19]. This is beyond the scope of this class but there are references that I can point you to if you are interested.

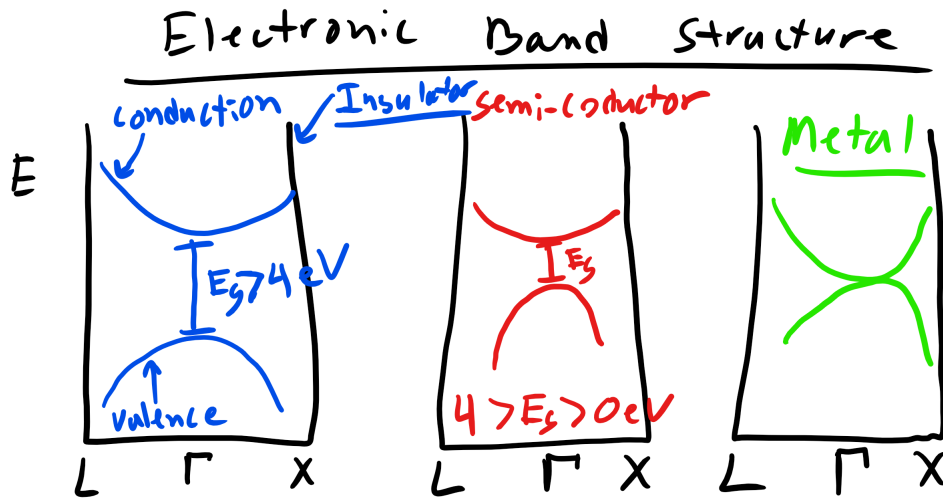


Figure 10-1: Electronic band structure.

10.2 Electronic Band Structure and Block Waves

When discussing electronic, optical, and magnetic properties it is critical to understand the **electronic band structure** of different materials. The **electronic band structure** of materials illustrates the range of **energies that an electron may occupy** and some **energies that are forbidden**[17, 18, 19]. To better understand this let's take a look at the band structure of several broad classes of materials specifically **insulators**, **metals**, and **semi-conductors**. [17, 18, 19] Before we take a look at the band structures in terms of electrical properties insulators are a class of materials that are poor at conducting electrons, metals are excellent conductors, and semi-conductors are in between and we can see this by looking at the band structure below:

Let's start with the metals and look at the band that is highlighted in blue. This band is the **conduction band** so and you can see that it is in contact with the **valence band** below it[17, 18, 19]. This means that electrons occupy the conduction bands at room temperature. This allows metals to be good electron conductors and contributes to their electrical properties. Now we can see for the two other materials that there appears to be a gap between the valence and conduction bands. This is referred to as a **bandgap** it is essentially an energy gap or a space where electrons cannot exist. The origin of this bandgap can be derived from quantum mechanics[17, 18, 19]. Electrons have particle-wave duality and they typically encounter a periodic lattice of atoms. This periodicity in the arrangement of atoms will similarly induce a periodic potential and thus the waveform of the electron will also be periodic. This is the theorem that **Block** developed and one can then solve Schrodinger's equation to find the energy states[17, 18, 19]. This is obviously very hard to do but it is the periodic nature of the lattice that leads this bandgap.

So for semi-conductors and insulators the valence and conduction electrons are separate and at room temperature you probably will not find many electrons in the conduction band. However, the difference between semi-conductors and insulators is the magnitude of the bandgap[17, 18, 19]. Clearly the bandgap is much larger for insulators than for semi-conductors. **In fact in this class the rule will be if the bandgap is greater than 4eV we will consider this an insulator.**[17, 18, 19]

10.3 Optical Properties

We can also use bandgaps to understand why materials appear a particular color. For example, copper is redish in color and this is related tot the band structure. The energy gap between the 4s and 3d shells is approximately 2.2eV[17, 18, 19]. We can relate this energy to wavelength using Plank's equation

$$E = \frac{hc}{\lambda} \quad (10.1)$$

where h is Plank's constant, c is the speed of light, and λ is wavelength. This equates to a wavelength of approximately 562nm which is in the copper color range[17, 18, 19].

10.4 Magnetic Properties

Finally I want to briefly discuss different types of magnetic materials specifically **diamagnetic, paramagnetic, ferromagnetic, and superparamagnetic**[17, 18, 19]. Let's start with **diamagnetic** materials like carbon, lead, copper, water, and mercury[17, 18, 19]. Diamagnetic materials initially do not have magnetic moment and it is only when an external magnetic field is applied the material will then exhibit some induced magnetic field in the opposite direction of the applied field[17, 18, 19]. This is a purely quantum mechanical effect and actually leads to the magnetic levitation observed in classic examples like the levitating frog.

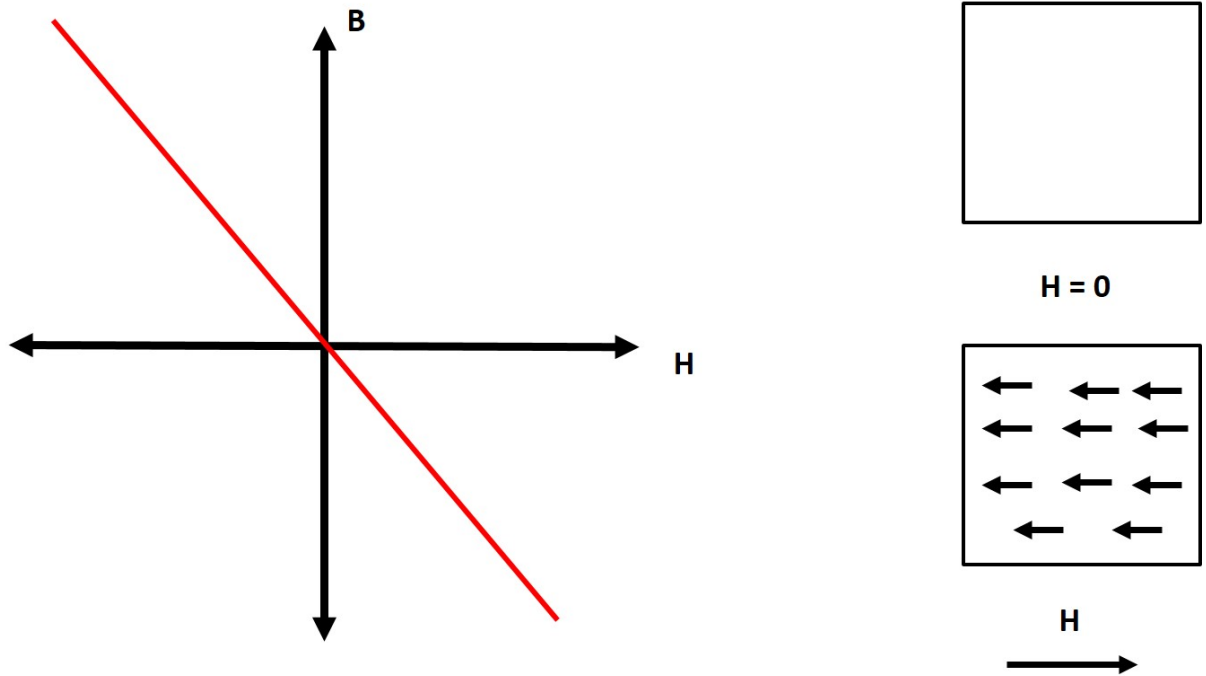


Figure 10-2: Diamagnetic material B vs H curve.

Parmagnetic materials (tungsten, aluminum, sodium, lithium) initially have no net magnetic field and the magnetic moments point in random directions. As the applied field, H , increase the magnetic field strength (B), gradually increases but all moments are never fully aligned with the applied field, we do not see saturation[17, 18, 19].

Ferromagnetic materials (cobalt, iron, nickel, chromium-oxide) initially have a net magnetic moment and will align with an applied field. You can see this net moment in the measurement of magnetic coercivity, H_c , the material also exhibits magnetic saturation, M_s , and magnetic remanence, M_r [17, 18, 19]. Magnetic saturation is when the material is completely aligned with the applied field, the magnetic remanence is the magnetic field remaining after the applied field has been removed and the coercivity is the applied field required to reduce the magnetic field to zero after reaching magnetic saturation[17, 18, 19].

Superparamagnetic materials have to be no the order of nanometers and only have a single magnetic domain[17, 18, 19]. You see that superparamagnetic particles also exhibit magnetic saturation however there is no coercivity. This is important because it takes a minimal amount of energy to magnetize these materials but for magnetic storage you would want ferromagnetic materials and your data is much more difficult to erase[17, 18, 19].

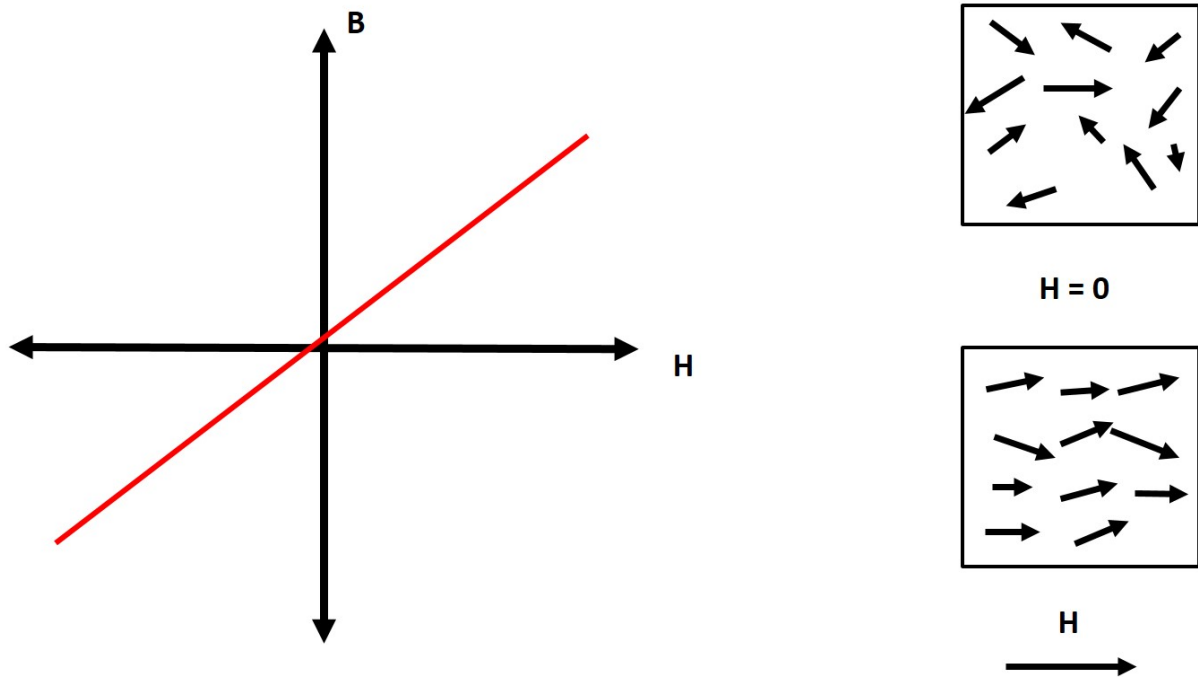


Figure 10-3: Paramagnetic material B vs H curve.

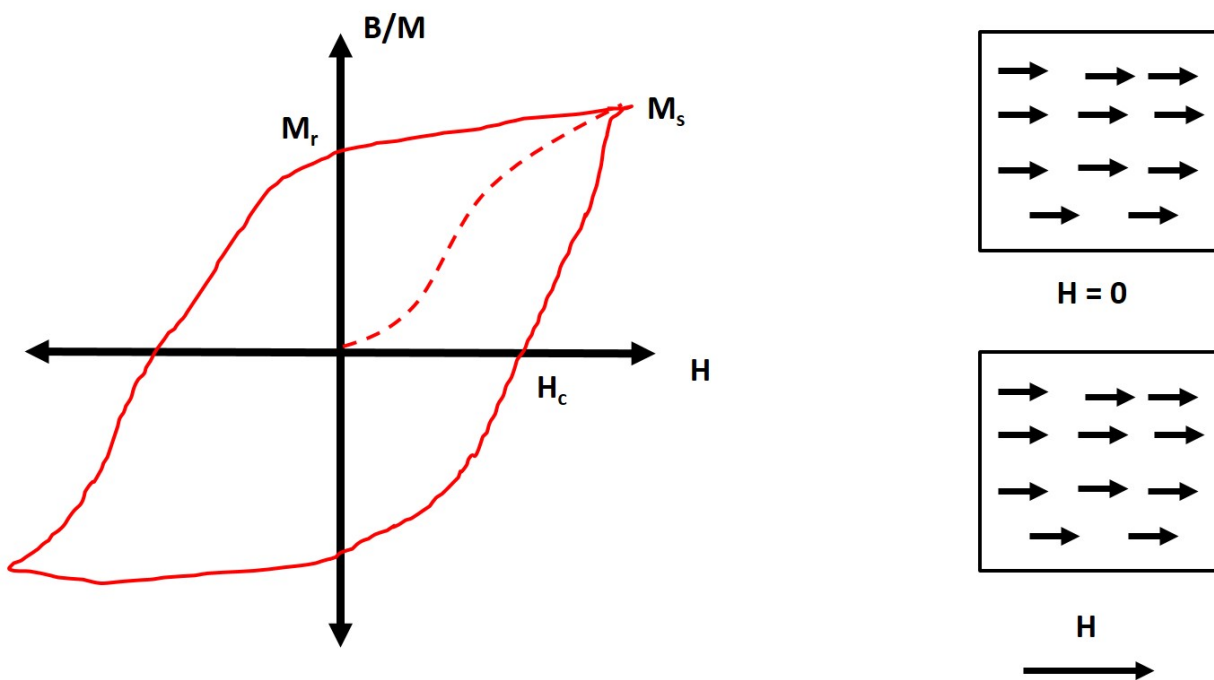


Figure 10-4: Ferromagnetic material B vs H curve.

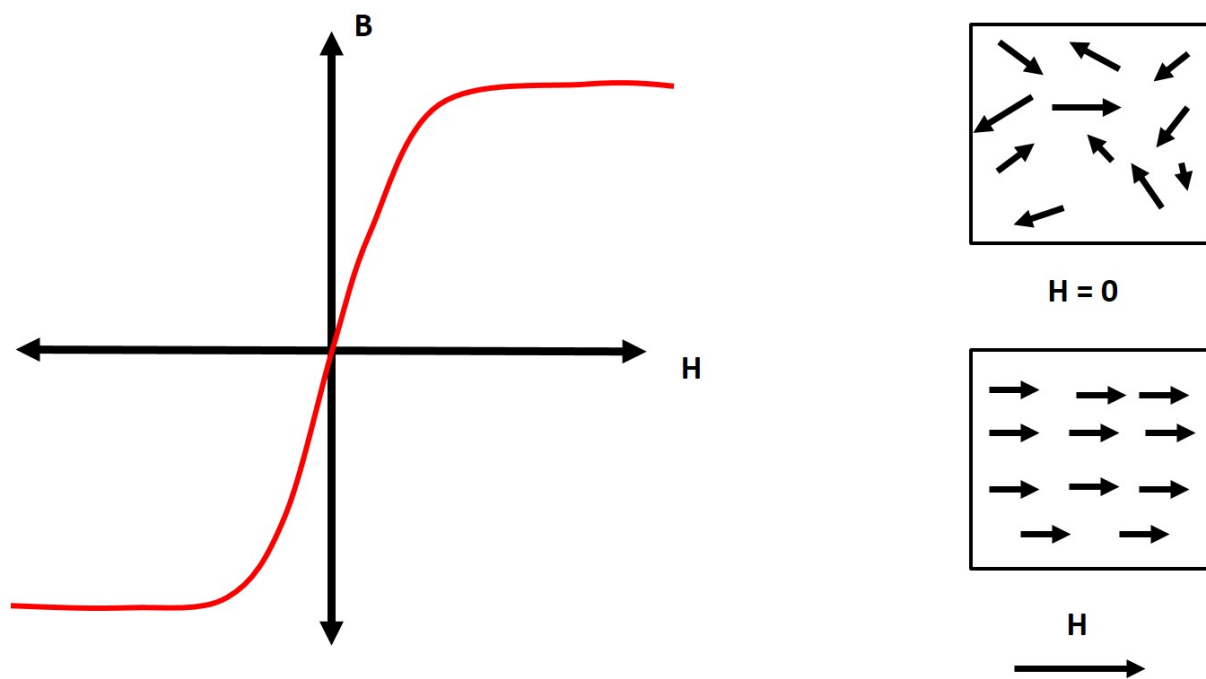


Figure 10-5: Superparamagnetic material B vs H curve.

THIS PAGE INTENTIONALLY LEFT BLANK

Bibliography

- [1] Callister. *Materials Science and Engineering: An Introduction, Tenth Edition*. John Wiley & Sons, Incorporated, December 2017.
- [2] Sam Allen and Edwin L. Thomas. *The Structure of Materials*. Wiley, February 1999. Google-Books-ID: JgtpQgAACAAJ.
- [3] Keministi. English: Newman projections of butane conformations & their relative energy differences (not total energies). Conformations form when butane rotates about one of its single covalent bond. Torsional/dihedral angle is shown on x-axis., September 2018.
- [4] Original: DornelfVector:DePiep. English: Hexagonal close packed crystal structure (vectorised from png), July 2012.
- [5] Ficheiro:Empilement compact.svg.
- [6] Zureks. Polski: Schematyczne przedstawienie dyslokacji krystalicznej - dyslokacja śrubowa, 2008.
- [7] Javier Bartolomé Vílchez. English: Scheme of the Burgers' vector in edge and screw dislocations, July 2008.
- [8] Robert W. Balluffi, Sam Allen, and W. Craig Carter. *Kinetics of Materials*. Wiley, December 2005. Google-Books-ID: i9jPjwEACAAJ.
- [9] Darrel J. Irvine. Thermodynamics., September 2009.
- [10] Krystn Van Vliet and John M. Maloney. Mechanical behavior of materials., September 2010.
- [11] 2D_geometric_strain png: Sanpazderivative work: Mircalla22. English: Deformation of an infinitesimal rectangular material element., August 2009.
- [12] Yet-Ming Chiang. *Physical Ceramics*. John Wiley Sons, 1997. Google-Books-ID: aBYtswEACAAJ.
- [13] Reid Van Lehn and Alfredo Alexander-Katz. Polymer physics., September 2011.
- [14] Robert J. Young and Peter A. Lovell. *Introduction to Polymers, Third Edition*. CRC Press, June 2011. Google-Books-ID: ImQg2MK8NtkC.
- [15] Michael Rubinstein and Ralph H. Colby. *Polymer Physics*. OUP Oxford, June 2003. Google-Books-ID: RHksknEQYsYC.
- [16] 718 Bot at English Wikipedia. English: personal production. Diffusion and usage unrestricted, July 2008.

- [17] Stephen Blundell. *Magnetism in Condensed Matter*. OUP Oxford, October 2001. Google-Books-ID: OGHGmgEACAAJ.
- [18] Kittel. *INTRODUCTION TO SOLID STATE PHYSICS, 7TH ED*. Wiley India Pvt. Limited, 2007. Google-Books-ID: F9Qu5c.hUaUC.
- [19] Anthony Mark Fox and Department of Physics and Astronomy Mark Fox. *Optical Properties of Solids*. Oxford University Press, 2001.